LATERAL LOAD ANALYSIS
OF
MULTI-STOREY WALL-FRAME STRUCTURES

by

© DAMIEN K. W. LEUNG, B.Eng.

A Thesis

Submitted to the School of Graduate Studies

in Partial Fulfilment of the Requirements

for the Degree

Master of Engineering

McMaster University

July 1980

MULTI-STOREY WALL-FRAME STRUCTURES

MASTER OF ENGINEERING (1980)
(Civil Engineering)

McMASTER UNIVERSITY
Hamilton, Ontario.

TITLE: Lateral Load Analysis of Multi-Storey Wall-Frame Structures

AUTHOR: Damien K. W. Leung, B.Eng. (McMaster University)

SUPERVISOR: Dr. W. K. Tso

NUMBER OF PAGES: xvi, 358

ABSTRACT

This thesis studies the behaviour of multi-storey wall-frame structures subjected to lateral and/or torsional loads. A planar structure with rotational and vertical restraints imposed between the wall and the frame is analysed. Parametric studies of a nominal structure are presented to examine the general effects of such restraints and structure height on wall-frame interaction. In the light of the understanding acquired from this two-dimensional analysis, a more general method of analysis for three-dimensional wall-frame structures is developed. For both methods, the variation of structural properties along the structure height is considered. A more flexible method of analysis for general three-dimensional building structures analogous to the stiffness matrix method is also presented. Applying this method to determine the structure stiffness matrix and using the lumped-mass approach, an attempt is made to study the free-vibration dynamic responses of the Banco de America Building both before and after damage was sustained by the building during the Managua earthquake of December 23, 1972. Lastly, conclusions regarding the behaviour and design of wall-frame structures are drawn, and the applicabilities and limitations of the three-dimensional analytical methods developed in this thesis discussed.

ACKNOWLEDGEMENTS

I wish to express my profound gratitude to Dr. W. K. Tso for his patient guidance and continual encouragement in carrying out the research which culminated in the present thesis.

The financial support of this research by the Department of Civil Engineering and Engineering Mechanics, McMaster University, through a research and teaching assistantship is gratefully acknowledged.

I also wish to thank my dear wife, Fanny, for her endurance during my research programme and for the careful typing of this thesis.

TABLE OF CONTENTS

4 THREE-DIMENSIONAL ANALYSIS OF UNIFORM WALL-FRAME STRUCTURES

APPENDIX

LIST OF FIGURES

LIST OF TABLES

CHAPTER I

INTRODUCTION

1.1 HIGH-RISE BUILDINGS

Since the turn of the century, there has been a growing trend towards high-rise construction as an economical and efficient means to meet with ever-increasing demands for usable space for residential and commercial purposes in urban centres.

In regard to the economical and structural feasibilities of tall buildings, the overwhelming concern to the engineer lies in the structural performance of these buildings against lateral loads caused by wind or earthquakes. Thus, in order to cope with such diverse structural requirements — weighed against the functional and architectural counterparts — as may be called for by a particular building while achieving economy and efficiency, various types of lateral load structural systems have evolved over the past few decades. Principal among these systems are, in the order of their emergence amid the trend for taller buildings, the moment-resisting frame system, the shear wall

system, the wall-frame system, and the tube system.

The general complexity of these high-rise building systems, along with the paramount need for an adequate design, has led to extensive research efforts in the development of efficient and reliable analytical techniques to assist in the design of these structures.

1.2 REVIEW OF PAST WORKS

The various methods of lateral load analysis which have been proposed for different structural systems will be reviewed herein in order to provide an overview of the state of art in lateral load analysis:

(1) Moment-Resisting Frame System

Before the advent of the digital computer, the analysis and design of frame-type structures in the design office depended on approximate hand methods. The portal frame method and the cantilever method are among the first of these methods and have been widely used. Other methods involve replacing the multi-bay frame with a single-bay equivalent frame [39] or with a column subjected to rotational constraints at floor levels [22]. Chan [7] has presented a hand method for the analysis of multi-storey, multi-bay frames. Axial deformations of all columns are considered in the analysis.

With the availability of digital computers, an exact analysis based on matrix methods [50] of plane frame and three-dimensional frame structures is possible, and many plane frame and space frame programs with various capabilities have since been developed. The use of a space frame program in general requires enormous computer storage and

is costly. In this connexion, Weaver and Nelson [81] developed a stiffness matrix method of analysis for three-dimensional frame structures in which the number of degrees of freedom for the total structure is reduced by assuming the floor slabs to act as rigid diaphragms, so that each floor undergoes three rigid-body displacements, namely, two horizontal displacements and one rotation about a vertical axis, while each joint has three degrees of freedom, namely, one vertical displacement and two rotations about two perpendicular horizontal axes.

(2) Shear Wall System

The shear wall system has been shown to be an efficient lateral load system for buildings reaching up to about 250 feet. Since the 1960's, considerable research work has been carried out to develop efficient techniques for the analysis of shear wall structures of various configurations. These techniques include the stiffness matrix method and its analogies, the finite element method [85], finite difference methods, and various methods which are based upon the concept of treating the structure as a continuous body by replacing the horizontal stiffening elements such as lintel beams with continuous media.

By the stiffness matrix method, a plane shear wall is replaced by an equivalent column to which rigid arms are

attached at floor levels to simulate the effect of wall width. Thus, planar coupled shear walls have been modelled as an equivalent frame [63] and accordingly analysed as such using a standard plane frame program. However, this approach will result in a need for substantial computer storage. Stafford Smith [68] proposed a modified beam method for symmetrical planar coupled shear walls. By this method, the effect of wall width is accounted for by modifying the properties of the connecting beams so that no dummy rigid arms are required. Others [27, 28] have attempted to account for the effect of wall width on the adjoining beams by directly modifying the element stiffness matrices of these beams. Jenkins and Harrison [33] applied the stiffness matrix method to analyse plane shear wall assemblies by developing special element stiffness matrices. Heidebrecht and Swift [31] presented a method based on the stiffness matrix approach for the analysis of asymmetrical coupled shear walls. Applying Vlasov's thin-walled beam theory [80], an additional degree of freedom for warping is introduced for each open-section wall element in deriving its element stiffness matrix. Connecting beams are assumed to be connected to the shear center of the associated wall section. The element stiffness matrices for individual wall elements and beams on a given floor are assembled to form the corresponding storey stiffness matrix. The stiffness

matrix of the whole structure is then obtained by superimposing these storey stiffness matrices.

The finite element method has been used to analyse planar shear wall structures [37, 46]. By the method, a plane wall is divided into a mesh of tiny elements of some geometric shape. Appropriate shape functions defining the mode of deformation of the typical element are prescribed so that compatibility and continuity in deformation along inter-elemental boundaries are maintained. Subsequent solution procedures are analogous to those of the stiffness matrix method. However, the feasibility of applying the finite element method to three-dimensional shear wall structures is all but minimal because of the enormous computer capacity and computing time that will be required, and the immense work involved in the process of data preparation.

A finite difference method has been proposed by Elkholy [21] for the analysis of plane coupled shear walls. In this method, a set of simultaneous equations are derived based on equilibrium and compatibility conditions. Variations in dimensional properties along the height of the structure and in the number of wall piers are allowed.

An abundance of analytical methods, or continuum methods as they are usually referred to, in which the discrete connections between shear walls are replaced by continuous laminae of equivalent structural properties, have

been proposed by various researchers. In all these methods, rigid diaphragm action of the floor system and constant structure height are assumed. Equilibrium conditions, and compatibility and/or continuity conditions at the midspan of the continuous connecting laminae are observed, thereby resulting in a set of governing differential equations. Solutions to these differential equations subject to appropriate boundary conditions are then sought.

The continuum approach was first applied to a planar uniform coupled shear wall by Beck [2]. Similar analyses were also presented by Rosman [56, 57], and Coull and Choudhurry [13, 14]. Stepwise changes in structural and dimensional properties along the height of the structure [15, 18, 49, 72, 78], various foundation effects [10, 11, 73, 77], inelastic behaviour [48, 84], effects of local wall deformation [43], unequal wall sections [38], and multi-bays [32] have also been considered. The effective width [79] and the bending stiffness [51] of floor slabs connecting shear walls have also been studied. Coull and Irwin [16] proposed a method of analysis for three-dimensional shear wall structures that are comprised of uniform single or coupled shear walls arranged in parallel planes. The basic approach of the method is analogous to that of the stiffness matrix method of analysis. A flexibility matrix with respect to lateral deflection is determined by an appropriate continuum

method for each planar shear wall assembly, and is inverted to obtain the corresponding stiffness matrix. The stiffness matrix of the overall structure can thus be obtained by superimposing those of the shear wall assemblies. After solving for the displacements of the overall structure, loads are distributed to each shear wall assembly.

Continuum analyses of shear wall systems with non-planar wall sections, based on Vlasov's thin-walled beam theory [80], have been proposed by various researchers. A torsional analysis of open-section shear walls has been presented by Heidebrecht and Stafford Smith [30], while the torsional behaviour of core-wall structures has been studied by Michael [44], Rosman [58], and Tso and Biswas [74,75]. The last two authors have also presented an analysis of two non-planar uniform shear walls of variable cross-section coupled by a row of connecting beams [76]. Gluck and Gellert [23] presented an analysis of a general three-dimensional uniform coupled shear wall system. A more comprehensive analysis allowing for stepwise changes in structural properties along the height of the structure was proposed by Biswas [4].

(3) Wall-Frame System

The wall-frame system consists of two major components, namely, the shear wall and the frame, which are distinct from each other in structural behaviour under lateral loads.

Various methods of analysis including iteration methods, finite difference methods, the stiffness matrix method and its analogies, the finite element method, and continuum methods have been proposed. Rosenblueth and Holtz [54] proposed an iterative procedure for the analysis of a planar shear wall-frame system which consists of a single shear wall connected to rigid frames. By the method, it is assumed that contraflexural points in the columns and girders occur at midspans, that the frame shear in a given storey is proportional to the average slope in that storey, and that the shear forces and moments in the beams connected to the wall are proportional to the flexural slope of the wall. In deriving the frame stiffness, axial effects of the columns are neglected. The method requires an initial estimation of the shear distribution in the wall. From this the wall moment and the slope of the deflected wall are found, thereby leading to a new estimate of the wall shear. Convergence is accelerated by an extrapolation procedure. Two methods were developed in the analysis to obtain a rapid first approximation of the wall shear. Axial effects in the wall due to shear forces in the connecting beams are neglected. Cardan [6] used a similar approach and considered the shear wall as being subjected to continuous distributions of external loads and of reactions from parallel frames connected to the wall. Constant dimensional properties and midspan con-

tra[redacted]exural points in the columns and beams, except those beams that are connected to the wall, are assumed. Shears taken by frames are assumed to be proportional to the slope of deflection of the wall. Axial effects of columns and the wall are neglected. A second order differential equation with the slope of the wall as the unknown is obtained. An iteration method has been proposed by Khan and Sbarounis [36], in which a planar shear wall-frame system is treated as consisting of a wall system and a frame system. Initially, the wall is assumed to take all the external loads and its resulting deflected shape is computed. Forcing the frame system to assume this deflected shape, the moments throughout the frame are computed, either by moment distribution or by an iterative modified slope-deflection procedure. From these member moments, the total shear in each storey of the frame, and the moments and forces applied on the wall by the wall-frame connecting members are determined. Subjecting the wall to the combined action of the external loads and this set of interacting moments and forces, a new deflected shape is computed for the wall. The entire process is then repeated until the deflected shape of the wall attains the required accuracy. The moments and forces in all members can then be computed based on the final deflected shape of the overall system. The analysis can include shear deformation of the wall, axial deforma-

tions of the columns, plastic hinge formation in the wall, rotation of the foundation, and variation of structural properties with height. Influence curves have been presented as a design aid. Gould [26] treated the planar shear wall-frame system as a cantilever beam supported at floor levels by a system of translational and rotation springs. Finite difference techniques are used to solve the fourth order beam equation, thereby giving the wall deflection at each floor level. The unknown spring forces and moments can thus be computed. The shear wall is then analysed as a cantilever beam subjected to these spring reactions. Rosman [57] analysed the shear wall-frame structure as a combination of a flexural beam and a shear beam tied together by pin-ended inextensible links. The shear stiffness of the shear beam, which represents the frame, is derived on the assumption of midspan contraflexural points in the columns and girders in the frame and of negligible axial deformations in the columns. With the use of an energy approach the analysis results in a second order differential equation with the wall moment as the unknown. Parme [47] presented an analysis which consists of relating the total load at each floor level of the planar shear wall-frame structure to the displacements of that floor and the two floors above and below. Thus, at each level an equation is set up in terms of the relative stiffnesses of the columns, girders

and shear wall, and the applied loading. This leads to a number of simultaneous equations equal to the number of floors. Axial deformations in the columns and the effect of wall rotation on the girder moments are neglected. Goyal and Sharma [27] presented a matrix analysis of the planar shear wall-frame structure by replacing the wall with an equivalent column and incorporating the wall width effect into the element stiffness matrix of the adjoining beams. Grundy and Wathen [28] presented a similar analysis but included stability effects. Oakberg and Weaver [46] and others applied the finite element method by dividing the plane wall into a mesh of small plate elements. Macleod [40] proposed a simple hand method by which the wall and the frame are assumed to be linked together at the top only, thereby implying constant shear in the frame. A simple equation presented by the same author [39] is used to determine the frame stiffness. Heidebrecht and Stafford Smith [29] adopted the concept of the flexural-shear system and derived a fourth order differential equation with the lateral deflection of the structure as the unknown. The wall-frame connections are assumed to be pin-ended. Design curves for three common types of loading conditions have been presented. The analysis has also been extended for the dynamic analysis of uniform shear wall-frame structure and to include stepwise changes in structural properties along the height of

the structure.

Analytical methods have also been proposed for three-dimensional wall-frame structures. Clough, King, and Wilson [9] presented a modified stiffness matrix method for the analysis of a building structure which is comprised of parallel frames and shear walls. The latter are replaced by equivalent columns with rigid arms at floor levels. Rigid diaphragm action of the floor system and a symmetric distribution of stiffness are assumed so that each parallel frame is subjected to the same lateral deflection at any floor level. A tri-diagonal stiffness matrix is developed for each frame, and is reduced by recursion relationships to the corresponding lateral frame stiffness. The lateral stiffness of the complete building is then obtained by superimposing all lateral frame stiffnesses. Webster [82] presented another modified stiffness matrix method for an asymmetric structure consisting of parallel frames and shear walls. The latter are replaced by equivalent columns while the effect of wall width is incorporated into the element stiffness matrices of the adjoining connecting beams. Effects of resisting elements normal to the load direction are neglected. The method consists of the construction of a stiffness matrix for each parallel frame in the structure, and its subsequent reduction by matrix partitioning methods to the corresponding lateral stiffness matrix. By considering the lateral and

rotational equilibrium of the building in translating and rotating as a rigid body, a matrix equation is obtained. Solving this equation gives the lateral and rotational displacements of the structure and subsequently the loads in each parallel frame. Winokur and Gluck [83] presented a method which is conceptually analogous to the approach of the stiffness matrix method. The structure is divided into its major resisting elements, which can be frames or shear walls. Lateral stiffness matrices are derived for individual elements. Assuming the floor slabs to act as rigid diaphragms, equilibrium equations for the overall structure are formulated. These when solved yield the translational displacements and rotations of the overall structure. Loads can subsequently be distributed to the resisting components. In the analysis, axial deformations of columns and walls, and coupling between walls or between walls and frames are neglected. Goldberg [25] presented an analysis for panel-type buildings taking into account the deformation of floor slabs in their own planes. Axial strains of columns are neglected. The analysis is based upon the slope-deflection theory and a Timoshenko beam analogy. A matrix equation is set up for each floor of the structure based on the equilibrium conditions at the various wall-floor intersections and beam-column joints. A process of matrix substitution and elimination is carried out to obtain the displacement

vector for the lowest floor level. Displacements at higher levels are then computed by back-substitution. Internal moments and shears are subsequently computed for all columns, walls, and floor panels from the displacements. Majid and Croxton [41] proposed an analysis for building structures consisting of a grillage system of parallel floor slabs and shear walls, and parallel skeletal frames. Asymmetric arrangements of the parallel frames and walls are permitted. The deformation of the slabs in their own planes is considered. The stiffness matrix method is used to construct influence coefficients for the frames and the grillage. These coefficients are then used in conjunction with a force method to satisfy compatibility conditions at the junctions of the structure and its overall equilibrium. Applying the concept of the stiffness matrix method, Stomato and Stafford Smith [71] have presented an analysis of a three-dimensional structure which is comprised of a network of arbitrarily oriented planar resisting panels. Each panel may consist of a frame, shear walls, or a combination of the two, is assumed to have only in-plane stiffness and no torsional stiffness, and is assigned one degree of freedom for in-plane translational displacement. Its in-plane stiffness matrix and behaviour with respect to distribution of loads within itself are assumed to have been known. At those intersections where two panels meet, it is assumed that only vertical forces act,

and a third degree of freedom for vertical displacement is assigned for each of the planels. Rigid diaphragm action of the floor system is assumed. Subsequent solution procedures are analogous to those of the stiffness matrix method. A method based on energy considerations has been presented by Chriss [8] for analysing structures which consist of shear walls and frames linked together by floor slabs that are assumed to act as rigid diaphragms but are flexible out of plane. The shear walls are assumed to have biaxial bending stiffness and torsional stiffness, while the frames are assumed to have in-plane stiffness by frame action and out-of-plane stiffness by cantilever action of the columns. The minimum total potential theorem is applied, resulting in an equation which when solved yields the two translational displacements and the rotational displacement at each floor of the overall structure. In the analysis, coupling between walls and between walls and frames is neglected. Stomato and Mancini [70] proposed a continuum analysis for a three-dimensional structure consisting of uncoupled walls and frames. Rigid diaphragm action of the floor system is assumed. The frames are replaced by shear beams. The torsional characteristics of open-section walls are included. Rutenberg and Heidebrecht [60] presented a similar analysis but considered only plane shear walls.

(4) Tube System

The tube system is an efficient structural system for very tall buildings. It consists of the framed-tube system, the tube-in-tube system, and the rigid-tube system.

The framed-tube system is essentially a tubular structure comprised of closely spaced columns interconnected by stiff spandrel beams. Its behaviour consists of cantilever action as a tube and shearing action in the parallel frames. Khan and Navinchandra [35] proposed a method in which the parallel frames are assumed to be resisting the total external shear while the tube action is accounted for by considering the tube as consisting of two channels whose webs are formed from the parallel frames. Coull and Subedi [19] proposed a method in which the structure is replaced by an equivalent plane frame so that it can be analysed by a plane frame program. An approximate shear wall-frame analysis [29] can also be used to analyse framed-tube structures by treating the parallel frames as shear beams and the normal frames as flexural beams. Chan [7] presented an analysis based on an energy approach. The method includes the out-of-plane bending of the columns in the normal frames and results in three coupled differential equations. The number of differential equations can be reduced to one by neglecting the out-of-plane bending of the columns. Coull and Bose [12] replaced the framed-tube structure by an equiva-

lent orthotropic tube and made simplifying assumptions regarding stress distribution in the equivalent tube. Moreover, an exact analysis using space frame programs is also possible.

The tube-in-tube structure is a hybrid structure formed of the framed-tube system and the shear wall system linked together by floor slabs. Therefore it can be analysed approximately as a shear beam linked to a flexural beam [29]. Coull and Subedi [20] proposed a method in which flexibility matrices are obtained for the outer framed-tube and the inner shear wall structure using appropriate established methods. The corresponding stiffness matrices are then determined by inverting these flexibility matrices. By superimposing the stiffness matrices, the total stiffness matrix for the overall structure is obtained. The overall deformation of the structure can then be solved for, after which loads are distributed between the inner and the outer tubes.

The rigid-tube system is basically an improved version of the tube-in-tube system with the shear walls spanning across the full width and length of the framed-tube. Thus it may be approximately analysed as a shear wall-frame system as in the case of the tube-in-tube system.

The analytical methods reviewed above can be classi-

fied under two basic categories, each of which is founded on a characteristic approach. The two distinct approaches are in general referred to as the discrete approach and the continuum approach.

The basic concept of the discrete approach, of which the matrix methods and the finite element method are representative, consists of dividing the structure in question into a finite number of small and interconnected elements, and defining the behaviour of the overall structure as the resultant of the interaction among the constituent elements and expressing it in terms of the displacements or forces at the joints where two or more elements meet or where an element is bounded by an external medium. The small constituent element can be an individual line element such as columns and beams, as in the case of the matrix methods of analysis, or it can be a small well-defined region within a structural member, as in the case of the finite element method. Thus the theoretical accuracy of the approach is in general dependent upon an accurate understanding of the behaviour of the respective typical element when subjected to external loads. As far as building structures are concerned, while the finite element method is called for only in more refined analyses, the stiffness matrix method – in contrast to the flexibility matrix method – has almost become the standard analytical technique. Within the limits of its

basic assumption, that all members are line elements, the stiffness matrix method will provide exact results, this being solely due to the well-established understanding of the behaviour of such line members based on the classical beam theory. The method also provides both versatility and flexibility in that it imposes no restrictions regarding the variation of structural properties in, and the configuration of the structure concerned. As has been mentioned previously on several occasions, however, the method does have several limitations. Firstly, without modification, the method is limited to structures which can be reasonably approximated by an assembly of line elements, as in the case of frame type structures. It is immediately evident that the method will encounter difficulty in dealing with non-planar shear wall sections, though not so much with the planar counterpart where the equivalent column analogy can be applied directly. In fact, in analysing general three-dimensional shear wall structures, the method may be found to be inconvenient and inefficient in regard to data preparation and computing time, respectively, if not entirely inapplicable. Secondly, owing to the large number of variables contributed by the numerous "small elements" normally present in a high-rise building, the method invariably requires fast and large-capacity computers. Thirdly, round-off errors accumulated over numerous mathematical operations

may undermine the accuracy of the method. Last but not least, the method does not provide a meaningful physical interpretation of the behaviour of the structure as an integrated system, and much less a visualisation of the interaction among the various structural components that make up the structure.

In the continuum approach, the structure under consideration is envisioned as comprising one or more media continuous throughout the height of the structure and possessing certain equivalent structural properties. The approach is essentially based upon a well-defined mathematical model of the structure, and invariably involves the use of differential equations. The behaviour of the model is described by a relatively small number of critical parameters, and force and displacement variables which are inter-related. Thus, the interaction among these parameters and variables, and their effects on the behaviour of the structure can be visualised readily.

The accuracy of a continuum analysis basically depends on how well the mathematical model contains the actual behaviour of the structure, and also on how well the assumptions on which the analysis is based are satisfied by the actual problem being considered. The approach has been shown best suited to the analysis of high-rise shear wall struc-

tures, wherein the walls do qualify as continuous media while the horizontal stiffening elements, contributed by floor slabs or lintel beams, can reasonably be replaced by continuous media of equivalent structural properties. While the approach has been applied primarily to shear wall problems, its performance in the analysis of framed-tube structures [12] and shear wall-frame structures [29, 60, 70] has also been found to be adequate.

In the light of the weakness of conventional matrix methods and the finite element method in dealing with general shear wall structures, the advantages of applying continuum methods to these structures, in such capacities as efficiency, convenience in data preparation, accuracy, and computer resource requirements, are obvious. Notwithstanding, a continuum analysis by itself in general does suffer several drawbacks, which are:

(1) Structural properties are assumed to be constant throughout the entire height of the structure.

(2) The structure must be continuous up to the very top so that no variation of structure height across its plan is allowed.

(3) Such an analysis usually lacks generality in that it can only be applied to structures which fit the particular physical model for which the analysis is intended.

Of these drawbacks, the first can be relieved by the use of the transfer matrix technique, thereby allowing stepwise structural changes along the height of the structure, while the others have limited the general application of continuum analyses.

1.3 SCOPE OF THESIS

A general review of research work in the lateral load analysis of high-rise building structures carried out in the past couple of decades has been presented. The general advantages and disadvantages of the two major categories of analytical methods which have resulted from these years of research efforts, namely, the discrete methods and the continuum methods, have also been discussed.

The scope of the present thesis thereby consists of two parts:

The first part consists in the investigation of the problem of wall-frame interaction in two-dimensional and three-dimensional wall-frame structural systems, taking into account the effect of vertical interaction between the shear wall and the frame.

The second part of the thesis is to address some of the difficulties that may likely arise in analysing a general building structure using currently available discrete and continuum methods. It consists in presenting a viable, flexible, and versatile technique for the lateral load analysis of a general building structure. By this method, a general building structure is envisioned as consisting of a combination of substructures each of which constitutes an independent analytical system by itself and thereby pertains to a

specific analytical method. Basically, the method puts together a broad spectrum of distinct analytical techniques, whether discrete, continuum, or experimental, to meet with diverse analytical needs.

In the following chapters, the response of a uniform planar wall-frame structure to lateral loads will be investigated in Chapter II, while the effect of stepwise structural changes along the height of the structure will be considered in Chapter III. An analysis of a general three-dimensional uniform wall-frame structure will be presented in Chapter IV, and that of the non-uniform counterpart in Chapter V. A more general three-dimensional analysis of an arbitrary building structure will be presented in Chapter VI. The free-vibration dynamic response of a three-dimensional building structure will be studied in Chapter VII. A model study on the dynamic response of an actual building, namely, the Banco de America Building, will also be presented. Finally, a summary of the more important findings regarding wall-frame interaction will be provided in Chapter VIII.

CHAPTER II

UNIFORM PLANAR WALL-FRAME STRUCTURES

2.1 INTRODUCTION

The wall-frame structure is widely used in buildings comprising twenty to forty storeys in height. Architecturally, the frame allows open space for commercial purposes while the shear wall can serve as enclosures for service cores and as partitions. Structurally, the structure acts as both a lateral load-resisting system and a gravity load-bearing system. In regard to its capacity as a lateral load-resisting system, the wall-frame structure is a complex structure in which two distinct structure types are tied together and interact to resist external loads.

When subjected to lateral loads, a plane shear wall behaves primarily as a flexural cantilever, and consequently develops a deflected shape that is convex to the initial undeformed position as shown in Figure 2-1. A frame is a discontinuous and jointed structure comprising an assembly of beam and column members. When subjected to lateral loads, it develops moments, shears, and axial forces in its beam and column members to resist the shearing and overturning

effects of the external loads. Thus, the lateral deflection of a frame consists of two effects, namely, (i) web drift, which is mainly due to the bending deformation of the beams and columns, and (ii) chord drift, which is due to the axial deformation of the column members. Of the two effects, web drift in general predominates and gives the frame a deflected shape which is concave to the initial undeformed position as shown in Figure 2-1. The chord drift effect causes rocking of the floors, and is of significance only in relatively tall and slender frames.

As a result of these incompatible physical behaviours of the two structure types, a redistribution of loads will occur when the two are tied together by floor slabs or lintel beams and hence forced to act compatibly (Figure 2-1). In general, near the base of the system, most of the external loads are resisted by the wall component while near the top, in addition to resisting most or even all of the external loads there, the frame component often acts to restrain the wall from excessive sidesway and hence is required to take on additional loads. Owing to this interaction, the wall-frame system presents a very efficient lateral load-resisting system for relatively tall buildings because effective stiffness and deflection control are provided by the frame towards the top of the building, where the wall is relatively flexible. Moreover, in the light of this pattern of

load distribution, it is clear that the frame may sustain a considerable portion of the external shear and overturning effects. Neglecting the contribution of the frame to lateral load resistance is therefore an undue over-simplification and will possibly lead to overdesigning the wall and underdesigning the frame.

Besides providing better efficiency over the shear wall system and the moment-resisting frame system, the wall-frame system also presents an extremely promising structural system in the perspective of seismic design. The system combines both stiffness, which is mainly due to the shear wall whereby interstorey drift is reduced (and hence non-structural damage), and ductility, which can be built into the frame members at planned locations. Thus a three-stage seismic strategy is possible: energy dissipation at selected locations, such as the wall-frame connections, during the initial tremors of an earthquake, major lateral resistance due to the shear wall, and final back-up from the frame system. The frame system can further act as the ultimate gravity load support in preventing or delaying total collapse.

A number of analytical methods have been proposed for the analysis of planar wall-frame structures. These have been reviewed in Chapter I. The methods proposed by Rosenblueth and Holtz[54], and by Khan and Sbarounis[36]

involve iterative procedures and therefore cannot be condensed into a set of design charts or design equations for regular use in the design office. Gould[26] reduced a flexible wall-frame configuration to a cantilever beam supported by concentrated elastic reactions. However, the method results in a number of simultaneous equations equal to the number of floors of the structure. Thus, solution by hand is virtually impossible. Parme[47] neglected the effect of wall rotation on the wall-frame connecting beams, which may lead to a serious under-estimation of the shear forces in these beams. The method also results in a number of simultaneous equations equal to the number of floors. Although the number of unknowns in each equation is limited to five so that hand calculation is still possible with the aid of a desk calculator, design charts or equations cannot be prepared for efficient regular use. MaCleod's method[40] is simple to apply, but its accuracy is questionable. Methods by Cardan[6], Rosman[57], and Heidebrecht and Stafford Smith [29] are based upon modelling the structure as a continuous flexural-shear system so that closed form solutions are obtained and hence design charts or equations can be set up. Cardan considered moment-resisting beams between the frame and the wall but neglected the axial effects caused in the wall by the shears in these beams. The other authors assumed such beams to be pin-ended.

In this chapter, a method of analysis for a uniform planar wall-frame structure in which the wall and the frame are connected by moment-resisting beams will be presented. The method will be based on the continuum approach. The shear beam analogy will be used to account for the horizontal shearing behaviour of the frame. The effect of axial deformations in the frame columns due to the shear forces in the connecting beams will be included. The analysis allows other types of end conditions for the connecting beams to be considered. Examples will be worked out to verify the proposed analysis. Based on the results of these examples, the limitations of the proposed theory will be discussed. Finally, a parametric study of a nominal wall-frame structure will be presented.

2.2 NOTATIONS

The following notations will be used in this chapter:

A_b = effective shear area of connecting beam.

A_{ci} = cross-sectional area of column i (i=1,2,...n).

A_w = cross-sectional area of shear wall.

d_{ci} = distance of column i from centroid of frame.

d_f = equivalent moment arm of resultant couple formed by chord drift-induced axial forces in columns of frame.

E = elastic modulus.

f_c = axial effect factor for column 1 ($1.1 \leq f_c \leq 1.4$).

G = shear modulus.

GA = shear stiffness of frame as shear beam.

h, H = floor height and structure height, respectively.

I_b = moment of inertia of connecting beam section.

I_{ci} = moment of inertia of column i.

I_{gi} = moment of inertia of girder i.

I_w = moment of inertia of shear wall section.

ℓ_b = length of connecting beam.

ℓ_f, ℓ_w = distances from midspan of connecting beam to frame centroid and wall centroid, respectively.

ℓ_{gi} = length of girder i.

$M(z)$ = external overturning moment at height z.

n = number of columns in frame.

P = concentrated load at top of structure.

p = intensity of uniformly distributed load.

$\bar{p}$ = top intensity of triangularly distributed load.

$q(z)$ = beam shear intensity at height z.

$T(z)$ = axial force in wall at height z.

$T_{ci}(z)$ = axial force in column i at height caused by chord drift.

$V(z)$, V_o = external horizontal shear at height z and at base of structure, respectively.

V_f, V_w, V_b = internal horizontal shear due to frame, wall, and connecting beams, respectively.

$y(z)$ = lateral deflection of structure at height z.

z = height variable with respect to foundation of structure.

Eqn(s) = Equation(s).

2.3 STATEMENT OF PROBLEM

The elevation of a generalised uniform planar wall-frame structure is shown in Figure 2-2. The wall and the frame are connected by floor slabs or connecting beams at all floors. In the case of floor slabs acting as connections, these are replaced by connecting beams of appropriate equivalent properties. For ease of reference, the columns and the rows of girders are numbered as shown in Figure 2-2. The following assumptions are made in the analysis:

1. Rigid diaphragm action of the floor system is assumed so that the shear wall and the frame are confined to the same lateral deflection at any floor level.
2. Structure height, floor height, and the structural properties of the wall, frame, and connecting beams are constant.
3. Contraflexural points are assumed at the midspan of the connecting beams and the columns and girders of the frame.
4. For simplicity, shear deformation is neglected for the shear wall, columns, and girders.
5. The frame contains at least two columns and is assumed to be extended so that one-half of the span of the connecting beam at each floor is included as a beam member of the frame.

6. The frame is replaced by a continuous shear beam having a constant shear stiffness of GA in approximation of the horizontal shear resistance of the frame. The derivation of GA is given in Appendix A.
7. The connecting beams are assumed to be fixed-ended at both ends, and are replaced by a band of continuous laminae of equivalent structural properties throughout the entire height of the structure.
8. Elastic behaviour is assumed.
9. The foundation of the structure is assumed to be rigid.

By the assumption of rigid diaphragm action, the overall lateral deflection of the structure is governed by one single displacement function $y(z)$. By the assumption of fixed-ended connecting laminae, rotational and vertical translational constraints are imposed on the wall and the frame. These constraints result in a distribution of shear forces, denoted by $q(z)$, in the laminae. When a cut is made at the midspan of the laminae, this shear distribution will be exposed as shown in Figure 2-3. However, no moment distribution will occur at the cut because of the assumption of midspan contraflexural points in the laminae. The shear distribution will result in an axial force, denoted by $T(z)$, in the wall.

Thus there are altogether three unknown variables,

namely, y, q, and T. Therefore three equations are required in order to achieve a solution. One of these can be obtained by considering the horizontal equilibrium of the overall structure, another by considering the vertical equilibrium of the shear wall, and the third one by considering the compatibility of deformation at the midspan cut of the laminae.

2.4 FORMULATION OF ANALYSIS

2.4.1 EQUILIBRIUM CONDITIONS

2.4.1.1 Horizontal Shear Force Equilibrium

The internal horizontal resisting shear force at height z due to the shearing action of the frame is, by definition of its shear stiffness GA, given by

$$V_f(z) = GA \cdot y'(z) \qquad (2\text{-}1a)$$

The shear force in the wall due to lateral deflection is given by

$$V_w(z) = - EI_w y'''(z) \qquad (2\text{-}1b)$$

where E is the elastic modulus and I_w is the moment of inertia of the wall section.

If an imaginary cut is made along the vertical centreline of the connecting laminae, a shear distribution of intensity q(z) will be exposed as shown in Figure 2-3. By considering the moment equilibrium of an elemental section, of depth dz, of the wall with the attached laminae as shown in Figure 2-4, the horizontal shear induced in the wall by the shear distribution q(z) can be shown to be given by

$$V_b(z) = \ell_w \cdot q(z) \qquad (2\text{-}1c)$$

where ℓ_w is the distance between the wall centroid and the midspan of the connecting laminae.

It is noted that the contribution of q(z) to the shear resistance of the frame has already been taken into account by the GA term and hence need not be accounted for separately.

Thus, to maintain horizontal shear force equilibrium, there is obtained

$$V_f(z) + V_w(z) + V_b(z) = V(z)$$

or
$$-EI_w y''' + GA \cdot y' + \ell_w q = V \qquad (2\text{-}2)$$

where V(z) is the external shear at height z.

2.4.1.2 Vertical Equilibrium of Wall

By considering the vertical equilibrium of an elemental section of depth dz of the wall as shown in Figure 2-4, there is obtained

$$\frac{dT(z)}{dz} = -q(z) \qquad (2\text{-}3)$$

where T(z) is the axial force at height z in the wall.

Accordingly, T(z) is given by

$$T(z) = \int_z^H q(\bar{z})\, d\bar{z} \qquad (2\text{-}4)$$

2.4.2 COMPATIBILITY CONDITIONS

A third equation will be obtained by considering the compatibility of deformation at the midspan of the connecting laminae. Consider an imaginary cut at the midspan of the laminae whereby the beam shear distribution is exposed as shown in Figure 2-3. Points at the frame side of the cut will undergo vertical displacements relative to points at the wall side due to six effects, namely, (1) flexural deformation of the wall, (2) axial deformation of the wall due to T(z), (3) flexural and shear deformation of the laminae, (4) rotation of the joints formed by the connecting beams and column 1, (5) axial deformation of column 1 due to q(z), and (6) axial deformation of column 1 due to the chord drift effects of the frame.

Letting the vertical displacement of the point on the frame side of the cut relative to that on the wall side at height z due to the i^{th} effect mentioned above be denoted by δ_i, and referring to Figure 2-5, there is obtained:

$$\delta_1 = \ell_w y'(z) \qquad (2\text{-}5)$$

$$\delta_2 = -\frac{1}{EA_w}\int_0^z T(\bar{z})\, d\bar{z} \qquad (2\text{-}6)$$

where A_w is the cross-sectional area of the wall.

$$\delta_3 = -\frac{q(z)}{E\gamma} \qquad (2\text{-}7)$$

where γ is the connecting beam stiffness factor including the effect of shear deformation and is given by

$$\gamma = \frac{12EI_b}{\ell_b^3 h}\left(1 + \frac{12EI_b}{\ell_b^2 A_b G}\right)^{-1} \qquad (2\text{-}7a)$$

in which I_b, ℓ_b, and A_b are respectively the moment of inertia, length, and effective shear area of the discrete connecting beam.

The rotation of the joint between the connecting beam and column 1 at height z can be shown to be a function of y'(z), and is given by

$$\theta = 2\left[\, 2 + \frac{I_{g1}h}{I_{c1}\ell_{g1}} + \frac{I_b h}{I_{c1}\ell_b}\,\right]^{-1} y' \qquad (2\text{-}8)$$

where I_{c1} is the moment of inertia of column 1, while I_{g1} and ℓ_{g1} are respectively the moment of inertia and length of girder 1. A detailed derivation of θ is given in Appendix A.

Therefore, there is obtained

$$\delta_4 = \ell_e y' \qquad (2\text{-}9a)$$

where

$$\ell_e = \ell_b\left(2 + \frac{I_{g1}h}{I_{c1}\ell_{g1}} \quad \frac{I_b h}{I_{c1}\ell_b}\right)^{-1} \qquad (2\text{-}9b)$$

The effect of the beam shear distribution q(z) on the

frame can be recognised by reverting the shear beam model back to the real frame. Thus there will be a series of discrete shear forces acting at the midspan cut of the connecting beams. These discrete shear forces can be represented by a set of vertical forces of the same corresponding magnitudes and a set of moments acting at the connecting beam-column joints as shown in Figure 2-6a. The vertical forces will give rise to a direct axial force component in column 1. Owing to the restraint of the girders — considering there is at least one row of girders in the frame — This axial force will be slightly smaller than will be obtained by simple summation of the vertical forces acting at the joints. For frames of general proportions, however, the discrepancy can be taken to be negligible. Meanwhile, the moments will give rise to shear forces in the girders. These shears will in general be of significant magnitude only in the girders which are connected to columns 1 and 2 because of shear lag effects. The shears in these girders will result in axial forces in columns 1 and 2. In column 1, this second axial force effect will act in the same direction as the direct axial force component. Its magnitude depends on the relative stiffnesses of the girders and columns of the frame, and the length of the connecting beams. For frames and connecting beams of general proportions, it varies between 10 % and 40 % of the magnitude of the direct axial force compo-

-nent. Thus in order to reflect to a reasonable extent the actual axial force caused by the connecting beam shears in column 1, a factor f_c ranging between 1.1 and 1.4 is introduced. Therefore, there is obtained

$$\delta_5 = -\frac{1}{EA_{c1}} \int_0^H f_c T(\bar{z})\, d\bar{z} \qquad (2\text{-}10)$$

where A_{c1} is the cross-sectional area of column 1. Recommendations regarding the use of f_c are given in Appendix B.

Finally, axial forces are also induced in the columns because of the chord drift effects of the frame. The moment-resisting effect M_c of these axial forces about the centroid of an n-column frame (defined by the first moments of area of the constituent columns), where n is greater than 1, is given by

$$M_c = \sum_{i=1}^{n} T_{ci} d_{ci} \qquad (2\text{-}11a)$$

where d_{ci} and T_{ci} are respectively the distance from the frame centroid of and the chord drift-induced axial force in column i.

Assuming that each column deforms axially in proportion to its respective distance from the frame centroid and that all the axial forces in the columns on one side of the frame centroid act in the same direction while those on the other side act in an opposite direction (Figure 2-5(f)), it

can be shown that

$$M_c = T_{c1} d_f \qquad (2\text{-}11b)$$

where d_f is defined as the equivalent moment arm of the resultant couple due to the chord drift-induced axial forces and, for an n-column frame with n greater than 1, is given by

$$d_f = \frac{1}{d_{c1}} \sum_{i=1}^{n} d_{ci}^2 \qquad (2\text{-}11c)$$

Referring to Figure 2-6b, the moment equilibrium of the total structure about an axis normal to the plane of the structure and through the midspan of the connecting laminae at height z is expressed by the following equation:

$$EI_w y'' + T\ell_w + f_c T\frac{\ell_b}{2} - (f_c - 1)T\left(\ell_{g1} + \frac{\ell_b}{2}\right) + M_c = M(z) \qquad (2\text{-}11d)$$

where M(z) is the external overturning moment at height z.

Therefore, T_{c1} is given by

$$T_{c1} = \frac{1}{d_f}\left\{ M - EI_w y'' - T\left[\ell_w + \frac{\ell_b}{2} - (f_c - 1)\ell_{g1}\right]\right\} \qquad (2\text{-}11e)$$

Accordingly, it can be shown that

$$\delta_6 = \frac{\ell_f}{d_{c1}} \int_0^H \frac{T_{c1}}{EA_{c1}}\, d\bar{z} \qquad (2\text{-}11f)$$

where ℓ_f is the distance between the midspan of the connecting beams and the frame centroid.

Therefore, by compatibility of deformation at the cut, there is obtained

$$\delta_1 + \delta_2 + \delta_3 + \delta_4 + \delta_5 + \delta_6 = 0$$

This leads to the following compatibility equation:

$$\mu y' - \frac{q}{E\gamma} - s \int_0^z T \, d\bar{z} + \rho \int_0^z M \, d\bar{z} = 0 \qquad (2\text{-}12)$$

where $\rho = \ell_f/(d_{c1} d_f E A_{c1})$ (2-12a)

$$\mu = \ell_w + \ell_e - \rho E I_w \qquad (2\text{-}12b)$$

$$s = \bar{s} + 1/(EA_o) \qquad (2\text{-}12c)$$

with $\bar{s} = \rho [\, \ell_w + \ell_b/2 - (f_c - 1)\ell_{g1} \,]$ (2-12d)

$$\frac{1}{A_0} = 1/A_w + f_c/A_{c1} \qquad (2\text{-}12e)$$

2.4.3 DERIVATION OF FINAL DIFFERENTIAL EQUATION AND SOLUTION

Considering Eqns(2-2) and (2-12), there are altogether three unknowns, namely, $y(z)$, $q(z)$, and $T(z)$. $T(z)$ can be related to $q(z)$ by the use of Eqn(2-3). Thus,

either y(z) or q(z) will have to be eliminated in order to arrive at the final differential equation. In the following, it is attempted to eliminate y(z).

Re-arranging Eqn(2-12), there is obtained

$$y' = \frac{1}{\mu}\left(\frac{q}{E\gamma} + s\int_0^z T\,d\bar{z} - \rho\int_0^z M\,d\bar{z}\right) \qquad (2\text{-}13)$$

Differentiating Eqn(2-13) twice leads to the following equations:

$$y'' = \frac{1}{\mu}\left(\frac{q'}{E\gamma} + s\,T - \rho\,M\right) \qquad (2\text{-}14)$$

$$y''' = \frac{1}{\mu}\left(\frac{q''}{E\gamma} + s\,T' - \rho\,M'\right) \qquad (2\text{-}15)$$

Making use of Eqn(2-3) and the relationship $V = -M'$, there is obtained from Eqn(2-15)

$$y''' = \frac{1}{\mu}\left(\frac{q''}{E\gamma} - s\,q + \rho\,V\right) \qquad (2\text{-}16)$$

By further differentiations of Eqn(2-16), there is obtained:

$$y^{iv} = \frac{1}{\mu}\left(\frac{q'''}{E\gamma} - s\,q' + \rho\,V'\right) \qquad (2\text{-}17)$$

$$y^{v} = \frac{1}{\mu}\left(\frac{q^{iv}}{E\gamma} - s\,q'' + \rho\,V''\right) \qquad (2\text{-}18)$$

From Eqn(2-2), the following two equations can be obtained by differentiation:

$$- EI_w y^{iv} + GA\, y'' + \ell_w q' = V' \qquad (2\text{-}19)$$

$$- EI_w y^{v} + GA\, y''' + \ell_w q'' = V'' \qquad (2\text{-}20)$$

Finally, it can be shown that by substituting Eqns(2-16) and (2-18) into Eqn(2-20) and collecting like terms, the following differential equation is obtained:

$$q^{iv} - \beta\, q'' + \phi\, q = - \psi\, V'' + \zeta\, V \qquad (2\text{-}21)$$

where

$$\beta = \frac{\ell_w \mu \gamma}{I_w} + s\, E\, \gamma + \frac{GA}{EI_w} \qquad (2\text{-}21a)$$

$$\phi = \frac{GA}{EI_w} \cdot s\, E\, \gamma \qquad (2\text{-}21b)$$

$$\psi = \left(\frac{\mu}{EI_w} + \rho \right) \cdot E\gamma \qquad (2\text{-}21c)$$

$$\zeta = \frac{GA}{EI_w} \cdot \rho \cdot E\gamma \qquad (2\text{-}21d)$$

The complete solution to Eqn(2-21) consists of a complementary function, q_H, and a particular integral, q_p. It can be shown that for all structures

$$\beta^2 > 4\phi \qquad (2\text{-}22)$$

so that the complementary function is given by

$$q_H = C_1\cosh(m_1 z) + C_2\sinh(m_1 z) + C_3\cosh(m_2 z) + C_4\sinh(m_2 z) \qquad (2\text{-}23)$$

where $$m_1 = \frac{1}{\sqrt{2}}[\,\beta + \sqrt{(\beta^2-4\phi)}\,]^{1/2} \qquad (2\text{-}23a)$$

$$m_2 = \frac{1}{\sqrt{2}}[\,\beta - \sqrt{(\beta^2-4\phi)}\,]^{1/2} \qquad (2\text{-}23b)$$

and C_1, C_2, C_3, and C_4 are constants to be determined by considerations of boundary conditions.

The particular integral, q_p, depends on the actual loading conditions. Considering a combination of the following three loading cases:

(a) a concentrated load P at the top,

(b) a uniformly distributed load of intensity p throughout the entire height of the structure,

(c) a triangularly distributed load of intensity $\bar{p}$ at the top and zero intensity at the base,

the particular integral can be shown to be given by

$$q_p = \frac{\zeta}{\phi}\{\,P + p(H-z) + \frac{\bar{p}}{H}[\,\frac{\psi}{\zeta} - \frac{\beta}{\phi} + \frac{1}{2}(\,H^2 - z^2\,)\,]\,\} \qquad (2\text{-}24)$$

Thus the complete solution to Eqn(2-21) subject to the above-mentioned load combination is given by

$$q = q_H + q_P \qquad (2\text{-}25)$$

with q_H and q_P given by Eqns(2-23) and (2-24) respectively.

The four constants in Eqn(2-23), namely, C_1, C_2, C_3, and C_4, are to be determined from the following boundary conditions:

(a) As a geometric condition, the slope of the deflection curve is zero at the base. Thus,

$$y'|_{z=0} = 0 \qquad (2\text{-}26)$$

Therefore, from Eqn(2-12), there is obtained

$$q|_{z=0} = 0 \qquad (2\text{-}27)$$

(b) Axial force and wall moment vanish at the top. Thus,

$$y''|_{z=H} = 0 \qquad (2\text{-}28)$$

$$T|_{z=H} = 0 \qquad (2\text{-}29)$$

Therefore, from Eqn(2-14), there can be obtained

$$q'_{z=H} = 0 \qquad (2\text{-}30)$$

(c) Making use of Eqns(2-26) and (2-27), there is obtained from Eqn(2-2):

$$- EI_w y'''|_{z=0} = V_o \qquad (2\text{-}31)$$

or $$y'''|_{z=0} = - V_o/(EI_w) \qquad (2\text{-}32)$$

where V_o is the total external base shear and is given by

$$V_o = P + pH + \bar{p}H/2 \qquad (2\text{-}33)$$

Substituting Eqns(2-27) and (2-32) into Eqn(2-16), there is obtained

$$q''|_{z=0} = - \psi V_o \qquad (2\text{-}34)$$

(d) Applying Eqns(2-28) and (2-30) to Eqn(2-19), there is obtained

$$y^{iv}|_{z=H} = - V'/(EI_w)|_{z=H} \qquad (2\text{-}35)$$

Substituting Eqns(2-30) and (2-35) into Eqn(2-17), there is obtained

$$q'''|_{z=H} = - \psi V'|_{z=H} \qquad (2\text{-}36)$$

Since

$$V'|_{z=H} = - (p+\bar{p}) \qquad (2\text{-}37)$$

therefore, Eqn(2-36) becomes

$$q'''|_{z=H} = \psi (p + \bar{p}) \qquad (2\text{-}38)$$

Applying Eqn(2-25) to Eqns(2-27), (2-30), (2-34), and (2-38) leads to a system of four simultaneous equations from which the constants C_1, C_2, C_3, and C_4, can be determined. The axial force in the wall, T, can then be obtained from Eqn(2-4), and other quantities such as wall moment, wall shear, and frame shear through Eqns(2-13) to (2-15). The lateral deflection of the structure can be found by integrating Eqn(2-13).

2.5 CONSIDERATION OF OTHER CONNECTING BEAM END CONDITIONS

The foregoing analysis assumes fixities at both ends of the connecting beam. However, it can be modified to accomodate the following different end conditions (Figure 2-7):

(1) Pin at Wall and Fixity at Frame (Pin-Fix)

In the proposed analysis, the contraflexural point in the connecting beam is assumed to be located at the midspan. In contrast, this particular case of pin (wall)-fix (frame) configuration amounts to assuming the contraflexural point to be located at the wall-beam joint. Thus, for the frame, the connecting beam is in effect replaced by another beam of twice the true length so that the shear stiffness of column 1 is now given by

$$GA_1 = \frac{12EI_{c1}}{h^2}\left[\,1 + \frac{2I_{c1}}{h\left(I_{g1}/\ell_{g1} + I_b/2\ell_b\right)}\right]^{-1} \qquad (2\text{-}39)$$

For the wall, ℓ_w is now the distance between the wall centroid and the wall-beam joint. Moreover, the new beam stiffness factor including shear deformation can be shown to be

$$\gamma_{pf} = \frac{3I_b}{\ell_b^3 h}\left[\,1 + \frac{3EI_b}{\ell_b^2 A_b G}\,\right]^{-1} \qquad (2\text{-}40)$$

(2) Fixity at Wall and Pin at Frame (Fix-Pin)

Following a similar line of argument to that given in (1) above, the contraflexural point in the connecting beam is now located at the connecting beam-column joint. Thus the shear stiffness of column 1 is given by

$$GA_1 = \frac{12EI_{c1}}{h^2}\left[1 + \frac{2I_{c1}}{h(I_{g1}/\ell_{g1})}\right]^{-1} \qquad (2\text{-}41)$$

ℓ_w is then given by the distance between the wall centroid and column 1 of the frame. The new connecting beam stiffness factor is given by

$$\gamma_{fp} = \gamma_{pf} \qquad (2\text{-}42)$$

(3) Pins at Both Ends of Connecting Beam (Pin-Pin)

The proposed analysis can be suited to this particular configuration by simply assuming a very flexible connecting beam. As γ tends to zero, q goes to zero so that Eqn(2-2) becomes

$$-EI_w y''' + GA\, y' = V \qquad (2\text{-}43)$$

It is noted this equation is similar to that used in Heidebrecht's analysis[29], where the connecting beams are assumed to be hinged at both ends.

2.6 EXAMPLES AND DISCUSSION OF RESULTS

2.6.1 VERIFICATION OF PROPOSED ANALYSIS

Three example structures have been solved using the proposed analysis. The three structures are similar in configuration and dimensional properties except for the number of storeys: one consists of ten storeys, another twenty storeys, and the third thirty storeys. For ease of reference, the three cases are labelled E-10, E-20, and E-30 respectively. Their common dimensional properties are given in Table 2-1. In each case, the connecting beams are assumed to be fixed-ended, and a uniformly distributed lateral load of intensity 22kN/m (1.5K/ft) is applied. In order to minimise the influence of the empirical factor f_c on the results given by the proposed theory, the appropriate value of f_c for each case has been determined by analysing the respective frame using SAP-IV [62]. For each frame, f_c has been found to be about 1.2 in the intermediate storeys. Thus f_c is set at 1.2 for all three example structures.

The results of lateral deflection, connecting beam shear, interstorey shear in the wall, and wall moment are shown in Figures 2-8a through 2-8d for the 10-storey example (Case E-10), in Figures 2-9a through 2-9d for the 20-storey example (Case E-20), and in Figures 2-10a through 2-10d for the 30-storey example (Case E-30). The three examples have also been solved using SAP-IV and the corresponding results

presented in the respective figures for comparison. In using SAP-IV, the wall is replaced by an equivalent column with rigid arms attached at floor levels to simulate the effect of the finite wall width.

In order to evaluate the general effects of fixed-ended connecting beams on the behaviour of wall-frame systems, the 20-storey structure of Case E-20 has also been solved with pin-ended connecting beams. The results for lateral deflection, interstorey wall shear, and wall moment for this case — labelled E-20P — are presented in the same figures as for Case E-20 for comparison. The corresponding results given by SAP-IV are also shown.

For each of the four cases, lateral deflections have been normalised relative to the top deflection $(y_c)_t$ of the respective cantilever wall subjected to the same loading alone, and wall moments relative to the respective external base moment M_o. Thus, the general advantages of wall-frame systems over shear wall systems in controlling building sway and in reducing moment loads in the wall can be immediately inferred from these results (Figures 2-8a and 2-8d, Figures 2-9a and 2-9d, and Figures 2-10a and 2-10d).

Considering the results for Cases E-10, E-20, and

E-30, the following observations can be made:

(1) In regard to lateral deflection, the result for Case E-10 is slightly overestimated by the proposed analysis while those for Case E-20 and E-30 are under-estimated. This can be accounted for by two facts: (a) In the shear beam representation of the frame, the value of the GA term adopted pertains to an intermediate storey of the frame so that the average shear stiffness of the frame tends to be under-estimated (Appendix A), and (b) chord drift effects are neglected in evaluating the GA term so that — not considering the under-estimation mentioned in (a) — the actual stiffness of the frame tends to be over-estimated. These facts imply that with a relatively short frame such as the one in Case E-10, in which chord drift is relatively insignificant, the structure deflection will tend to be over-estimated, whereas with a relatively tall and slender frame such as those in Cases E-20 and E-30, in which chord drift becomes significant, the structure deflection will tend to be under-estimated.

(2) For all three cases, the wall shears at the base are over-estimated by the proposed analysis. This is due to the prescribed geometric condition of zero slope

at the base, which implies that the frame does not take any horizontal shear at the base so that all of the external base shear will be taken up by the wall. Moreover, the maximum connecting beam shear is overestimated in these examples.

(3) Neglecting chord drift effects in evaluating the GA term implies that the general accuracy of the proposed theory may tend to decline with taller and slenderer frames. Hence, while close agreement is generally observed in all three cases, larger discrepancies are found in the results of the 30-storey structure of Case E-30, especially in the lateral deflection for which a 20% discrepancy relative to the corresponding result given by SAP-IV is observed at the top. However, the accuracies of such parameters as connecting beam shear, wall shear (and hence frame shear), and wall moment are found to be generally adequate.

Comparing the results of lateral deflection, wall shear and wall moment for Cases E-20 and E-20P (Figure 2-9a, 2-9c, and 2-9d), the following observations can be made:

(1) The fixed-ended beams considerably improve the efficiency of the overall structure with respect to structure deflection, and reduce the moment load in the

wall. Moreover, interstorey shear in the wall is increased, thereby implying a corresponding decrease in interstorey shear in the frame.

(2) In terms of comparative accuracy relative to the results of SAP-IV, Case E-20 (with fixed-ended connecting beams) fares better than Case E-20P (with pin-ended connecting beams). This observation can be explained as follows: chord drift effects are included in formulating the compatibility equation and are related to the shears in the connecting beams. Thus, these effects will be effectively considered or "activated" only if there is relatively strong coupling between the wall and the frame, such being the case when the connecting beams are fixed-ended.

In the light of the results of the examples presented above, it can be said that the proposed analysis tends to under-estimate lateral deflections and over-estimate interstorey wall shears near the base, and that its accuracy with the lateral deflection parameter is much more sensitive to the height of the structure than with other parameters. It has also been found that changes in the value of f_c within the suggested range induce changes of the order of only one or two percent in the general results of the worked examples. Experience based on these and other worked examples tends

to show that when

$$\bar{\alpha} = \sqrt{(\kappa GA/EI_w)} \cdot H < 6 \qquad (2\text{-}44)$$

and when the effective stiffness of the connecting beam section is of the same order of magnitude as that of the average girder section in the frame, the error bounds of the proposed theory for top defection, maximum beam shear, interstorey wall shear at the base, and wall moment at the base relative to the corresponding results of an "exact" analysis by matrix methods are approximately - 20%, + 5%, + 10%, and ± 5%, respectively, where positive precentages indicate over-estimation, and negative percentages under-estimation. Incidentally, the values of $\bar{\alpha}$ for Cases E-10, E-20, and E-30 are respectively 1.74, 3.48, and 5.22. When the wall-frame connections are relatively flexible compared to the girders in the frame, as in Case E-20P, the error bound for top deflection many increase considerably while those for the other parameters remain relatively stable.

Finally, the assumption of midspan contraflexural points in the connecting beams can be shown to be justified. The moments which would appear at the midspan of the connecting beams, if that assumption were not made, can be determined (Appendix C). These moments for Case E-20 are shown in Figure 2-11, where their magnitudes can be seen to be only a few per cent of the end moments of the respective

connecting beams.

2.6.2 DISTRIBUTION OF LOAD BETWEEN WALL AND FRAME

In order to obtain a clear picture of the pattern of load distribution between the wall and the frame in relation to the provisions for the seismic design of a wall-frame system laid down in the NBCC (1977) [45], the 20-storey structure of Case E-20 has been solved using a triangular load distribution of intensity 44kN/m (3.0K/ft) at the top in simulation of a lateral seismic loading. The resulting interstorey shears in the wall and the frame of this example structure are normalised with respect to the external base shear and are plotted as shown in Figure 2-12. The external shears along the height of the structure, normalised with respect to the external base shear, are also plotted as shown in part (a) of the same figure.

Referring to Figure 2-12, the major shear resistance due to the wall in the lower part of the structure (part(a)) and the increasing relative contribution of the frame towards the top (part(b)) can be observed. It can also be observed from part(b) that the critical frame shear is located at about 0.35H.

In regard to the design of the frame in a wall-frame system, the distribution of interstorey shear in the frame is of particular interest. Cases 2 and 3 of Table 4.1.9.A,

Sentence 4.1.9.1.(7), NBCC (1977), stipulate that in a "dual structural system" such as the wall-frame system, the frame shall have the capacity to resist not less than 25 per cent of the total lateral force, or the load which is apportioned it in accordance with its stiffness relative to that of the wall, whichever is critical. Therefore, when a curve which represents a load equal to 25 per cent of the external load is drawn as shown in Figure 2-12(b), it can be concluded that for this particular example, the design of the bottom three storeys of the frame will be governed by the requirement of resisting not less than 25 per cent of the total lateral load while that of the remaining storeys will be governed by the requirement of resisting the load that is apportioned the frame in interacting with the wall.

2.7 PARAMETRIC STUDY OF A NOMINAL STRUCTURE

The solution to the final differential equation is rather complex so that, while design equations can still be set up for regular use in the design office, general design curves are not possible. However, it is felt that a parametric study of a nominal structure is still helpful in gaining some insights into the behaviour of wall-frame systems. To this end, a nominal wall-frame structure with fixed-ended connecting beams has been selected for an investigation of the effects of the following two parameters:

(1) stiffness of the connecting beam – by varying the dimensions of the beam section,

and (2) structure height – by varying the number of storeys.

The basic dimensional properties of the nominal structure are identical to those of the 20-storey structure of worked example E-20. The value of f_c is set at 1.2. A uniformly distributed load of 22 kN/m (1.5K/ft) is assumed in all cases. For the parameter of connecting beam stiffness, the following rectangular beam sections are taken: (a) 50 mm (2 in.) square (which is practically equivalent to having pin-pin end conditions); (b) 762 mm (30 in.) x 203 mm (8 in.) deep; (c) 762 mm (30 in.) x305 mm (12 in.) deep; (d) 203 mm (8 in.) x 610 mm (24 in.) deep; and (e) 457 mm (18 in.) x 610 mm (24 in.) deep. The relative stiffnesses for these

beam sections are respectively 0.00, 0.06, 0.20, 0.45, and 1.00. For the parameter of structure height, the following numbers of storeys are taken: (a) 10; (b) 15; (c) 20; (d) 25; (e) 30; and (f) 35.

The results for lateral deflection, connecting beam shear, frame shear, and wall moment for the various connecting beam stiffnesses are presented in Figure 2-13a through Figure 2-13d, while those for the various structure heights are shown in Figure 2-14a through Figure 2-14d. In each case, lateral deflections are normalised with respect to the top deflection of the cantilever wall subjected to the same loading alone, connecting beam shears and frame shears with respect to the external base shear, and wall moments with respect to the external base moment.

From Figures 2-13a,2-13c, and 2-13d, the significant contribution of strong wall-frame coupling to reducing building sway, shear load in the frame, and wall moment can be inferred. From Figure 2-13b, a larger increase in beam shears with beam stiffness in the critical region, which occurs between 0.3H and 0.5H for various beam stiffnesses, than near the top of the structure can also be observed. From Figures 2-14a and 2-14d,the increasing efficiency of the wall-frame system in deflection control and in reducing the moment load in the wall with taller buildings is noted. These two figures also tend to show that increase in the

general efficiency of the wall-frame system tends to become marginal when the structure exceeds about 35 storeys in height. This finding corresponds to current thinking that wall - frame structures are efficient lateral load systems up to about 40 storeys. Figure 2-14b shows a considerable increase in the maximum lintel shear with structure height and a tendency for the increase to become marginal when the number of storeys exceeds 35. The figure also shows the critical region of lintel shear shifting from 0.5H in low-rises down to about 0.2H in very tall buildings, and shows a relative decrease in the efficiency of the connecting beams in the top storeys with taller structures. Finally, Figure 2-14c shows that the critical frame shear in wall-frame systems occurs near the mid-height in low-rises and shifts down to about 0.25H in very tall buildings.

2.8 CONCLUSION

A method of analysis has been presented for the study of the response of uniform planar wall-frame structures to lateral loads. The analysis is based upon the continuum approach. The shear wall is treated as a flexural cantilever, the connecting beams are replaced by a continuous medium of equivalent structural properties, and the frame is modelled as a shear beam in approximation of its horizontal shearing action. The actual behaviour of the frame as a discrete structure concerning such effects as axial deformations in the columns and shear lag is also given consideration when dealing with the problem of vertical compatibility. The analysis leads to a fourth order heterogeneous ordinary differential equation in the beam shear intensity. Explicit solutions can be obtained for three common loading conditions. Other types of wall-frame coupling configurations can also be accomodated by the proposed theory. Examples have been worked out to verify the analysis and their results compared with those given by a matrix method frame program (SAP-IV). Good agreement has been observed. Besides reinforcing previous findings regarding the significant contribution of the frame in a wall-frame structure, these examples have also demonstrated the further benefits of wall-frame coupling by moment-resisting beams. Based on the results of the examples, limitations of the proposed

analysis have been discussed in order to provide some useful insights into the behaviour of wall-frame structures.

In comparison with similar theories dealing with wall-frame interaction, it is believed that the proposed analysis offers a more comprehensive treatment of the interaction among the three basic elements of a general wall-frame structure, namely, the frame, the wall, and the wall-frame connections.

Last but not least, it should be noted that besides furnishing a means to analyse planar wall-frame structures, the proposed analysis contributes towards a basic understanding of the problem of wall-frame interaction and thereby provides a premise upon which a general three-dimensional analysis can be pursued.

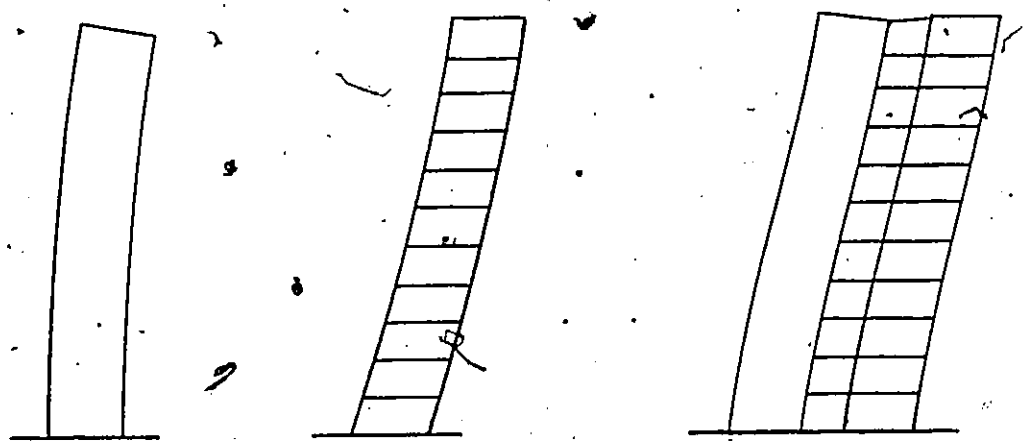

FIG. 2-1: MODES OF DEFLECTION

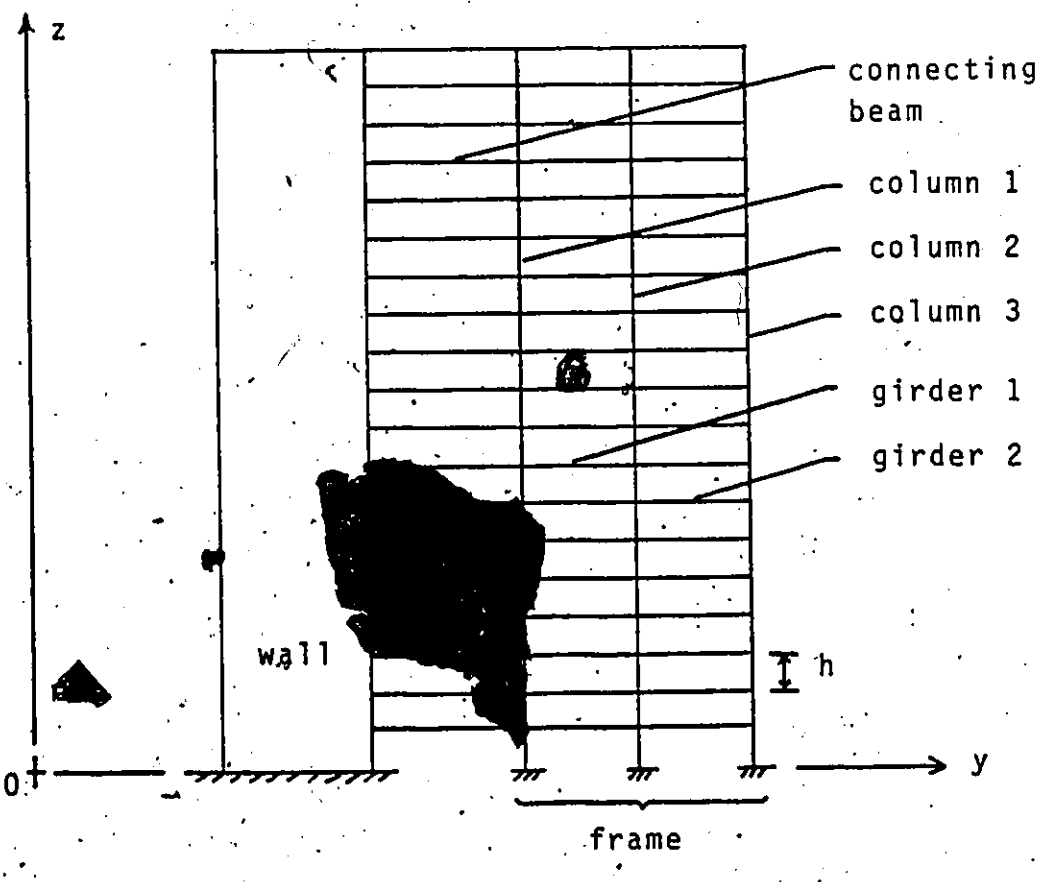

FIG. 2-2: PLANAR WALL-FRAME STRUCTURE

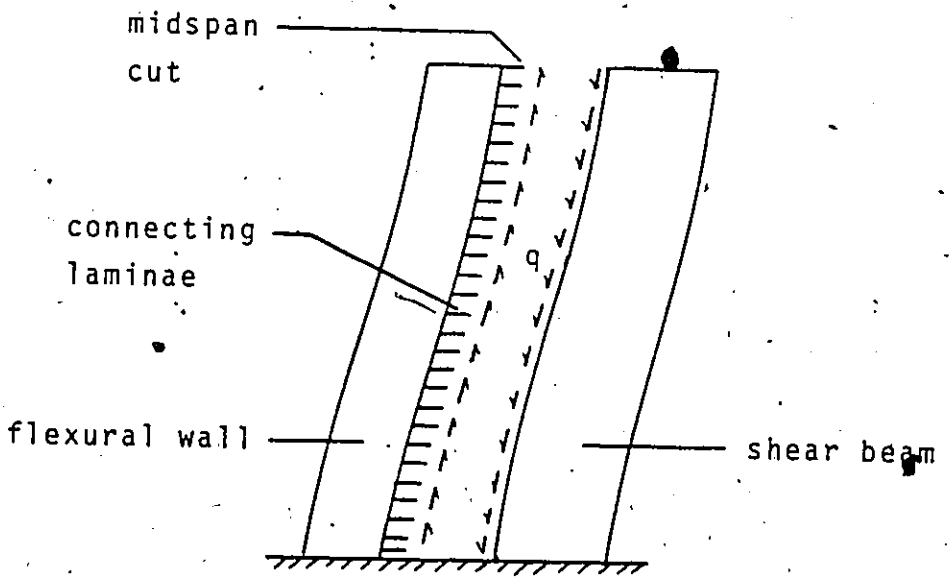

FIG. 2-3: DISTRIBUTED SHEAR IN CONNECTING LAMINAE

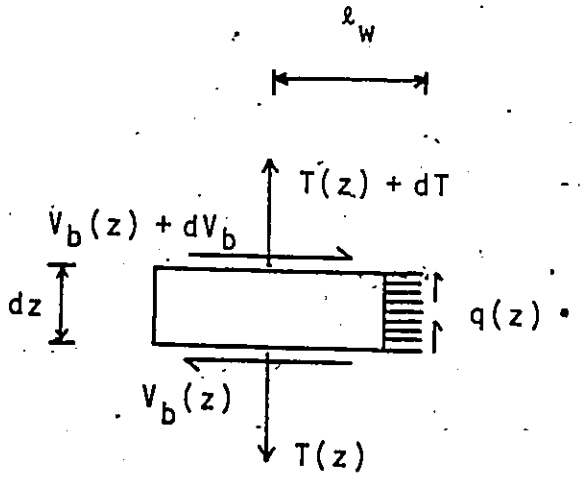

FIG. 2-4: FORCES ACTING ON ELEMENTAL WALL SECTION DUE TO DISTRIBUTED SHEAR q(z)

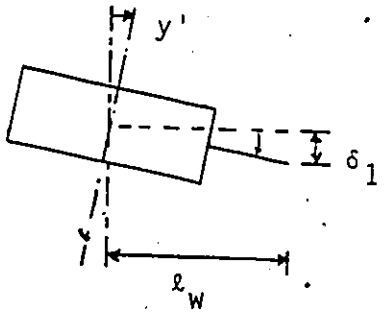

(a) wall rotation

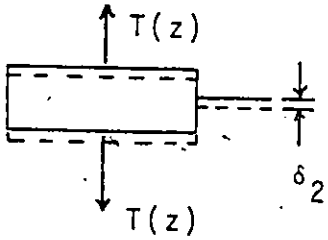

(b) axial deformation of wall

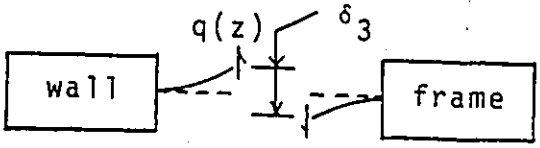

(c) shear and flexural deformation of laminae

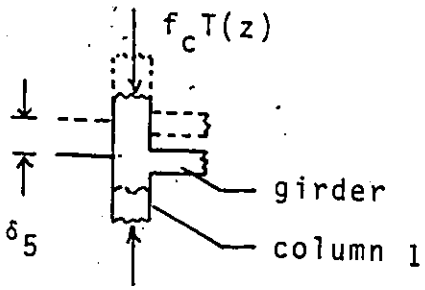

(e) axial deformation of column 1

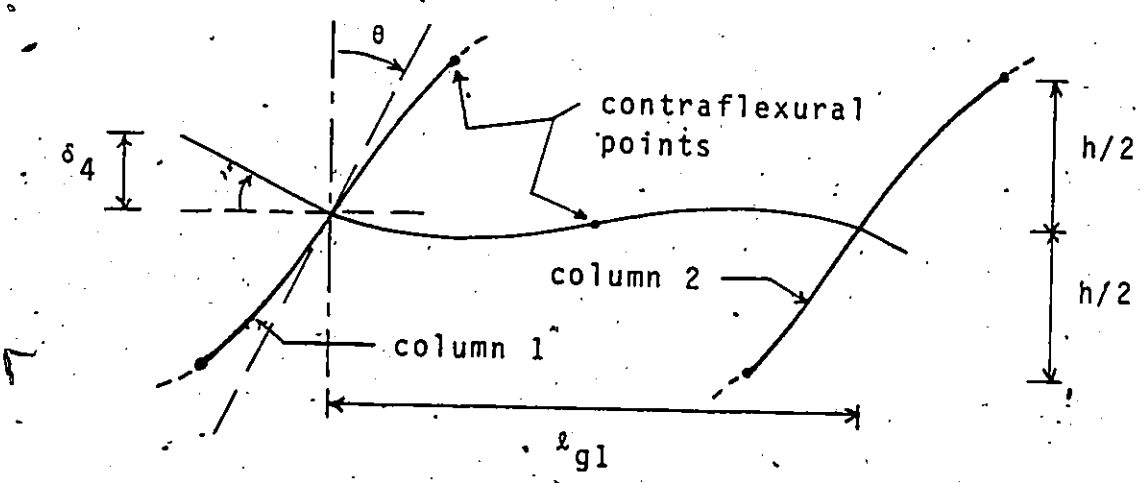

(d) rotation of connecting beam-column joint

FIG. 2-5: RELATIVE DISPLACEMENTS AT MIDSPAN CUT OF CONNECTING BEAM AT HEIGHT z

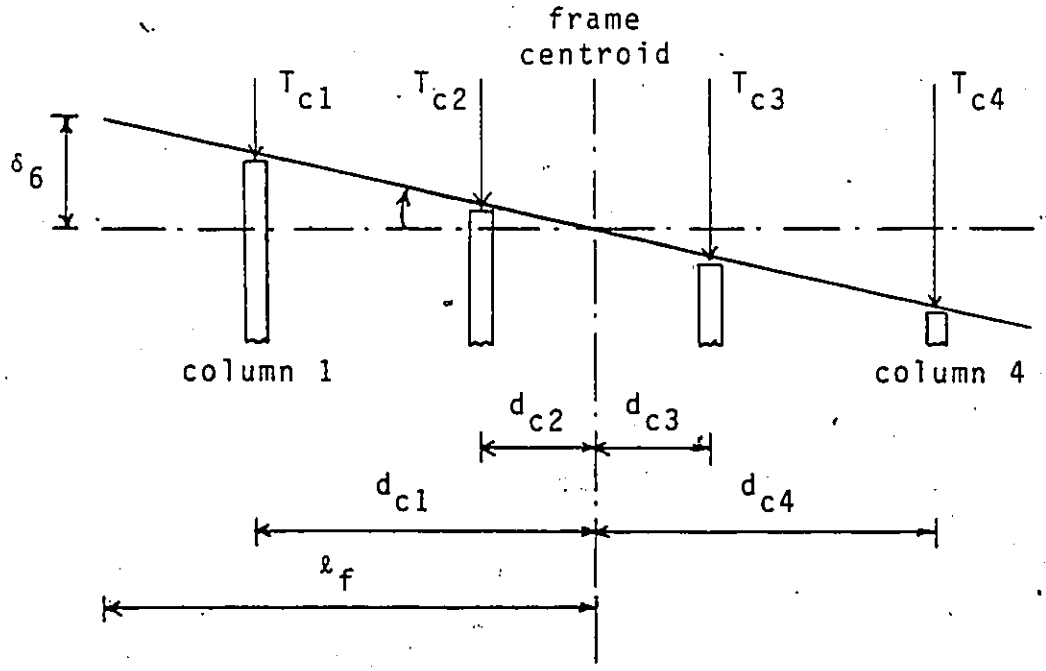

(f) effect of chord drift

(FIG. 2-5 CONTINUED)

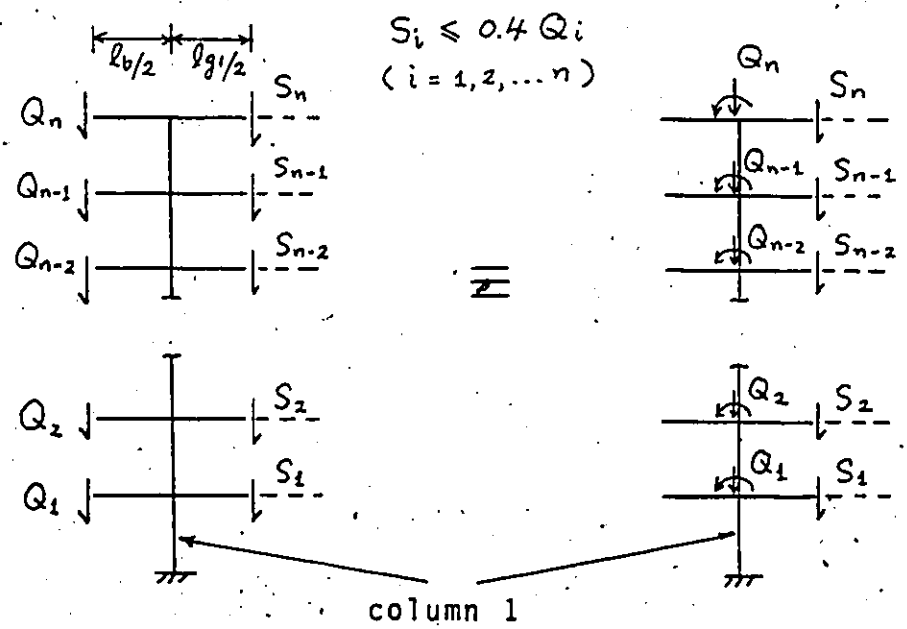

FIG. 2-6a: EFFECT OF CONNECTING BEAM SHEAR ON COLUMN 1

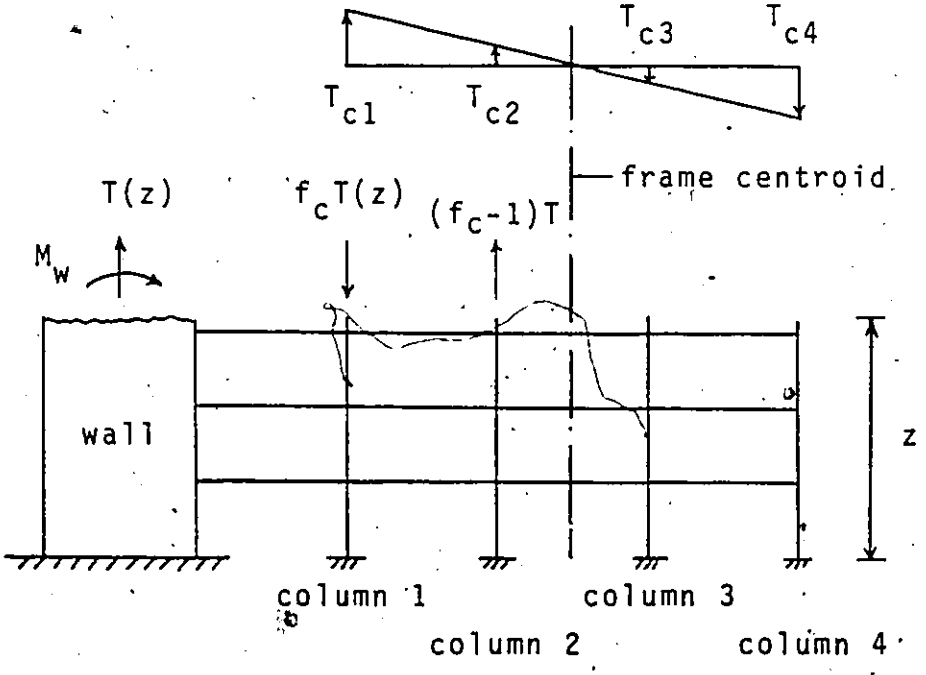

FIG. 2-6b: MOMENT EQUILIBRIUM OF STRUCTURE

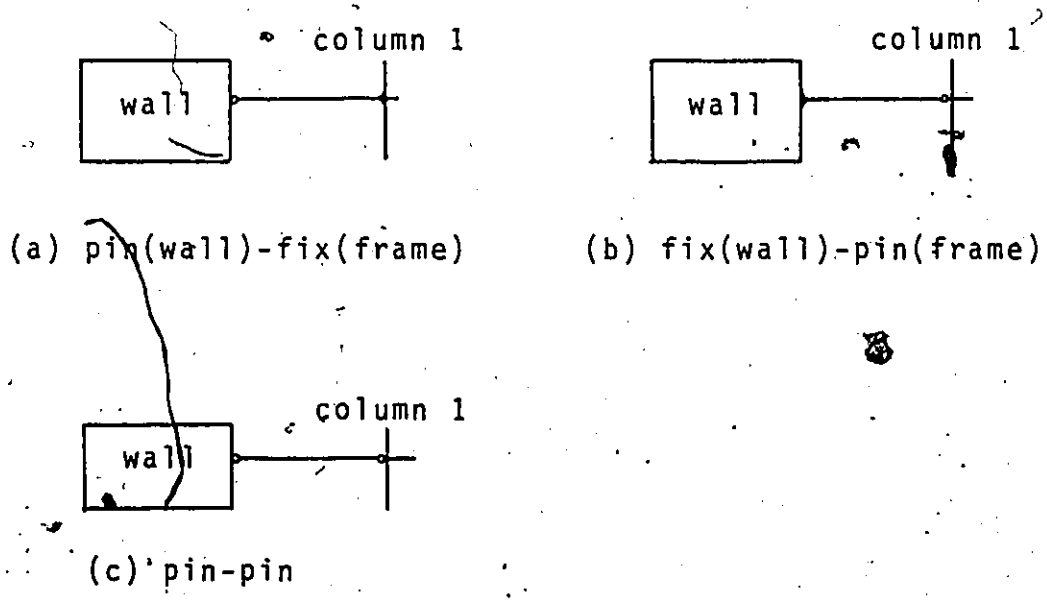

FIG. 2-7: CONNECTING BEAM CONFIGURATIONS

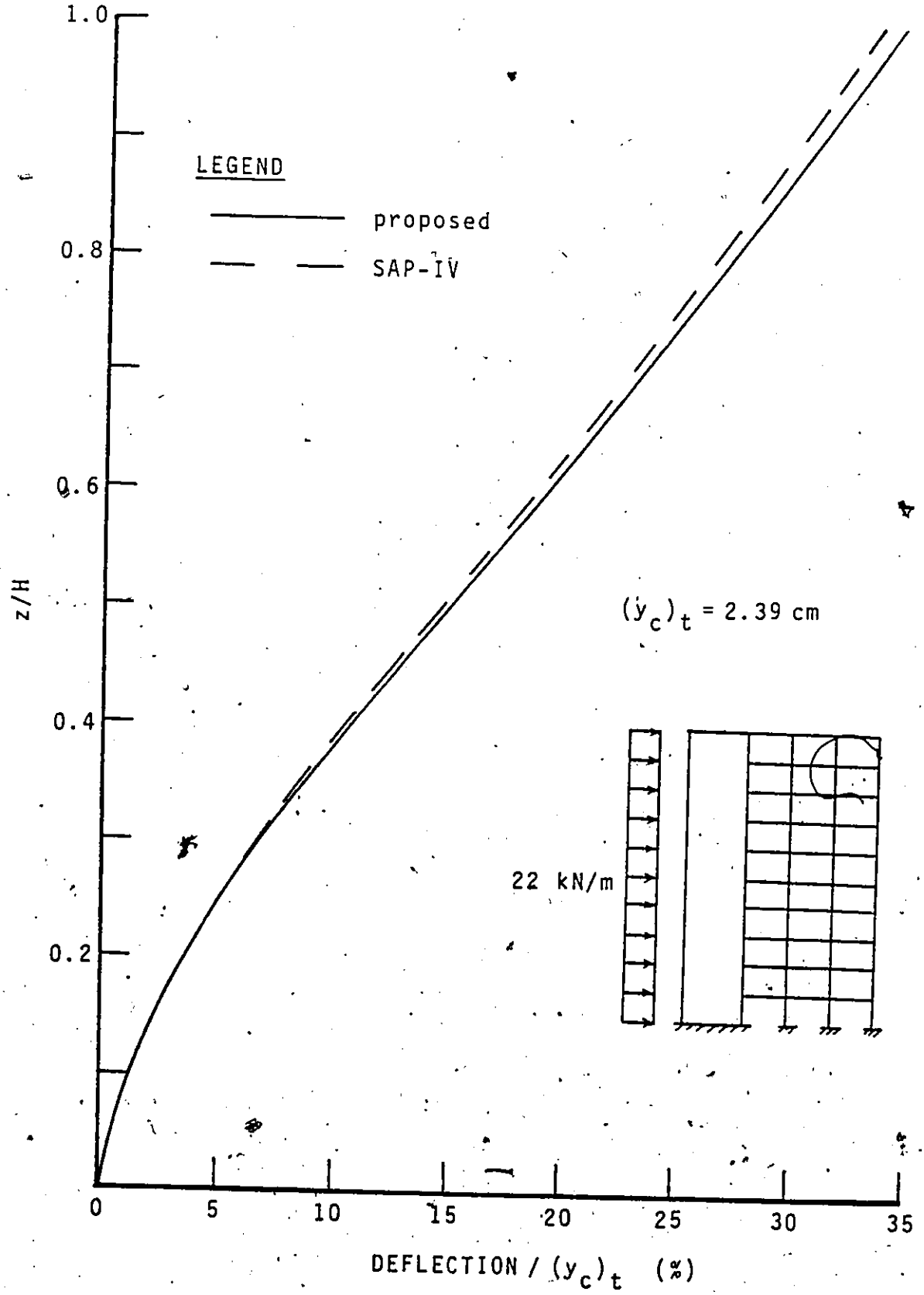

FIG. 2-8a: CASE E-10 — LATERAL DEFLECTION

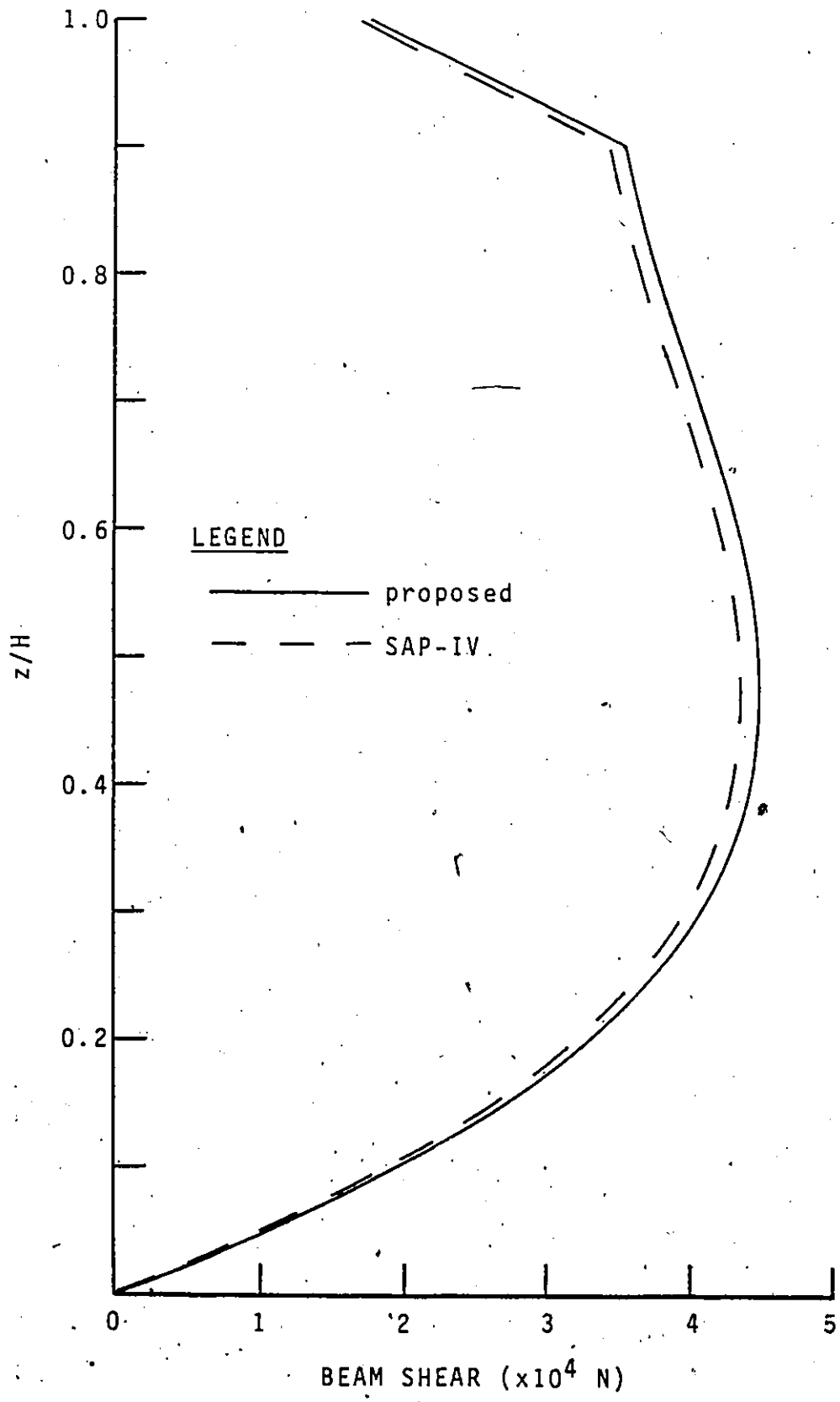

FIG. 2-8b: CASE E-10 — CONNECTING BEAM SHEARS

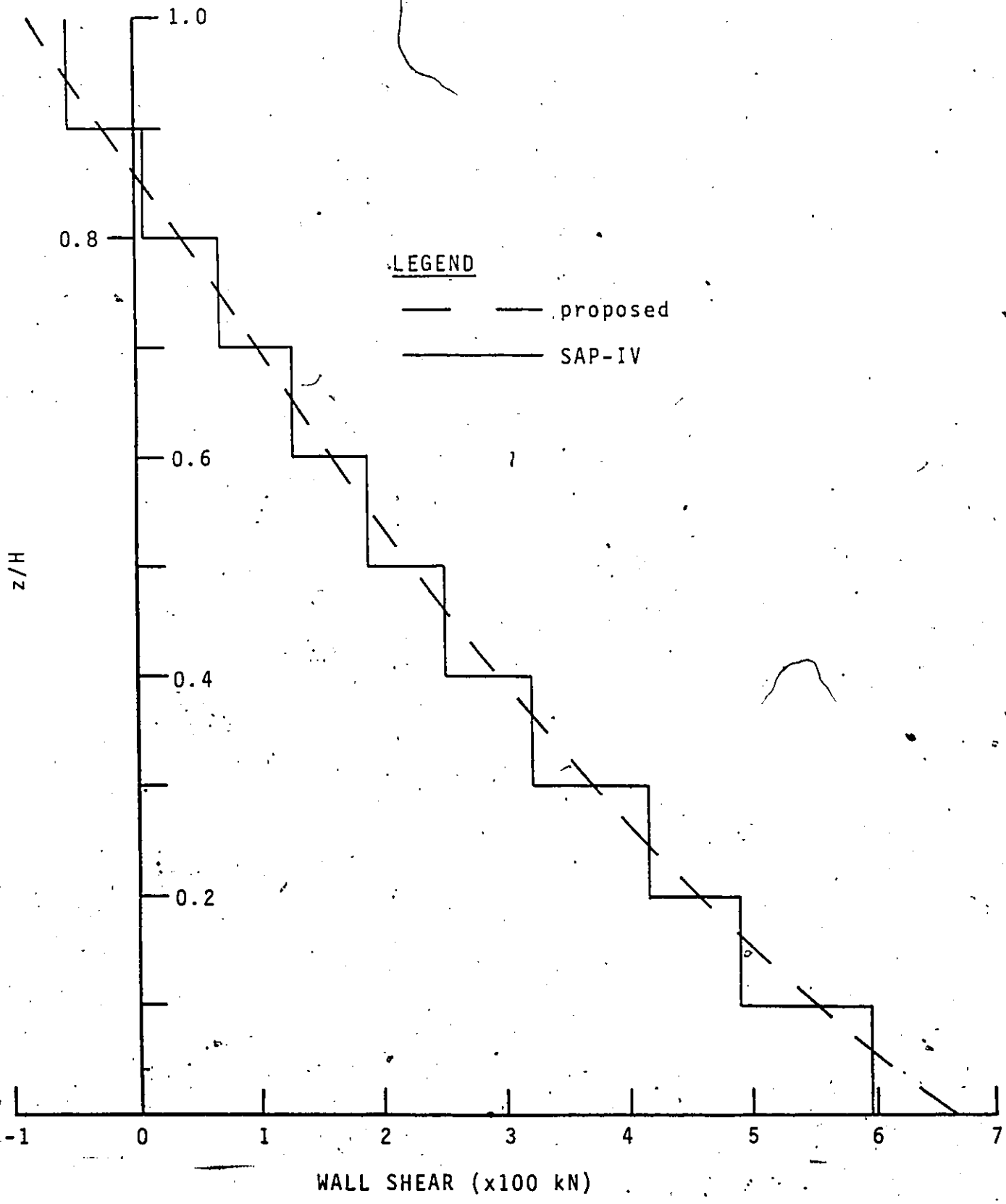

FIG. 2-8c: CASE E-10 — INTERSTOREY WALL SHEAR

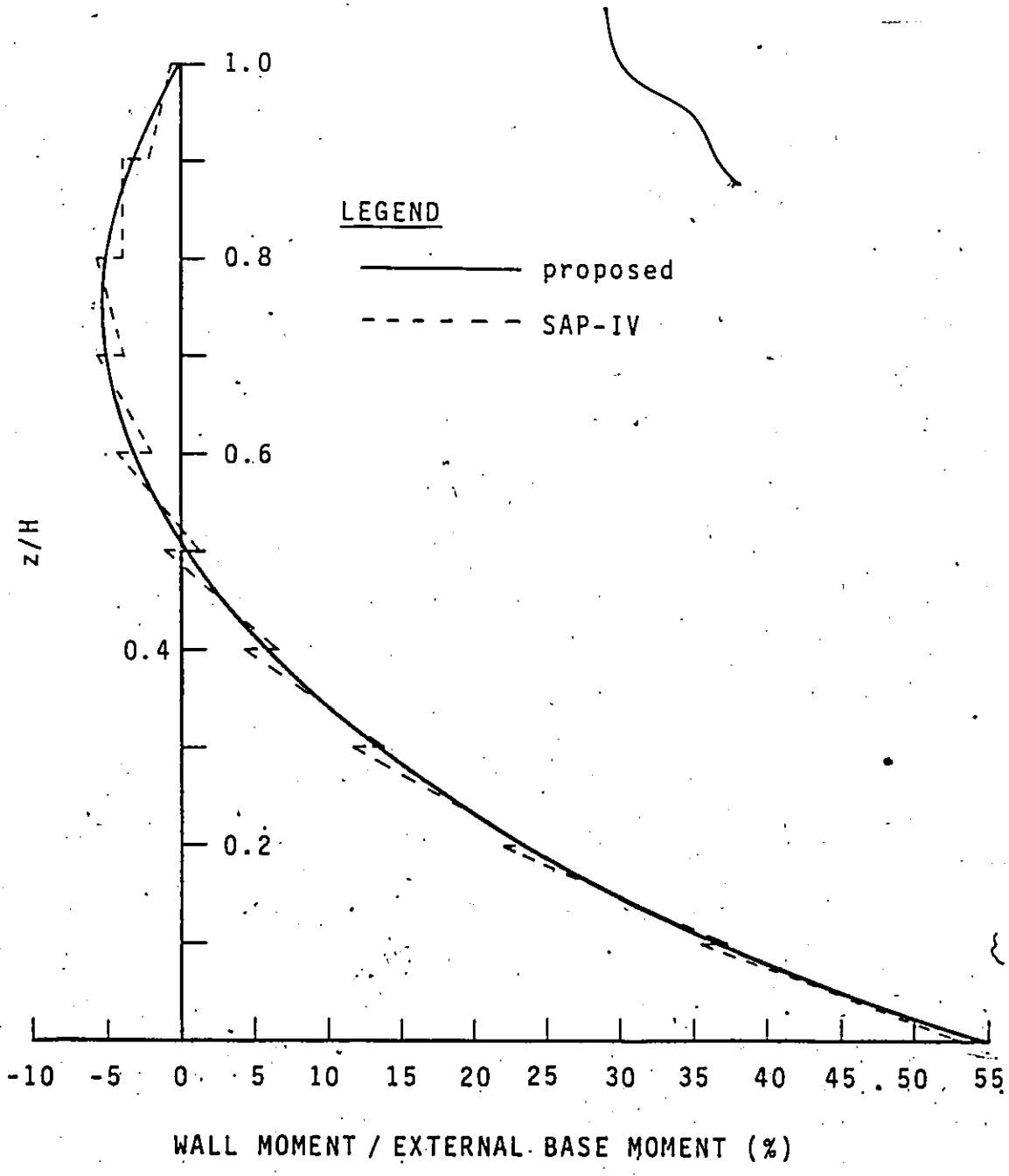

FIG. 2-8d: CASE E-10 — WALL MOMENT

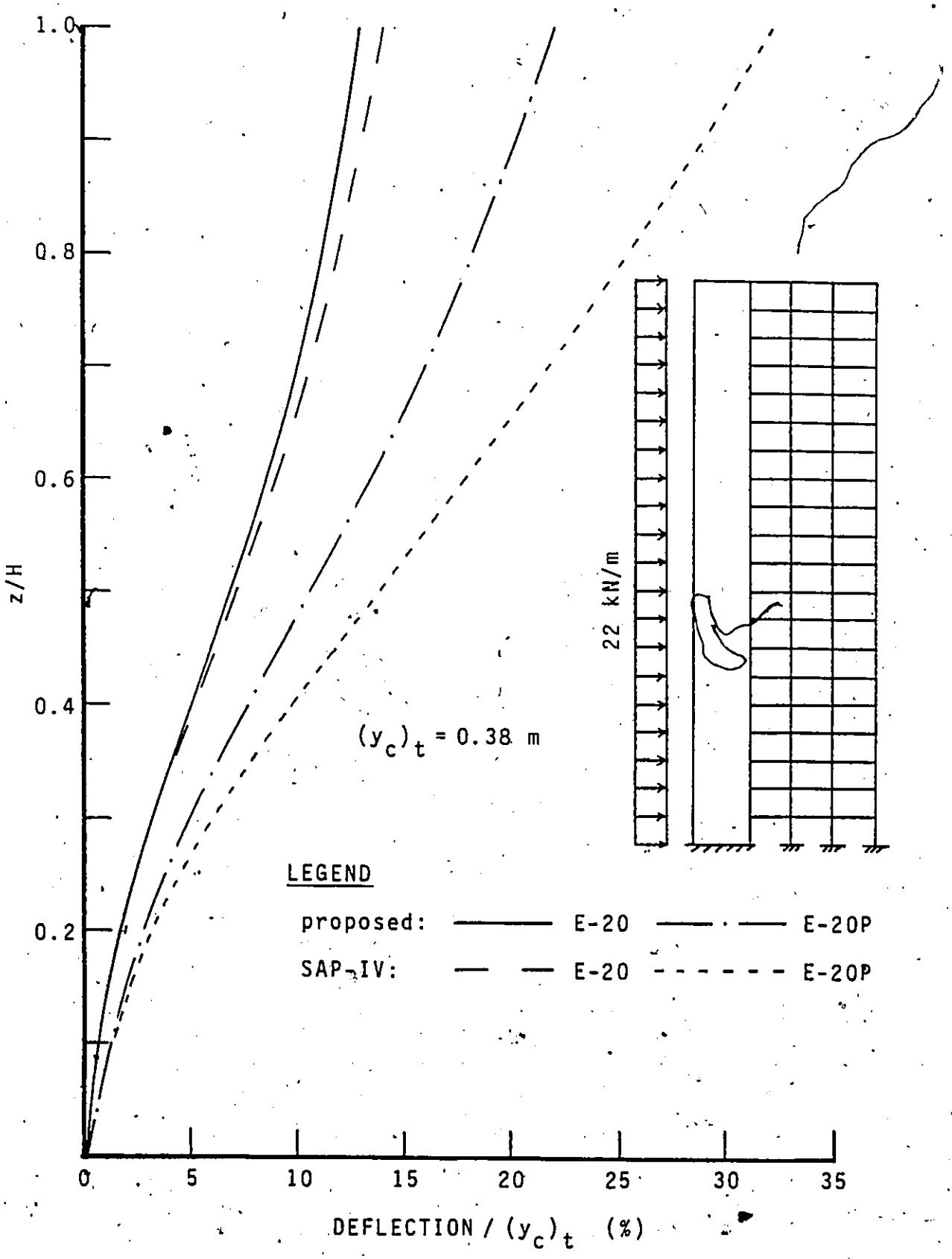

FIG. 2-9a: CASES E-20 AND E-20P — LATERAL DEFLECTION

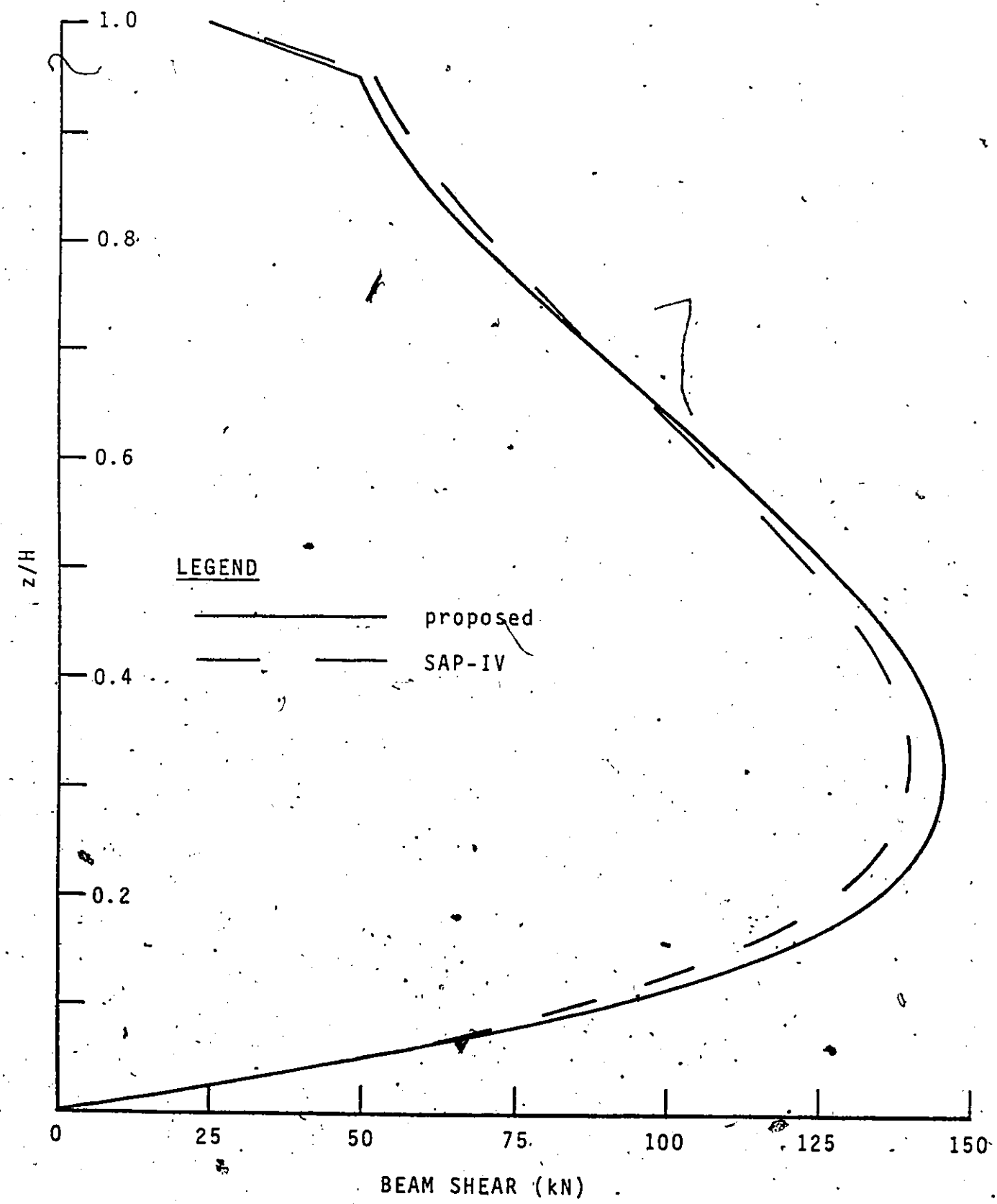

FIG. 2-9b: CASE E-20 — CONNECTING BEAM SHEARS

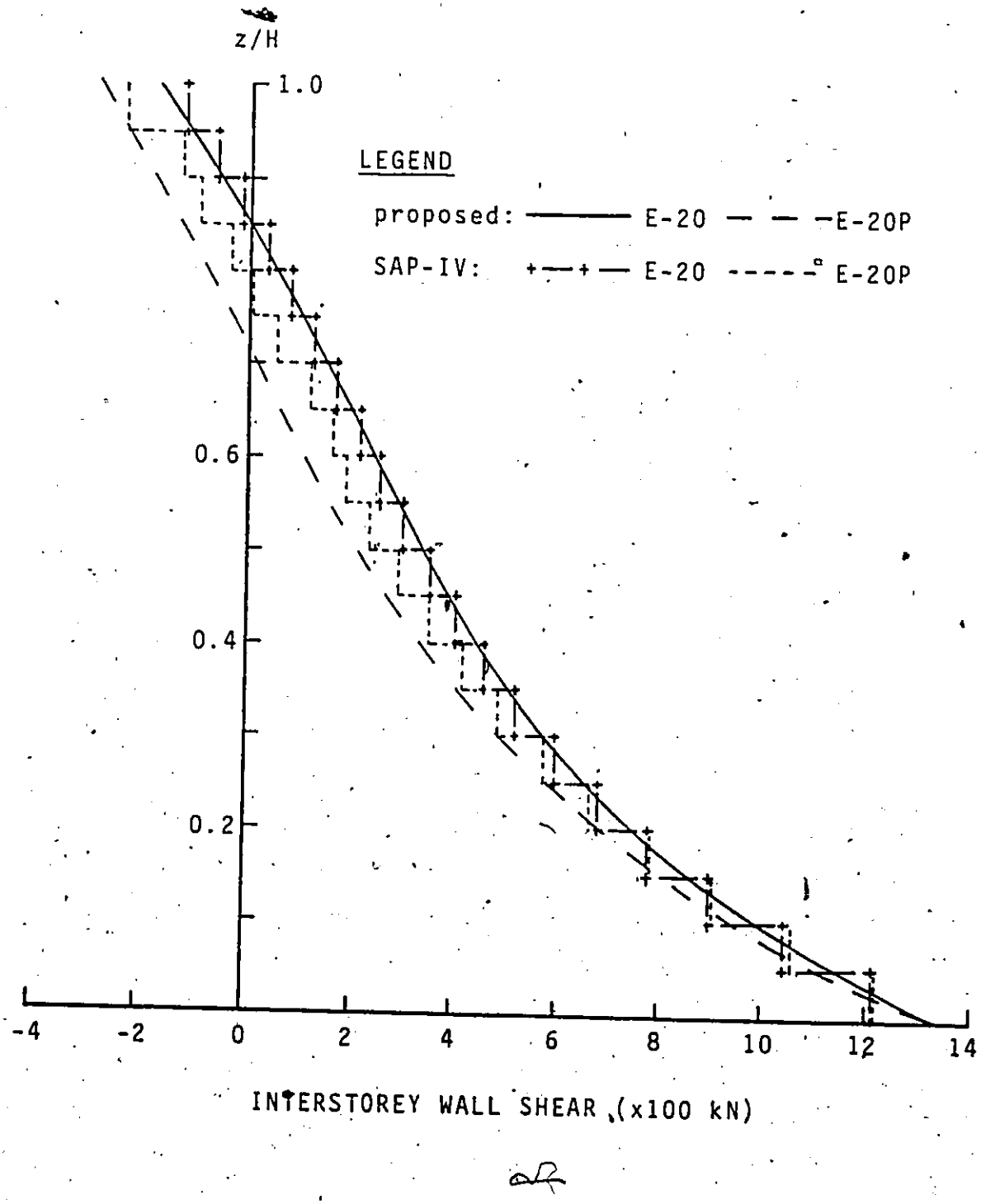

FIG. 2-9c: CASES E-20 AND E-20P — INTERSTOREY WALL SHEAR

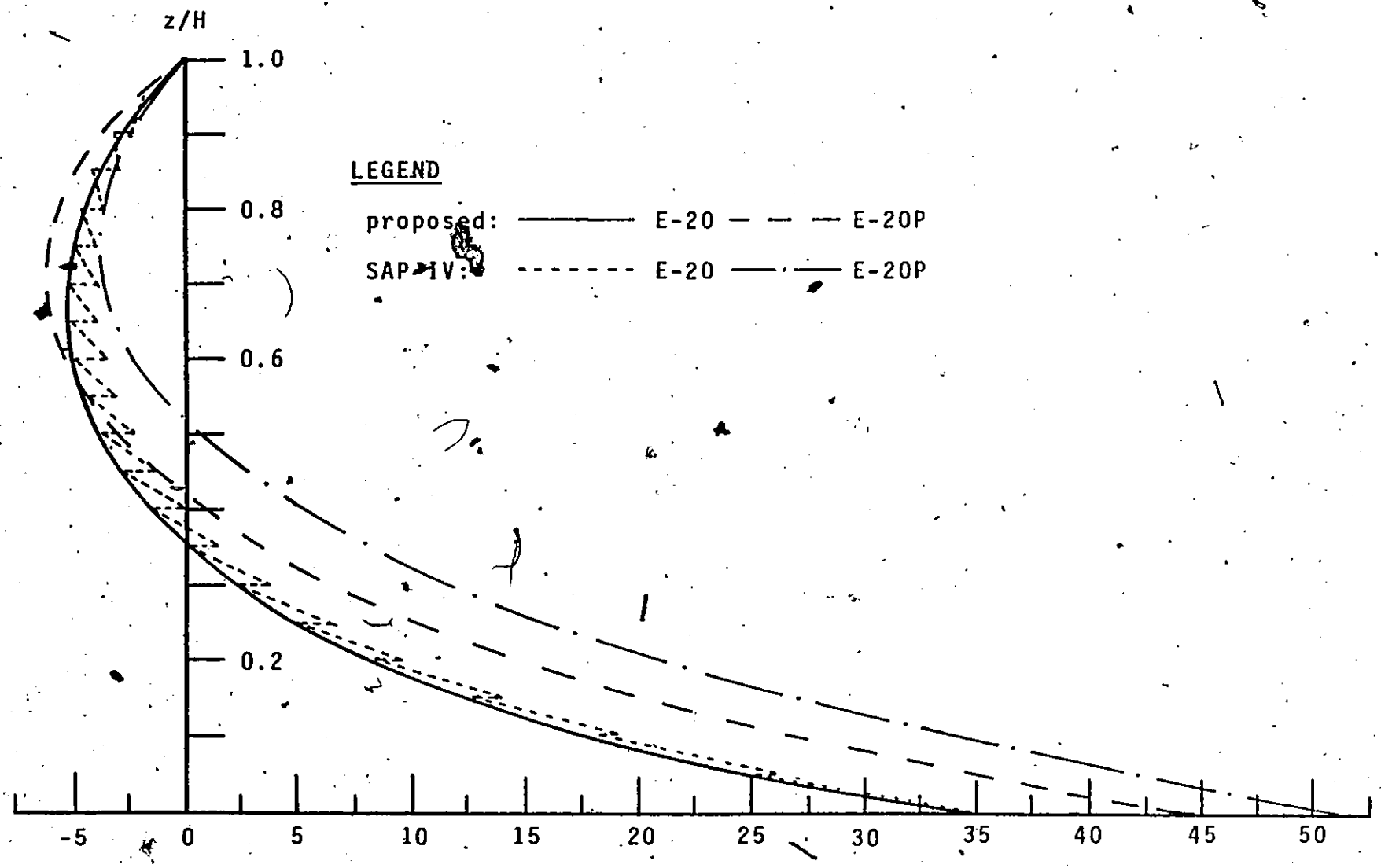

FIG. 2-9d: CASES E-20 AND E-20P — WALL MOMENT

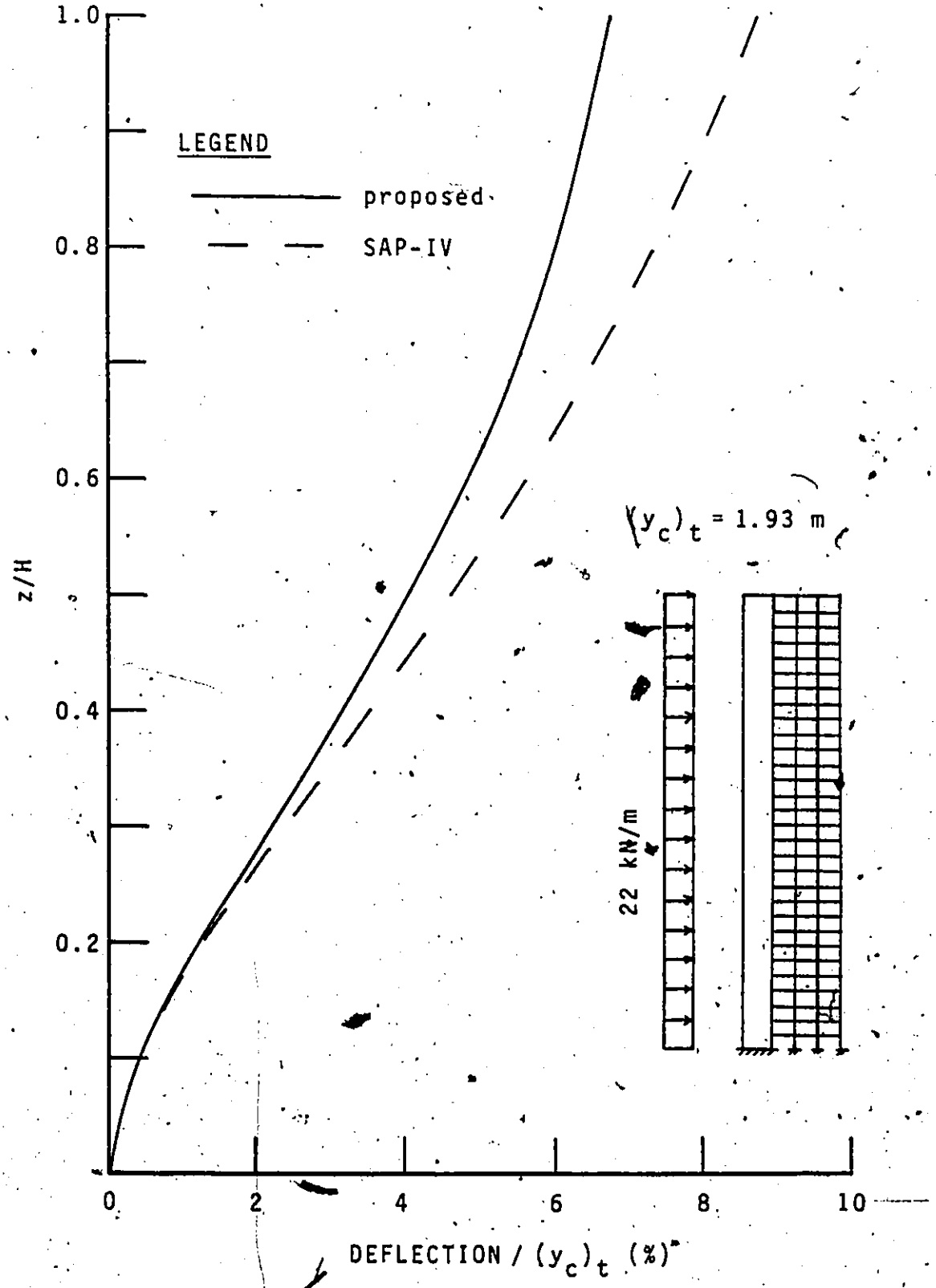

FIG. 2-10a: CASE E-30 — LATERAL DEFLECTION

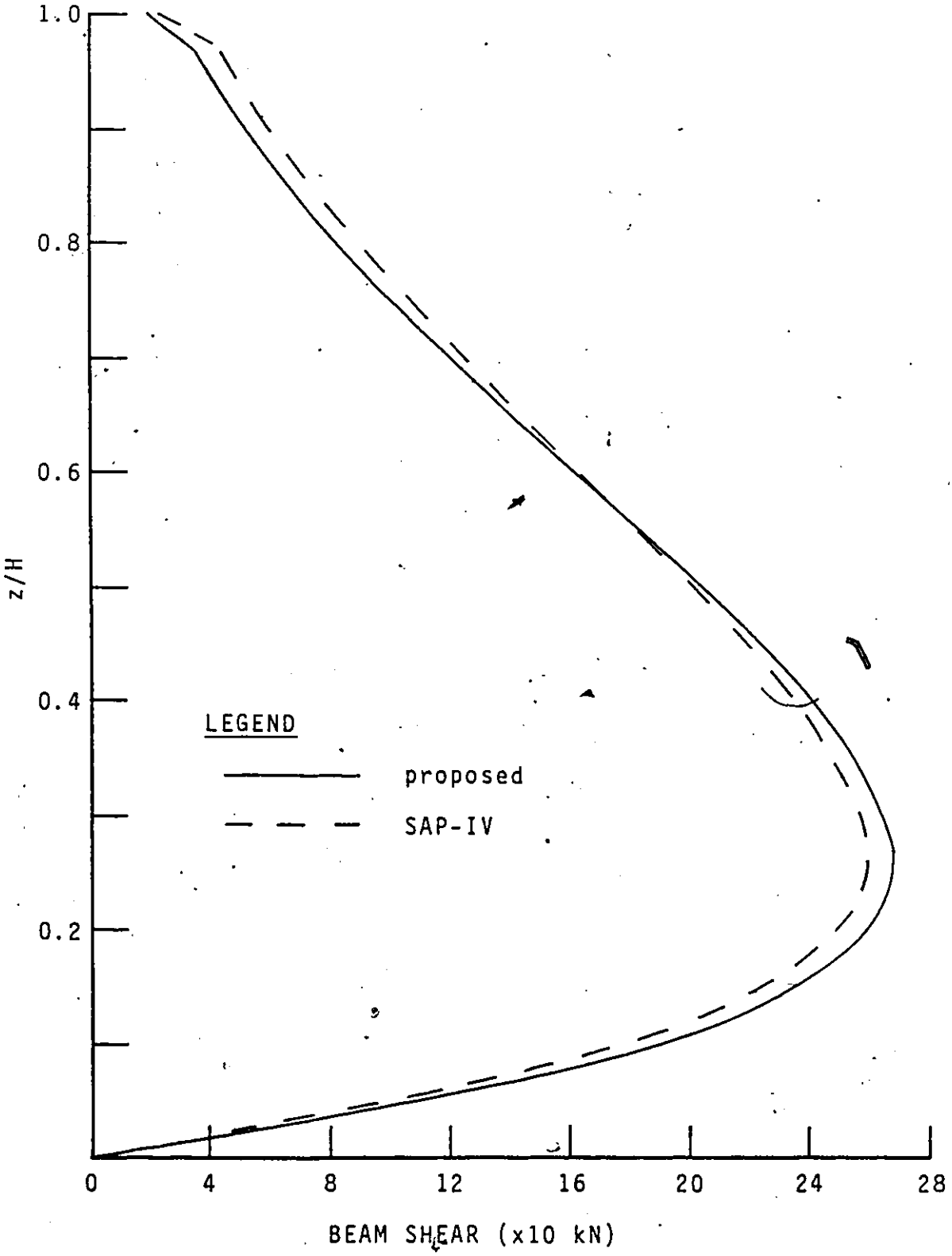

FIG. 2-10b: CASE E-30 — CONNECTING BEAM SHEARS

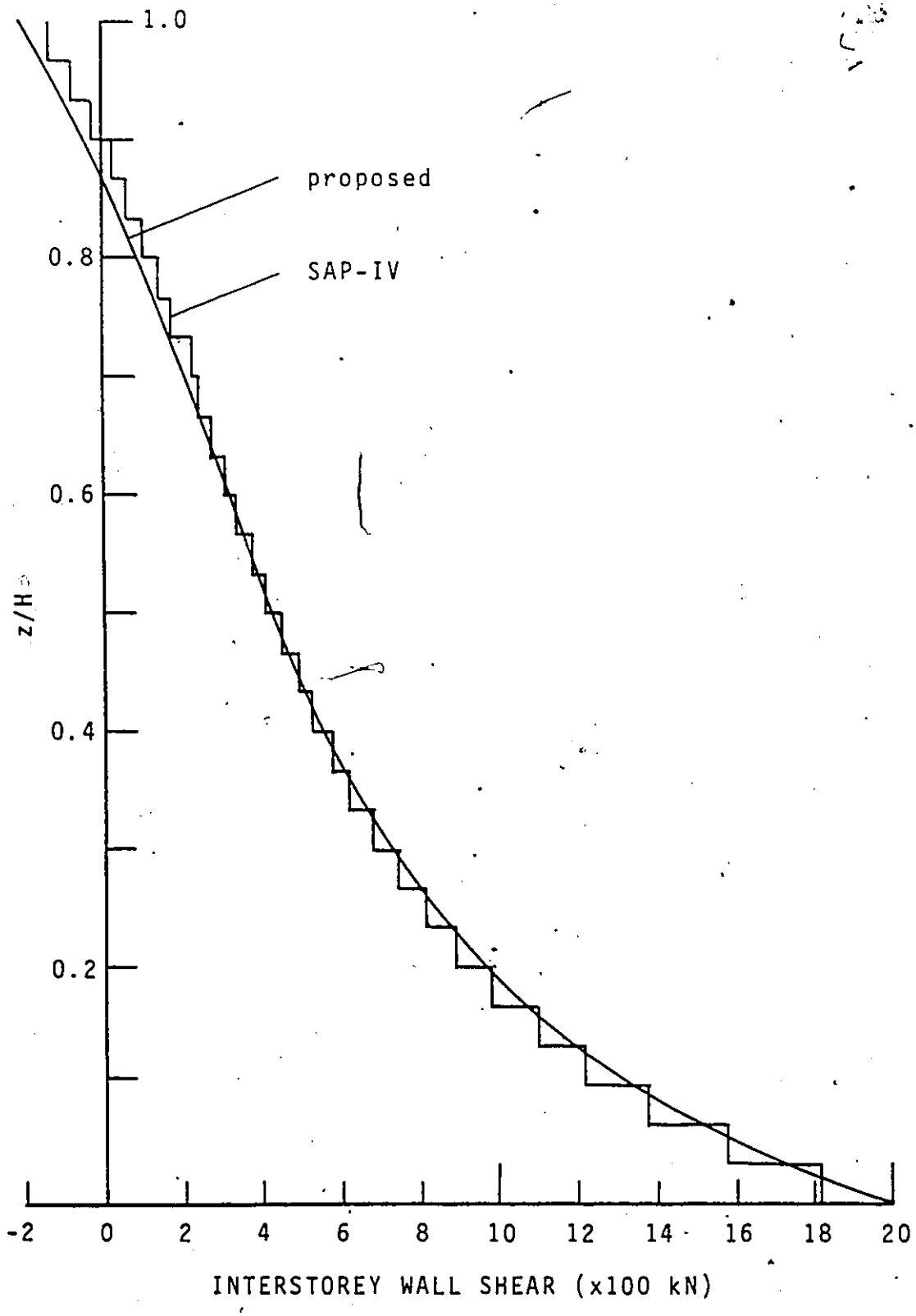

FIG. 2-10c: CASE E-30 — INTERSTOREY WALL SHEAR

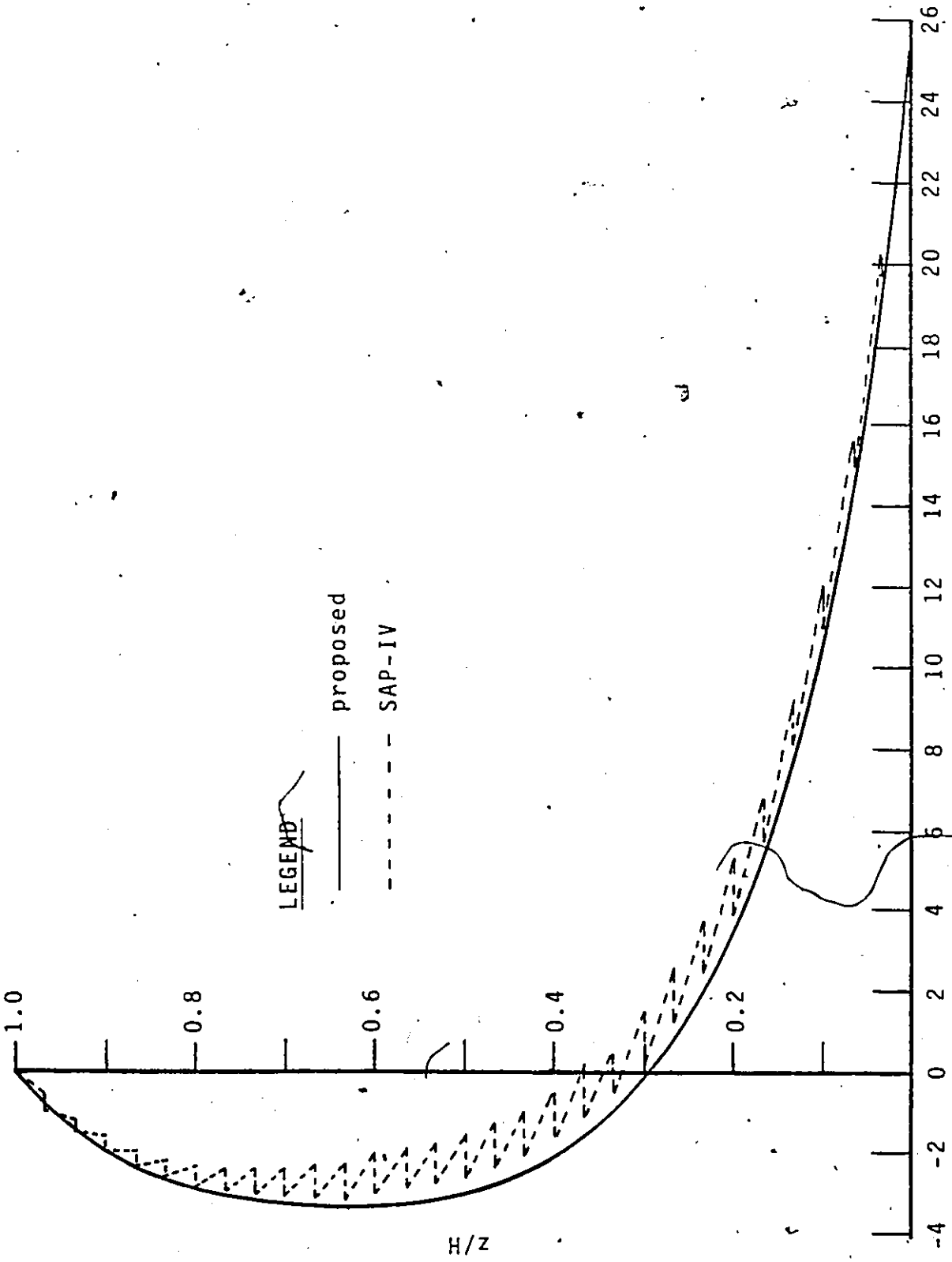

FIG. 2-10d: CASE E-30 — WALL MOMENT

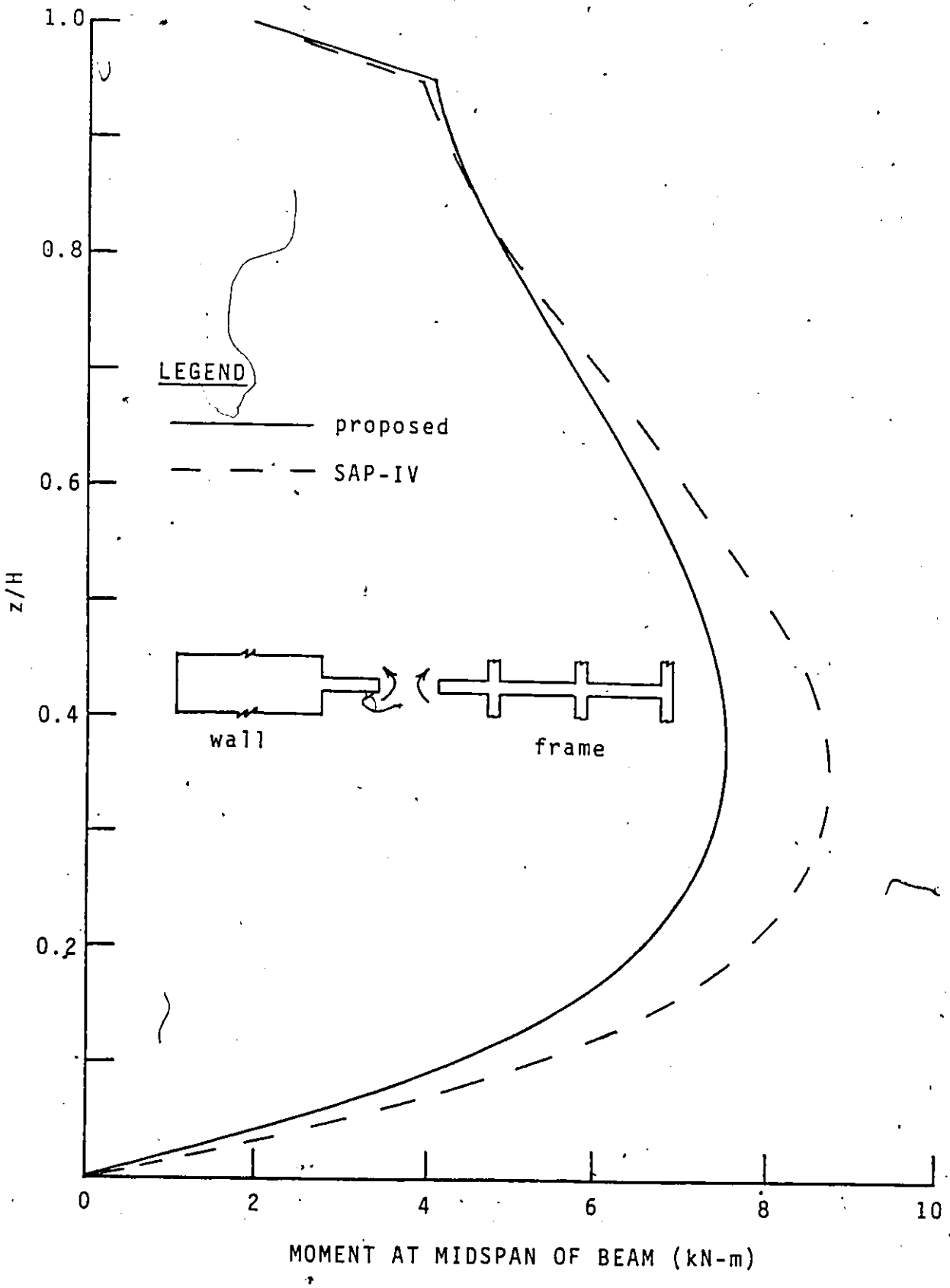

FIG. 2-11: MOMENTS AT MIDSPAN OF CONNECTING BEAM

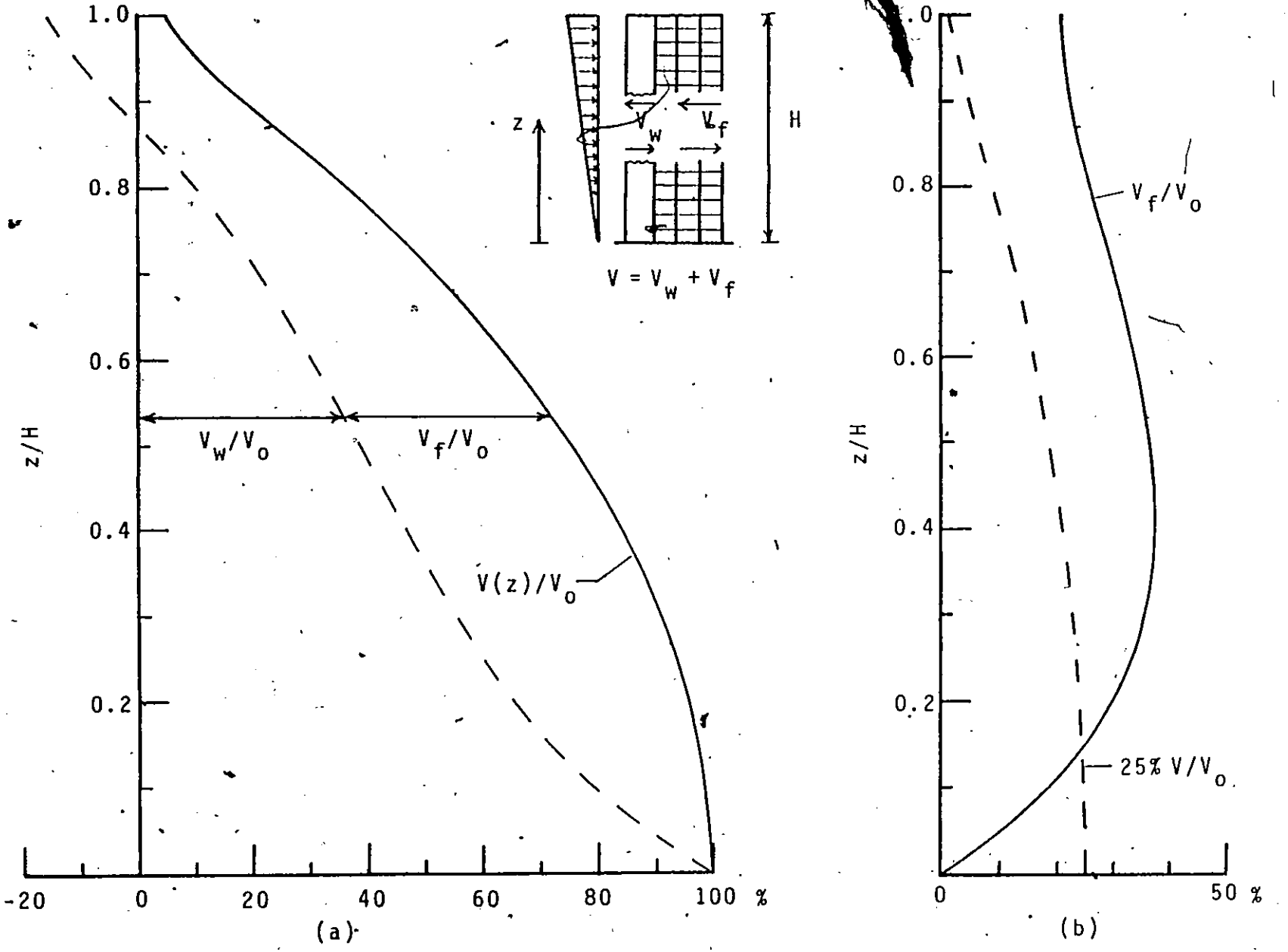

FIG. 2-12: LOAD DISTRIBUTION BETWEEN WALL AND FRAME

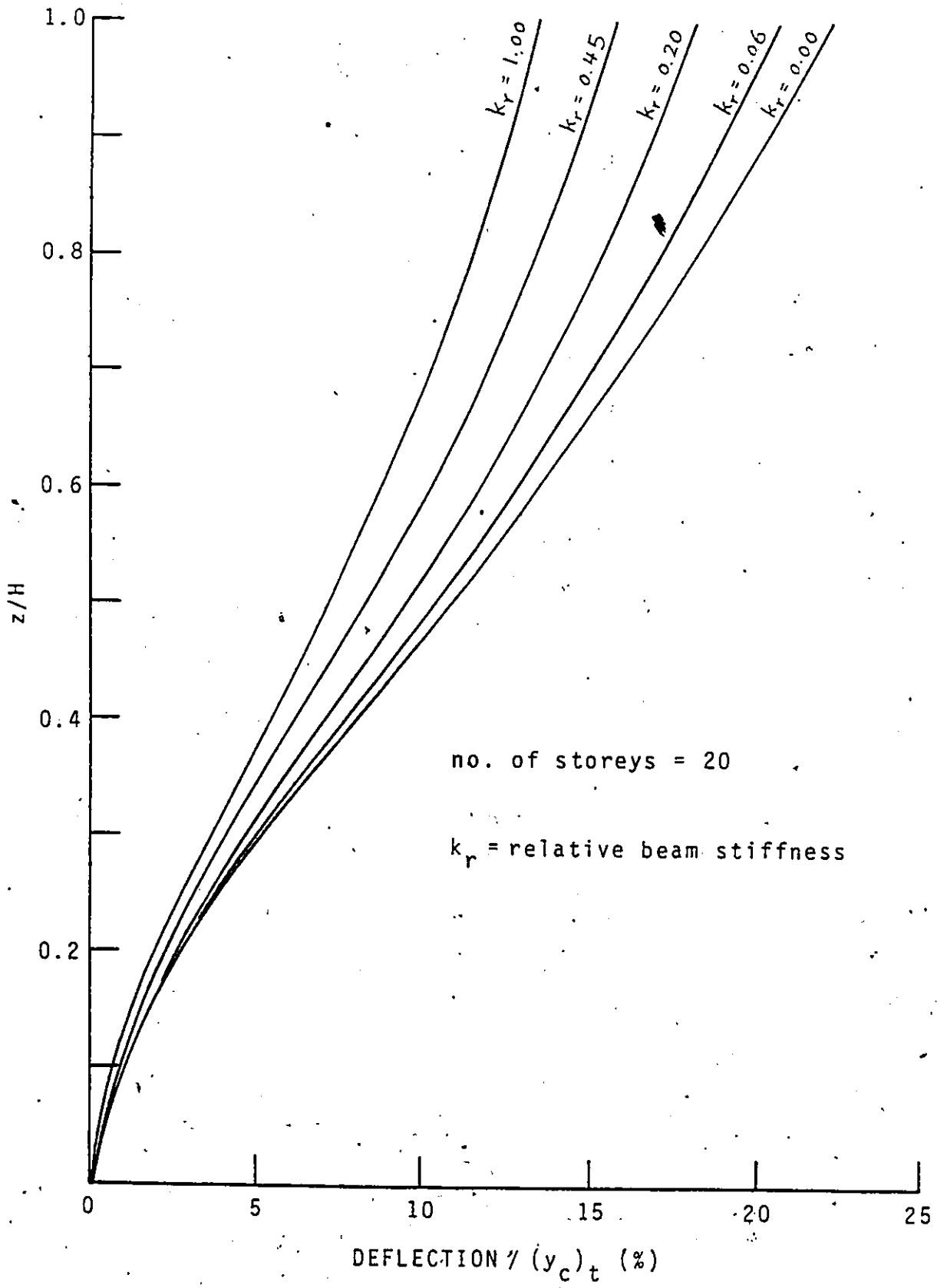

FIG. 2-13a: EFFECT OF BEAM STIFFNESS ON LATERAL DEFLECTION

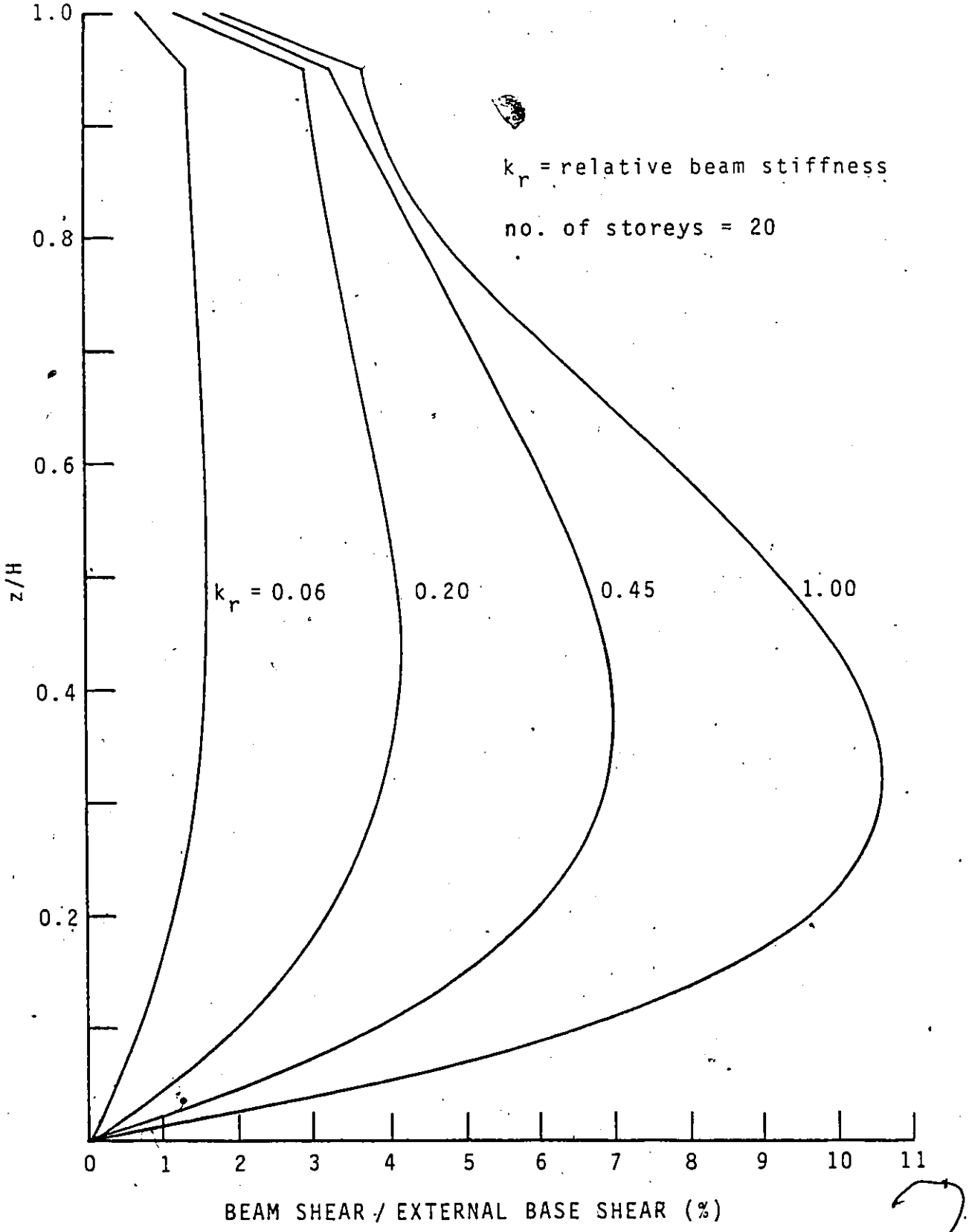

FIG. 2-13b: EFFECT OF BEAM STIFFNESS ON BEAM SHEARS

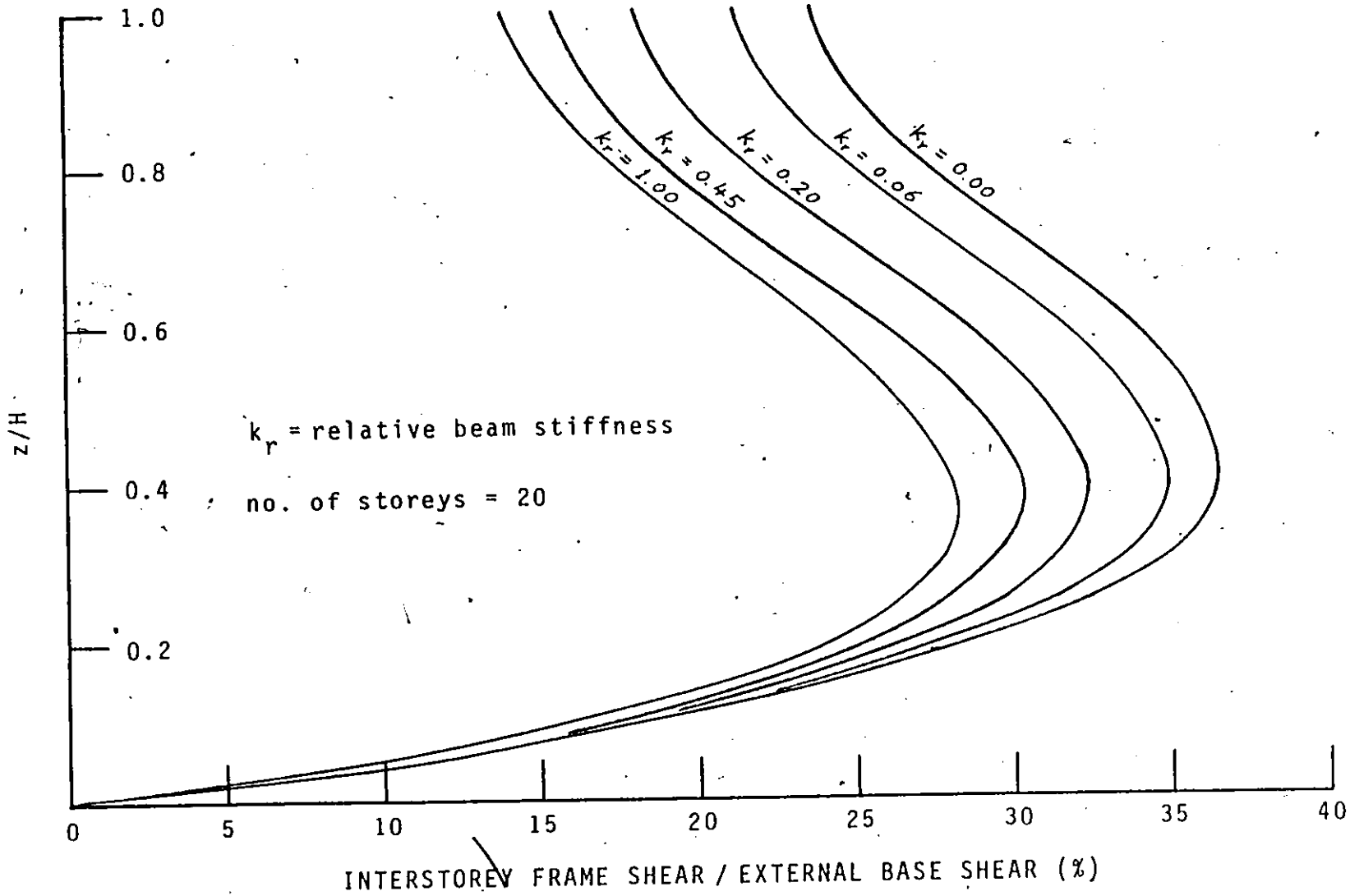

FIG. 2-13c: EFFECT OF BEAM STIFFNESS ON INTERSTOREY FRAME SHEAR

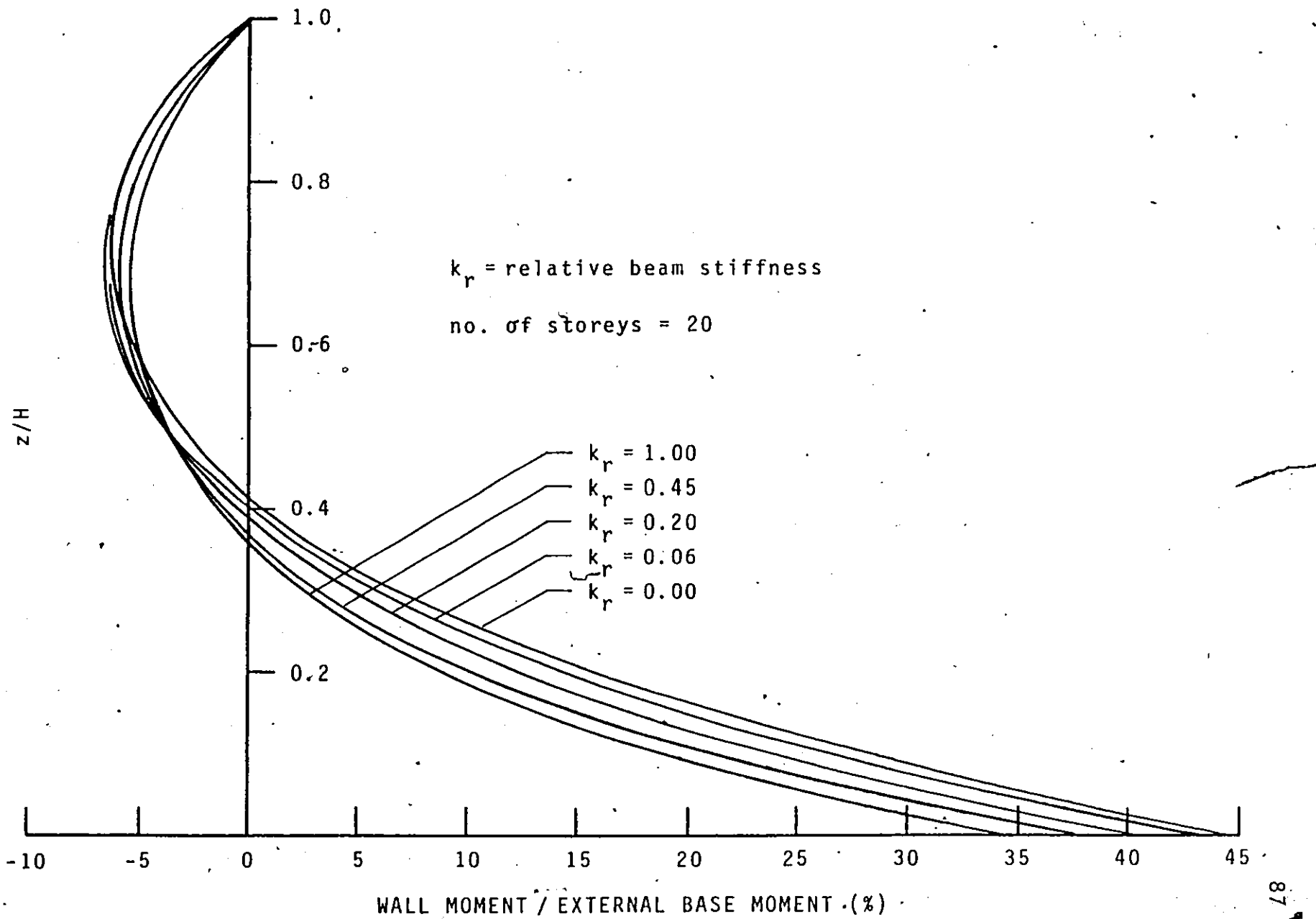

FIG. 2-13d: EFFECT OF BEAM STIFFNESS ON WALL MOMENT

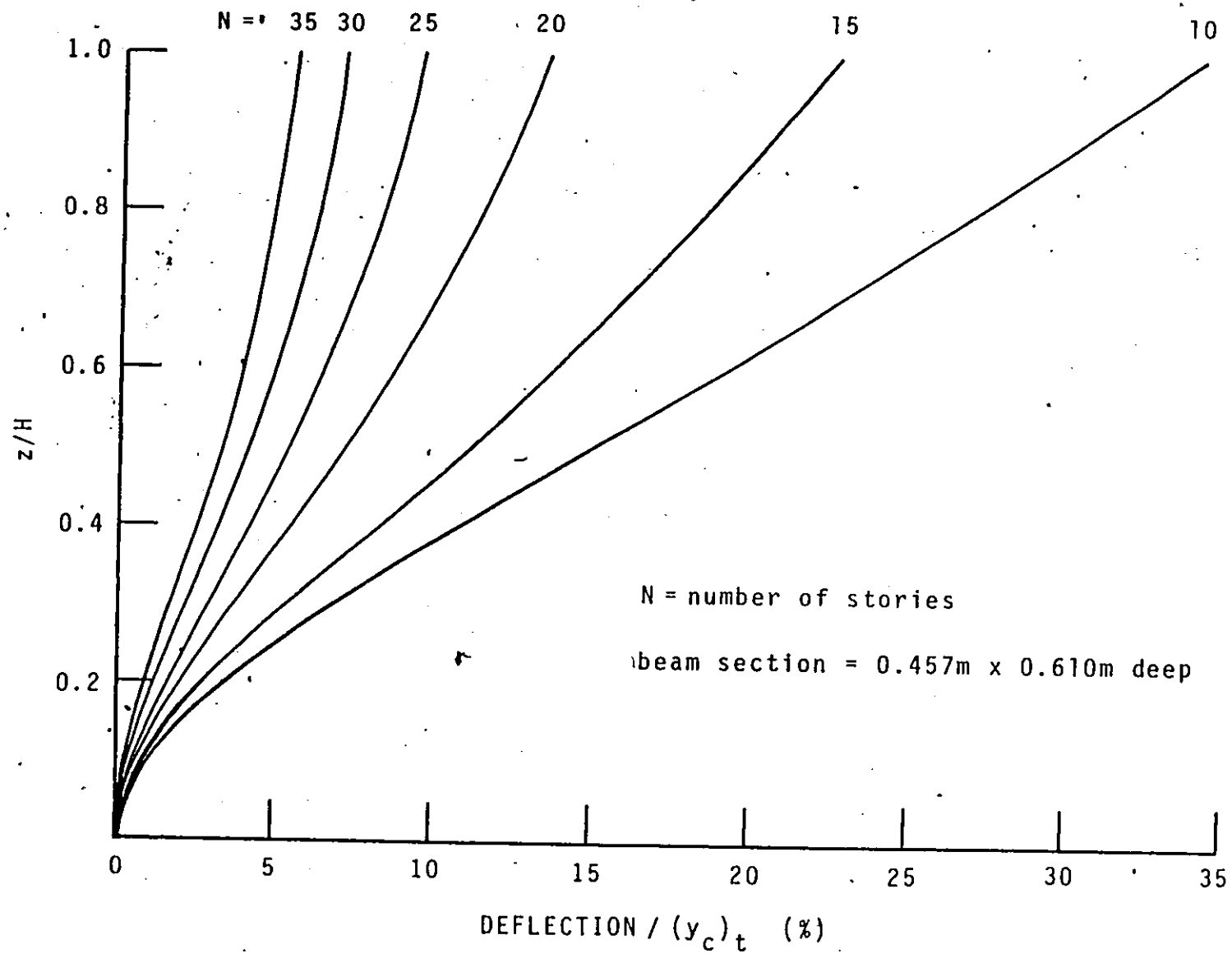

FIG. 2-14a: EFFECT OF STRUCTURE HEIGHT ON LATERAL DEFLECTION

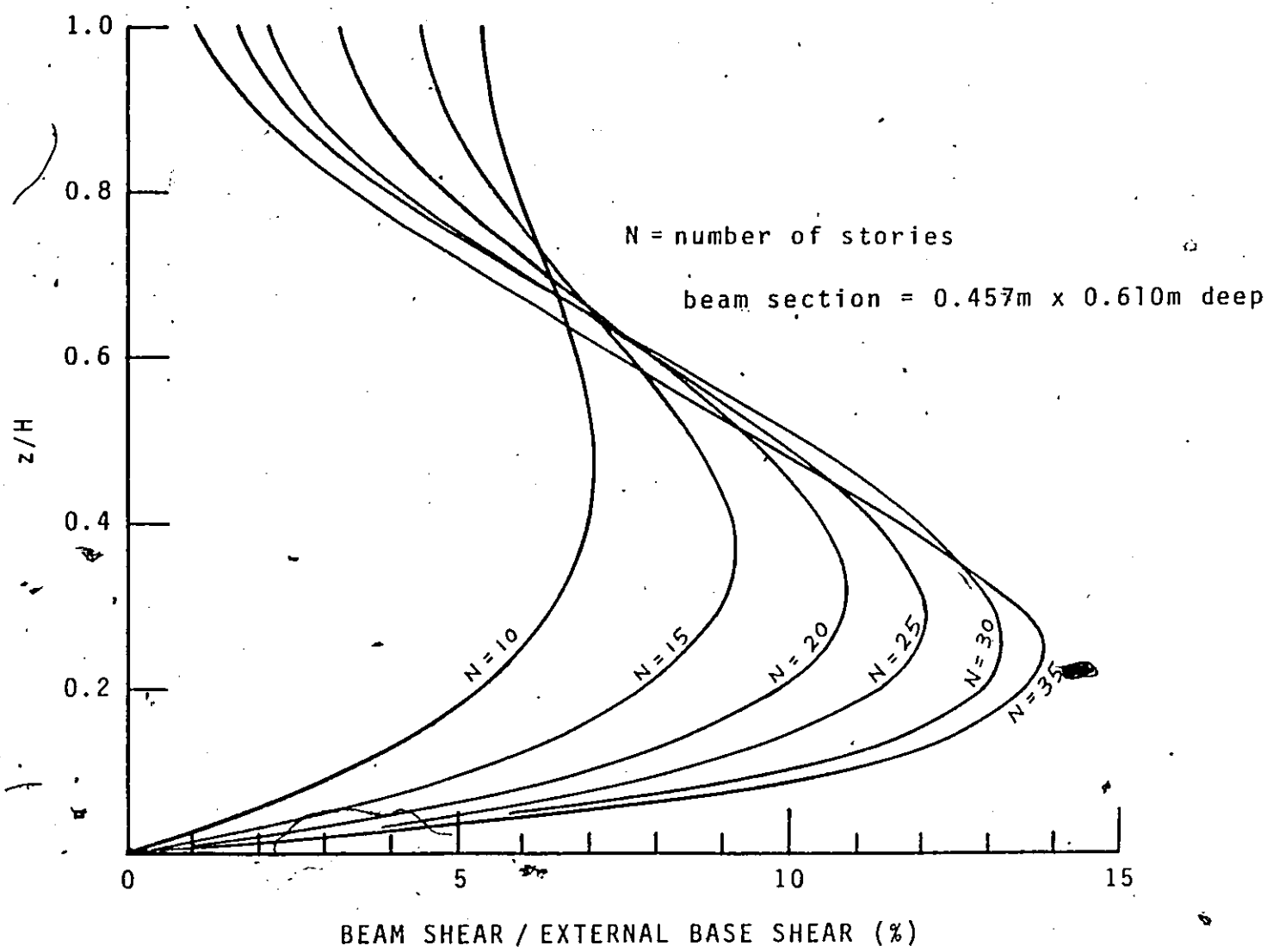

FIG. 2-14b: EFFECT OF STRUCTURE HEIGHT ON BEAM SHEARS

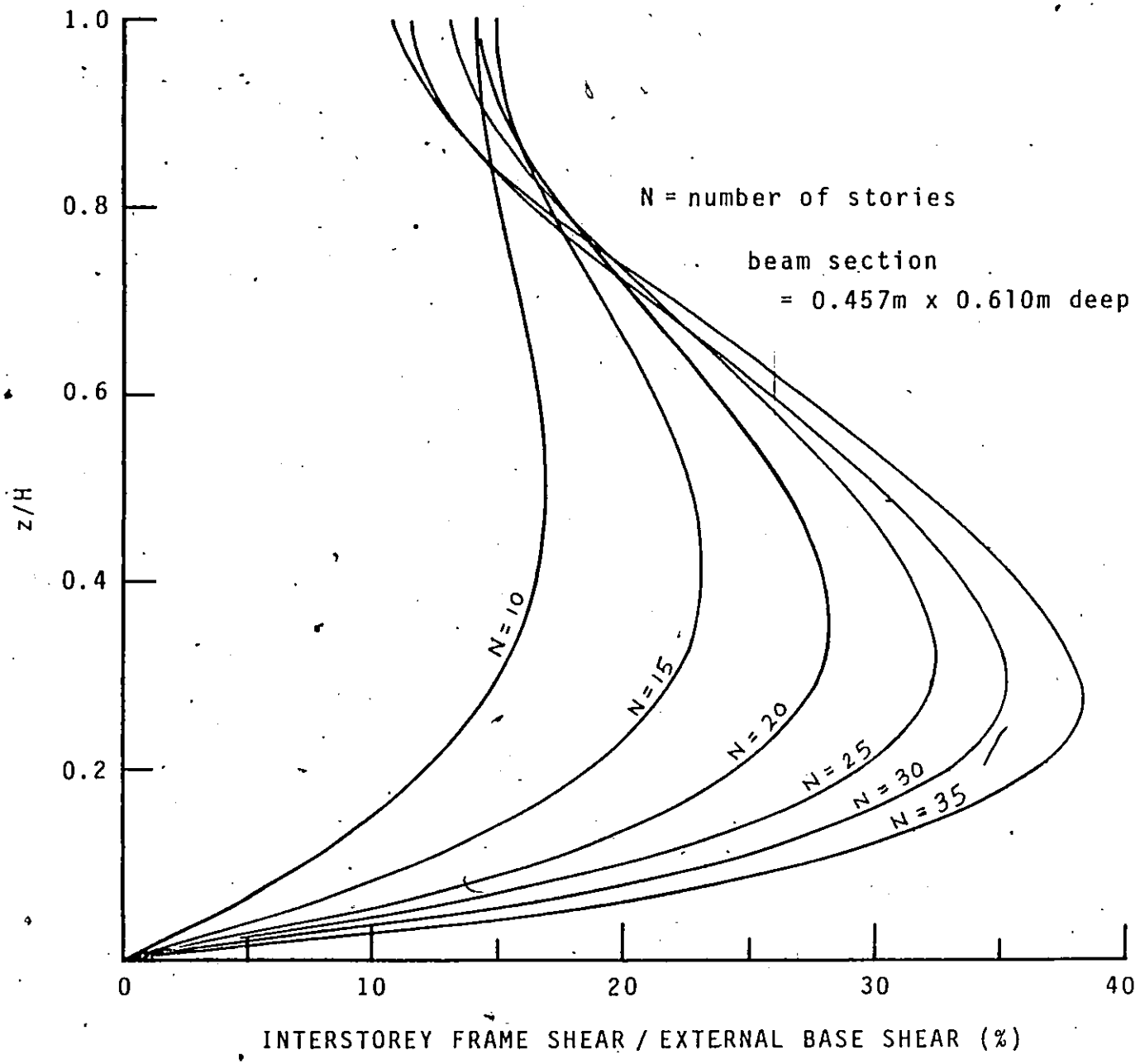

FIG. 2-14c: EFFECT OF STRUCTURE HEIGHT ON INTERSTOREY FRAME SHEAR

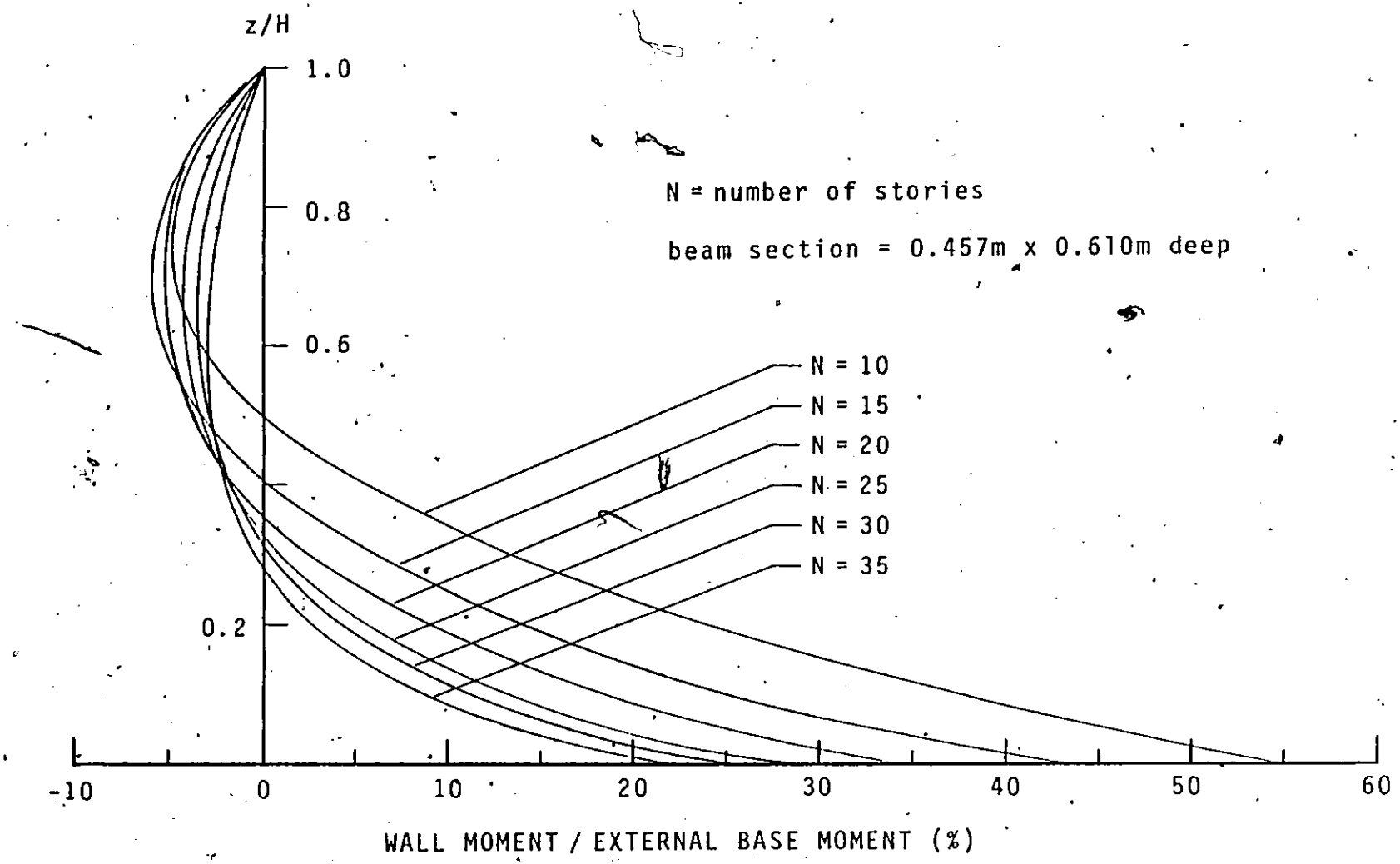

FIG. 2-14d: EFFECT OF STRUCTURE HEIGHT ON WALL MOMENT

TABLE 2-1 : COMMON DIMENSIONAL PROPERTIES OF WORKED EXAMPLES

number of bays in frame	2
bay width	4.57 m (15 ft)
column section	0.762mx0.762m(2.5ftx2.5ft)
girder section	0.457mx0.610m deep(1.5ftx2.0ft)
connecting beam section	0.457mx0.610m deep(1.5ftx2.0ft)
length of conn. beam	4.57 m (15 ft)
shear area of conn. beam	0.232 m^2(2.5 ft^2)
wall section	0.254mx6.10m(0.833ftx20ft)
floor height	3.05 m (10 ft)
Young's modulus	$2.07x10^{10}$ N/m^2(432000 ksf)
Poisson's ratio	0.15

CHAPTER III

NON-UNIFORM PLANAR WALL-FRAME STRUCTURES

3.1 INTRODUCTION

One of the basic assumptions made in the continuum analysis proposed in Chapter II is the uniformity of structural properties along the entire height of the shear wall-frame structure. However, in real structures, stepwise variations in structural properties along the height do occur for architectural and/or economical reasons. These variations include changes in floor height, material properties, and the sectional properties of the shear wall, the connecting beams and the columns and girders of the frame. Such stepwise non-uniformity can be accomodated by using the transfer matrix technique in conjunction with the continuum analysis.

The transfer matrix technique has been used in the analysis of a planar coupled shear wall structure by Tso and Chan [78], and in the torsional analysis of open section core structures [30] and the analysis of a planar shear wall-frame structure [29] by Heidebrecht and Stafford Smith. The basic principle of the technique is that the non-uniform

structure in question can be divided into a number of uniform segments. Each individual segment, being uniform within itself, can be analysed by the respective continuum analysis. The responses, in terms of deformation and force variables, of adjacent segments can then be inter-related by considerations of equilibrium and compatibility at the common boundaries between segments. These inter-relationships eventually culminate in a single relationships between the responses at the top and base of the structure. Boundary conditions for the overall structure can then be applied to solve for these responses. Based on these known responses and the relationships derived earlier between segments, the response at any height in the structure can be determined accordingly.

In this chapter, an analysis of a non-uniform planar wall-frame structure will be presented. An example will be illustrated to verify the proposed anslysis.

3.2 NOTATIONS

The following notations are used in this chapter. When a notation contains the i subcript, the quantity represented by the notation is meant to pertain to the i^{th} segment of the total structure unless otherwise stated. For simplicity and wherever appropriate, a group of notations which pertain to the same segment will be placed inside brackets with the associated subscript placed outside them; e.g., $(EI_w)_i$.

A_{bi} = effective shear area of connecting beam.

A_{cji} = cross-sectional area of column j (j=1,2,...n).

A_{wi} = cross-sectional area of shear wall.

d_{cji} = distance of column j from centroid of frame.

d_{fi} = equivalent moment arm of resultant couple formed by chord drift-induced axial forces in columns.

E_i, G_i = elastic modulus and shear modulus, respectively.

f_{ci} = axial force factor for column i ($1.1 \leq f_{ci} \leq 1.4$).

GA_i = shear stiffness of frame as shear beam.

h_i, H_i, H = floor height, length of segment, structure height.

I_{bi} = moment of inertia of connecting beam section.

I_{cji} = moment of inertia of column j.

I_{gj} = moment of inertia of girder j.

I_{wi} = moment of inertia of shear wall section.

ℓ_{fi}, ℓ_{wi} = distances from midspan of connecting beam to

ℓ_{bi} = length of connecting beam.

ℓ_{gj} = length of girder j.

$M_i(z)$ = external overturning moment at height z.

n = number of columns in frame (n > 1).

N = number of segments in total structure.

P_i = concentrated load at station i.

$q_i(z)$ = beam shear intensity at height z.

$T_i(z)$ = axial force in wall at height z.

$T_{cji}(z)$ = chord drift-induced axial force in column j at height z.

$V_i(z)$ = external horizontal shear at height z.

$y_i(z)$ = lateral deflection of structure at height z.

z, $\hat{z}$ = height variables with respect to bottom of segment i and bottom of structure, resp.

Eqn(s) = Equation(s).

3.3 STATEMENT OF PROBLEM

The non-uniform planar wall-frame structure under consideration is one in which changes in the structural properties of the shear wall, the frame, and the connecting medium occur at a number of discrete levels along the height H of the structure. Permissible changes include changes in floor height, material properties, and the sectional properties of the shear wall, the connecting medium, and the columns and girders of the frame. One limitation is that the centroidal axis of the shear wall remains unchanged throughout the entire height of the structure. The connecting medium can be floor slabs or lintel beams. In the case of the former, connecting beams of appropriate equivalent structural properties are substituted. In this analysis, all connecting beams are assumed to be fixed-ended at both ends.

A schematic picture of the wall-frame structure with stepwise structural changes is given in Figure 3-1. Each discrete level of change, including the top and the base of the structure, is defined as a station. The part of the structure between two stations is defined as a segment. Within each segment, no structural change is permitted. Applied lateral loads are represented by a number of concentrated loads acting at the stations. No loads are permitted within each segment. Stations and segments are numbered in

ascending order starting from the base. Assuming there are N segments in the structure, the base is taken to be station zero, the next higher station to be station 1, and so forth. Thus, the top of the structure is denoted as station N. Segment i is then the part of the structure between stations (i-1) and i. The elevation of a typical segment, say, segment i, of the wall-frame structure is shown in Figure 3-2. For ease of reference, the columns and girders are numbered as shown in the same diagram.

The collection of deformation and force quantities which defines the state at any particular location along the height of the structure is called a state vector. The state vectors immediately above and below station i are denoted by $\{\Phi\}_{iA}$ and $\{\Phi\}_{iB}$ respectively. Thus it follows that the state vectors at the top and the bottom of segment i are $\{\Phi\}_{iB}$ and $\{\Phi\}_{(i-1)A}$ respectively (Figure 3-3). Referring to Figure 3-3, the shear force and moment acting on segment i at the top are denoted by V_{iB} and M_{iB}, respectively, while those at the base are denoted by $V_{(i-1)A}$ and $M_{(i-1)A}$, respectively. The shear forces acting just above and below station i are denoted by V_{iA} and V_{iB} respectively, and the moments by M_{iA} and M_{iB} respectively. The concentrated load acting at station i is denoted by P_i.

In the analysis, the following assumptions are made:

1. Rigid diaphragm action of the floor system is assumed.
2. The height of the structure is constant across its plan.
3. Contraflexural points are assumed to be located at the midspan of the connecting beams and the columns and girders of the frame.
4. Shear deformation is neglected for the shear wall, columns, and girders.
5. The frame contains at least two columns and is assumed to be extended so that one-half of the span of the connecting beam at each floor level is included as a beam member of the frame.
6. The frame is replaced by a continuous shear beam with an equivalent shear stiffness of GA_i in segment i of the total structure.
7. The connecting beams are fixed-ended, and are replaced by a band of continuous laminae of equivalent structural properties.
8. Elastic behaviour is assumed.
9. The foundation of the structure is assumed to be rigid.

3.4 ANALYSIS OF TYPICAL SEGMENT — SEGMENT i

The analysis of a typical segment is essentially similar to that of a uniform wall-frame structure subjected to a concentrated load at the top. Thus the analysis proposed in Chapter II can be utilised here.

3.4.1 EQUILIBRIUM CONDITIONS

At any height z relative to the base of the segment, the horizontal shear force equilibrium is given by

$$-(EI_w)_i y_i''' + GA_i y_i' + \ell_{wi} q_i = V_{iB} \qquad (3\text{-}1)$$

Consideration of the vertical equilibrium of an elemental wall section of depth dz leads to

$$\frac{dT_i(z)}{dz} = - q_i(z) \qquad (3\text{-}2)$$

The axial force at height z in the wall is therefore given by

$$T_i(z) = T_{iB} + \int_z^{H_i} q_i(\bar{z})\, d\bar{z} \qquad (3\text{-}3)$$

where H_i is the length of segment i and T_{iB} is the axial force acting in the wall at the top of segment i.

3.4.2 COMPATIBILITY CONDITIONS

Referring to Section 2.4.2, and observing an initial relative vertical displacement δ_{ti} at the base of the segment due to the axial deformations of the wall and column 1 accumulated over all segments below segment i, the equation for vertical compatibility at the midspan of the connecting laminae is given by

$$\mu_i y_i' - \frac{q_i}{E_i \gamma_i} - s_i \int_0^z T_i d\bar{z} + \rho_i \int_0^z M_i d\bar{z} + (\rho EI_w)_i y'_{(i-1)A} + \delta_{ti} = 0 \qquad (3\text{-}4)$$

where $\mu_i = (\ell_w + \ell_e - \rho EI_w)_i$ (3-4a)

$\rho_i = [\ \ell_f/(d_{c1} d_f E A_{c1})\ ]_i$ (3-4b)

γ_i = stiffness factor of connecting laminae including shear deformation

$$= \frac{12 I_{bi}}{(\ell_b^3 h)_i} [\ 1 + \frac{12 (EI_b)_i}{(\ell_b^2 A_b G)_i}\ ]^{-1} \qquad (3\text{-}4c)$$

$s_i = \bar{s}_i + 1/(EA)_i$ (3-4d)

with $1/A_i = (1/A_w + f_c/A_{c1})_i$ (3-4e)

$\bar{s}_i = \rho_i [\ \ell_w + \ell_b/2 - (f_c - 1)\ell_{g1}\ ]_i$ (3-4f)

In Eqns(3-4e) and (3-4f), f_{ci} is the factor which allows for the larger axial force induced in column 1 by the lintel shears than that induced in the wall. In general, it varies between 1.1 and 1.4. The term $(\rho EI_w)_i y'_{(i-1)A}$ in Eqn(3-4) is derived from the integration of the wall moment term shown in Eqn(2-11d). The total initial relative displacement at the base of segment i, δ_{ti}, consists of three components such that

$$\delta_{ti} = \delta_{wi} + \delta_{ci} + \delta_{di} \qquad (3\text{-}4g)$$

where δ_{wi}, δ_{ci}, and δ_{di} are the initial relative displacements at the base of segment i due to the axial force in the wall, the beam shear-induced axial force in column 1, and the chord drift-induced axial force in the same column, respectively, accumulated over all segments below i, and are given by

$$\delta_{wi} = - \sum_{j=1}^{i-1} \frac{1}{(EA_w)_j} \int_0^{H_j} T_j \, d\bar{z} \qquad (3\text{-}4h)$$

$$\delta_{ci} = - \sum_{j=1}^{i-1} \frac{1}{(EA_{cl})_j} \int_0^{H_j} f_{cj} T_j \, d\bar{z} \qquad (3\text{-}4i)$$

$$\delta_{di} = \sum_{j=1}^{i-1} (\rho d_f)_j \int_0^{H_j} T_{clj} \, d\bar{z} \qquad (3\text{-}4j)$$

3.4.3 DERIVATION OF FINAL DIFFERENTIAL EQUATION AND SOLUTION

Re-arranging Eqn(3-4), there is obtained

$$y_i' = \frac{1}{\mu_i}\left[\frac{q_i}{E_i\gamma_i} + s_i \int_0^z T_i d\bar{z} - \rho_i \int_0^z M_i d\bar{z} - (\rho EI_w)_i y'_{(i-1)A} - \delta_{ti}\right] \quad (3\text{-}5)$$

Successive differentiations of Eqn(3-5) and the use of Eqn(3-2) lead to the following equations:

$$y_i'' = \frac{1}{\mu_i}\left[\frac{q_i'}{E_i\gamma_i} + s_i T_i - \rho_i M_i\right] \quad (3\text{-}6)$$

$$y_i''' = \frac{1}{\mu_i}\left[\frac{q_i''}{E_i\gamma_i} - s_i q_i - \rho_i M_i'\right] \quad (3\text{-}7)$$

$$y_i^{iv} = \frac{1}{\mu_i}\left[\frac{q_i'''}{E_i\gamma_i} - s_i q_i' - \rho_i M_i''\right] \quad (3\text{-}8)$$

$$y_i^{v} = \frac{1}{\mu_i}\left[\frac{q_i^{iv}}{E_i\gamma_i} - s_i q_i'' - \rho_i M_i'''\right] \quad (3\text{-}9)$$

Differentiating Eqn(3-1) twice yields the following equations:

$$-(EI_w)_i y_i^{iv} + GA_i y_i'' + \ell_{wi} q_i' = 0 \quad (3\text{-}10)$$

$$-(EI_w)_i y_i^{v} + GA_i y_i''' + \ell_{wi} q_i'' = 0 \quad (3\text{-}11)$$

Substituting Eqns(3-7) and (3-9) into Eqn(3-11), and noting the following relationships:

$$M_i = M_{iB} + V_{iB}(H_i - z) \tag{3-12a}$$

$$M_i' = - V_{iB} \tag{3-12b}$$

$$M_i'' = M_i''' = 0 \tag{3-12c}$$

there is obtained

$$q_i^{iv} - \beta_i q_i'' + \phi_i q_i = \zeta_i V_{iB} \tag{3-13}$$

where

$$\beta_i = \left(\frac{\ell_w \mu \gamma}{I_w} \right)_i + (sE\gamma)_i + \left(\frac{GA}{EI_w} \right)_i \tag{3-13a}$$

$$\phi_i = \left(\frac{GA}{EI_w} \cdot sE\gamma \right)_i \tag{3-13b}$$

$$\zeta_i = \left(\frac{GA}{EI_w} \cdot \rho E\gamma \right)_i \tag{3-13c}$$

With reference to Section 2.4.4, the complete solution to Eqn(3-13) is given by:

$$q_i(z) = C_{1i}\cosh(m_i z) + C_{2i}\sinh(m_i z) + C_{3i}\cosh(n_i z) + C_{4i}\sinh(n_i z) + (\zeta/\phi)_i V_{iB} \qquad (3\text{-}14)$$

where

$$m_i = \frac{1}{\sqrt{2}}\left[\beta_i + \sqrt{(\beta_i^2 - 4\phi_i)}\right]^{1/2} \qquad (3\text{-}14a)$$

$$n_i = \frac{1}{\sqrt{2}}\left[\beta_i - \sqrt{(\beta_i^2 - 4\phi_i)}\right]^{1/2} \qquad (3\text{-}14b)$$

3.5 TRANSFER MATRIX TECHNIQUE

The transfer matrix technique consists in deriving relationships between the states at the top and bottom of each segment and between the states just above and below each station, and finally obtaining a single relationship between the states at the top and bottom of the overall structure. Boundary conditions of the overall structure can then be applied to solve for the unknowns in the two boundary states. Any intermediate state can accordingly be determined by a process of back-substitution through the derived relationships between adjacent states.

3.5.1 SEGMENT TRANSFER MATRIX FOR SEGMENT i

The state vectors at the top and bottom of segment i, namely, $\{\Phi\}_{iB}$ and $\{\Phi\}_{(i-1)A}$ respectively, are defined as follows:

$$\{\Phi\}_{iB} = \text{col.}\{q,\ q',\ q''',\ T,\ y,\ y',\ V,\ M\}_{iB} \qquad (3\text{-}15)$$

$$\{\Phi\}_{(i-1)A} = \text{col.}\{q,\ q',\ q''',\ T,\ y,\ y',\ V,\ M\}_{(i-1)A} \qquad (3\text{-}16)$$

Making use of the equations derived in Section 3.4, any intermediate state at height z within the segment, denoted by $\{\Phi(z)\}_i$, can be related to a vector $\{R\}_i$ through an 8x8 matrix $[\lambda(z)]_i$ such that

$$\{\Phi(z)\}_i = [\lambda(z)]_i \{R\}_i \tag{3-17}$$

where

$$\{R\}_i = \text{col.}\{C_{1i}, C_{2i}, C_{3i}, C_{4i}, T_{iB}, y_{iB}, V_{iB}, M_{iB}\} \tag{3-17a}$$

The matrix $[\lambda(z)]_i$ is shown in details in Appendix D.

The state vectors $\{\Phi\}_{iB}$ and $\{\Phi\}_{(i-1)A}$ are therefore given by

$$\{\Phi\}_{iB} = [\lambda(z=H_i)]_i \{R\}_i \tag{3-18}$$

$$\{\Phi\}_{(i-1)A} = [\lambda(z=0)]_i \{R\}_i \tag{3-19}$$

and can be related to each other by a segment transfer matrix $[F]_i$ such that

$$\{\Phi\}_{iB} = [F]_i \{\Phi\}_{(i-1)A} \tag{3-20}$$

where $$[F]_i = [\lambda(z=H_i)]_i [\lambda(z=0)]_i^{-1} \tag{3-20a}$$

3.5.2 STATION TRANSFER MATRIX FOR STATION i

From considerations of continuity requirements between segments and equilibrium conditions at stations, the state vector at the top of segment i, $\{\Phi\}_{iB}$, can further be related to that at the bottom of segment (i-1), $\{\Phi\}_{iA}$, by a station transfer matrix $[S]_i$ and a load transfer vector $\{L\}_i$

such that

$$\{\Phi\}_{iA} = [S]_i\{\Phi\}_{iB} + \{L\}_i \qquad (3\text{-}21)$$

The elements of $[S]_i$ and $\{L\}_i$ are determined from the following continuity and equilibrium requirements:

(1) The lateral displacements just above and below station i are equal. Thus,

$$y_{iA} = y_{iB} \qquad (3\text{-}22a)$$

(2) The slopes of the deflection curve just above and below station i are equal. Thus,

$$y'_{iA} = y'_{iB} \qquad (3\text{-}22b)$$

(3) The axial forces in the wall just above and below station i are equal. Thus,

$$T_{iA} = T_{iB} \qquad (3\text{-}22c)$$

(4) The internal moments of the wall just above and below station i are equal. Thus,

$$y''_{iA} = [(EI_w)_i/(EI_w)_{(i+1)}]\, y''_{iB} \qquad (3\text{-}22d)$$

The external moments just above and below station i are also equal. Thus,

$$M_{iA} = M_{iB} \tag{3-22e}$$

(5) The horizontal equilibrium of station i leads to

$$V_{iA} = V_{iB} - P_i \tag{3-22f}$$

(6) Applying Eqn(3-5) at the top of segment i and at the bottom of segment (i+1) separately, and making use of Eqn(3-22b), there is obtained

$$q_{iA} = \frac{(E\gamma)_{i+1}}{(E\gamma)_i} q_{iB} + (E\gamma)_{i+1}\{(\mu_{i+1} - \mu_i) + [(\rho EI_w)_{i+1} - (\rho EI_w)_i]\} y'_{iB} \tag{3-22g}$$

(7) Substituting Eqn(3-6) into Eqn(3-22d) and utilising Eqns(3-22c) and (3-22e), there is obtained

$$q'_{iA} = \frac{\alpha_i}{\alpha_{i+1}} q'_{iB} + \xi_i T_{iB} + n_i M_{iB} \tag{3-22h}$$

where

$$\alpha_i = [I_w/(\mu\gamma)]_i \tag{3-22i}$$

$$\xi_i = [(sEI_w/\mu)_i - (sEI_w/\mu)_{i+1}]/\alpha_{i+1} \tag{3-22j}$$

$$n_i = -[(\rho EI_w/\mu)_i - (\rho EI_w/\mu)_{i+1}]/\alpha_{i+1} \tag{3-22k}$$

(8) Substituting Eqn(3-6) into Eqn(3-10) for y_i'', and isolating the y^{iv} term, there is obtained

$$y^{iv} = \left(\frac{GA}{EI_w}\right)_i \left\{\frac{1}{\mu_i}\left[\frac{q_i'}{E_i\gamma_i} + s_i T_i - \rho_i M_i\right]\right\} + \left(\frac{\ell_w}{EI_w}\right)_i q_i' \qquad (3\text{-}22\ell)$$

Equating Eqn(3-22ℓ) to Eqn(3-8), and noting that $M_i'' = 0$, there is obtained

$$q_i''' = \beta_i q_i' + \phi_i T_i - \zeta_i M_i \qquad (3\text{-}22m)$$

Applying Eqn(3-22m) at the top of segment i and at the base of segment (i+1) separately, and making use of Eqns(3-22c), (3-22e), and (3-22h), the following continuity equation is obtained:

$$q_{iA}''' = U_i q_{iB}''' + \Gamma_i q_{iB}' + \psi_i M_{iB} \qquad (3\text{-}22n)$$

where $$U_i = \left[\beta_{i+1}\xi_i + \phi_{i+1}\right]/\phi_i \qquad (3\text{-}22p)$$

$$\Gamma_i = \left[\beta_{i+1}\alpha_i/\alpha_{i+1} - U_i\beta_i\right] \qquad (3\text{-}22q)$$

$$\psi_i = \left[U_i\zeta_i + \beta_{i+1}\eta_i - \zeta_{i+1}\right] \qquad (3\text{-}22r)$$

The station transfer matrix $[S]_i$ and the load transfer vector $\{L\}_i$ can thus be constructed from Eqns(3-22a) through (3-22r). Details of $[S]_i$ and $\{L\}_i$ are given in Appendix E.

3.5.3 STRUCTURE TRANSFER MATRIX

Applying Eqns(3-20) and (3-21) to each segment and station of the structure, respectively, the following equations are obtained:

$$
\begin{aligned}
\{\Phi\}_{1B} &= [F]_1\{\Phi\}_o \\
\{\Phi\}_{1A} &= [S]_1\{\Phi\}_{1B} + \{L\}_1 \\
\{\Phi\}_{2B} &= [F]_2\{\Phi\}_{1A} \\
&\cdots\cdots\cdots\cdots\cdots \\
\{\Phi\}_{NB} &= [F]_N\{\Phi\}_{(N-1)A} \\
\{\Phi\}_{NA} &= [S]_N\{\Phi\}_{NB} + \{L\}_N
\end{aligned}
\qquad (3\text{-}23)
$$

Taking note that $[S]_N$ is an identity matrix, the N^{th} station need not be considered if the load at that station, P_N, is considered as one of the boundary conditions. By successive substitutions of Eqns(3-23), the relationships between the states at the top and bottom of the structure can be established as

$$\{\Phi\}_{NB} = [\bar{F}]\{\Phi\}_o + \{\bar{L}\} \qquad (3\text{-}24)$$

where $[\bar{F}]$ = structure transfer matrix

$$= \prod_{i=1}^{i=N} ([S]_i [F]_i) \qquad (3\text{-}25)$$

$\{\bar{L}\}$ = structure load vector

$$= \sum_{i=1}^{N-1} \left(\prod_{r=i+1}^{N} [S]_r [F]_r \right) \{L\}_i \qquad (3\text{-}26)$$

It is to be noted that in Eqn(3-25) and Eqn(3-26), the " Π " operation represents pre-multiplication.

3.5.4 BOUNDARY CONDITIONS FOR TOTAL STRUCTURE

The state vectors $\{\Phi\}_{NB}$ and $\{\Phi\}_o$ can be determined from the following boundary conditions:

(1) At the base, as geometric requirements,

$$y_o = 0 \qquad (3\text{-}27a)$$

$$y'_o = 0 \qquad (3\text{-}27b)$$

(2) Applying Eqn(3-4) at the base of segment 1 and utilising Eqn(3-27b), there is obtained

$$q_o = 0 \qquad (3\text{-}27c)$$

(3) At the top, axial forces and moments vanish. Thus,

$$T_{NB} = 0 \qquad (3\text{-}27d)$$

$$M_{NB} = 0 \qquad (3\text{-}27e)$$

$$y''_{NB} = 0 \qquad (3\text{-}27f)$$

Therefore, from Eqn(3-6) applied at the top, there is obtained

$$q'_{NB} = 0 \qquad (3\text{-}27g)$$

(4) In the light of Eqns(3-27d) through (3-27g), the following condition is obtained by applying Eqn(3-22m) at the top of the structure:

$$q'''_{NB} = 0 \qquad (3\text{-}27h)$$

Furthermore, at the top,

$$V^{\theta}_{NB} = P_N \qquad (3\text{-}27i)$$

Substituting the above boundary conditions into Eqn(3-24) leads to a set of simultaneous equations from which the state vectors $\{\Phi\}_{NB}$ and $\{\Phi\}_o$ can be determined completely. Any intermediate state vector can then be found using Eqn(3-23).

3.6 VERIFICATION OF PROPOSED ANALYSIS

An example of a 20-storey non-uniform wall-frame structure has been worked out using the proposed technique. The structure consists of a frame with two bays, each bay being 4.57m (15ft) wide, and a 6.10m (20ft) wide shear wall coupled together by fixed-ended connecting beams of length 4.57m (15ft) as shown in Figure 3-4. The structure is divided into three uniform segments. The dimensional properties pertinent to each segment are shown in Table 3-1. f_{ci} is taken to be 1.2 for all segments. A uniformly distributed load of intensity 22kN/m (1.5K/ft) is approximated by a series of concentrated loads acting at floor levels: 33.4kN (7.5K) at the top and 66.8kN (15K) at each of the remaining floor (except the ground level) as shown in Figure 3-4. Results for lateral deflection, beam shear, interstorey shear in the wall, and wall moment are shown in Figure 3-5 through Figure 3-8. The corresponding results given by SAP-IV [62] are also shown in the same figure for comparison. Good agreement can be observed.

3.7 CONCLUSION

A method of analysis of non-uniform planar wall-frame structure subjected to lateral loads has been presented. The proposed method combines the convenience of the continuum approach and the flexibility of the transfer matrix technique. While structural properties must remain constant within a segment, changes are permitted between segments. The only limitation regarding such change is that the vertical centroidal axis of the wall must remain constant throughout the entire height of the structure. Lateral loadings are approximated by a number of concentrated loads applied at each floor level where a station is defined.

An example has been worked out using the proposed analysis and the results checked with a matrix method frame program (SAP-IV). Close agreement has been observed.

Use of the transfer matrix technique in conjunction with the continuum approach renders the latter capable of analysing structures with stepwise changes in structural properties, which include changes in floor height, material properties, and the sectional properties of the structural members. It allows the structure to be analysed as a discrete system by the inclusion of as many segments as there are storeys. It also provides a convenient way of obtaining the flexibility matrix of the structure. By inverting this matrix, the corresponding stiffness matrix is obtained.

The stiffness matrix can then be used to determine the dynamic properties of the structure.

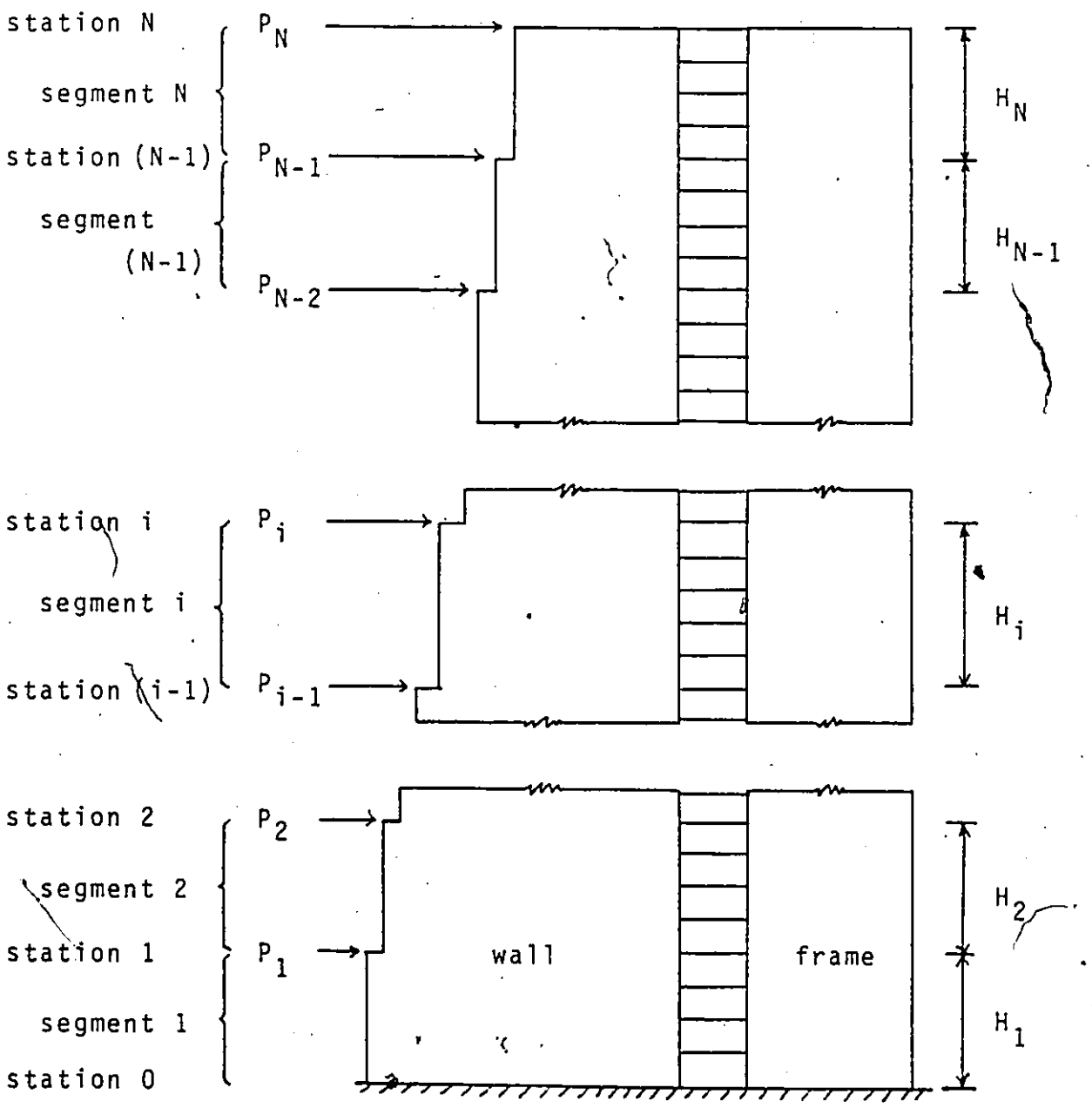

FIG. 3-1: SCHEMATIC REPRESENTATION OF NON-UNIFORM WALL-FRAME STRUCTURE

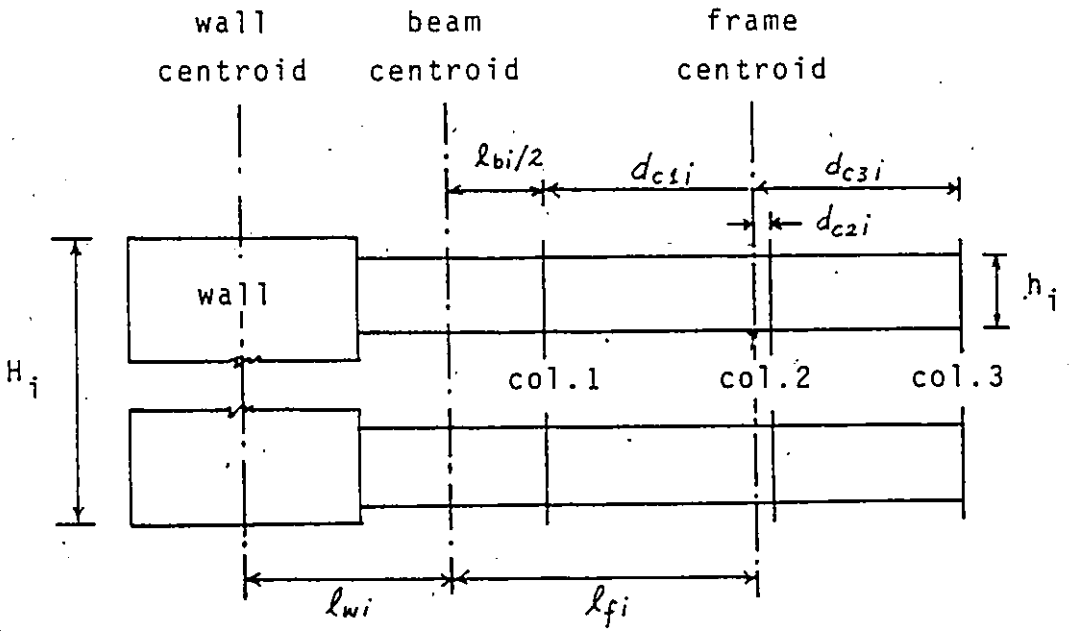

FIG. 3-2: ELEVATION OF TYPICAL SEGMENT (SEGMENT i)

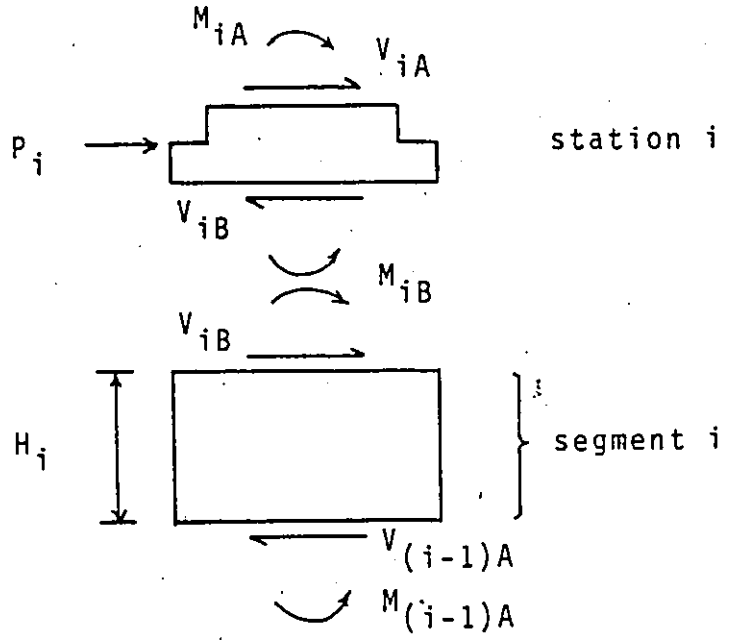

FIG. 3-3: FORCES AND MOMENTS ACTING ON STATION i AND SEGMENT i

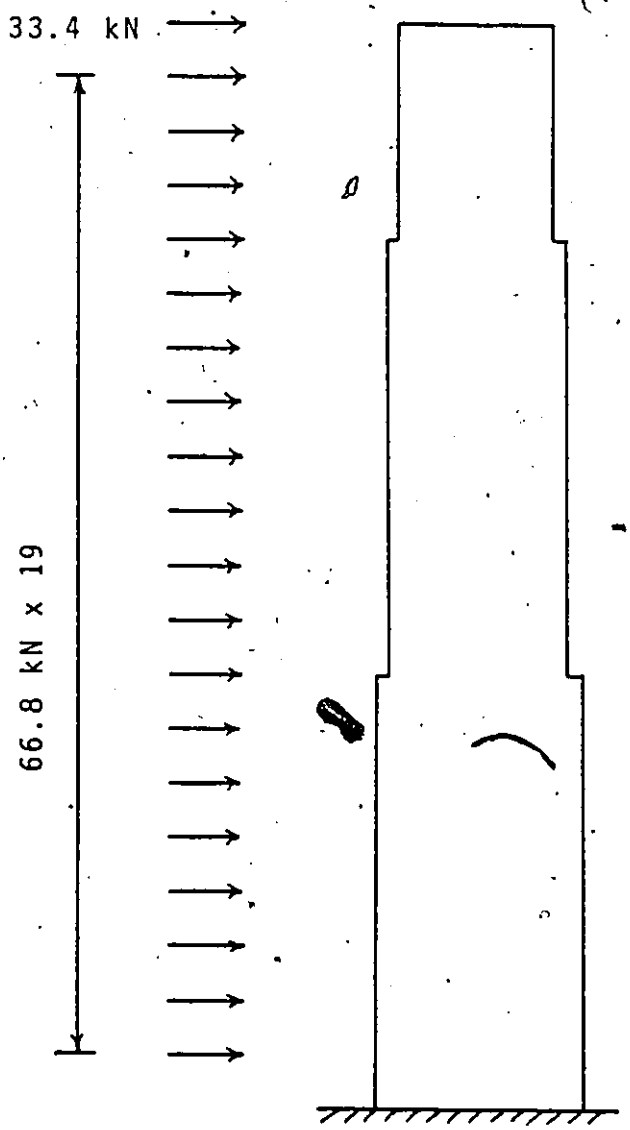

FIG. 3-4: LOADING CONDITIONS OF EXAMPLE STRUCTURE

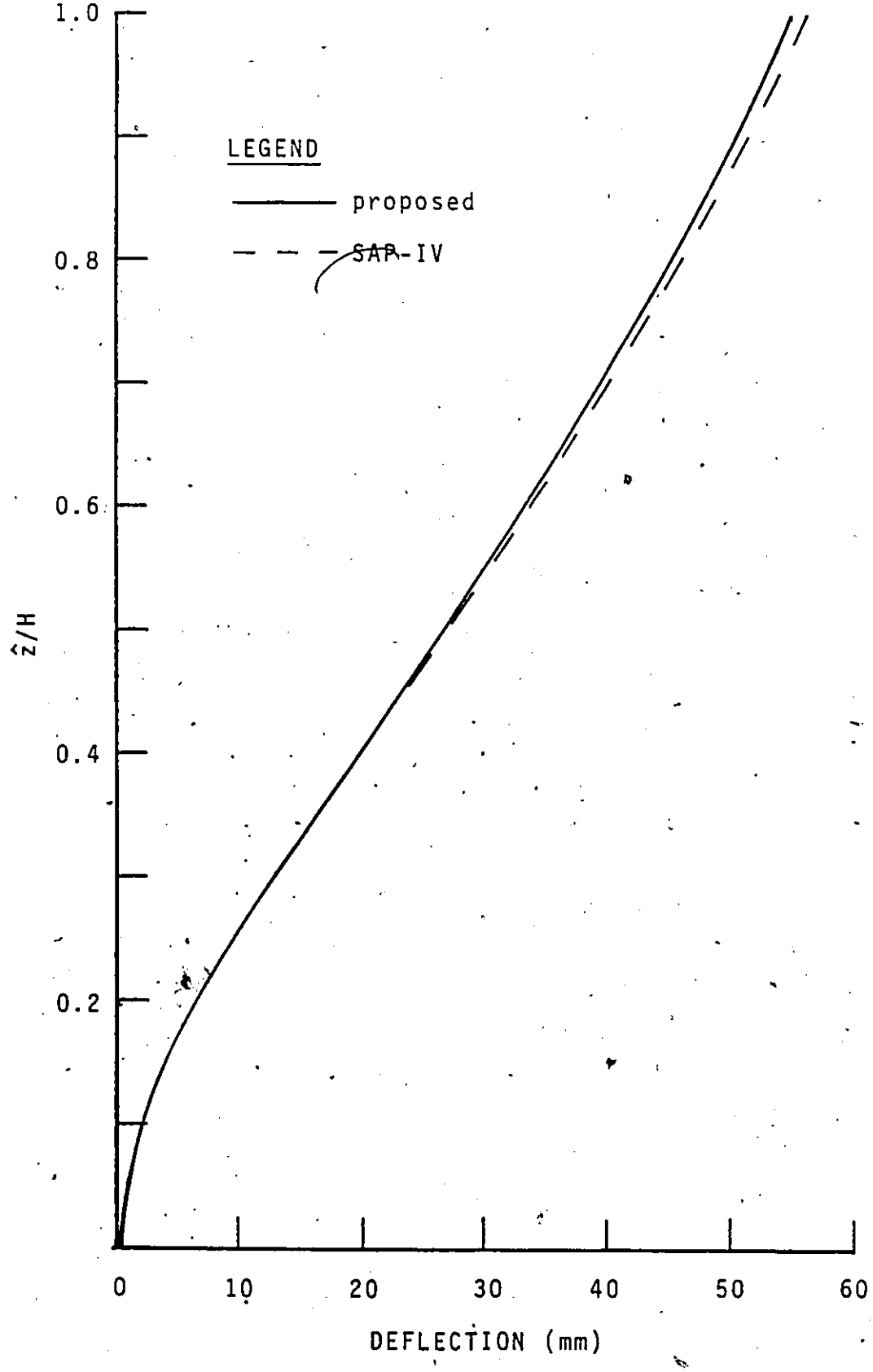

FIG. 3-5: NON-UNIFORM EXAMPLE – LATERAL DEFLECTION

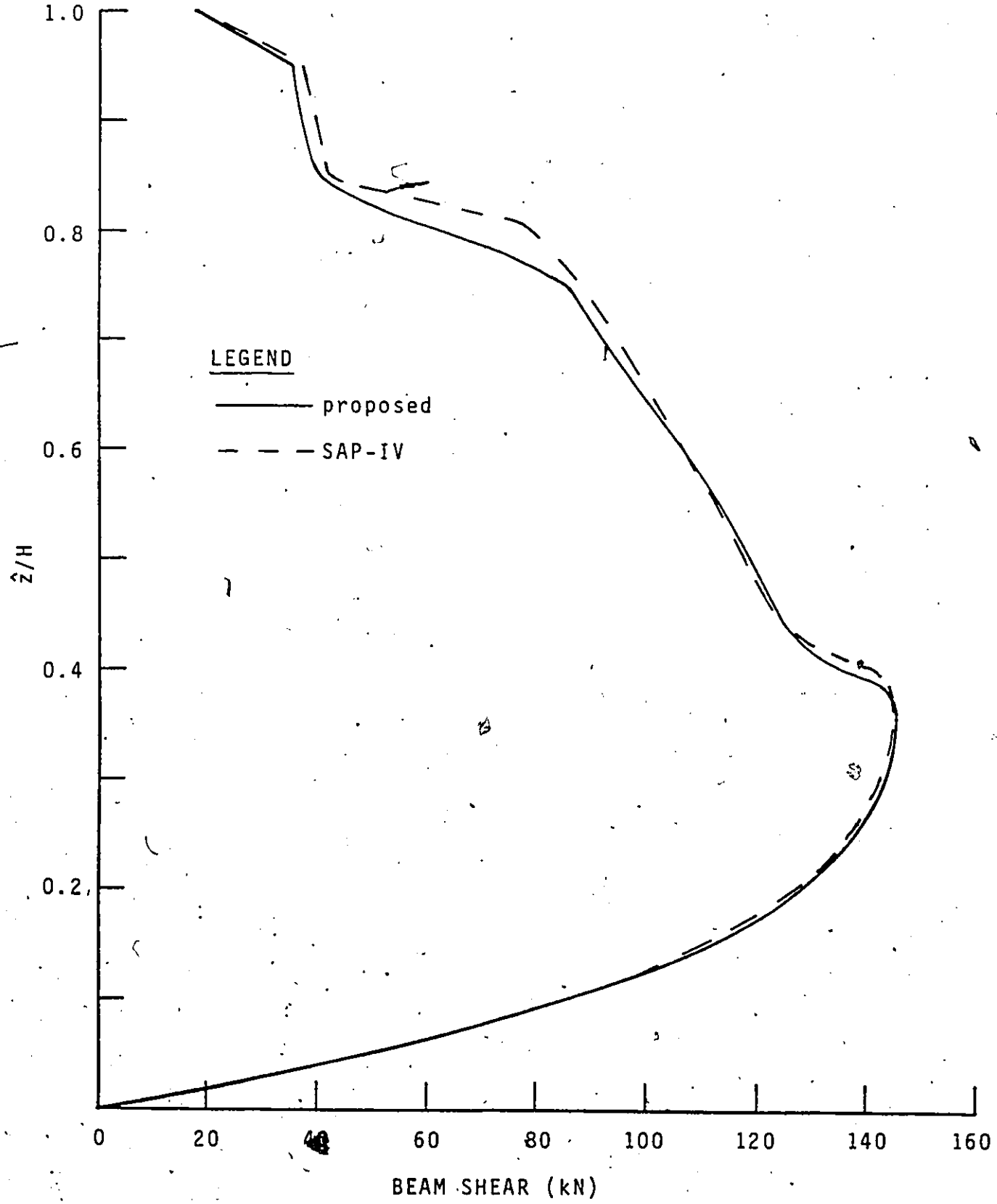

FIG. 3-6: NON-UNIFORM EXAMPLE — CONNECTING BEAM SHEAR

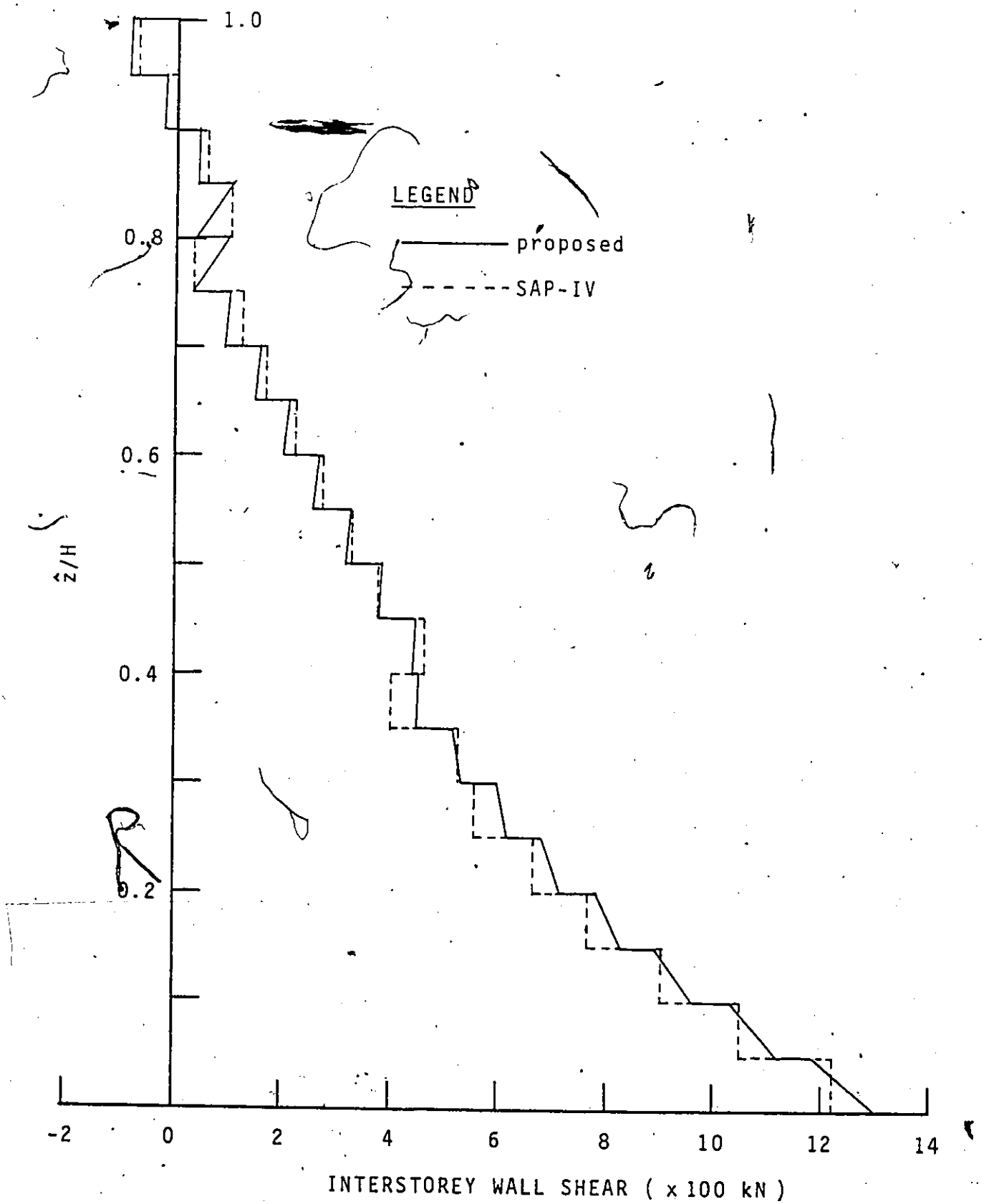

FIG. 3-7: NON-UNIFORM EXAMPLE — INTERSTOREY WALL SHEAR

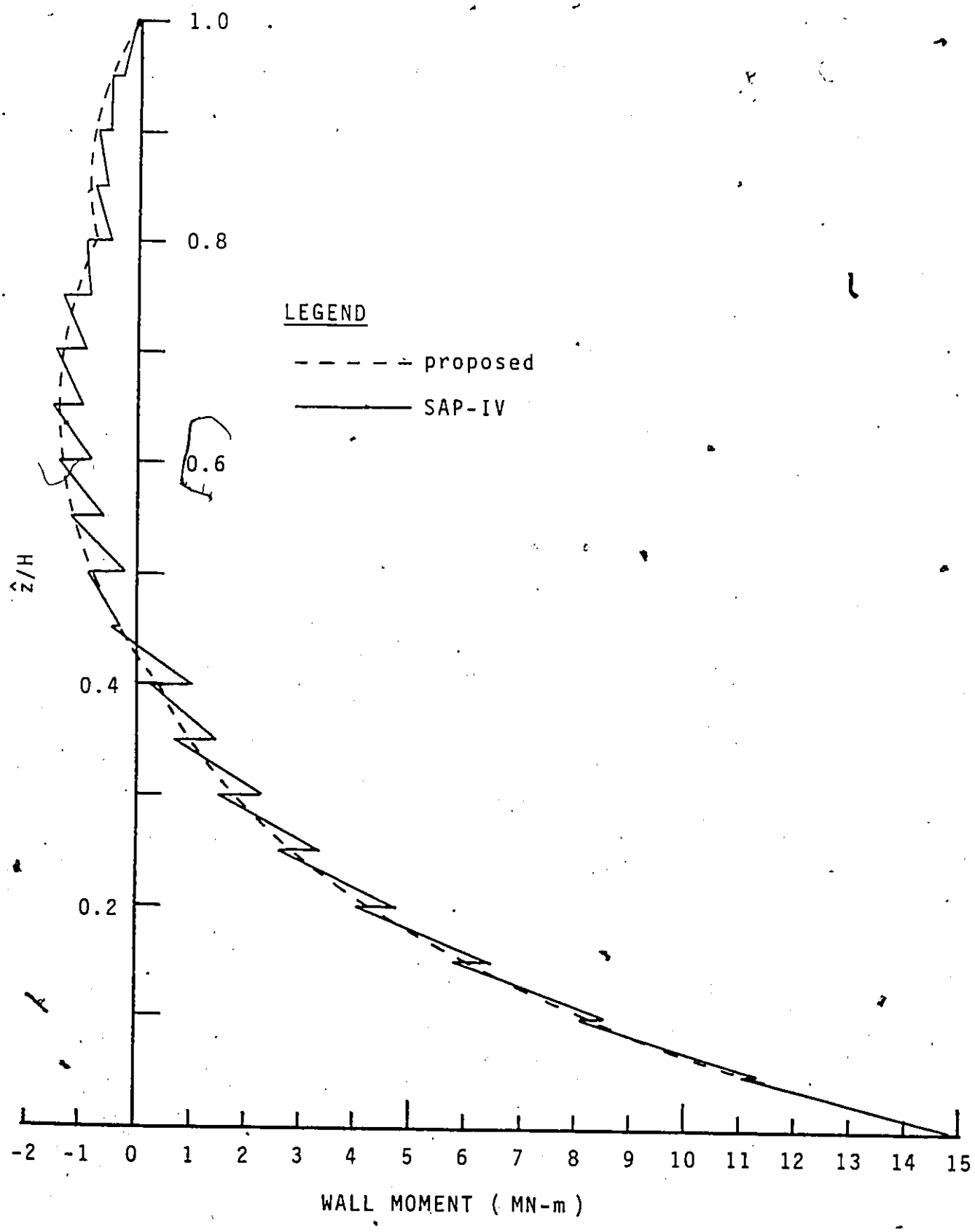

FIG. 3-8: NON-UNIFORM EXAMPLE – WALL MOMENT

TABLE 3-1 : DIMENSIONAL PROPERTIES OF EXAMPLE STRUCTURE

	segment		
	1	2	3
column section	762mm square (30in.sq.)	660mm square (26in. sq.)	559mm square (22in.sq.)
girder and conn. beam sections	508mmx610mm (20"x24"deep)	457mmx610mm (18"x24"deep)	406mmx508mm (16"x20"deep)
wall thickness	305mm (12in.)	254mm (10in.)	203mm (8in.)
no. of storeys	8	8	4
shear area factor of conn.beam	5/6	5/6	5/6
floor height	3.05m (10ft)		
length of conn. beam	4.57m (15ft)		
bay width	4.57m (15ft)		
Young's modulus	20,700MPa (432,000ksf)		
Poisson's ratio	0.15		

CHAPTER IV

THREE-DIMENSIONAL ANALYSIS OF UNIFORM WALL-FRAME STRUCTURES

4.1 INTRODUCTION

The structural layout of a general wall-frame building often exhibits asymmetry due to architectural reasons. When such a building is subjected to lateral loads caused by wind or seismic forces, torsional deformation of the building will be incurred in addition to horizontal translational displacements. Under such circumstances, a general three-dimensional analysis becomes necessary in order to ascertain the loads acting on the various resisting components of the building structure.

A multitude of three-dimensional methods of analysis for wall-frame structures have been proposed by various researchers. These have been reviewed in Chapter I. Many of these methods are limited to wall-frame structures comprised of parallel planar assemblages of walls and frames [9, 25, 41, 60, 82], while others consider arbitrarily oriented planar assemblages [71] or simple uncoupled open-section shear walls and frames [8, 70]. Of all these analyses, none

considers general coupling between walls or between walls and frames.

In this chapter, a general three-dimensional analysis of uniform wall-frame structures will be presented. Based on Vlasov's thin-walled beam theory [80], the shear walls will be generally treated as thin-walled beams. The frames will be modelled as shear beams in approximation of their horizontal shearing action. The out-of-plane stiffness of floor slabs will be approximated by connecting beams properly located and having appropriate stiffnesses. Vertical compatibility between interconnected shear walls or interconnected shear walls and frames via connecting beams will be taken into account. However, vertical compatibility between intersecting frames is not enforced. In deriving the vertical compatibility condition between a shear wall and a frame, the effect of shear lag in transmitting axial effects in the columns of the latter will be considered. Rigid diaphragm action of the floor system will be assumed so that the overall deformation of the wall-frame structure can be defined by only three displacement functions representing horizontal translations in two perpendicular directions and rotation about a vertical axis. After the theory is presented, an example will be solved and the results compared with those from a three-dimensional matrix method program. Advantages and limitations of the theory will also be discussed.

4.2 NOTATIONS

The following symbols will be used in this chapter:

A_{bk}, $\bar{A}_{bi}$, $\hat{A}_{bj}$ = shear areas of k^{th} band of type 1, i^{th} band of type 2, and j^{th} band of type 3 connecting beams, respectively.

A_m, A_{cji} = cross-sectional areas of wall m and column C_{ji}, respectively.

$[\tilde{A}]$ = axial deformation matrix (Appendix G).

d_{cji} = in-plane distance of column C_{ji} from centroid of respective frame ($i = 1, 2, \ldots \bar{n}_\ell$).

E, G = Young's modulus and shear modulus, respectively.

$f_{j\ell}$ = axial effect factor for column C_{j1} of frame ℓ.

GA_ℓ = equivalent shear stiffness of frame ℓ.

h, H = storey height and structure height, respectively.

K, I, J = numbers of type 1, type 2, and type 3 connecting beams, respectively.

$\tilde{I}_{bk}$, $\bar{I}_{bi}$, $\hat{I}_{bj}$ = moments of inertia of k^{th} band of type 1, i^{th} band of type 2, and j^{th} band of type 3 connecting beams, respectively.

$\bar{I}_{xm}$, $\bar{I}_{ym}$ = principal moments of inertia of wall m about $\bar{X}_m$- and $\bar{Y}_m$-axes, respectively.

I_{xm}, I_{ym}, I_{xym} = moments of inertia of wall m about global X- and Y-directions, and product of inertia with respect to global X- and Y-directions, respectively.

$\bar{I}_{\omega m}$ = principal sectorial moment of inertia of wall m.

J_m = St. Venant's torsional stiffness of wall m.

ℓ_{bk}, $\bar{\ell}_{bi}$, $\hat{\ell}_{bj}$ = clear span lengths of k^{th} band of type 1, i^{th} band of type 2, and j^{th} band of type 3 connecting beams, respectively.

ℓ_{gcl}, I_{gcl} = length and moment of inertia, respectively, of girder connected to column C_{jl}.

$\{L\}$ = col. $\{ -V_x \quad -V_y \quad -Q_t \}$

L, M = numbers of frames and shear walls, respectively.

$\bar{n}_\ell$ = number of columns in frame ℓ.

$\{P_x \; P_y \; P_t\}$col. = vector of concentrated loads at top.

$\{p_x \; p_y \; p_t\}$col. = vector of uniformly distributed loads.

$\{\bar{p}_x \; \bar{p}_y \; \bar{p}_t\}$col. = vector of triangularly distributed loads.

$Q_t(z)$, Q_{to} = applied torque at z and base torque, respectively.

q_k, $\bar{q}_i$, $\hat{q}_j$ = distributed shears in k^{th} band of type 1, i^{th} band of type 2, and j^{th} band of type 3 connecting laminae, respectively.

r_{xk}, r_{yk} = distances between centroids of walls connected by k^{th} band of type 1 beams along the X- and Y-directions, respectively.

$\hat{r}_{xj}$, $\hat{r}_{yj}$ = distances between centroid of wall m and midspan of the j^{th} band of type 3 beams that connects the wall to a frame, measured along the X- and Y-directions, respectively.

$r_{\theta k}$, $\bar{r}_{\theta i}$, $\hat{r}_{\theta j}$ = effective sectorial co-ordinates at the midspan of the k^{th} band of type 1, i^{th} band of type 2, and j^{th} band of type 3 beams, respectively.

$T_m(z)$ = axial force at centroid of wall m at height z.

$V_x(z)$, $V_y(z)$ = external X-direction and Y-direction horizontal shears, respectively, at height z.

V_{xo}, V_{yo} = external X-direction and Y-direction base shears, respectively.

X, Y, Z, O = global axes and origin.

$\bar{X}_m$, $\bar{Y}_m$ = principal axes of wall m.

$\bar{X}_\ell$, $\bar{Y}_\ell$ = local axes of frame ℓ.

x_{cji}, y_{cji} = global co-ordinates of column C_{ji}.

x_{em}, y_{em} = global co-ordinates of centroid of wall m.

x_{cm}, y_{cm} = global co-ordinates of shear centre of wall m.

$x_{o\ell}$, $y_{o\ell}$ = global co-ordinates of origin of local axes

of frame ℓ.

$\bar{x}_{cm}$, $\bar{y}_{cm}$ = co-ordinates of shear centre of wall m with respect to O along the $\bar{X}_m$- and $\bar{Y}_m$-directions, respectively.

$\bar{x}_{o\ell}$, $\bar{y}_{o\ell}$ = co-ordinates of origin of local axes of frame ℓ with respect to O along the $\bar{X}_\ell$- and $\bar{Y}_\ell$-directions, respectively.

x_{bk}, y_{bk} = global co-ordinates of midspan of k^{th} band of type 1 beams.

$\hat{x}_{bj}$, $\hat{y}_{bj}$ = global co-ordinates of midspan of j^{th} band of type 3 beams.

z = height variable along the Z-axis.

γ_k, $\bar{\gamma}_i$, $\hat{\gamma}_j$ = stiffness factors of k^{th} band of type 1, i^{th} band of type 2, and j^{th} band of type 3 connecting laminae, respectively, including effect of shear deformation.

$\mu_{j\ell}$ = rotation factor of joints formed by j^{th} band of type 3 beams and column C_{j1} of frame ℓ.

$\xi(z)$, $\eta(z)$, $\theta(z)$ = horizontal displacements of O in X- and Y-directions and rotation of structure about the Z-axis, respectively, at height z.

ξ_m, η_m, θ_m = horizontal displacements of shear center of wall m in $\bar{X}_m$- and $\bar{Y}_m$-directions and rotation of same about the vertical, respectively.

ξ_ℓ, η_ℓ, θ_ℓ = horizontal displacements of O_ℓ of frame ℓ in $\overline{X}_\ell$- and $\overline{Y}_\ell$-directions and rotation of same about the vertical, respectively.

ϕ_m, ϕ_ℓ = orientations of the local co-ordinate systems of wall m and frame ℓ, respectively, relative to the global co-ordinate system.

$\hat{\phi}_{bj}$ = acute angle between the j^{th} band of type 3 beams and the plane of the associated frame.

ω_{km}, ω_{kn} = sectorial co-ordinates at midspan cut of k^{th} band of type 1 beams with respect to the shear centres of wall m and wall n respectively.

ω_{ia}, ω_{ib} = sectorial co-ordinates at either side of midspan cut of i^{th} band of type 2 beams with respect to the shear centre of the respective wall.

$\hat{\omega}_{jm}$ = sectorial co-ordinate at midspan cut of j^{th} band of type 3 beams with respect to the shear centre of wall m.

$\{\Delta\}$ = generalised displacement vector
= col. $\{ \xi(z), \eta(z), \theta(z) \}$.

Eqn(s) = Equation(s).

col. = column vector.

4.3 STATEMENT OF PROBLEM

Consider a uniform three-dimensional wall-frame structure consisting of M shear walls, L plane frames, and N bands of connecting beams. Assuming rigid diaphragm action of the floor system, the overall deformation of the structure will be defined by three continuous generalised displacement functions. Referring to an arbitrarily located orthogonal global co-ordinate system defined by origin O, horizontal axes X and Y, and vertical axis Z, these displacement functions will be denoted by $\xi(z)$, $\eta(z)$, and $\theta(z)$ representing the horizontal displacements of O in the X- and Y-directions and the rotation of the structure about the Z-axis, respectively (Figure 4-1).

The shear walls can be any open-sections of arbitrary shapes in plan. The global co-ordinates of the centroid G_m and the shear centre S_m of the m^{th} wall, where m = 1, 2, ... M, are denoted by (x_{em}, y_{em}) and (x_{cm}, y_{cm}) respectively. The principal horizontal axes of the wall section are denoted by $\bar{X}_m$ and $\bar{Y}_m$ oriented at an angle ϕ_m relative to the global counterparts. Displacements of the shear centre S_m in the $\bar{X}_m$- and $\bar{Y}_m$-directions and about the vertical are denoted by $\xi_m(z)$, $\eta_m(z)$, and $\theta_m(z)$ respectively. The geometry of a typical shear wall in plan view is shown in Figure 4-2.

The frames can be arbitrarily located and oriented.

To relate the translational and rotational displacements of the frames to those of the total structure, a local co-ordinate system is specified for each frame. Thus, for the ℓ^{th} frame, where $\ell = 1, 2, \ldots L$, the local co-ordinate system consists of origin O_ℓ at its centroid, which is defined by the first moment of column areas and is located at $(x_{O\ell}, y_{O\ell})$ in the global X - Y plane, horizontal axes $\overline{X}_\ell$ and $\overline{Y}_\ell$ with $\overline{X}_\ell$ lying in the plane of the frame, and vertical axis $\overline{Z}_\ell$ through O_ℓ. The overall deformation of the frame as a unit will be defined by the displacements of O_ℓ in the $\overline{X}_\ell$- and $\overline{Y}_\ell$-directions and about the $\overline{Z}_\ell$-axis, denoted by $\xi_\ell(z)$, $\eta_\ell(z)$, and $\theta_\ell(z)$, respectively. The geometry of a typical frame in plan view is shown in Figure 4-3.

Coupling between shear walls via connecting beams can occur in any fashion. Coupling can also occur between a frame and a wall. When this is the case, it is assumed that the frame and the wall are not coupled to other shear walls. An example of a possible configuration is shown in Figure 4-4. Referring to Figure 4-4, three types of connecting beams can be distinguished. A type 1 beam connects two individual shear walls, a type 2 beam connects two points, a and b, of the same wall, and a type 3 beam connects a shear wall and a frame. Of the total N beams, it is assumed that there are K type 1 beams, I type 2 beams, and J type 3 beams so that $N = K + I + J$. The locations of the

midspans of the k^{th} band of type 1 connecting beams and the j^{th} band of type 3 connecting beams are defined by global co-ordinates (x_{bk}, y_{bk}) and $(x_{\hat{bj}}, y_{\hat{bj}})$ respectively.

The geometry of two non-planar shear walls, walls m and n, connected by the k^{th} band of type 1 beams is shown in Figure 4-5. Similarly, that of a non-planar shear wall with the i^{th} band of type 2 beams is given in Figure 4-6, and that of a non-planar shear wall, wall m, and frame ℓ connected by the j^{th} band of type 3 beams in Figure 4-7. For ease of reference, the columns of frame ℓ which is coupled to shear wall m via the j^{th} band of type 3 beams are labelled C_{ji}, with i = 1, 2, 3, ..., $\bar{n}_\ell$, where $\bar{n}_\ell$ is the number of columns in frame ℓ, and with C_{j1} denoting the column which adjoins the connecting beams.

In addition to the assumption of rigid diaphragm action, the following assumptions are made in the analysis:

(1) The sectional properties of walls, columns, girders, and connecting beams, spans of girders and connecting beams, and storey heights are assumed to be constant throughout the entire height of the structure.

(2) The height of the structure is constant across its plan.

(3) The proportions of the shear walls are such that Vlasov's thin-walled beam theory can be applied.

(4) The out-of-plane stiffnesses of floor slabs are ap-

proximated by equivalent connecting beams of appropriate stiffnesses.

(5) The mid-points of connecting beams, girders and columns are assumed to be contraflexural points.

(6) For each band of type 3 beams, which connect frames and walls, one-half of the span of the connecting beam at each floor is considered to be a member of the respective frame.

(7) The discrete connecting beams are further replaced by uniformly and continuously distributed connecting laminae with equivalent properties throughout the entire height of the structure.

(8) Each frame ℓ is replaced by a shear beam having a constant shear stiffness of GA_ℓ in approximation of the horizontal shear resistance of the frame [29].

(9) The out-of-plane stiffness of each frame is negligible.

(10) Linearly elastic behaviour is assumed for all structural elements.

(11) The foundation of the structure is rigid.

Considering an overall view of the analysis, there can be envisioned altogether (N + 3) independent unknown variables that need to be determined. These unknown variables are the three generalised displacement functions and the N

shear distributions in the N band of connecting laminae. Therefore, (N + 3) equations are required in order to achieve a solution. These equations can be obtained by (a) considering the overall equilibrium of the total structure, which will yield three equations of equilibrium, and (b) considering the problem of compatibility in deformation in each band of the connecting laminae, which will yield N compatibility equations. Thus, (N + 3) equations will be available for determining the (N + 3) unknowns. Once these unknowns are solved, all other quantities can be found accordingly.

4.4 CO-ORDINATE TRANSFORMATION

The assumption of rigid diaphragm action renders all points at the same height z in the plan of the total structure to undergo the same rotation so that $\theta_m(z) = \theta_\ell(z) = \theta(z)$. Meanwhile, the following relationships for co-ordinate transformation holds:

(1) For frame ℓ,

$$\begin{Bmatrix} \xi_\ell \\ \eta_\ell \\ \theta_\ell \end{Bmatrix} = \begin{bmatrix} \cos\phi_\ell & \sin\phi_\ell & -\bar{y}_{o\ell} \\ -\sin\phi_\ell & \cos\phi_\ell & \bar{x}_{o\ell} \\ 0 & 0 & 1 \end{bmatrix} \begin{Bmatrix} \xi \\ \eta \\ \theta \end{Bmatrix} \qquad (4\text{-}1a)$$

where $\bar{x}_{o\ell}$ and $\bar{y}_{o\ell}$ are the co-ordinates of O_ℓ measured with respect to O along the $\bar{X}_\ell$- and $\bar{Y}_\ell$-directions, respectively.

(2) For wall m,

$$\begin{Bmatrix} \xi_m \\ \eta_m \\ \theta_m \end{Bmatrix} = \begin{bmatrix} \cos\phi_m & \sin\phi_m & -\bar{y}_{cm} \\ -\sin\phi_m & \cos\phi_m & \bar{x}_{cm} \\ 0 & 0 & 1 \end{bmatrix} \begin{Bmatrix} \xi \\ \eta \\ \theta \end{Bmatrix} \qquad (4\text{-}1b)$$

where $\bar{x}_{cm}$ and $\bar{y}_{cm}$ are the co-ordinates of S_m measured with respect to O along the $\bar{X}_m$- and $\bar{Y}_m$- directions, respectively.

Finally, co-ordinates that are measured with respect to a particular reference point along the directions of a local co-ordinate system, denoted by $(\bar{x}, \bar{y})$, can be transformed into co-ordinates measured with respect to the same reference point along the global directions, denoted by (x, y), according to the following relationship:

$$\begin{Bmatrix} \bar{x} \\ \bar{y} \end{Bmatrix} = \begin{bmatrix} \cos\phi & \sin\phi \\ -\sin\phi & \cos\phi \end{bmatrix} \begin{Bmatrix} x \\ y \end{Bmatrix} \qquad (4\text{-}1c)$$

where ϕ is the orientation of the local co-ordinate system in question with respect to the global counterpart.

4.5 EQUILIBRIUM CONDITIONS

The horizontal shear force equilibrium and the torsional equilibrium of the total structure are maintained by internal forces, moments, and couples contributed by the shear walls, frames, and connecting laminae. A general sign convention for the forces and moments acting on a typical structural element is given in Appendix F.

4.5.1 HORIZONTAL SHEAR FORCE EQUILIBRIUM

Referring to Figure 4-8, in which the shear forces acting on wall m in its principal directions are shown, the shear force components acting on the wall in the global X- and Y-directions are respectively given by

$$V^x_{wm} = - E\bar{I}_{ym}\xi'''_m \cos\phi_m + E\bar{I}_{xm}\eta'''_m \sin\phi_m \qquad (4\text{-}2a)$$

$$V^y_{wm} = - E\bar{I}_{ym}\xi'''_m \sin\phi_m - E\bar{I}_{xm}\eta'''_m \cos\phi_m \qquad (4\text{-}2b)$$

Making use of Eqn(4-1b), it can be shown that Eqn(4-2a) becomes

$$V^x_{wm} = - EI_{ym}\xi''' - EI_{xym}\eta''' + EI_{ycm}\theta''' \qquad (4\text{-}3)$$

where I_{ym}, I_{xm}, and I_{xym} are the moments of inertia and product moment of inertia of wall m with respect to the global directions, while I_{ycm} is defined by

$$I_{ycm} = y_{cm} I_{ym} - x_{cm} I_{xym} \tag{4-4}$$

Summing up the contributions from all M walls, the total shear force in the X-direction due to the walls is given by

$$V_w^x = - EI^*_{yy} \xi''' - EI^*_{xy} \eta''' + EI^*_{yc} \theta''' \tag{4-5}$$

where
$$\left.\begin{aligned} I^*_{yy} &= \sum_{m=1}^{M} I_{ym} \\ I^*_{xy} &= \sum_{m=1}^{M} I_{xym} \\ I^*_{yc} &= \sum_{m=1}^{M} I_{ycm} \end{aligned}\right\} \tag{4-6}$$

Likewise, it can be shown that the total horizontal shear force in the Y-direction due to all M shear walls is given by

$$V_w^y = - EI^*_{xy} \xi''' - EI^*_{xx} \eta''' - EI^*_{xc} \theta''' \tag{4-7}$$

where
$$\left.\begin{aligned} I^*_{xx} &= \sum_{m=1}^{M} I_{xm} \\ I^*_{xc} &= \sum_{m=1}^{M} I_{xcm} \end{aligned}\right\} \qquad (4\text{-}8)$$

with
$$I_{xcm} = x_{cm} I_{xm} - y_{cm} I_{xym} \qquad (4\text{-}9)$$

The in-plane horizontal shear force acting on frame ℓ is given by

$$\bar{V}_{f\ell} = GA_\ell \xi'_\ell \qquad (4\text{-}10)$$

Therefore, the horizontal shear force components acting on frame ℓ in the X- and Y-directions are respectively given by

$$V^x_{f\ell} = GA_\ell \xi'_\ell \cos\phi_\ell \qquad (4\text{-}11)$$

$$V^y_{f\ell} = GA_\ell \xi'_\ell \sin\phi_\ell \qquad (4\text{-}12)$$

Expressing Eqns(4-11) and (4-12) in terms of the global displacement variables, there is obtained

$$V^x_{f\ell} = GA_\ell \cos^2\phi_\ell \xi' + GA_\ell \sin\phi_\ell \cos\phi_\ell \eta' - \bar{y}_{o\ell} GA_\ell \cos\phi_\ell \theta' \qquad (4\text{-}13)$$

$$V^y_{f\ell} = GA_\ell \sin\phi_\ell \cos\phi_\ell \xi' + GA_\ell \sin^2\phi_\ell \eta' - \bar{y}_{o\ell} GA_\ell \sin\phi_\ell \theta' \qquad (4\text{-}14)$$

Therefore, summing up the contributions from all L frames, the total horizontal shears acting in the X- and Y-directions are given by V_f^x and V_f^y, respectively, such that

$$V_f^x = GA_{xx}\xi' + GA_{xy}\eta' - GA_{x\theta}\theta' \tag{4-15}$$

$$V_f^y = GA_{xy}\xi' + GA_{yy}\eta' - GA_{y\theta}\theta' \tag{4-16}$$

where
$$\left.\begin{aligned} GA_{xx} &= \sum_{\ell=1}^{L} (GA_\ell \cos^2\phi_\ell) \\ GA_{xy} &= \sum_{\ell=1}^{L} (GA_\ell \sin\phi_\ell \cos\phi_\ell) \\ GA_{yy} &= \sum_{\ell=1}^{L} (GA_\ell \sin^2\phi_\ell) \\ GA_{x\theta} &= \sum_{\ell=1}^{L} (\bar{y}_{o\ell} GA_\ell \cos\phi_\ell) \\ GA_{y\theta} &= \sum_{\ell=1}^{L} (\bar{y}_{o\ell} GA_\ell \sin\phi_\ell) \end{aligned}\right\} \tag{4-17}$$

Of the three types of connecting laminae, only type 1 and type 3 contribute resistance to externally applied horizontal shears. If an imaginary cut is made along the vertical centreline of the k^{th} band of type 1 connecting laminae, a distribution of shear forces $q_k(z)$ will be exposed. Assuming q_k to be positive if it acts upwards on wall m and downwards on wall n, where m < n, the shear

forces induced in walls m and n due to q_k can be obtained by considering the moment equilibrium of an elemental section of the walls dz in depth as shown in Figure 4-9. Thus the shear forces induced in wall m and wall n due to q_k and acting in the directions of the local principal axes of the respective walls are given by $\overline{V}_{xkm}$ and $\overline{V}_{ykm}$ for wall m, and $\overline{V}_{xkn}$ and $\overline{V}_{ykn}$ for wall n such that

$$\overline{V}_{xkm} = q_k \overline{x}_{bkm} \tag{4-18a}$$

$$\overline{V}_{ykm} = q_k \overline{y}_{bkm} \tag{4-18b}$$

$$\overline{V}_{xkn} = -q_k \overline{x}_{bkn} \tag{4-18c}$$

$$\overline{V}_{ykn} = -q_k \overline{y}_{bkn} \tag{4-18d}$$

where $(\overline{x}_{bkm}, \overline{y}_{bkm})$ and $(\overline{x}_{bkn}, \overline{y}_{bkn})$ are the co-ordinates of the midspan of the k^{th} band of connecting laminae with respect to the centroids and principal directions of wall m and wall n respectively.

The resultants of the above four shear force components in the global X- and Y-directions can be shown to be given by V^x_{bk} and V^y_{bk}, respectively, such that

$$V^x_{bk} = r_{xk} q_k \tag{4-19}$$

$$V^y_{bk} = r_{yk} q_k \tag{4-20}$$

where $r_{xk} = x_{en} - x_{em}$ (4-21a)

$r_{yk} = y_{en} - y_{em}$ (4-21b)

Therefore, the total horizontal shear forces in the X- and Y-directions due to the shear distributions in all type 1 connecting laminae are respectively given by

$$V_b^x = \sum_{k=1}^{K} r_{xk}\, q_k \qquad (4\text{-}22)$$

$$V_b^y = \sum_{k=1}^{K} r_{yk}\, q_k \qquad (4\text{-}23)$$

Contributions from type 3 laminae can be found likewise. Thus an imaginary cut is made in the j^{th} band of type 3 laminae that connects wall m and frame ℓ. For simplicity, the shear distribution thus exposed, denoted by $\hat{q}_j(z)$, is assumed to act upwards on wall m and downwards on frame ℓ. Taking note that half of the span of the connecting beam at each floor has been included as a member of frame ℓ in the evaluation of GA_ℓ, the effect of the shear distribution $\hat{q}_j$ on the frame has already been taken into account in computing the GA_ℓ value of the frame. Thus, the shear distribution $\hat{q}_j$ will induce additional shear forces only in the wall. Accordingly it can be shown that the horizontal shear forces induced in the wall due to the shear distribution $\hat{q}_j$ in the X-

and Y-direction are respectively given by $V^x_{\hat{b}j}$ and $V^y_{\hat{b}j}$ such that

$$V^x_{\hat{b}j} = \hat{r}_{xj}\ \hat{q}_j \tag{4-24a}$$

$$V^y_{\hat{b}j} = \hat{r}_{yj}\ \hat{q}_j \tag{4-24b}$$

where $$\hat{r}_{xy} = x_{\hat{b}j} - x_{em} \tag{4-24c}$$

$$\hat{r}_{yj} = y_{\hat{b}j} - y_{em} \tag{4-24d}$$

Therefore, the total horizontal shear forces in the X- and Y-directions due to all type 3 laminae are respectively given by

$$V^x_{\hat{b}} = \sum_{j=1}^{J} \hat{r}_{xj}\ \hat{q}_j \tag{4-25a}$$

$$V^y_{\hat{b}} = \sum_{j=1}^{J} \hat{r}_{yj}\ \hat{q}_j \tag{4-25b}$$

The horizontal shear force equilibrium equations in the X- and Y-directions are therefore given by

$$V^x_w + V^x_f + V^x_b + V^x_{\hat{b}} = V_x \tag{4-26}$$

$$V^y_w + V^y_f + V^y_b + V^y_{\hat{b}} = V_y \tag{4-27}$$

where V_x and V_y are the external shear in the X- and Y-directions repectively.

Substituting the appropriate equations previously derived into Eqns(4-26) and (4-27), there is obtained

$$EI^*_{yy}\xi''' + EI^*_{xy}\eta''' - EI^*_{yc}\theta''' - GA_{xx}\xi' - GA_{xy}\eta' + GA_{x\theta}\theta' - \sum_{k=1}^{K} r_{xk}q_k - \sum_{j=1}^{J} \hat{r}_{xj}\hat{q}_j = -V_x \qquad (4\text{-}28)$$

$$EI^*_{xy}\xi''' + EI^*_{xx}\eta''' + EI^*_{xc}\theta''' - GA_{xy}\xi' - GA_{yy}\eta' + GA_{y\theta}\theta' - \sum_{k=1}^{K} r_{yk}q_k - \sum_{j=1}^{J} \hat{r}_{yj}\hat{q}_j = -V_y \qquad (4\text{-}29)$$

4.5.2 TORSIONAL EQUILIBRIUM ABOUT Z-AXIS

The total internal torque of the structure consists of contributions from the shear walls, the frames, and all three types of connecting laminae.

Referring to Figure 4-8, the torque about the Z-axis due to the shear forces, warping torsion and St. Venant torsion of wall m is given by

$$Q_{wm} = -E\bar{I}_{\omega m}\theta'''_m + E\bar{I}_{ym}\bar{y}_{cm}\xi'''_m - E\bar{I}_{xm}\bar{x}_{cm}\eta'''_m + GJ_m\theta'_m \qquad (4\text{-}30a)$$

Using the geometric relations in Eqns(4-1b) and (4-1c), Eqn (4-30a) becomes

$$Q_{wm} = - EI_{\omega m}\theta''' + EI_{ycm}\xi''' - EI_{xcm}\eta''' + GJ_m\theta' \tag{4-30b}$$

where $$I_{\omega m} = \bar{I}_{\omega m} + I_{xm}x_{cm}^2 + I_{ym}y_{cm}^2 - 2I_{xym}x_{cm}y_{cm} \tag{4-30c}$$

Therefore , the total torque due to all shear walls about the Z-axis is given by

$$Q_w = EI^*_{yc}\xi''' - EI^*_{xc}\eta''' - EI^*_{\omega}\theta''' + GJ^*\theta' \tag{4-31}$$

where $$\left.\begin{aligned} I^*_{\omega} &= \sum_{m=1}^{M} I_{\omega m} \\ J^* &= \sum_{m=1}^{M} J_m \end{aligned}\right\} \tag{4-31a}$$

The torque about the Z-axis due to frame ℓ is given by

$$Q_{f\ell} = V^y_{f\ell}\, x_{o\ell} - V^x_{f\ell}\, y_{o\ell} \tag{4-32a}$$

Substituting Eqns(4-13) and (4-14) into Eqn(4-32a), and expressing $x_{o\ell}$ and $y_{o\ell}$ in terms of $\bar{x}_{o\ell}$ and $\bar{y}_{o\ell}$ using Eqn(4-1c), there is obtained

$$Q_{f\ell} = - \bar{y}_{o\ell} GA_\ell \cos\phi_\ell \xi' - \bar{y}_{o\ell} GA_\ell \sin\phi_\ell \eta' + \bar{y}^2_{o\ell} GA_\ell \theta' \qquad (4\text{-}32b)$$

Summing up contributions from all frames, the total torque about the Z-axis due to all frames is given by

$$Q_f = - GA_{\theta x} \xi' - GA_{\theta y} \eta' + GA_{\theta\theta} \theta' \qquad (4\text{-}33)$$

where

$$\left.\begin{aligned} GA_{\theta x} &= GA_{x\theta} \\ GA_{\theta y} &= GA_{y\theta} \\ GA_{\theta\theta} &= \sum_{\ell=1}^{L} \left(\bar{y}^2_{o\ell} GA_\ell \right) \end{aligned}\right\} \qquad (4\text{-}33a)$$

For the k^{th} band of type 1 laminae, horizontal shear force components and torques are induced in walls m and n due to $q_k(z)$, as shown in Figure 4-9. These shear force components have been given by Eqns(4-18a) through (4-18d). The torque effects about the Z-axis due to the shear force components in wall m and those in wall n are respectively given by

$$Q_{skm} = - \bar{V}_{xkm} \bar{y}_{cm} + \bar{V}_{ykm} \bar{x}_{cm} \qquad (4\text{-}34a)$$

$$Q_{skn} = - \bar{V}_{xkn} \bar{y}_{cn} + \bar{V}_{ykn} \bar{y}_{cn} \qquad (4\text{-}34b)$$

The direct torques induced in wall m and wall n due to warp-

ing of these walls caused by q_k are respectively given by

$$Q_{\omega km} = q_k \omega_{km} \qquad (4\text{-}34c)$$

$$Q_{\omega kn} = - q_k \omega_{kn} \qquad (4\text{-}34d)$$

where ω_{km} and ω_{kn} are the sectorial co-ordinates at the mid-span of the laminae band k relative to the shear centres of wall m and wall n respectively.

Thus, by substituting Eqns(4-18a) through (4-18d) into Eqns(4-34a) and (4-34b), and making use of the transformation relationship of Eqn(4-1c), the total torque about the Z-axis due to q_k can be shown to be given by

$$Q_{bk} = r_{\theta k} q_k \qquad (4\text{-}34e)$$

where $$r_{\theta k} = x_{cm} (y_{bk} - y_{em}) - y_{cm} (x_{bk} - x_{em})$$
$$- x_{cn} (y_{bk} - y_{en}) + y_{cn} (x_{bk} - x_{en})$$
$$+ \omega_{km} - \omega_{kn} \qquad (4\text{-}34f)$$

Therefore, the total torque due to all type 1 connecting laminae is given by

$$Q_b = \sum_{k=1}^{K} (r_{\theta k} q_k) \qquad (4\text{-}35)$$

For the i^{th} band of type 2 laminae, a torque $Q_{\bar{b}i}$ is induced in the respective wall due to the shear distribution in the laminae, denoted by $\bar{q}_i(z)$, such that

$$Q_{\bar{b}i} = \bar{r}_{\theta i}\ \bar{q}_i \qquad (4\text{-}36)$$

where $$\bar{r}_{\theta i} = \omega_{ia} - \omega_{ib} \qquad (4\text{-}36a)$$

Therefore, the total torque due to all type 2 laminae is given by

$$Q_{\bar{b}} = \sum_{i=1}^{I} (\bar{r}_{\theta i}\ \bar{q}_i) \qquad (4\text{-}37)$$

For the j^{th} band of type 3 laminae that connects wall m and frame ℓ, two shear force components and a torque component are induced in wall m. These shear force components have been given by Eqns(4-24a) and (4-24b). Thus, the torque about the Z-axis due to the j^{th} band of type 3 laminae is given by

$$\hat{Q}_{bj} = - V^{x}_{\hat{b}j}\ y_{cm} + V^{y}_{\hat{b}j}\ x_{cm} + \hat{\omega}_{jm}\ \hat{q}_j \qquad (4\text{-}38a)$$

where $\hat{\omega}_{jm}$ is the sectorial co-ordinate at the midspan of the laminae with respect to the shear centre of wall m. There-

fore, substituting Eqns(4-24a) and (4-24b) into Eqn(4-38a), there is obtained

$$Q_{\hat{b}j} = \hat{r}_{\theta j}\,\hat{q}_j \tag{4-38b}$$

where $$\hat{r}_{\theta j} = \hat{\omega}_{jm} + x_{cm}\,\hat{r}_{yj} - y_{cm}\,\hat{r}_{xj} \tag{4-38c}$$

Thus, the total torque due to all type 3 laminae is given by

$$Q_{\hat{b}} = \sum_{j=1}^{J} \hat{r}_{\theta j}\,\hat{q}_j \tag{4-39}$$

Therefore, the equation for the torsional equilibrium of the total structure about the Z-axis is given by

$$Q_w + Q_f + Q_b + Q_{\bar{b}} + Q_{\hat{b}} = Q_t \tag{4-40}$$

where Q_t is the applied torque about the Z-axis. Substituting the appropriate equations into Eqn(4-40), and reversing signs throughout, there is obtained

$$\begin{aligned} &- EI^*_{yc}\xi''' + EI^*_{xc}\eta''' + EI^*_{\omega}\theta''' - GJ^*\theta' \\ &+ GA_{\theta x}\xi' + GA_{\theta y}\eta' - GA_{\theta\theta}\theta' \\ &- \sum_{k=1}^{K} r_{\theta k}q_k - \sum_{i=1}^{I} \bar{r}_{\theta i}\bar{q}_i - \sum_{j=1}^{J} \hat{r}_{\theta j}\hat{q}_j = - Q_t \end{aligned} \tag{4-41}$$

Eqns(4-28), (4-29), and (4-41) are therefore the three equations of equilibrium for the total structure.

A force function of interest for the shear walls is the axial force function. For a wall m which is connected to other walls via more than one band of type 1 laminae, the axial force in the wall is given by

$$T_m(z) = \sum_{k,m}^{Bl} s_k \int_z^H q_k(\bar{z})d\bar{z} \qquad (4\text{-}42a)$$

where $\sum_{k,m}^{Bl}$ represents summation over all type 1 laminae bands connected to wall m. T_m is taken to be positive when it produces tension in the wall. s_k is +1 when the associated distributed shear acts upwards on the wall, and is -1 when it acts downwards. For a wall m which is connected to a frame via the j^{th} type 3 laminae band and assuming the associated distributed shear to act upwards on the wall, the axial force in the wall is given by

$$T_m(z) = \int_z^H \hat{q}_j(\bar{z})d\bar{z} \qquad (4\text{-}42b)$$

4.6 COMPATIBILITY CONDITIONS

It has been pointed out in Section 4.3 that (N+3) equations are required to achieve a solution. Three of these have been obtained from equilibrium considerations in the previous section; the other N equations will be obtained from the consideration of compatibility in deformation at the midspan of each band of connecting laminae. To this end, an imaginary cut is made at the midspan of each band of laminae, thereby exposing the associated shear distribution in the laminae (but no moment distribution because of the assumption of midspan contraflexural points). The vertical relative displacements of the laminae on either side of the cut are then calculated. An equation can thus be obtained for each band of laminae by ensuring vertical compatibility at the midspan of the respective band of laminae.

4.6.1 COMPATIBILITY EQUATIONS FOR TYPE 1 CONNECTING LAMINAE

For the k^{th} band of type 1 connecting laminae that connects walls m and n, there are four effects which give rise to relative vertical displacements at the cut. The first effect consists of the flexural deformations of the walls whereby the point at the cut on the side of wall m will undergo a vertical displacement relative to that on the

side of wall n given by

$$(\delta_1)_k = - \bar{x}_{bkm}\xi'_m - \bar{y}_{bkm}\eta'_m + \bar{x}_{bkn}\xi'_n + \bar{y}_{bkn}\eta'_n \qquad (4\text{-}43a)$$

The second effect is warping deformation of the walls; the associated relative displacement at the cut is given by

$$(\delta_2)_k = \omega_{km}\theta'_m - \omega_{kn}\theta'_n \qquad (4\text{-}43b)$$

The third effect is the axial deformations of the walls; the associated relative displacement is given by

$$(\delta_3)_k = + \int_o^z \frac{T_m}{EA_m}\, d\bar{z} - \int_o^z \frac{T_n}{EA_n}\, d\bar{z} \qquad (4\text{-}43c)$$

The fourth effect is the flexural and shear deformation of the connecting laminae; the resulting relative displacement is given by

$$(\delta_4)_k = + \frac{q_k}{E\gamma_k} \qquad (4\text{-}43d)$$

where γ_k = stiffness factor of the k^{th} band of type 1 connecting laminae including shear deformation

$$= \frac{12I_{bk}}{h\ell_{bk}^3[\ 1 + 12EI_{bk}/(\ell_{bk}^2 A_{bk} G)\ ]} \qquad (4\text{-}43e)$$

By compatibility at the midspan of the laminae,

$$(\delta_1)_k + (\delta_2)_k + (\delta_3)_k + (\delta_4)_k = 0 \qquad (4\text{-}44a)$$

Substituting Eqns(4-43a) through (4-43d) into Eqn(4-44a), and transforming the local displacement variables into the generalised ones and the local co-ordinates into the global counterparts using the geometric relationships of Eqns (4-1b) and (4-1c), there is obtained

$$r_{xk}\xi' + r_{yk}\eta' + r_{\theta k}\theta' - \int_o^z \frac{T_m}{EA_m}\, d\bar{z} + \int_o^z \frac{T_n}{EA_n}\, d\bar{z} - \frac{q_k}{E\gamma_k} = 0 \qquad (4\text{-}44b)$$

Referring to the coupled shear wall unit shown in Figure 4-5, T_m and T_n can be eliminated from Eqn(4-44b) by differentiating the equation twice, thereby obtaining the following equation:

$$r_{xk}\xi''' + r_{yk}\eta''' + r_{\theta k}\theta''' + \frac{1}{E}\left(\frac{1}{A_m} + \frac{1}{A_n}\right)q_k - \frac{q_k''}{E\gamma_k} = 0 \qquad (4\text{-}45)$$

4.6.2 COMPATIBILITY EQUATIONS FOR TYPE 2 CONNECTING LAMINAE

For the i^{th} band of type 2 connecting laminae, only warping of the associated wall section and the flexural and shear deformation of the laminae due to $\bar{q}_i$ will produce relative displacements at the midspan cut. The resulting compatibility equation is thus given by

$$\bar{r}_{\theta i}\,\theta' - \frac{\bar{q}_i}{E\bar{\gamma}_i} = 0 \qquad (4\text{-}46)$$

where $\bar{\gamma}_i$ = stiffness factor for the i^{th} band of type 2 connecting laminae including shear deformation

$$= \frac{12\bar{I}_{bi}}{h\bar{\ell}_{bi}^3[\,1 + 12E\bar{I}_{bi}/(\bar{\ell}_{bi}^2\bar{A}_{bi}G)\,]} \qquad (4\text{-}46a)$$

4.6.3 COMPATIBILITY EQUATIONS FOR TYPE 3 CONNECTING LAMINAE

For the j^{th} band of type 3 connecting laminae that connects wall m and frame ℓ, the relative displacement at the midspan cut arises from the following six effects:

(1) the lateral and warping deformation of the wall,

(2) the rotation of the joints formed by the connecting laminae and column C_{j1} from the frame,

(3) the flexural and shear deformation of the laminae,

(4) the axial deformation of the wall due to the shear distribution $\hat{q}_j$,

(5) the axial deformation of column C_{jl} due to $\hat{q}_j$,

and (6) the axial deformation of column C_{jl} due to the chord drift effects of the frame.

Referring to the coupled wall-frame unit shown in Figure 4-7, and denoting the vertical displacement of a point at the cut on the side of the wall relative to that on the side of the frame due to the i^{th} effect of the above six by $(\hat{\delta}_i)_j$, there can be obtained

$$(\hat{\delta}_1)_j = - \bar{\hat{x}}_{bjm}\xi'_m - \bar{\hat{y}}_{bjm}\eta'_m + \hat{\omega}_{jm}\theta'_m \qquad (4\text{-}47a)$$

where $(\bar{\hat{x}}_{bjm}, \bar{\hat{y}}_{bjm})$ are the co-ordinates of the midspan of the j^{th} band of type 3 connecting laminae with respect to the local co-ordinate system of wall m, and $\hat{\omega}_{jm}$ is its sectorial co-ordinate with respect to the shear centre of wall m.

$$(\hat{\delta}_2)_j = - \mu_{j\ell}\,\xi'_\ell \qquad (4\text{-}47b)$$

where $$\mu_{j\ell} = e_{j\ell}\hat{\ell}_{bj}\left[\frac{h\hat{I}_{bj}}{\hat{\ell}_{bj}I_{cjl}} + \frac{hI_{gjl}}{\ell_{gjl}I_{cjl}} + 2\right]^{-1} \qquad (4\text{-}47c)$$

In Eqn(4-47c), I_{cjl} is the moment of inertia of column C_{jl}, I_{gjl} and ℓ_{gjl} are the moment of inertia and length, respectively, of the girder that is connected to column C_{jl}, while $e_{j\ell}$ is +1, or -1, when the j^{th} band of type 3 laminae is located on the negative, or positive, portion of the $\bar{X}_\ell$-axis.

$$(\hat{\delta}_3)_j = \frac{\hat{q}_j}{E\hat{\gamma}_j} \tag{4-47d}$$

where $\hat{\gamma}_j$ = stiffness factor for the j^{th} band of type 3 connecting laminae including shear deformation

$$= \frac{12\hat{I}_{bj}}{h\hat{\ell}_{bj}^3[\,1 + 12E\hat{I}_{bj}/(\hat{\ell}_{bj}^2\hat{A}_{bj}G)\,]} \tag{4-47e}$$

$$(\hat{\delta}_4)_j = \int_o^z \frac{T_m}{EA_m}\, d\bar{z} \tag{4-47f}$$

$$(\hat{\delta}_5)_j = \int_o^z \frac{f_{j\ell}T_m}{EA_{cjl}}\, d\bar{z} \tag{4-47g}$$

where A_{cjl} is the cross-sectional area of column C_{jl}, and $f_{j\ell}$ is a factor which allows for the additional axial load on column C_{jl} due to $\hat{q}_j$ when the frame has not less than one row of girders. In general, $f_{j\ell}$ takes on a value ranging from 1.1 to 1.4.

In evaluating $(\hat{\delta}_6)_j$, the following assumptions are made:

(a) The effect of $\hat{q}_j$ in inducing axial forces in columns other than C_{j1} and C_{j2} is neglected.

(b) Regarding chord drift-induced axial deformations in the columns, columns to one side of the frame centroid act in tension while those to the other side act in compression, and each column C_{ji} deforms axially in proportion to its respective in-plane distance d_{cji} from the frame centroid.

The chord drift-induced axial force in column C_{j1}, denoted by T_{cj1}, can be determined by considering the moment equilibrium of the coupled shear wall-frame unit about the X-axis or the Y-axis. The external moments about the X- and Y-axes taken up by the unit, denoted by M^x_{wf} and M^y_{wf} respectively, are balanced by resisting moments contributed by the lateral deformation of the wall, the axial effects in the wall and columns C_{j1} and C_{j2} due to $\hat{q}_j$, and the chord drift-induced axial effects in all columns of the frame.

Referring to Figure 4-10, the moments about the X- and Y-axes due to the lateral deformation of wall m, denoted by M_{mx} and M_{my} respectively, can be shown to be

$$M_{mx} = EI_{xym}\xi'' + EI_{xm}\eta'' + EI_{xcm}\theta'' \qquad (4\text{-}47h)$$

$$M_{my} = EI_{ym}\xi'' + EI_{xym}\eta'' - EI_{ycm}\theta'' \qquad (4\text{-}47i)$$

Referring to Figure 4-11, the moments about the X- and Y-axes due to the beam shear-induced axial effects in wall m and columns C_{j1} and C_{j2} are respectively given by

$$M_{qjx} = - T_m y_{em} + T_m \ell_{yj\ell} \qquad (4\text{-}47j)$$

$$M_{qjy} = - T_m x_{em} + T_m \ell_{xj\ell} \qquad (4\text{-}47k)$$

where
$$\left.\begin{aligned} \ell_{xj\ell} &= f_{j\ell} x_{cj1} - (f_{j\ell} - 1) x_{cj2} \\ \ell_{yj\ell} &= f_{j\ell} y_{cj1} - (f_{j\ell} - 1) y_{cj2} \end{aligned}\right\} \qquad (4\text{-}47l)$$

with (x_{cj1}, y_{cj1}) and (x_{cj2}, y_{cj2}) being the global coordinates of columns C_{j1} and C_{j2}, respectively.

The moment contributed by the chord drift-induced axial forces in the frame columns about the $\bar{Y}_\ell$-axis is given by

$$\bar{M}_c = \sum_{i=1}^{\bar{n}_\ell} T_{cji} d_{cji} \qquad (4\text{-}47m)$$

where $\bar{n}_\ell$ is the number of columns in frame ℓ, and T_{cji} is the chord drift-induced axial force in column C_{ji}. T_{cji} is assumed to be positive when it produces tension in the res-

pective column.

By assumption (b), there is obtained

$$T_{cji} = (d_{cji}/d_{cjl})\, T_{cjl} \qquad (4\text{-}47n)$$

Therefore,

$$\bar{M}_c = T_{cjl}\, W_{j\ell} \qquad (4\text{-}47p)$$

where $W_{j\ell}$ is the equivalent moment arm of the couple about the $\bar{Y}_\ell$-axis due to the chord drift-induced axial forces in the frame columns such that

$$W_{j\ell} = \left(\sum_{i=1}^{\bar{n}_\ell} d_{cji}^2 \right) / d_{cjl} \qquad (4\text{-}47q)$$

The moment components due to $\bar{M}_c$ about the X- and Y-directions are respectively given by

$$M_{cx} = e_{j\ell} T_{cjl} W_{j\ell} \sin\phi_\ell \qquad (4\text{-}47r)$$

$$M_{cy} = e_{j\ell} T_{cjl} W_{j\ell} \cos\phi_\ell \qquad (4\text{-}47s)$$

where $e_{j\ell}$ is as defined in Eqn(4-47c).

Therefore, the moment equilibriums of the coupled shear wall-frame unit about the X- and Y-axes are respectively given by:

$$M^x_{wf} = M_{mx} + M_{qjx} + M_{cx} \qquad (4\text{-}47t)$$

$$M^y_{wf} = M_{my} + M_{qjy} + M_{cy} \qquad (4\text{-}47u)$$

Substituting the appropriate equations derived earlier into Eqns(4-47t) and (4-47u), there is obtained

$$M^x_{wf} = EI_{xym}\xi'' + EI_{xm}\eta'' + EI_{xcm}\theta'' - T_m(y_{em} - \ell_{yj\ell}) + e_{j\ell}T_{cj1}W_{j\ell}\sin\phi_\ell \qquad (4\text{-}47v)$$

$$M^y_{wf} = EI_{ym}\xi'' + EI_{xym}\eta'' - EI_{ycm}\theta'' - T_m(x_{em} - \ell_{xj\ell}) + e_{j\ell}T_{cj1}W_{j\ell}\cos\phi_\ell \qquad (4\text{-}47w)$$

Thus, T_{cj1} is given by either of the following two equations:

$$T_{cj1} = \{ M^y_{wf} - EI_{ym}\xi'' - EI_{xym}\eta'' + EI_{ycm}\theta'' + T_m(x_{em} - \ell_{xj\ell}) \} / (e_{j\ell}W_{j\ell}\cos\phi_\ell) \qquad (4\text{-}48a)$$

-or,

$$M^x_{wf} - EI_{xym}\xi'' - EI_{xm}\eta'' - EI_{xcm}\theta'' + T_m(y_{em} - \ell_{yj\ell}) \} / (e_{j\ell}W_{j\ell}\sin\phi_\ell) \qquad (4\text{-}48b)$$

In the light of assumption (b), there is obtained an

angle of rocking due to chord drift given by

$$r = \frac{1}{d_{cjl}} \left(\frac{1}{EA_{cjl}} \int_o^z T_{cjl}\, d\bar{z} \right) \qquad (4\text{-}49)$$

so that

$$(\hat{\delta}_6)_j = - \frac{D_{cjl}}{d_{cjl} EA_{cjl}} \int_o^z T_{cjl}\, d\bar{z} \qquad (4\text{-}50)$$

with $D_{cjl} = d_{cjl} + \hat{\ell}_{bj}/2$ (4-50a)

By compatibility at the midspan of the laminae,

$$(\hat{\delta}_1)_j + (\hat{\delta}_2)_j + (\hat{\delta}_3)_j + (\hat{\delta}_4)_j + (\hat{\delta}_5)_j + (\hat{\delta}_6)_j = 0 \qquad (4\text{-}51a)$$

Therefore, by substituting the appropriate equations derived previously into Eqn(4-51a), and transforming the local coordinates and displacement variables into the global counterparts, the following compatibility equation for the j^{th} band of type 3 laminae is obtained:

$$\hat{r}^*_{xj}\xi' + \hat{r}^*_{yj}\eta' + \hat{r}^*_{\theta j}\theta' - \frac{\hat{q}_j}{E\hat{\gamma}_j} - \frac{1}{E}\left(\frac{1}{A_m} + \frac{f_{j\ell}}{A_{cjl}}\right) \int_o^z T_m\, d\bar{z}$$

$$+ \frac{D_{cjl}}{d_{cjl} EA_{cjl}} \int_o^z T_{cjl}\, d\bar{z} = 0 \qquad (4\text{-}51b)$$

$$\text{where} \quad \left.\begin{aligned} \hat{r}^*_{xj} &= \hat{r}_{xj} + \mu_{j\ell}\cos\phi_\ell \\ \hat{r}^*_{yj} &= \hat{r}_{yj} + \mu_{j\ell}\sin\phi_\ell \\ \hat{r}^*_{\theta j} &= \hat{r}_{\theta j} - \mu_{j\ell}\,\bar{y}_{o\ell} \end{aligned}\right\} \qquad (4\text{-}51c)$$

If Eqn(4-48a) is used for T_{cj1}, the compatibility equation will take the following form:

$$(\hat{r}^*_{xj} - \rho_{xj}EI_{ym})\xi' + (\hat{r}^*_{yj} - \rho_{xj}EI_{xym})\eta' + (\hat{r}^*_{\theta j} + \rho_{xj}EI_{ycm})\theta'$$

$$- \left[\frac{1}{E}\left(\frac{1}{A_m} + \frac{f_{j\ell}}{A_{cj1}}\right) + \rho_{xj}(\ell_{xj\ell} - x_{em})\right] \int_o^z T_m \, d\bar{z}$$

$$- \frac{\hat{q}_j}{E\hat{\gamma}_j} + \rho_{xj} \int_o^z M^y_{wf} \, d\bar{z} = 0 \qquad (4\text{-}51d)$$

$$\text{where} \quad \rho_{xj} = D_{cj1}/(d_{cj1}EA_{cj1}e_{j\ell}W_{j\ell}\cos\phi_\ell) \qquad (4\text{-}51e)$$

If the laminae band is inclined to the plane of the frame such that the frame would have to be rotated through an acute angle of $\hat{\phi}_{bj}$ in order to be aligned with the laminae band but without overlapping it (Figure 4-12), the $\hat{\ell}_{bj}$ term in Eqns(4-47c) and (4-50a), and the $f_{j\ell}$ term will be replaced by $\hat{\ell}^*_{bj}$ and $f^*_{j\ell}$, respectively, such that

$$\hat{\ell}^*_{bj} = \hat{\ell}_{bj}\cos\hat{\phi}_{bj} \qquad (4\text{-}52a)$$

$$f^*_{j\ell} = (f_{j\ell} - 1)\cos\hat{\phi}_{bj} + 1 \qquad (4\text{-}52b)$$

where $$0 \leq \hat{\phi}_{bj} \leq \pi/2 \qquad (4\text{-}52c)$$

In order to eliminate T_m and M^y_{wf} from Eqn(4-51d), the equation is differentiated twice. It is noted that

$$\left(\int_0^z T_m \, d\bar{z} \right)'' = - \hat{q}_j \qquad (4\text{-}53a)$$

$$\left(\int_0^z M^y_{wf} \, d\bar{z} \right)'' = - V^x_{wf} \qquad (4\text{-}53b)$$

where V^x_{wf} is the shear force acting on the wall-frame unit in the X-direction and is given by

$$V^x_{wf} = V^x_{wm} + V^x_{f\ell} + V^x_{\hat{b}j} \qquad (4\text{-}53c)$$

where V^x_{wm}, $V^x_{f\ell}$, and $V^x_{\hat{b}j}$ are given by Eqns(4-2a), (4-13), and (4-25a), respectively. Therefore, differentiating Eqn(4-51d) twice and taking note of Eqns(4-53a), (4-53b), and (4-53c), there is obtained

$$\hat{r}^*_{xj}\xi''' + \hat{r}^*_{yj}\eta''' + \hat{r}^*_{\theta j}\theta''' + S_{xj}\hat{q}_j - \frac{\hat{q}''_j}{E\hat{\gamma}_j} - \rho_{xj}GA_\ell\cos^2\phi_\ell\xi'$$

$$- \rho_{xj}GA_\ell\sin\phi_\ell\cos\phi_\ell\eta' + \rho_{xj}\bar{y}_{o\ell}GA_\ell\cos\phi_\ell\theta' = 0 \qquad (4\text{-}54)$$

where $$S_{xj} = \frac{1}{E}\left(1/A_m + f_{j\ell}/A_{cj1}\right) + \rho_{xj}\left(\ell_{xj\ell} - x_{em} - \hat{r}_{xj}\right).$$

(4-54a)

If Eqn(4-48b) is used for T_{cj1} in lieu of Eqn(4-48a), a similar development will lead to

$$\hat{r}^*_{xj}\xi''' + \hat{r}^*_{yj}\eta''' + \hat{r}^*_{\theta j}\theta''' + S_{yj}\hat{q}_j - \frac{\hat{q}_j''}{E\hat{\gamma}_j} - \rho_{yj}GA_\ell \sin^2\phi_\ell \eta'$$

$$- \rho_{yj}GA_\ell \sin\phi_\ell \cos\phi_\ell \xi' + \rho_{yj}\bar{y}_{o\ell}GA_\ell \sin\phi_\ell \theta' = 0 \qquad (4\text{-}55)$$

where
$$\left.\begin{aligned} \rho_{yj} &= D_{cj1}/(d_{cj1}EA_{cj1}e_{j\ell}W_{j\ell}\sin\phi_\ell) \\ S_{yj} &= \frac{1}{E}\left(\frac{1}{A_m} + \frac{f_{j\ell}}{A_{cj1}}\right) \pm \rho_{yj}\left(\ell_{yj\ell} - y_{em} - \hat{r}_{yj}\right) \end{aligned}\right\} \quad (4\text{-}55a)$$

Thus, Eqns(4-45), (4-46), and (4-54) or (4-55) represent the governing compatibility equations for the type 1, type 2, and type 3 connecting laminae, respectively.

4.7 MATRIX PRESENTATION OF GOVERNING EQUATIONS

The three equations of equilibrium, namely. Eqns(4-28), (4-29), (4-41), can be written in matrix form as follows:

$$[K_o]\{\Delta\}''' - [K_s]\{\Delta\}' - [R_s]^T\{\tilde{q}\} - [\bar{R}]^T\{\bar{q}\} = \{L\} \qquad (4\text{-}56)$$

where

$$[K_o] = \begin{bmatrix} I^*_{yy} & I^*_{xy} & -I^*_{yc} \\ I^*_{xy} & I^*_{yy} & I^*_{xc} \\ -I^*_{yc} & I^*_{xc} & I^*_{\omega} \end{bmatrix} \qquad (4\text{-}56a)$$

$$[K_s] = \begin{bmatrix} GA_{xx} & GA_{xy} & -GA_{x\theta} \\ GA_{xy} & GA_{yy} & -GA_{y\theta} \\ -GA_{x\theta} & -GA_{y\theta} & (GA_{\theta\theta} + GJ^*) \end{bmatrix} \qquad (4\text{-}56b)$$

$$[R_s]^T = \begin{bmatrix} r_{x1} & r_{x2} & \cdots & r_{xK} & \hat{r}_{x1} & \hat{r}_{x2} & \cdots & \hat{r}_{xJ} \\ r_{y1} & r_{y2} & \cdots & r_{yK} & \hat{r}_{y1} & \hat{r}_{y2} & \cdots & \hat{r}_{yJ} \\ r_{\theta 1} & r_{\theta 2} & \cdots & r_{\theta K} & \hat{r}_{\theta 1} & \hat{r}_{\theta 2} & \cdots & \hat{r}_{\theta J} \end{bmatrix} \qquad (4\text{-}56c)$$

$$[\bar{R}]^T = \begin{bmatrix} 0 & 0 & \cdots & 0 \\ 0 & 0 & \cdots & 0 \\ \bar{r}_{\theta 1} & \bar{r}_{\theta 2} & \cdots & \bar{r}_{\theta I} \end{bmatrix} \qquad (4\text{-}56d)$$

$\{\Delta\}$ = generalised displacement vector

$$= \text{col.}\{\, \xi(z) \quad \eta(z) \quad \theta(z) \,\} \qquad (4\text{-}56e)$$

$\{\tilde{q}\}$ = combined distributed beam shear vector for type 1 and type 3 connecting laminae

$$= \text{col.}\{\, q_1 \; q_2 \; \cdots \; q_K \; \hat{q}_1 \; \hat{q}_2 \; \cdots \; \hat{q}_J \,\} \qquad (4\text{-}56f)$$

$\{\bar{q}\}$ = distributed beam shear vector for type 2 connecting laminae

$$= \text{col.}\{\, \bar{q}_1 \quad \bar{q}_2 \; \cdots \; \bar{q}_I \,\} \qquad (4\text{-}56g)$$

$\{L\}$ = load vector

$$= \text{col.}\{\, -V_x \quad -V_y \quad -Q_t \,\} \qquad (4\text{-}56h)$$

The I compatibility equations for type 2 laminae can be represented as follows:

$$[\bar{R}]\{\Delta\}' - [\bar{\Gamma}]\{\bar{q}\} = \{0\} \qquad (4\text{-}57)$$

where

$$[\bar{\Gamma}] = \frac{1}{E}\begin{bmatrix} 1/\bar{\gamma}_1 & 0 & \cdots & 0 \\ 0 & 1/\bar{\gamma}_2 & \cdots & 0 \\ \vdots & \vdots & & \vdots \\ 0 & 0 & \cdots & 1/\bar{\gamma}_I \end{bmatrix} \tag{4-57a}$$

The compatibility equations for type 1 and type 3 laminae can be combined together to form one single matrix equation as follows:

$$[R_c]\{\Delta\}''' - [\Psi]\{\Delta\}' + [\tilde{A}]\{\tilde{q}\} - [\tilde{\Gamma}]\{\tilde{q}\}'' = \{0\} \tag{4-58}$$

where

$$[R_c]^T = \begin{bmatrix} r_{x1} & r_{x2} & \cdots & r_{xK} & \hat{r}^*_{x1} & \hat{r}^*_{x2} & \cdots & \hat{r}^*_{xJ} \\ r_{y1} & r_{y2} & \cdots & r_{yK} & \hat{r}^*_{y1} & \hat{r}^*_{y2} & \cdots & \hat{r}^*_{yJ} \\ r_{\theta 1} & r_{\theta 2} & \cdots & r_{\theta K} & \hat{r}^*_{\theta 1} & \hat{r}^*_{\theta 2} & \cdots & \hat{r}^*_{\theta J} \end{bmatrix} \tag{4-58a}$$

$$[\Psi]^T = \begin{bmatrix} 0 & 0 & \cdots & G^x_1 & G^x_2 & \cdots & G^x_J \\ 0 & 0 & \cdots & G^y_1 & G^y_2 & \cdots & G^y_J \\ 0 & 0 & \cdots & G^\theta_1 & G^\theta_2 & \cdots & G^\theta_J \end{bmatrix} \tag{4-58b}$$

in which, if Eqn(4-48a) is used for T_{cj1},

$$\left.\begin{aligned} G_j^x &= \rho_{xj}\, GA_\ell \cos^2\phi_\ell \\ G_j^y &= \rho_{xj}\, GA_\ell \sin\phi_\ell \cos\phi_\ell \\ G_j^\theta &= -\rho_{xj}\, \bar{y}_{o\ell}\, GA_\ell \cos\phi_\ell \end{aligned}\right\} \qquad (4\text{-}58c)$$

or, if Eqn(4-48b) is used for T_{cjl},

$$\left.\begin{aligned} G_j^x &= \rho_{yj}\, GA_\ell \sin\phi_\ell \cos\phi_\ell \\ G_j^y &= \rho_{yj}\, GA_\ell \sin^2\phi_\ell \\ G_j^\theta &= -\rho_{yj}\, \bar{y}_{o\ell}\, GA_\ell \sin\phi_\ell \end{aligned}\right\} \qquad (4\text{-}58d)$$

with $j = 1, 2, \ldots, J$; and ℓ = number of frame associated with the j^{th} band of type 3 laminae.

$$[\tilde{r}] = \frac{1}{E}\begin{bmatrix} 1/\gamma_1 & 0 & \cdots & & & 0 \\ 0 & 1/\gamma_2 & & & & \vdots \\ \vdots & & \ddots & & & \\ & & & 1/\gamma_K & & \\ & & & & 1/\hat{\gamma}_1 & \\ & & & & & 1/\hat{\gamma}_2 \\ 0 & 0 & \cdots & & & 1/\hat{\gamma}_J \end{bmatrix} \qquad (4\text{-}58e)$$

The matrix $[\tilde{A}]$ is a square symmetric matrix of order (K+J). Its set-up depends on how the shear walls and frames are coupled to one another by the type 1 or type 3 connecting laminae. A detailed and illustrated discussion of the construction of the matrix is given in Appendix G.

4.8 FINAL DIFFERENTIAL EQUATION AND SOLUTION

Eliminating $\{\tilde{q}\}$ from Eqn(4-56) by the use of Eqn(4-57), there is obtained

$$[K_o]\{\Delta\}''' - [\bar{K}_s]\{\Delta\}' - [R_s]^T\{\tilde{q}\} = \{L\} \qquad (4\text{-}59)$$

where $$[\bar{K}_s] = [K_s] + [\bar{R}]^T [\bar{\Gamma}]^{-1} [\bar{R}] \qquad (4\text{-}59a)$$

Defining a 3 x 1 vector $\{e\}$ by the following relationship

$$\{\tilde{q}\} = [\tilde{\Gamma}]^{-1} [R_c]\{e\} \qquad (4\text{-}60)$$

there is obtained from Eqn(4-59)

$$\{e\} = [R_s^T\tilde{\Gamma}^{-1}R_c]^{-1}[K_o]\{\Delta\}''' - [R_s^T\tilde{\Gamma}^{-1}R_c]^{-1}[\bar{K}_s]\{\Delta\}' - [R_s^T\tilde{\Gamma}^{-1}R_c]^{-1}\{L\} \qquad (4\text{-}61)$$

Substituting Eqn(4-60) into Eqn(4-58), there is obtained

$$[R_c]\{e\}'' = [\tilde{A}\tilde{\Gamma}^{-1}R_c]\{e\} + [R_c]\{\Phi\}''' - [\Psi]\{\Delta\}' \qquad (4\text{-}62)$$

Substituting Eqn(4-61) into Eqn(4-62), there is obtained

$$[K_o]\{\Delta\}^{V} - [K_1]\{\Delta\}''' + [K_2]\{\Delta\}' = \{L\}'' - [B]\{L\} \tag{4-63}$$

where

$$\left.\begin{aligned} [B] &= [R_s]^T[\tilde{\Gamma}]^{-1}[\tilde{A}\tilde{\Gamma}^{-1}R_c][R_s^T\tilde{\Gamma}^{-1}R_c]^{-1} \\ [K_1] &= [B][K_o] + [R_s^T\tilde{\Gamma}^{-1}R_c] + [\bar{K}_s] \\ [K_2] &= [B][\bar{K}_s] + [R_s]^T[\tilde{\Gamma}]^{-1}[\Psi] \end{aligned}\right\} \quad (4\text{-}63a)$$

Eqn(4-63) can be reduced to a fourth order differential equation as shown below:

$$[K_o]\{\Delta\}^{iv} - [K_1]\{\Delta\}'' + [K_2]\{\Delta\} = \int\{F\}d\bar{z} + \{C_k\} \tag{4-64}$$

where

$$\left.\begin{aligned} \{F\} &= \{L\}'' - [B]\{L\} \\ \{C_k\} &= 3 \times 1 \text{ constant vector} \end{aligned}\right\} \quad (4\text{-}64a)$$

Thus Eqn(4-64) represents the final differential equation to the present problem. In order to achieve a solution to this equation, the structure being considered must (a) have a minimum of three bands of types 1 or 3 laminae so as to ensure the non-singularity of $[R_s^T\tilde{\Gamma}^{-1}R_c]$, and (b) be structurally stable.

The solution to Eqn(4-64) consists of a complementary function $\{\Delta_H\}$ and a particular integral $\{\Delta_p\}$. Noting that the characteristic equation of the homogeneous differential equation is of the form

$$| \lambda^4[K_0] - \lambda^2[K_1] + [K_2] | = 0 \qquad (4\text{-}65)$$

which when expanded yields an even polynomial of degree 12, the complementary function can be shown to be given by

$$\{\Delta_H\} = \sum_{i=1}^{6} [C_i \cosh(\lambda_i z)\{\phi\}_i + S_i \sinh(\lambda_i z)\{\phi\}_i] \qquad (4\text{-}66)$$

where, with $i = 1, 2, \ldots 6$, λ_i^2 is the i^{th} eigenvalue of Eqn(4-65), $\{\phi\}_i$ is the eigenvector associated with $|\lambda_i|$, while C_i and S_i constitute twelve arbitrary constants to be determined from the boundary conditions of the structure.

The particular integral depends on the actual loading conditions. Thus, considering a combination of the following three common loading cases:

(a) concentrated lateral loads along X and Y and a concentrated torque about Z at the top of the structure, denoted by P_x, P_y and P_t respectively,

(b) uniformly distributed lateral loads of intensities p_x and p_y along X and Y, respectively, and uniformly

distributed torques of intensity p_t about Z,

(c) triangularly distributed lateral loads of top intensities $\bar{p}_x$ and $\bar{p}_y$ along X and Y, respectively, and triangularly distributed torques of top intensity $\bar{p}_t$ about Z,

the particular integral can be shown to be given by

$$\{\Delta_p\} = [K_2]^{-1}\left[\left(\frac{z}{H}\right)\begin{Bmatrix}\bar{p}_x\\ \bar{p}_y\\ \bar{p}_t\end{Bmatrix} + [B][\hat{P}]\begin{Bmatrix}z\\ z^2\\ z^3\end{Bmatrix}\right.$$

$$\left. + [K_1][K_2]^{-1}[B][\hat{P}]\begin{Bmatrix}0\\ 2\\ 6z\end{Bmatrix}\right] + \{\bar{C}_k\} \qquad (4\text{-}67)$$

where

$$[\hat{P}] = \begin{bmatrix} V_{xo}, & -p_x/2, & -\bar{p}_x/(6H)\\ V_{yo}, & -p_y/2, & -\bar{p}_y/(6H)\\ Q_{to}, & -p_t/2, & -\bar{p}_t/(6H)\end{bmatrix} \qquad (4\text{-}67a)$$

$\{\bar{C}_k\}$ = constant vector

$$= \text{col.}\{\bar{C}_{k1}, \bar{C}_{k2}, \bar{C}_{k3}\} \qquad (4\text{-}67b)$$

In Eqn(4-67a), V_{xo}, V_{yo}, and Q_{to} represent the total base

shears in the X- and Y-directions and the total base torque about Z, respectively.

The complete solution to Eqn(4-64) is thus given by

$$\{\Delta\} = \{\Delta_H\} + \{\Delta_P\} \tag{4-68}$$

There are altogether fifteen constants, namely, C_i and S_i with $i = 1, 2, \ldots. 6$ and $\bar{C}_{k1}$, $\bar{C}_{k2}$, and $\bar{C}_{k3}$. These are determined from the following boundary conditions:

(a) There are no lateral or rotational displacements at the base. Thus,

$$\text{at } z = o, \{\Delta\} = o \tag{4-69a}$$

(b) The slope of the structure is zero and warping is not permitted at the base. Thus,

$$\text{at } z = o, \{\Delta\}' = o \tag{4-69b}$$

(c) Moments, bimoments, and axial forces vanish at the top. Therefore,

$$\text{at } z = H, \{\Delta\}'' = o \tag{4-69c}$$

(d) According to Eqns(4-44b), (4-46), and (4-52), the shear distributions in the connecting laminae vanish at the base. Therefore, from Eqn(4-56), there is obtained

$$\text{at } z = o,\ [K_o]\{\Delta\}''' = \{L\} \qquad (4\text{-}69d)$$

(e) Differentiating Eqns(4-44b), (4-46), and (4-52) once and noting Eqn(4-69c), it can be concluded that the first derivatives of the shear distributions in the connecting laminae vanish at the top. Therefore, differentiating Eqn(4-56) once and applying this condition and Eqn(4-69c), there can be obtained

$$\text{at } z = H,\ [K_o]\{\Delta\}^{iv} = \{L\}' \qquad (4\text{-}69e)$$

Eqns(4-69a) through (4-69e) thus constitute fifteen simultaneous equations, from which the constants can be found. The generalised displacements are then given by Eqn (4-68), while the local displacements of walls and frames can be determined by the use of the transformation relationships of Eqns(4-1a) and (4-1b). The shear distributions in the type 1 and type 3 laminae are given by Eqns(4-60) and (4-61), and those in type 2 laminae by Eqn(4-57). The axial stress σ_p at any point in shear wall m can be found from the

relation

$$\sigma_p = \frac{T_m}{A_m} - E(\xi''_m \bar{x}_p + \eta''_m \bar{y}_p + \theta''_m \bar{\omega}_p) \qquad (4\text{-}70)$$

where $(\bar{x}_p, \bar{y}_p)$ are the co-ordinates of the particular point relative to the local co-ordinate system of wall m and $\bar{\omega}_p$ is the sectorial co-ordinate of that point with respect to S_m. T_m is given by Eqn(4-42a) or Eqn(4-42b). For the plane frames, the horizontal interstorey shear forces are given by Eqn(4-10). With these shear forces and the associated beam shear distributions, if any, a plane frame program can be used to find the internal reactions of the frame members.

4.9 VERIFICATION OF PROPOSED ANALYSIS

A uniform 15-storey concrete wall-frame structure has been analysed using the proposed method. It consists of nine wall piers, three frames, three rows of type 1 connecting beams, and two rows of type 3 connecting beams as shown in Figure 4-13. Storey height is 3.50m (11ft 6in). Wall thickness is 0.20m (8in) for all walls. All column sections are 1.0m (39.4in) square and all connecting beam and girder sections are 0.20m x 1.0m deep. Shear deformation is neglected for all connecting beams, girders, columns, and walls. Young's modulus is taken to be 2.07×10^7 kN/m^2 (4.32×10^5 ksf). A uniform lateral load of 10kN/m (0.685klf) along the height of the structure is assumed to act at wall pier 4 in the direction of the Y-axis.

For comparison, the same structure has also been analysed using the SAP-IV computer program [62], whereby the wall piers are treated as equivalent columns with rigid arms attached at floor levels. The rotational displacements of the structure as computed by both methods are plotted as shown in Figure 4-14. Results for the X- and Y-translational displacements at the centriod of wall pier 4 are shown in Figures 4-15 and 4-16. The wall moments of wall pier 3 and those about the stronger axis of wall pier 9 are shown in Figures 4-17 and 4-18 respectively. Interstorey frame shears are shown in Fig-

ures 4-19 through 4-21 while connecting beam shears are shown in Figures 4-22 through 4-26. To demonstrate the stiffening effect of the frames, a separate analysis [4] has also been performed on the structure without the frames. Results for structure rotation and the translational displacements of wall pier 4 as found by the analysis are shown in Figures 4-14 through 4-16.

A comparison of the results produced by the proposed method and the SAP-IV computer program show close agreement in general. Frame shears near the base are seen to be underestimated by the proposed method as a result of the assumption of zero slope at the base of the structure. Beam shears are generally overestimated by the proposed method. Despite the significant discrepancies in the results of beam shears for some of the connecting beams, the trends of shear distribution in these beams as exposed by both methods compare reasonably well. From Figures 4-14 through 4-16, the significant contribution of the three frames to the overall stiffness of the structure can be observed.

Finally, it is of interest to note that the execution time required by the SAP-IV program for analysing the above example structure on the CDC CYBER 170/730 computer was about 126 decimal seconds while that required by the proposed method was about 2.5 decimal seconds only (not including time required for solving for the member reactions in the frames

by plane frame analysis). The proposed method has also the advantage of computing the stresses at wall joints directly whereas with SAP-IV, this has to be performed separately.

4.10 CONCLUSION

A three-dimensional method of analysis has been presented for the investigation of the response of general uniform wall-frame building structures to lateral and torsional loads. In the analysis, the shear walls can have arbitrary open-sectional shapes and are treated as thin-walled beams. The connecting beams between walls or between walls and frames are replaced by continuous media of equivalent structural properties. The frames are replaced by shear beams in approximation of their horizontal shear resistances. Despite the limitation that vertical compatibility is not enforced at columns which belong to more than one moment frame, vertical compatibility between shear walls or between shear walls and frames is considered. No restrictions are imposed on the numbers, locations, and orientations of the shear walls and frames. An example has been worked out and the results checked against those given by SAP-IV [62]. The contribution of the frames in this example structure has also been found to be considerable.

In spite of the drawback of the shear beam model in accounting for the effect of axial deformations in the columns on the lateral deflection of the frame, which may be a significant factor in tall and slender frames, the proposed method

does possess the following advantages over matrix methods of analysis:

(1) The proposed method in general requires considerably less computer time and smaller computer capacities than matrix methods. The process of data preparation is also less tedious and time-consuming for the proposed method than for matrix methods.

(2) During the course of the design process, clear insights in regard to the overall behaviour of the structure being studied can be more readily provided the designer by the proposed method than by matrix methods.

(3) Since the final governing differential equation, namely, Eqn(4-64), has lateral and rotational displacements as the variable, the proposed analysis can be readily extended into a dynamic analysis by including the appropriate inertial forces into the equilibrium equations.

Finally, it is believed that the proposed method of analysis does provide a useful means for the study of the behaviour of general uniform wall-frame building structures subjected to lateral and torsional loads.

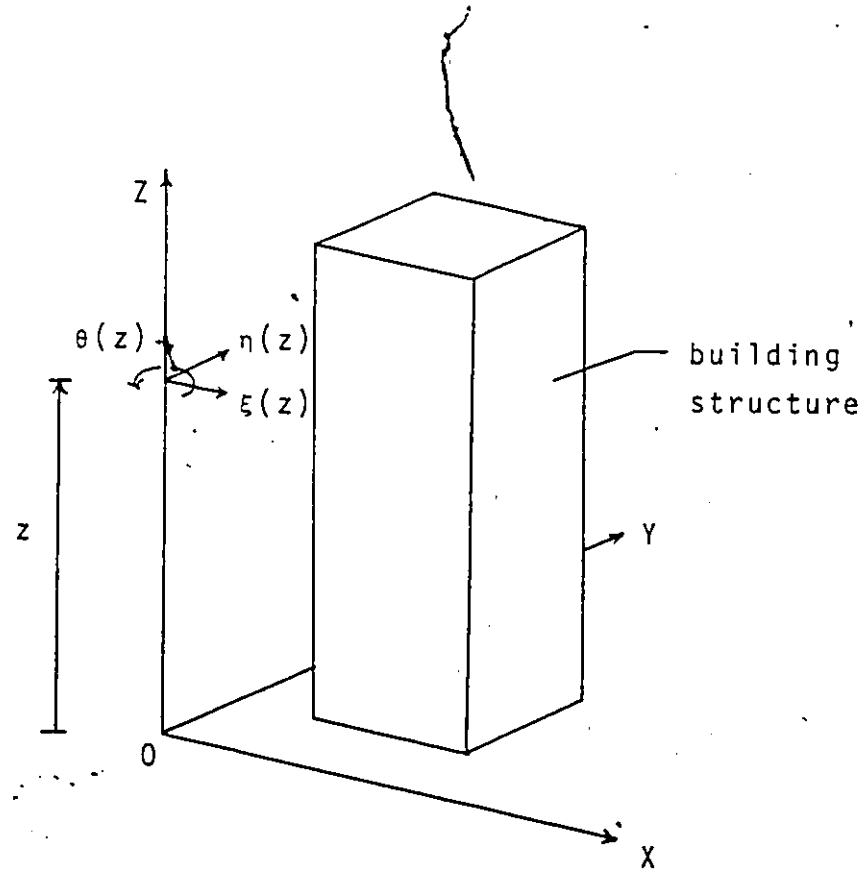

FIG. 4-1: GLOBAL CO-ORDINATE SYSTEM AND DISPLACEMENTS

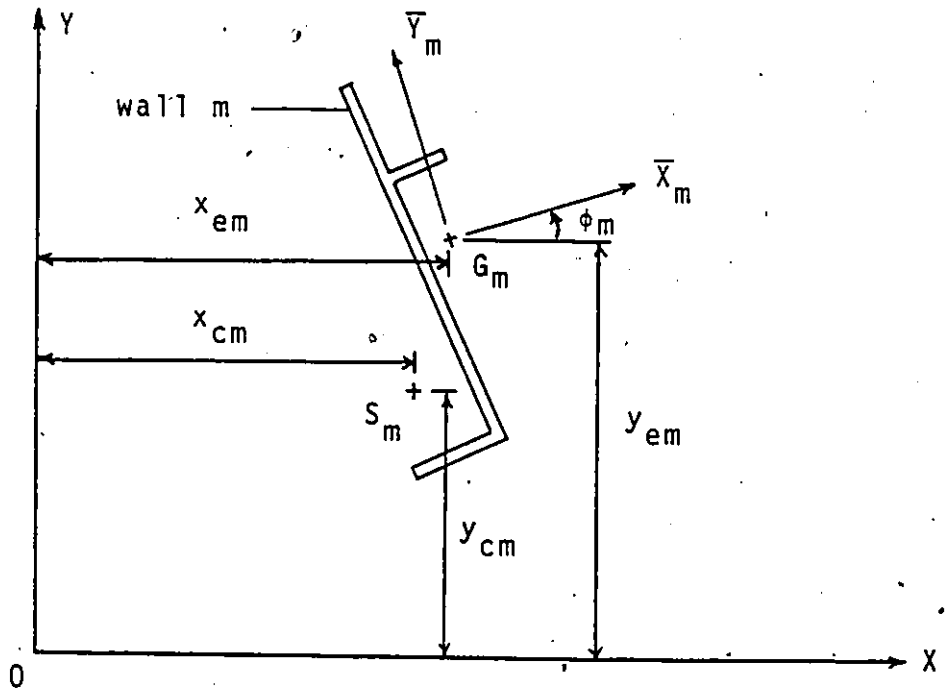

FIG. 4-2: GEOMETRY OF TYPICAL SHEAR WALL

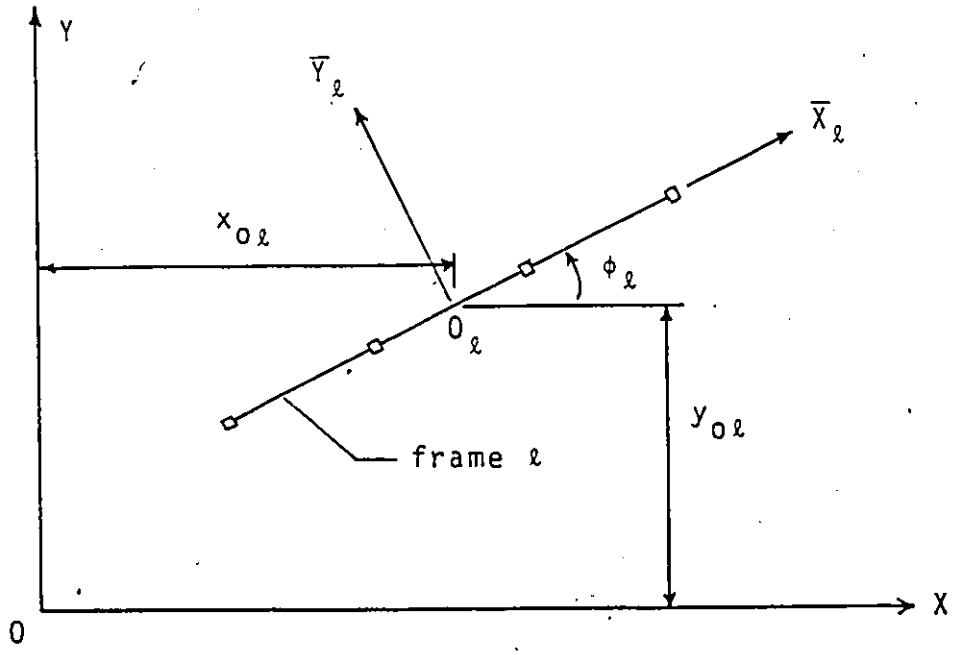

FIG. 4-3: GEOMETRY OF TYPICAL FRAME

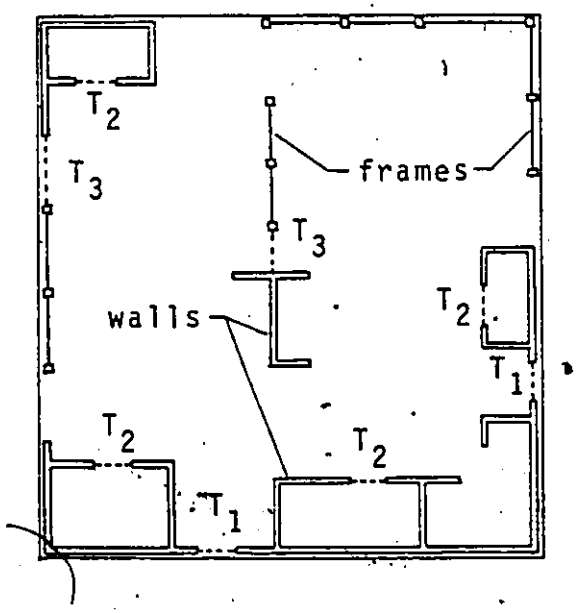

LEGEND

T_1 — type 1 beams

T_2 — type 2 beams

T_3 — type 3 beams

FIG. 4-4: EXAMPLE COUPLING CONFIGURATIONS

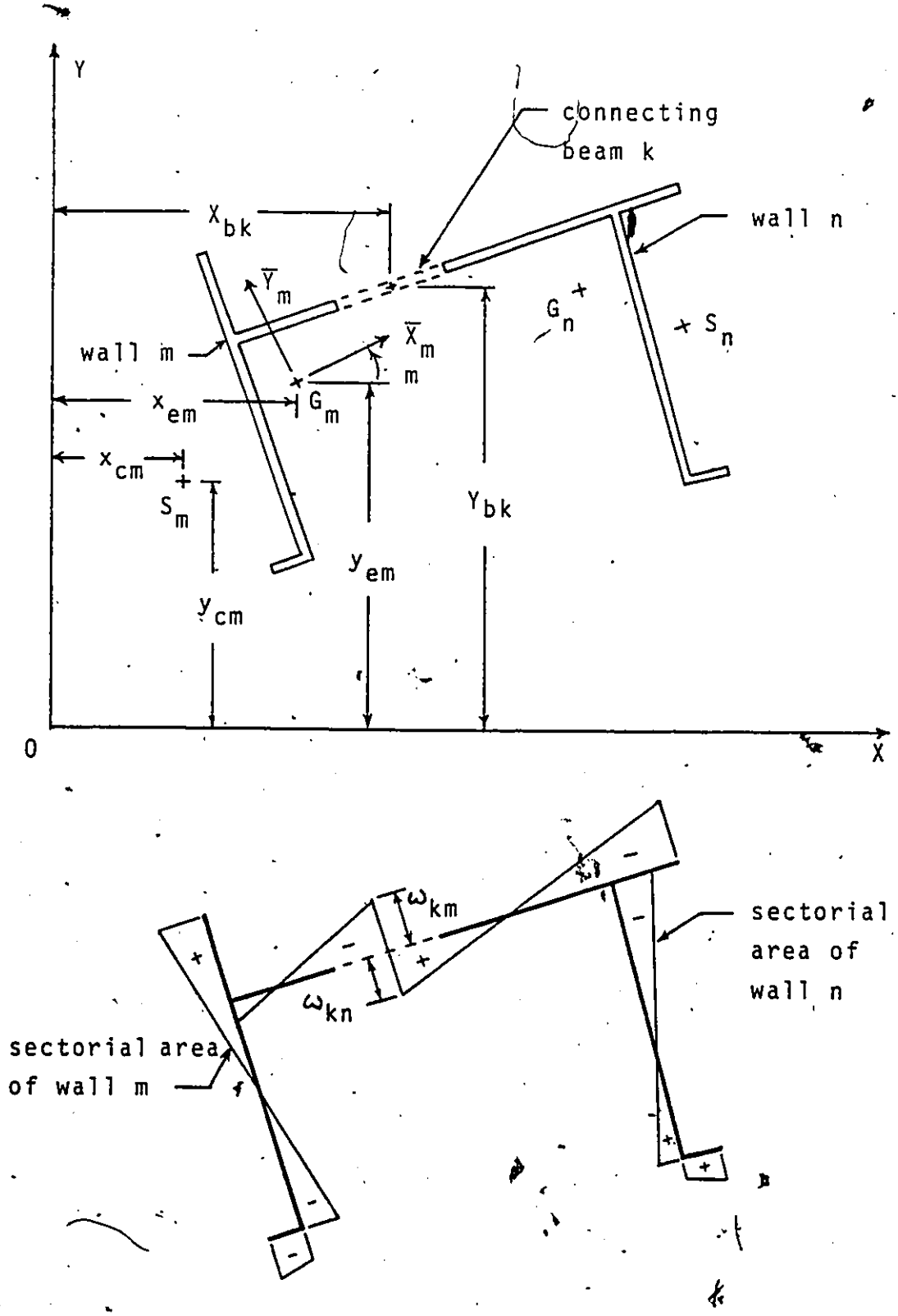

FIG. 4-5: COUPLING BY TYPE 1 CONNECTING BEAMS

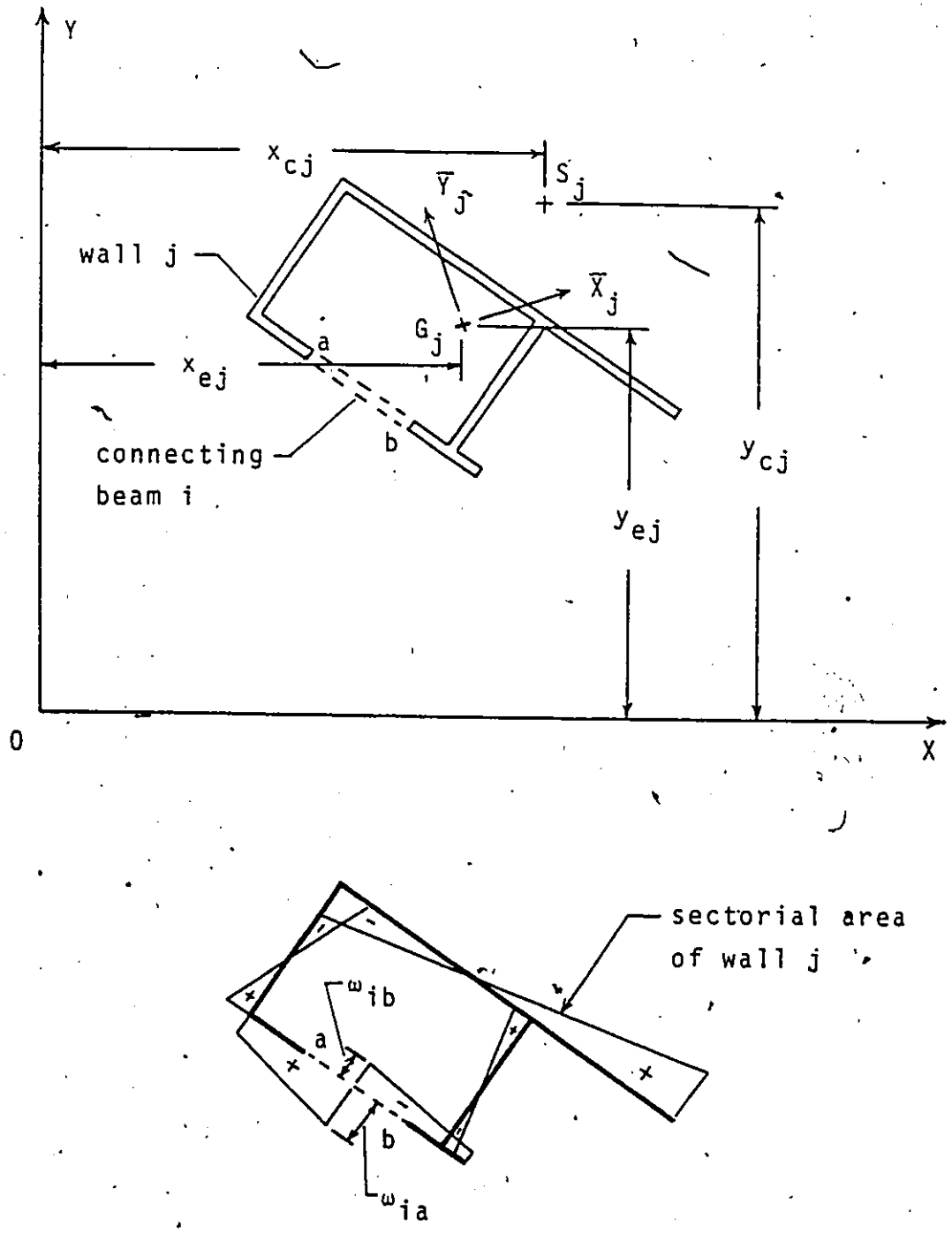

FIG. 4-6: COUPLING BY TYPE 2 CONNECTING BEAMS

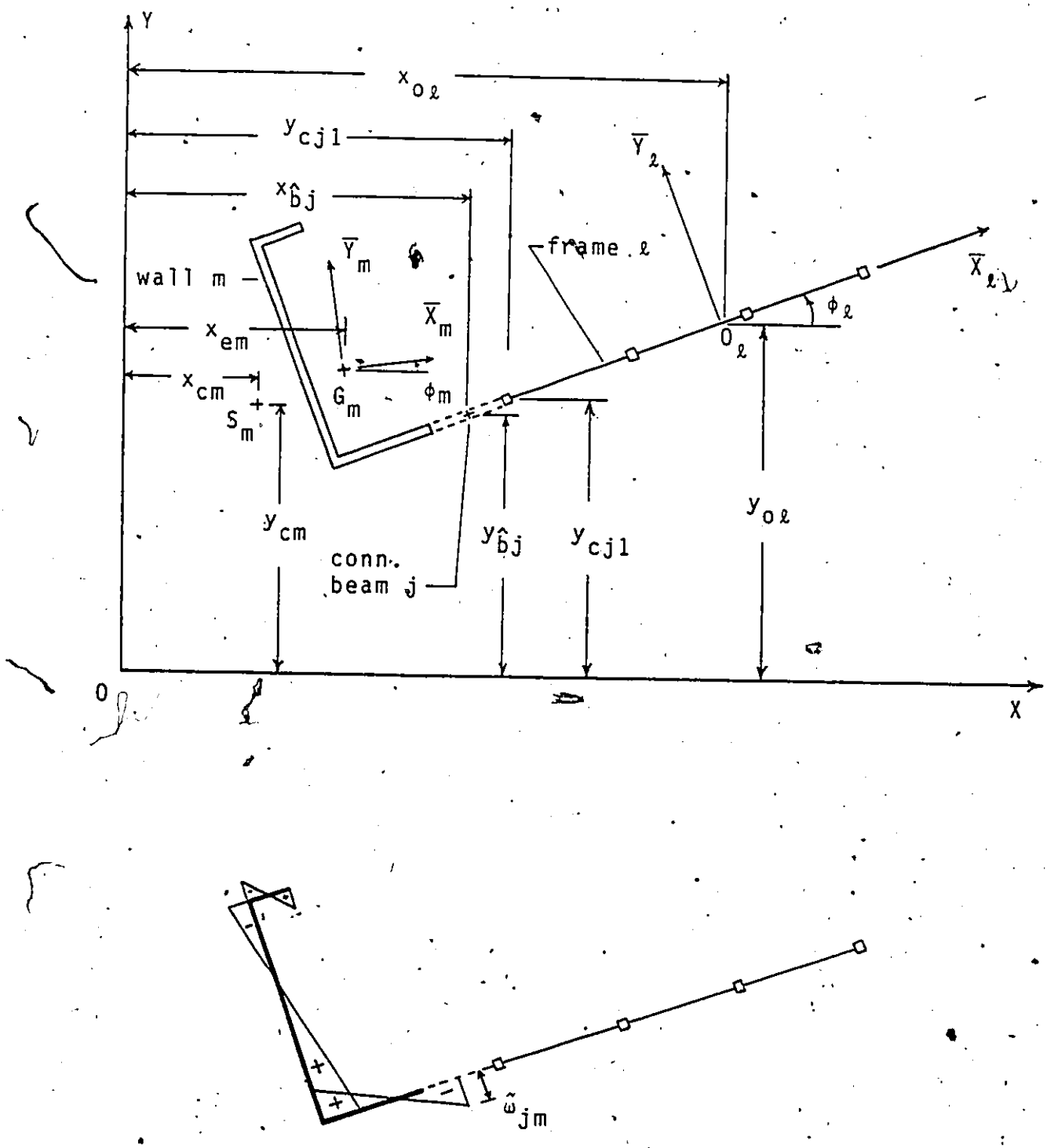

FIG. 4-7: COUPLING BY TYPE 3 CONNECTING BEAMS

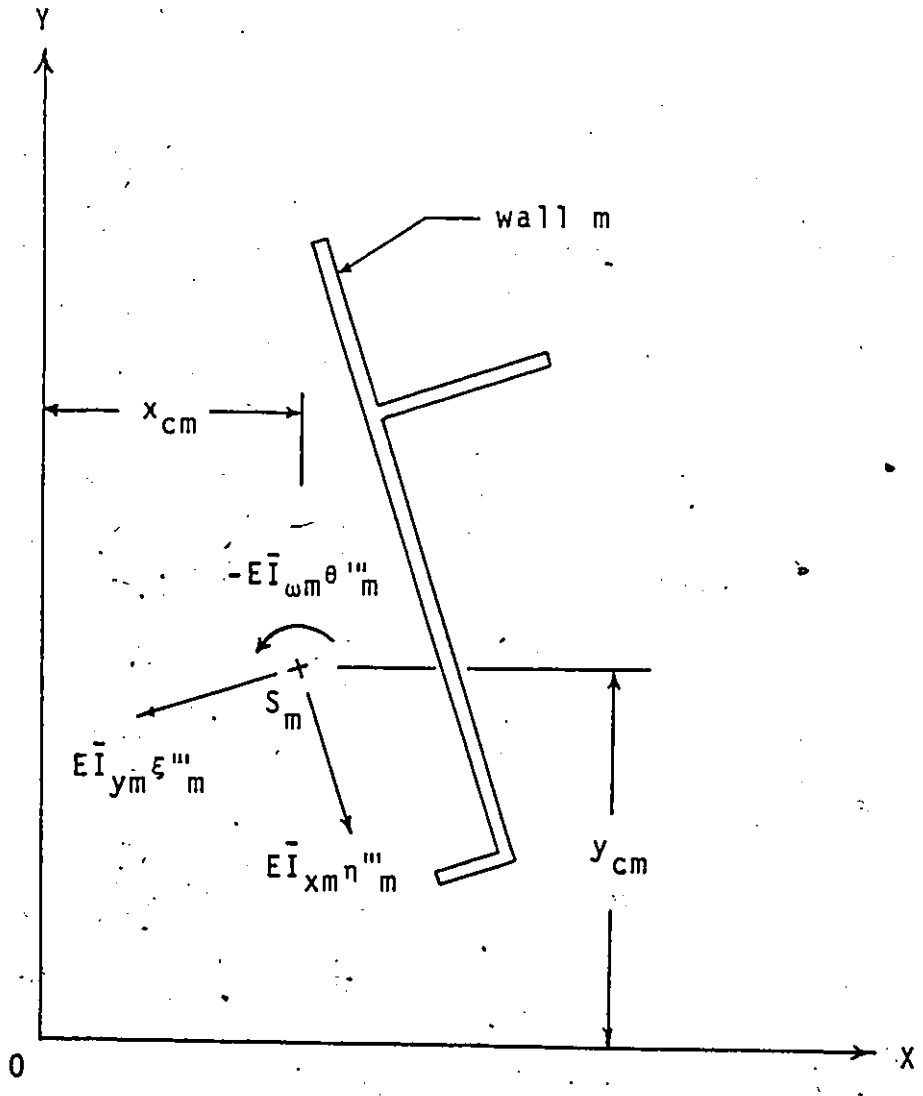

FIG. 4-8: SHEAR FORCES AND TORQUE ACTING ON WALL m

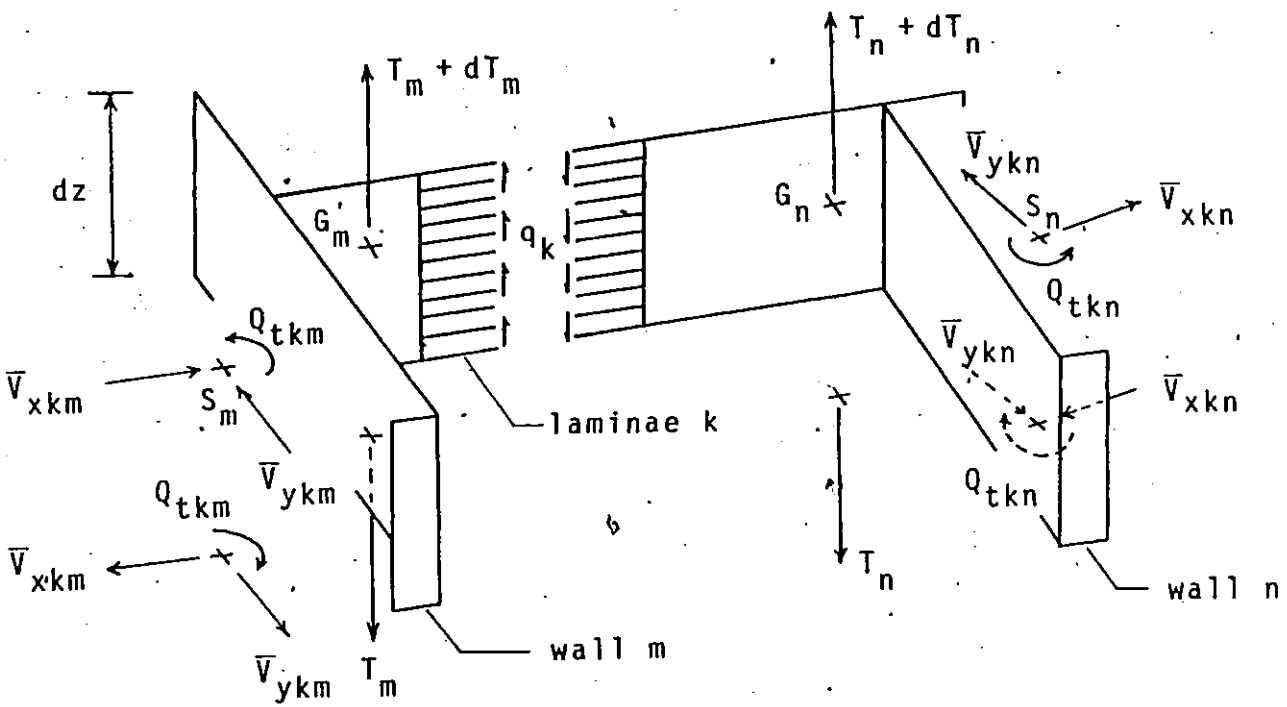

FIG. 4-9: FORCE AND TORQUE COMPONENTS ON WALLS m AND n DUE TO DISTRIBUTED SHEAR q_k

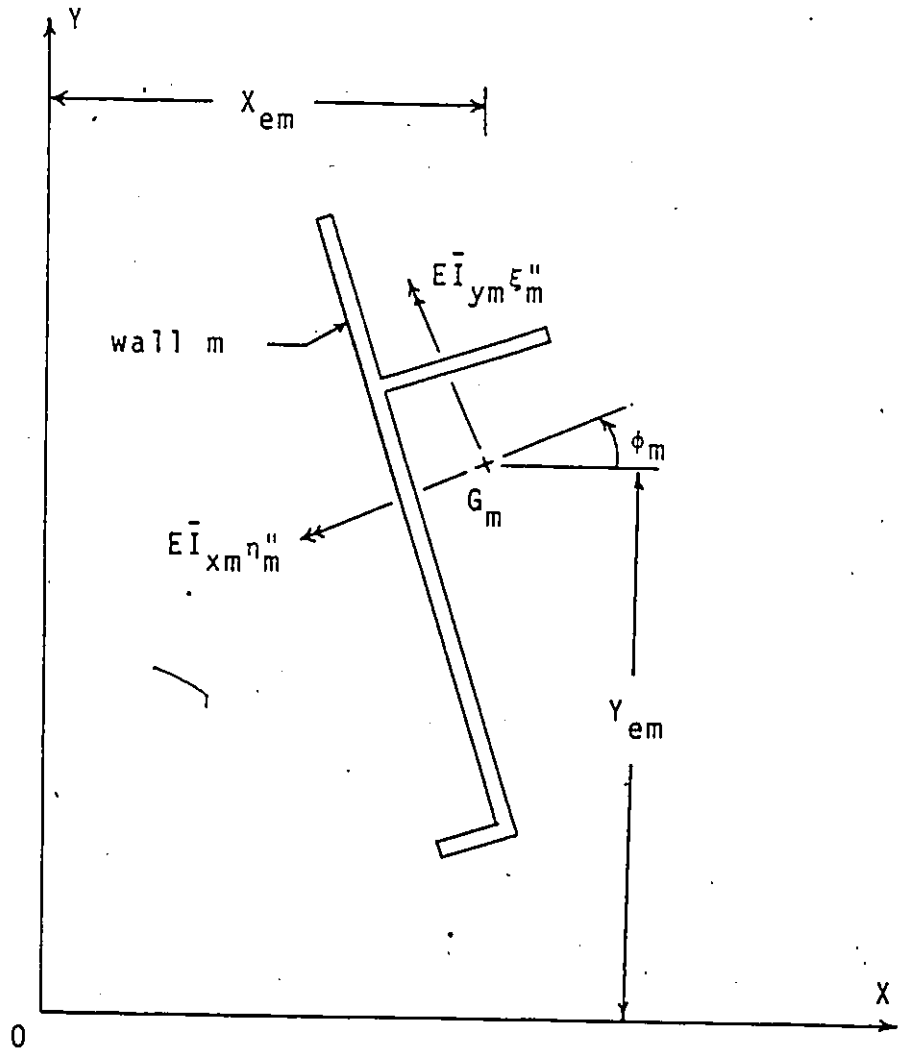

FIG. 4-10: MOMENTS ACTING ON WALL m

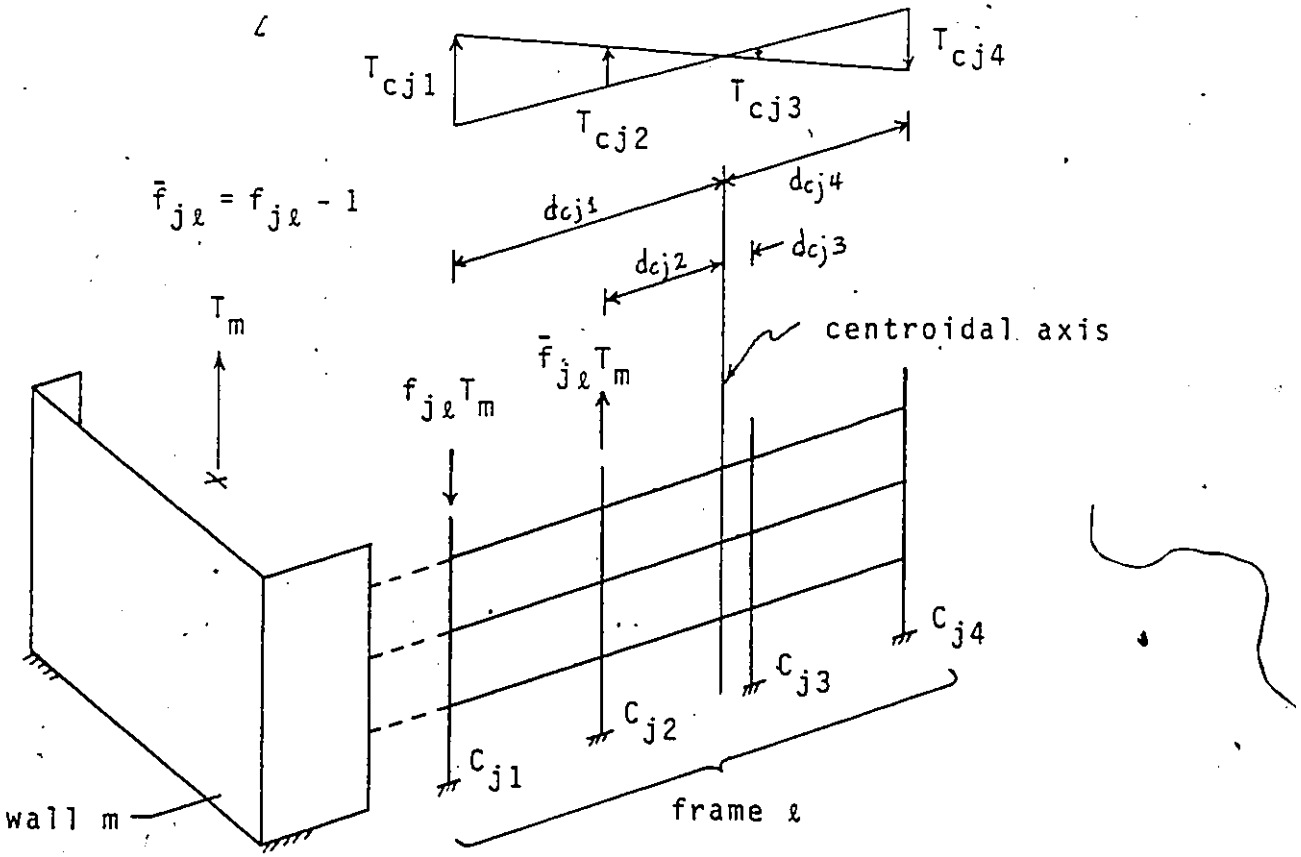

FIG. 4-11: AXIAL EFFECTS IN SHEAR WALL-FRAME UNIT

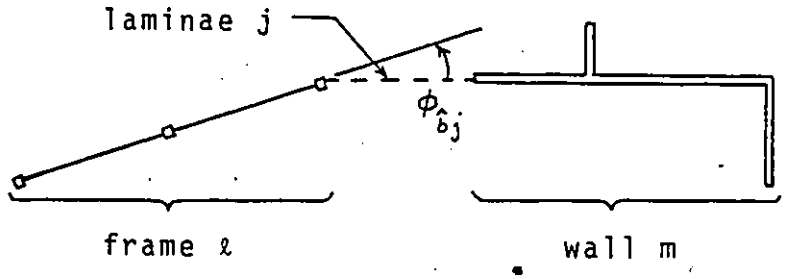

FIG. 4-12: TYPE 3 LAMINAE INCLINED TO PLANE OF CONNECTED FRAME

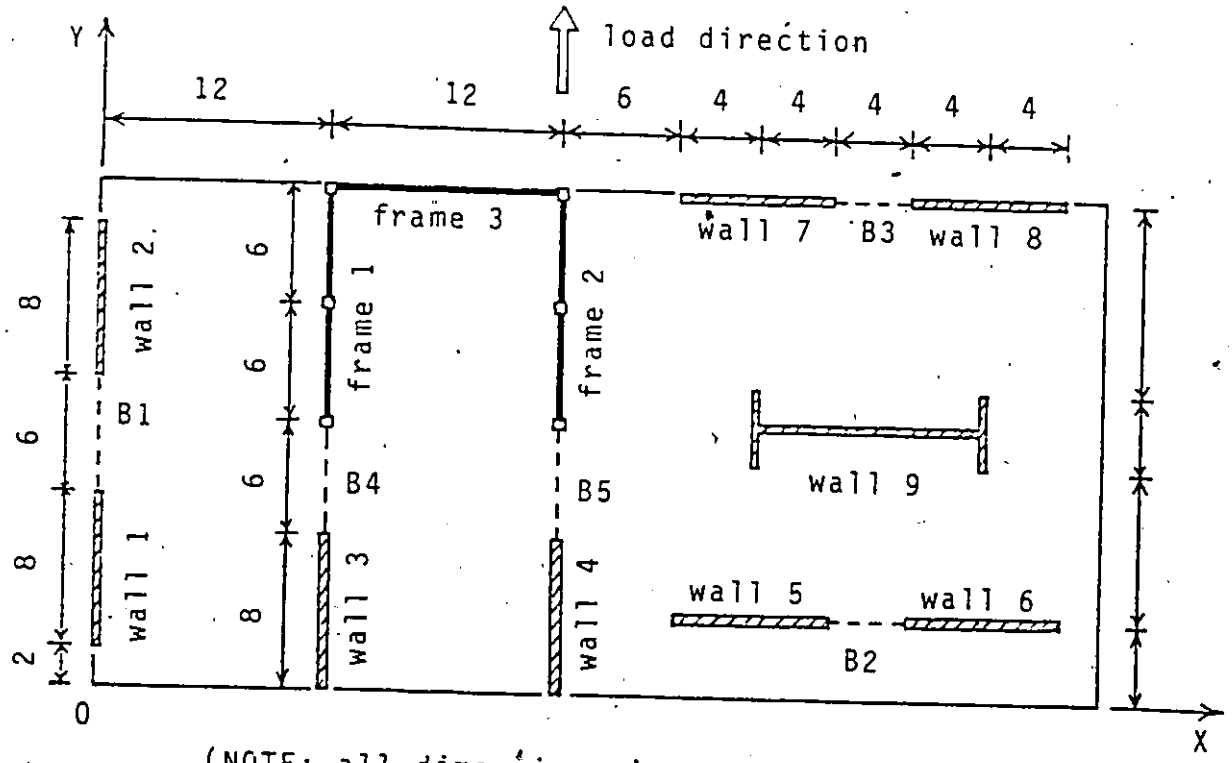

(NOTE: all dimensions in metres; connecting beams denoted by 'B1', 'B2', etc.)

STRUCTURAL DATA

wall thickness = 0.20 m

column section = 1.0 m square

girder section = 0.20 m x 1.0 m deep

conn. beam section = 0.20 m x 1.0 m deep

storey height = 3.50 m; no. of storeys = 15

Young's modulus = 20,700 MN/m^2

lateral load = 10 kN/m (applied at wall pier 4 in the direction of the Y-axis)

FIG. 4-13: PLAN OF EXAMPLE STRUCTURE

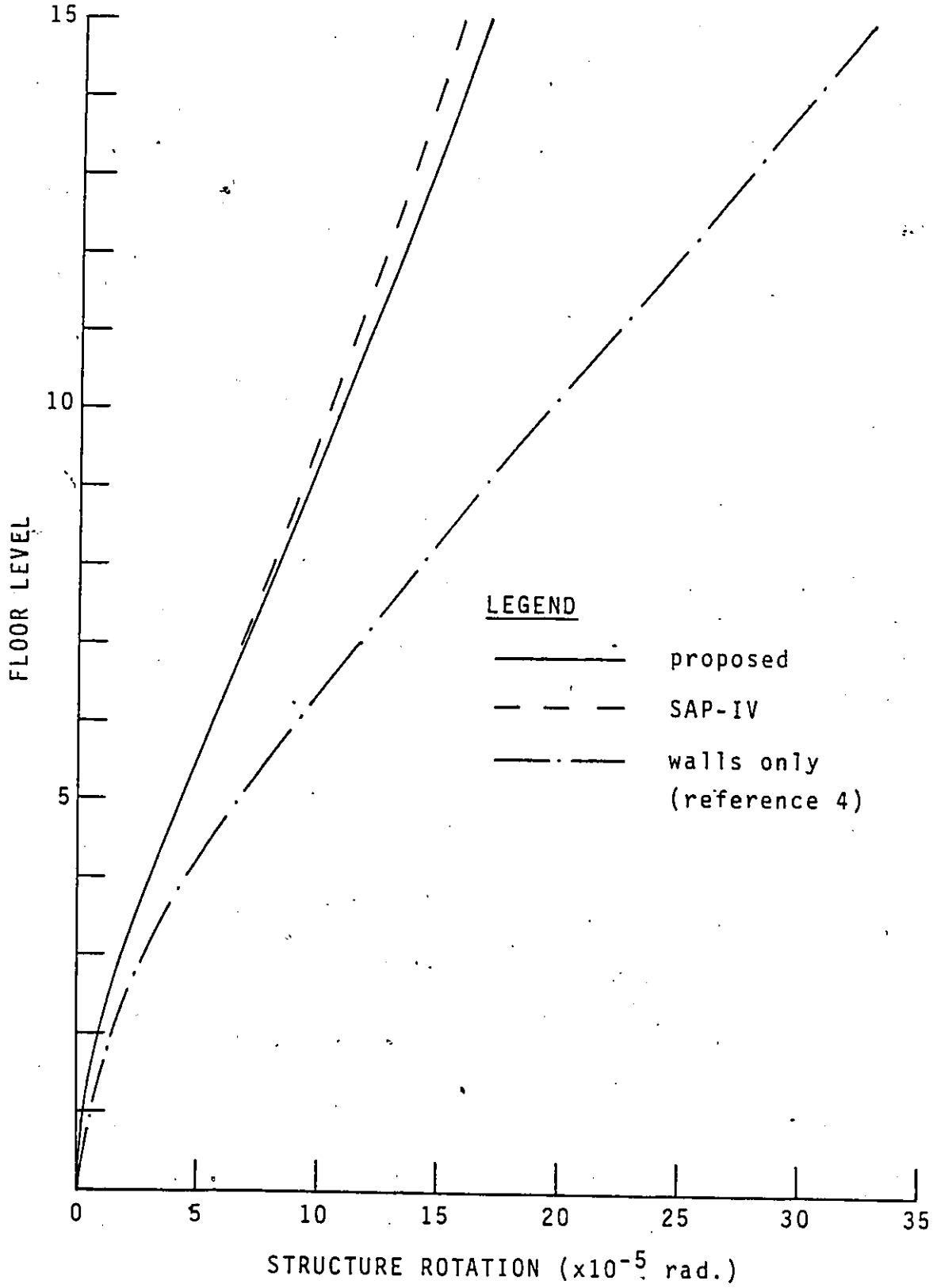

FIG. 4-14: ROTATION OF EXAMPLE STRUCTURE

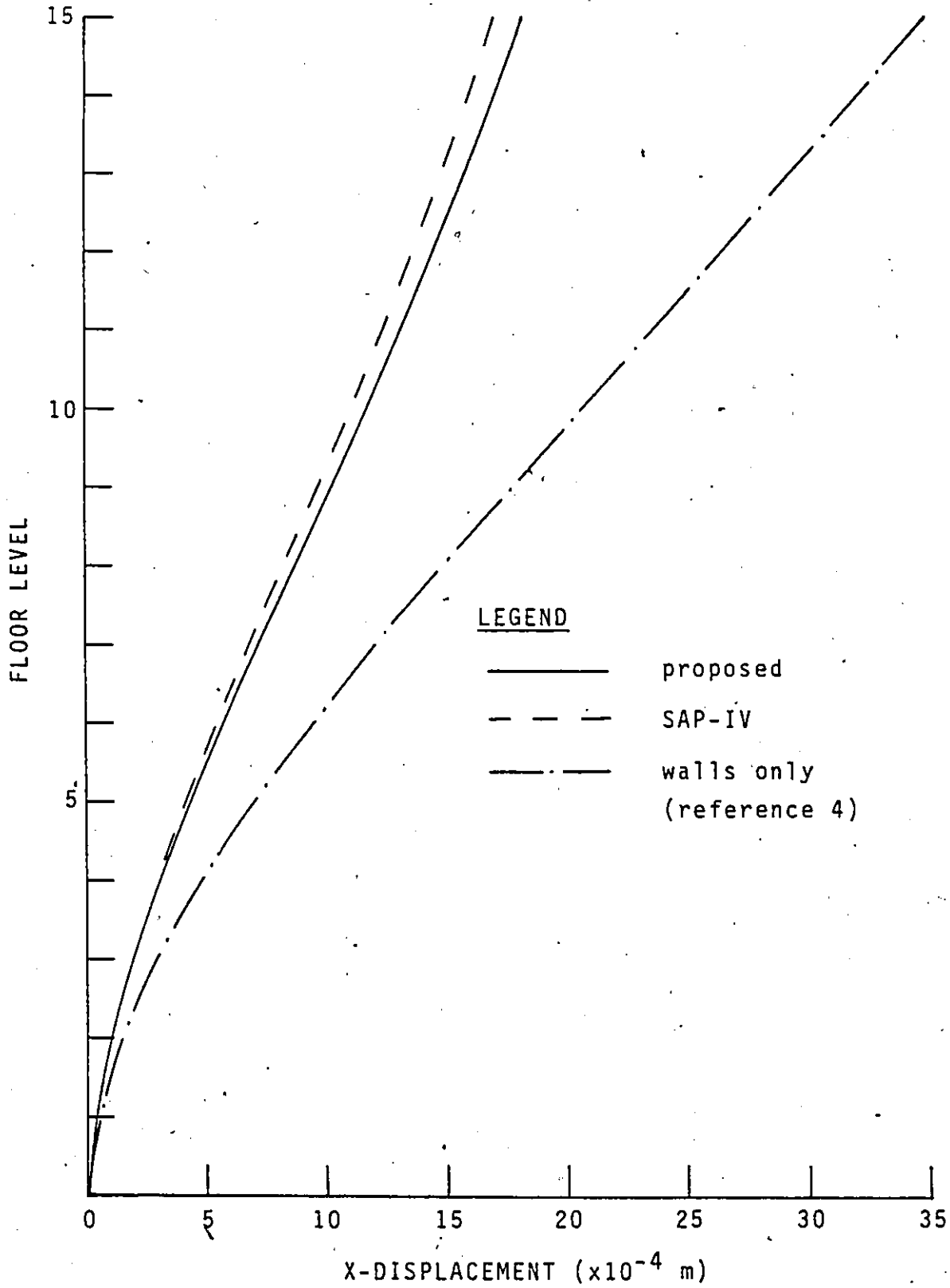

FIG. 4-15: X-DISPLACEMENT AT CENTROID OF WALL PIER 4

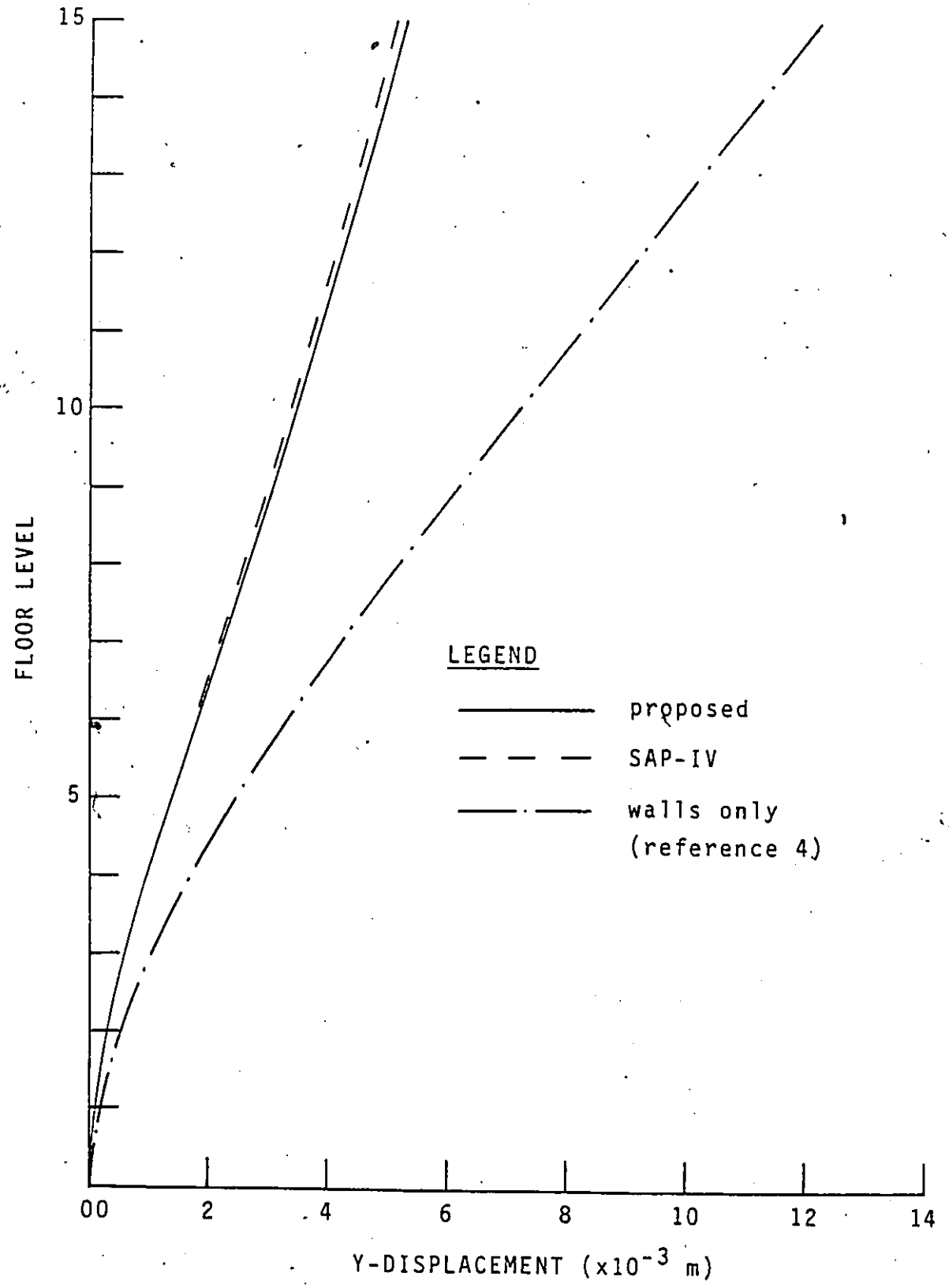

FIG. 4-16: Y-DISPLACEMENT AT CENTROID OF WALL PIER 4

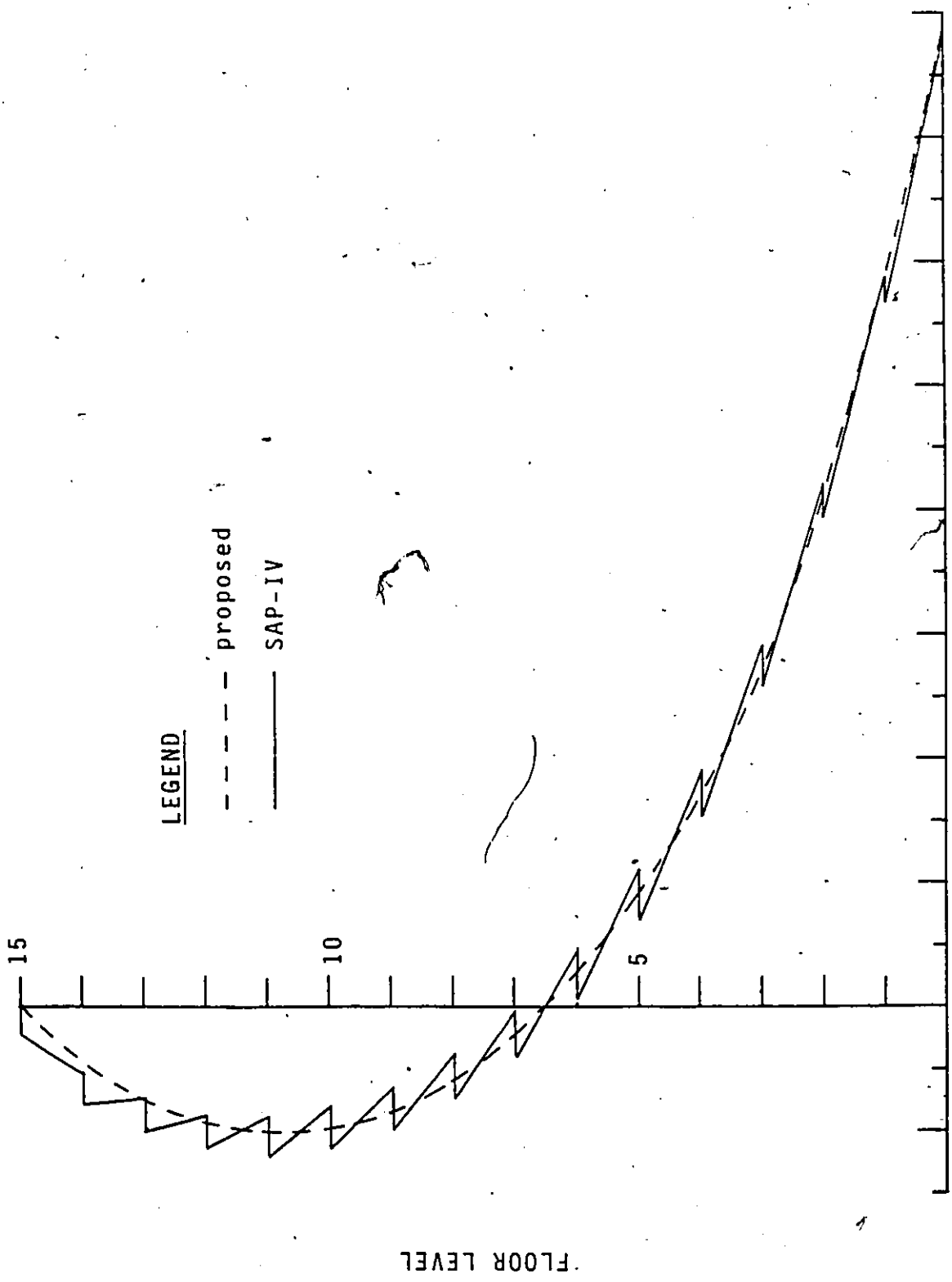

FIG. 4-17: INTERNAL MOMENT OF WALL PIER 3

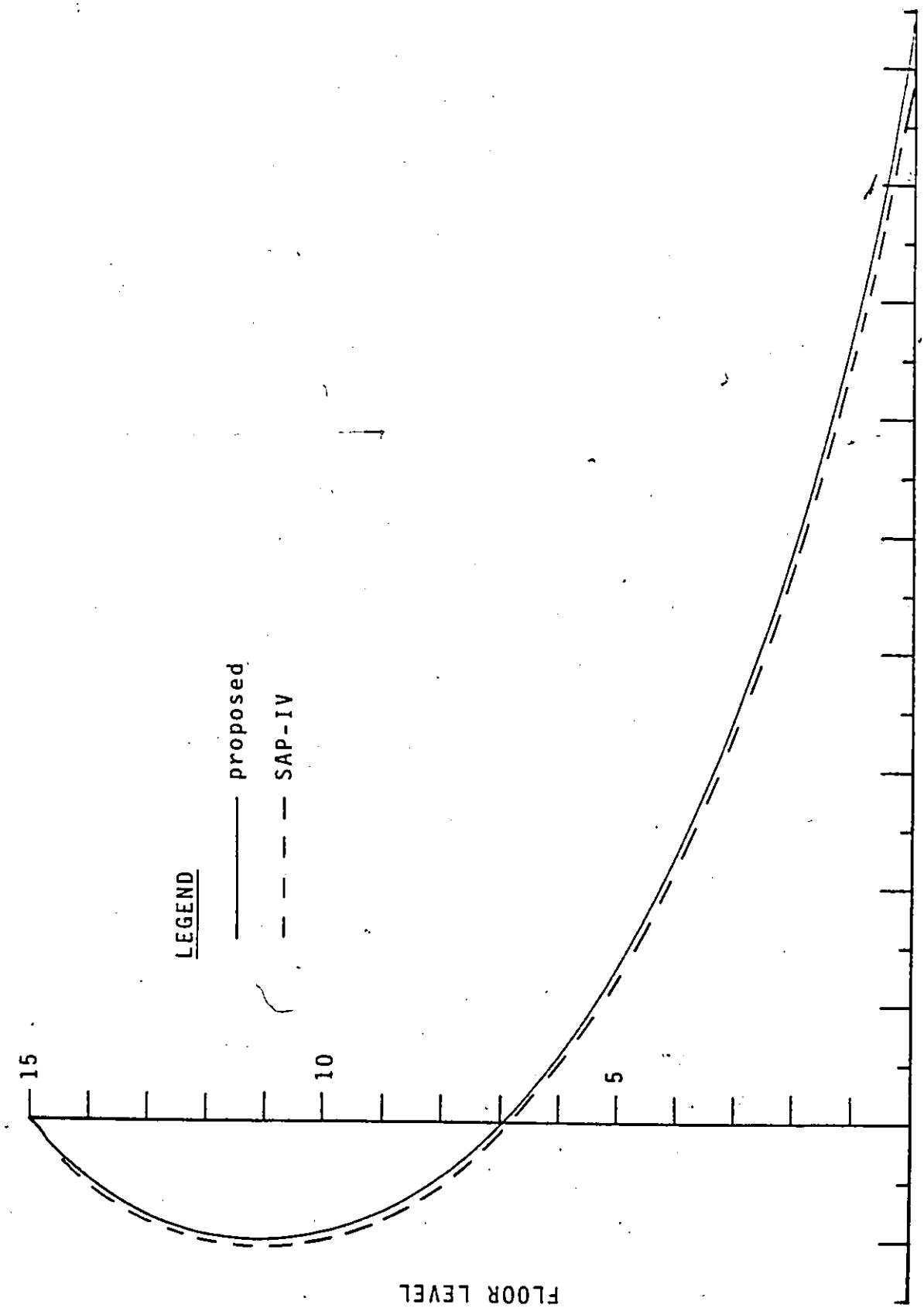

FIG. 4-18: INTERNAL MOMENT (ABOUT STRONG AXIS) OF WALL PIER 9

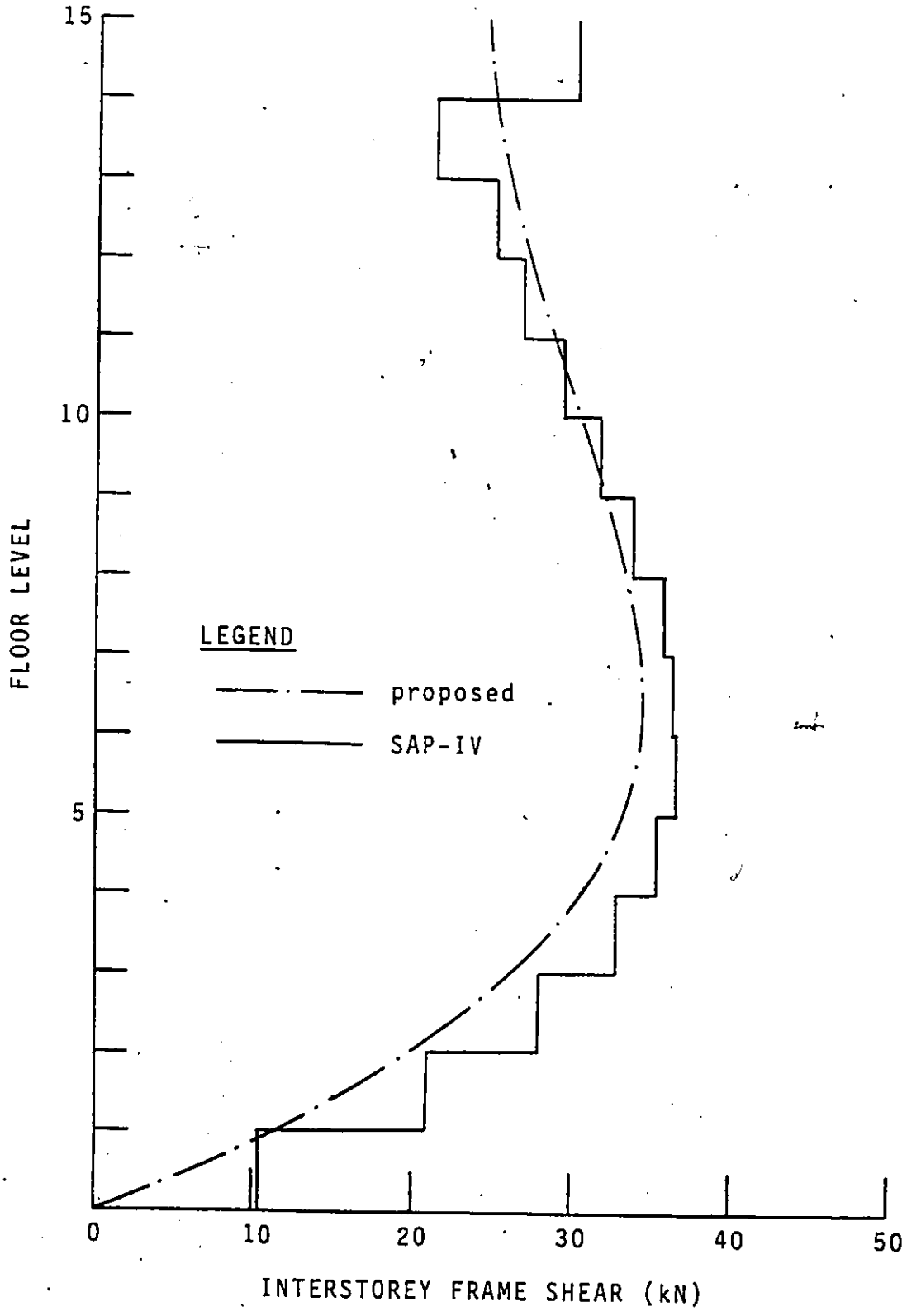

FIG. 4-19: INTERSTOREY SHEAR IN FRAME 1

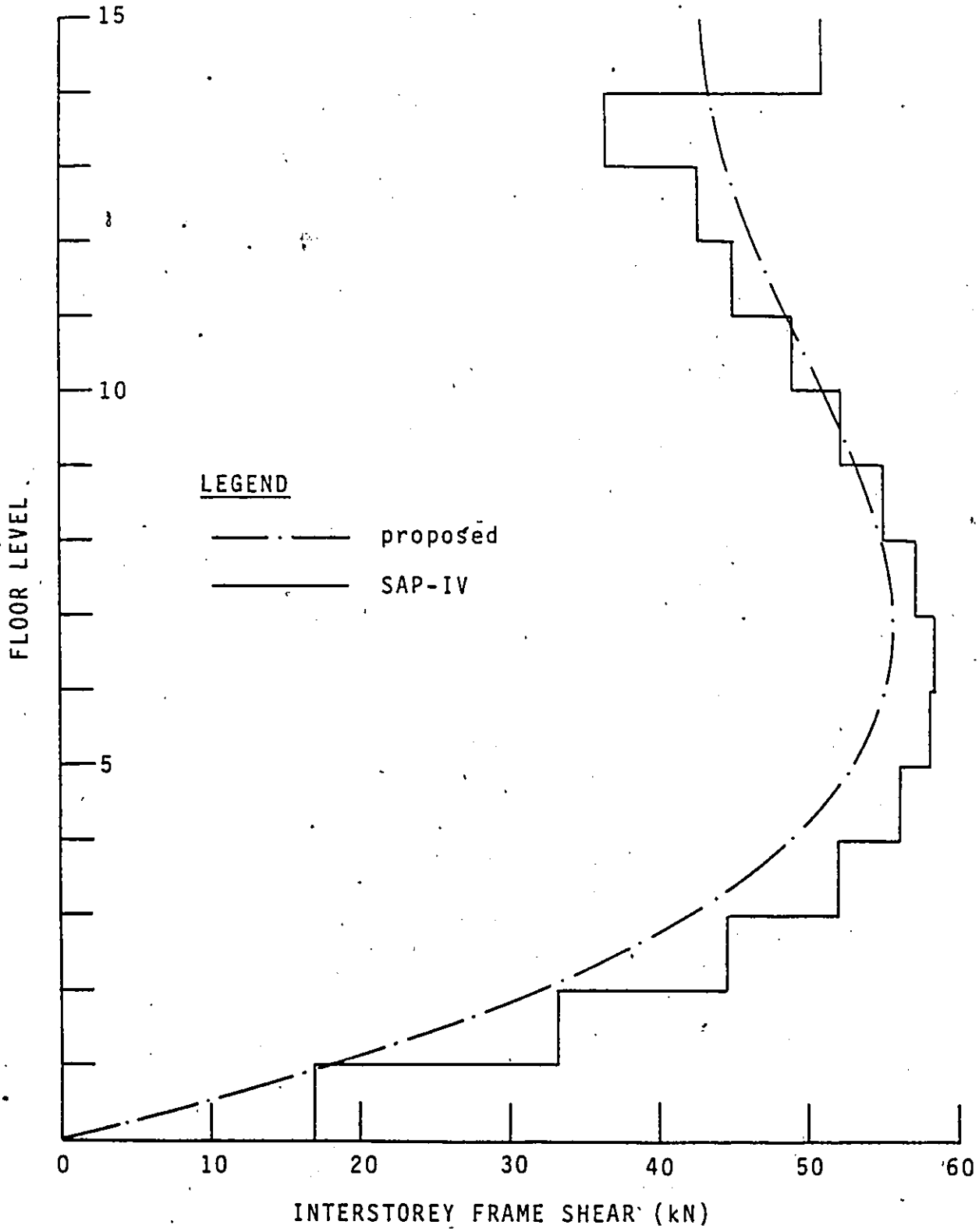

FIG. 4-20: INTERSTOREY SHEAR IN FRAME 2

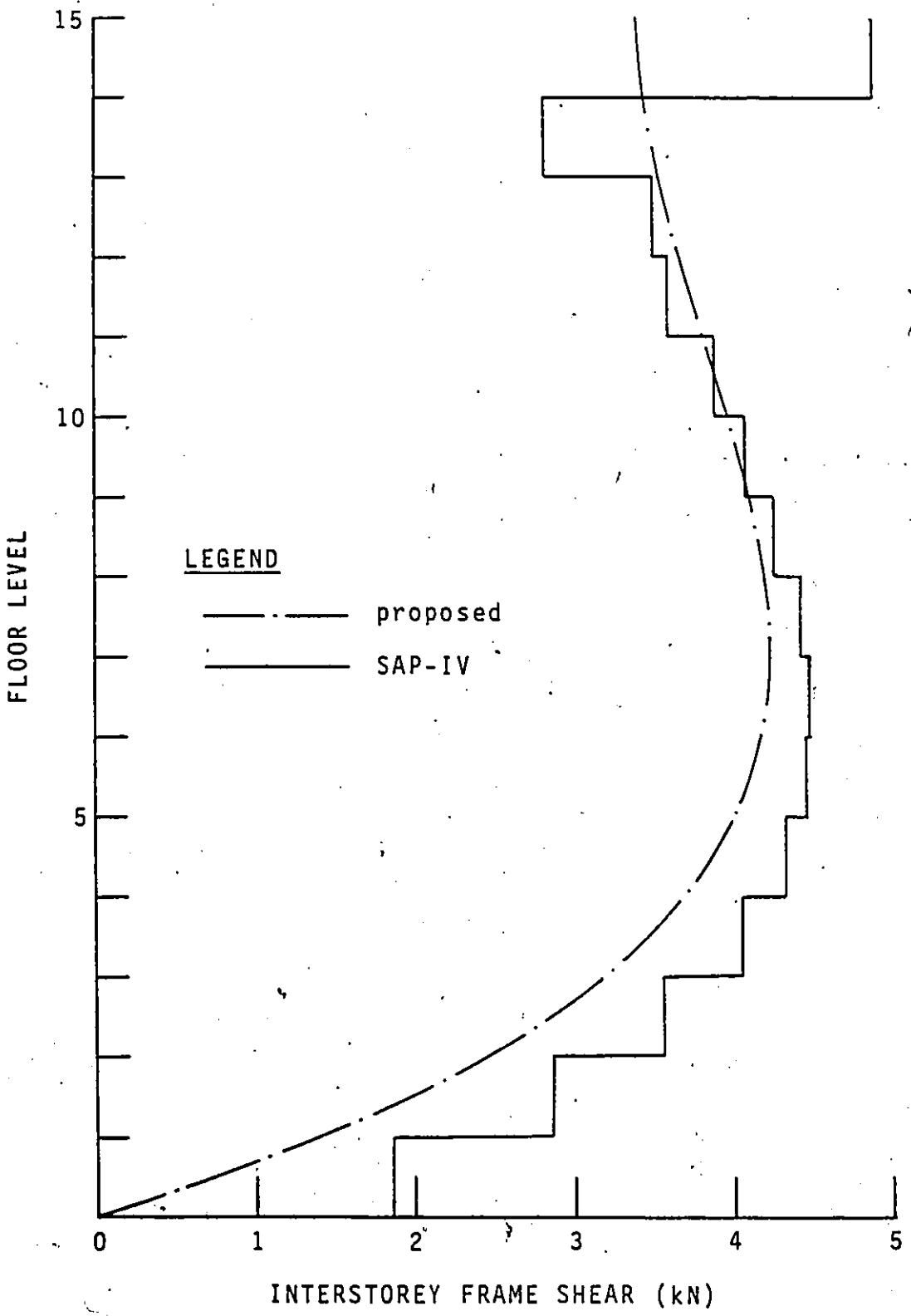

FIG. 4-21: INTERSTOREY SHEAR IN FRAME 3

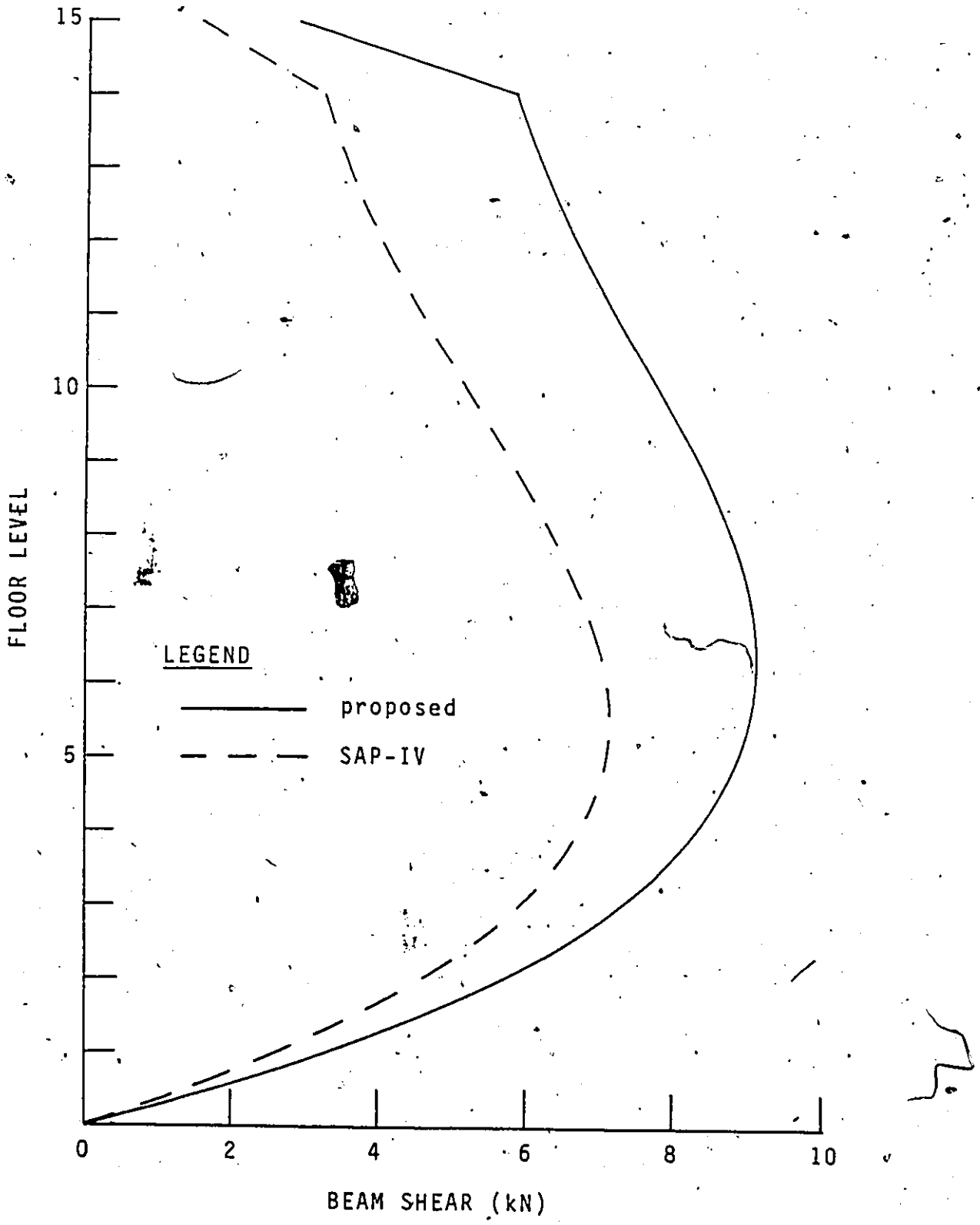

FIG. 4-22: SHEARS IN CONNECTING BEAM 1

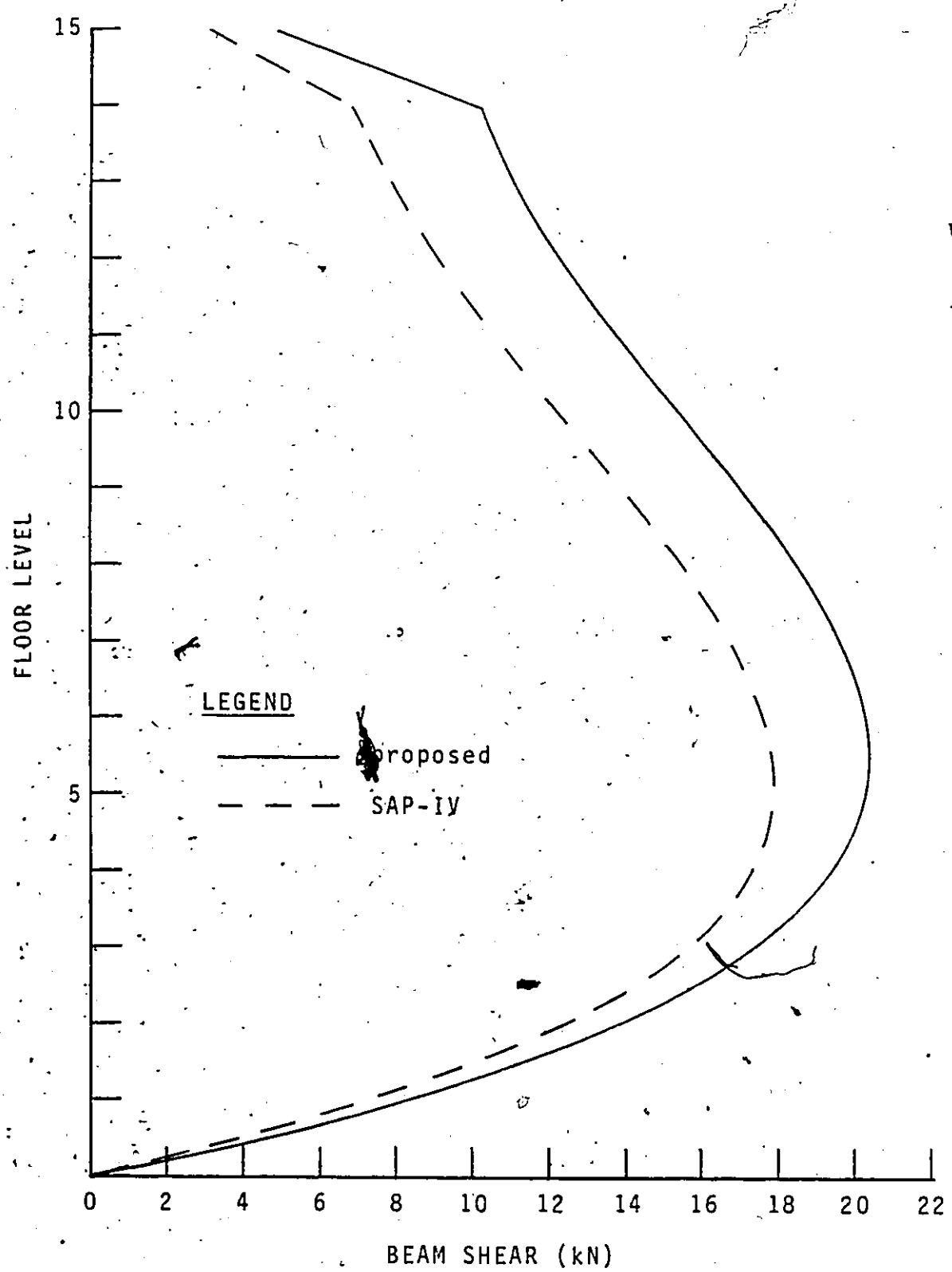

FIG. 4-23: SHEARS IN CONNECTING BEAM 2

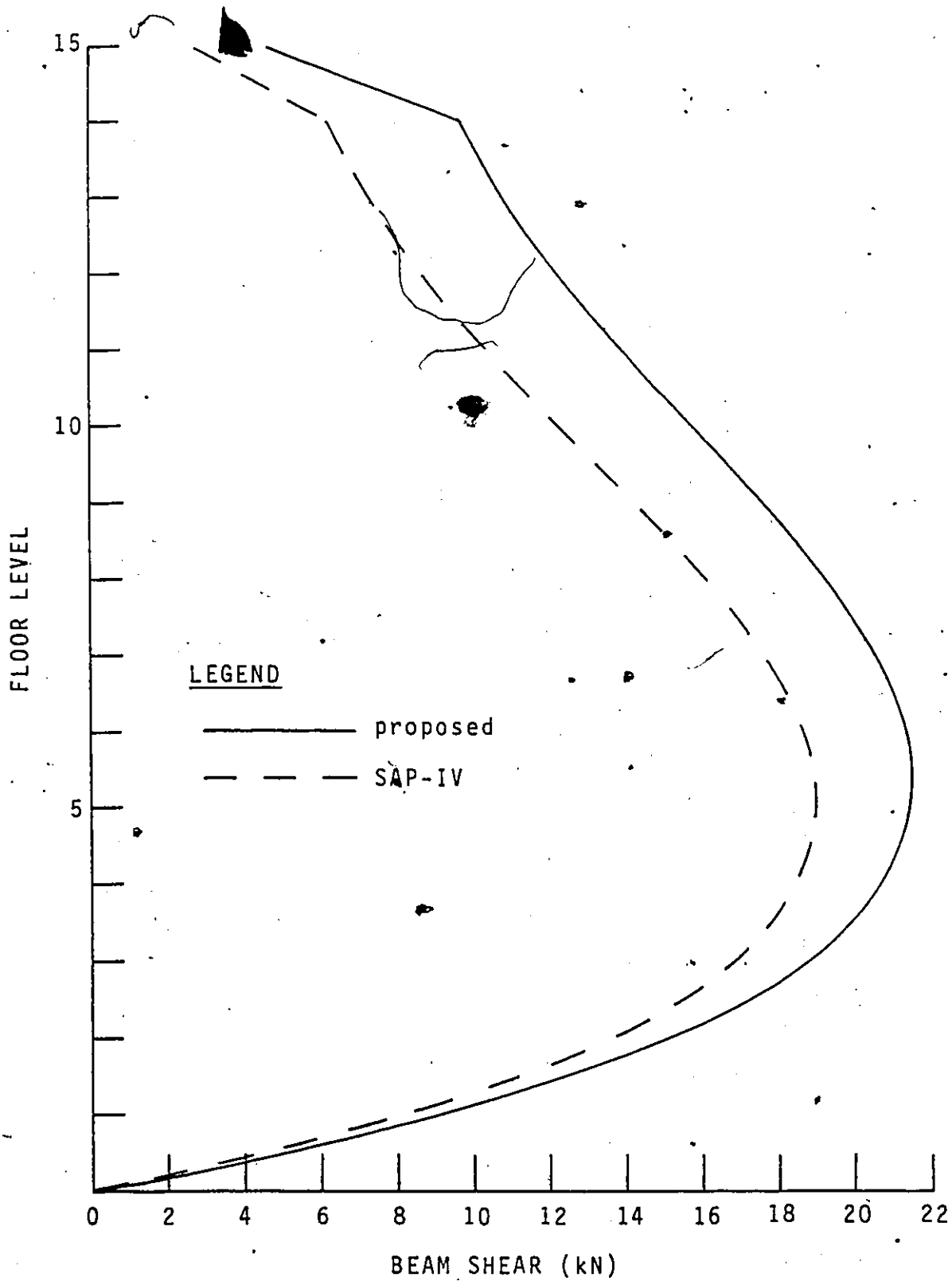

FIG. 4-24: SHEARS IN CONNECTING BEAM 3

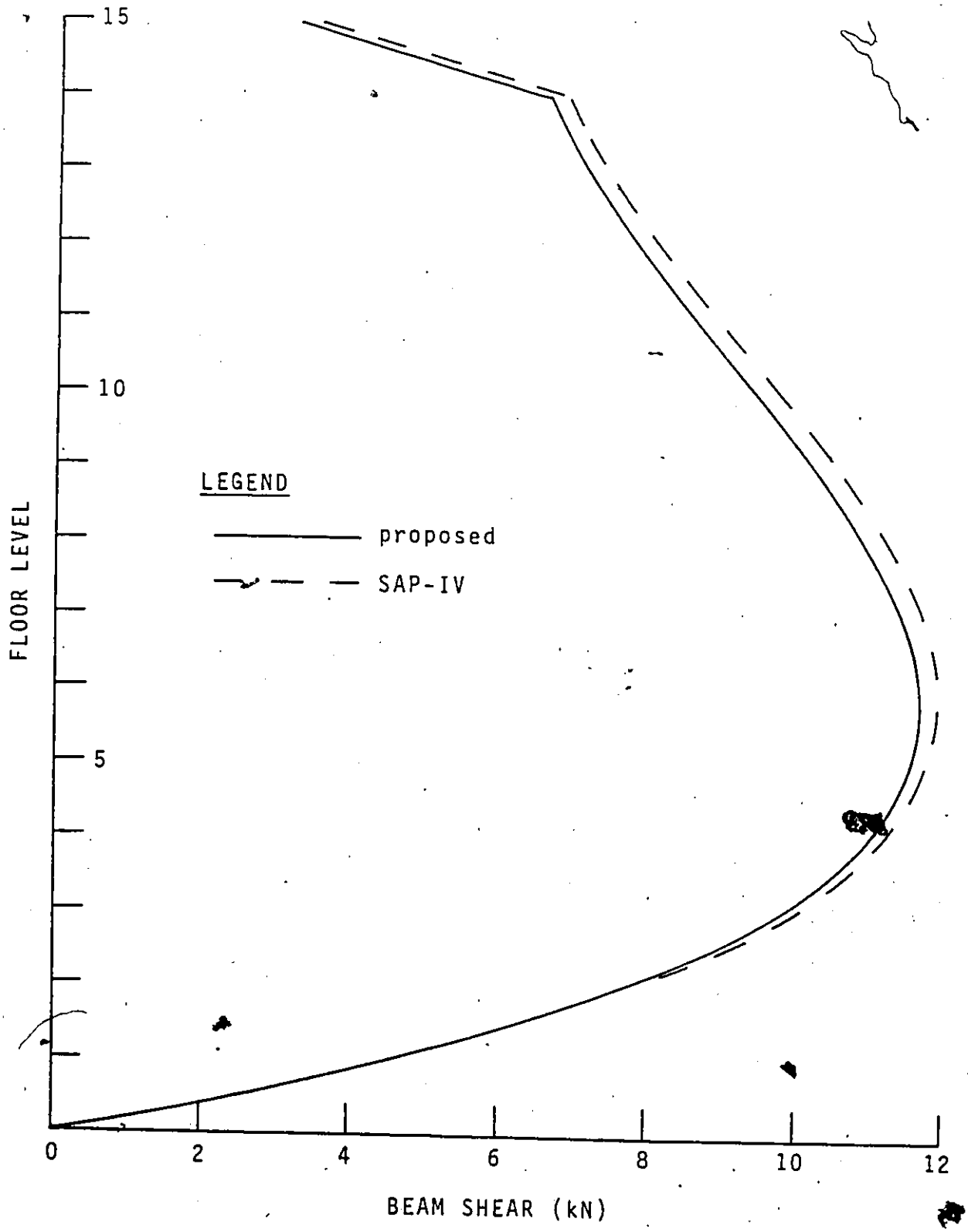

FIG. 4-25: SHEARS IN CONNECTING BEAM 4

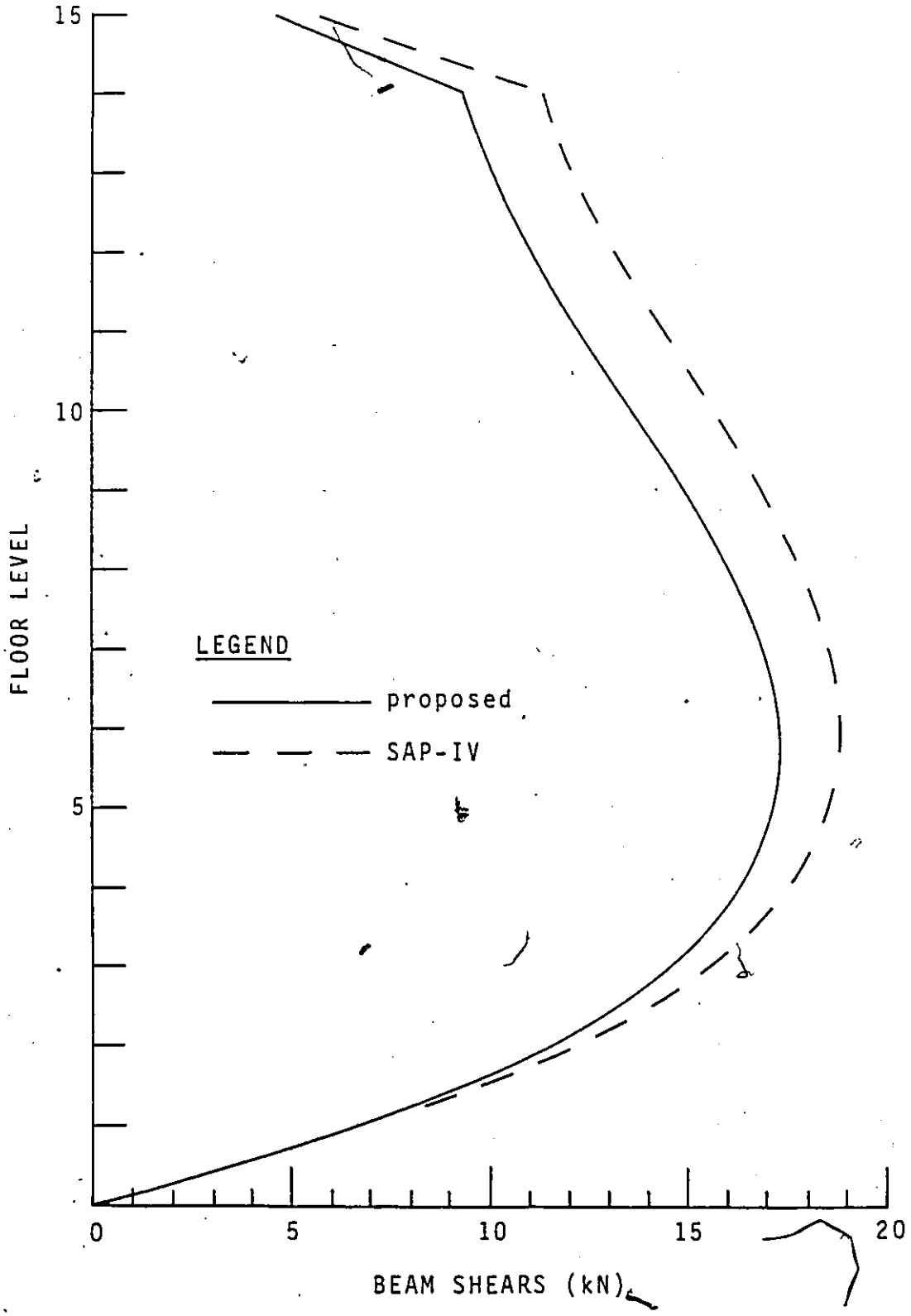

FIG. 4-26: SHEARS IN CONNECTING BEAM 5

CHAPTER V

THREE-DIMENSIONAL ANALYSIS OF NON-UNIFORM WALL-FRAME STRUCTURES

5.1 INTRODUCTION

As has been noted in Chapter III of this thesis, structural or dimensional variations along the height of a building structure usually occur because of architectural and/or economical reasons. These variations include changes in floor height, material properties, and the sectional properties of the structural elements such as walls, beams, and columns. In order to account for these structural or dimensional variations in three-dimensional wall-frame structures, the transfer matrix technique, which has been applied in Chapter III for the analysis of a non-uniform planar wall-frame structure and elsewhere [29, 30, 78], can be used in conjunction with the three-dimensional continuum analysis presented in Chapter IV.

In this chapter, a method of analysis for three-dimensional non-uniform wall-frame structures, which incorporates the continuum method presented in Chapter IV and the

transfer matrix technique, will be presented. The method allows for changes in floor height, material properties, and the sectional properties of the shear walls, connecting beams, and the columns and girders of the frames. Apart from these structural or dimensional changes, assumptions used in Chapter IV regarding the general configuration and modelling of the structure will apply.

5.2 NOTATIONS

The following notations will be used in this chapter. Unless otherwise stated, quantities with the subscript i pertains to segment i of the total structure. Throughout the chapter, for simplicity and whenever appropriate, a group of notations which pertain to the same segment will be placed inside a pair of brackets with the associated subscript placed outside them [e.g., $(Et)_i = E_i t_i$].

$[\tilde{A}]_i$ = axial deformation matrix (Appendix G).

E_i, G_i = elastic modulus and shear modulus, respectively.

$[F]_i$ = segment transfer matrix for segment i.

$[\overline{F}]$ = structure transfer matrix.

H_i = length of segment i.

H = total height of structure.

I, J, K = numbers of bands of type 2, type 3, and type 1 connecting laminae, respectively.

$\{L\}_i$ = load transfer vector for station i.

$\{\overline{L}\}$ = structure load vector.

N = number of segments in total structure.

M_{xiA}, M_{yiA} = internal moments about X- and Y-directions, respectively, at top of

station i.

M_{xiB}, M_{yiB} = internal moments about X- and Y-directions, respectively at bottom of station i.

P_{xi}, P_{yi}, P_{ti} = concentrated lateral loads in X- and Y-directions and torque, respectively, applied at station i.

$\{P\}_i$ = col. $\{ P_{xi} \;\; P_{yi} \;\; P_{ti} \}$.

Q_{tiA}, Q_{tiB} = internal torques just above and below station i, respectively.

$\{\tilde{q}\}_i$, $\{\tilde{q}\}_{iA}$, $\{\tilde{q}\}_{iB}$ = vectors of distributed beam shears for types 1 and 3 laminae at height z, at top of station i, and at bottom of station i, respectively.

$\{\bar{q}\}_i$, $\{\bar{q}\}_{iA}$, $\{\bar{q}\}_{iB}$ = vectors of distributed beam shears for types 2 laminae at height z, at top of station i, and at bottom of station i, respectively.

$[S]_i$ = station transfer matrix for station i.

T_{mi}, T_{miA}, T_{miB} = axial force in wall m at height z, at top of station i, and at bottom of station i, respectively.

t_i = relative thickness of shear walls in segment i.

V_{xiA}, V_{yiA} = internal shear forces in X- and Y-

directions, respectively, at top of station i.

V_{xiB}, V_{yiB} = internal shear forces in X- and Y-directions, respectively, at bottom of station i.

$\{V\}_{iA}$ = col. $\{ V_{xiA}, V_{yiA}, Q_{tiA} \}$.

$\{V\}_{iB}$ = col. $\{ V_{xiB}, V_{yiB}, Q_{tiB} \}$.

z, $\hat{z}$ = height variables with respect to base of segment i and structure, resp.

$\{\Delta\}_i$ = generalised displacement vector at height z.

= col. $\{ \xi_i(z) \quad \eta_i(z) \quad \theta_i(z) \}$.

$\{\Delta\}_{iA}$, $\{\Delta\}_{iB}$ = generalised displacement vectors at top and bottom of station i, respectively.

$\{\Phi(z)\}_i$ = state vector at height z [Eqn(5-18)].

$\{\Phi\}_{iA}$, $\{\Phi\}_{iB}$ = state vectors at top and bottom of station i, respectively.

Eqn(s) = Equation(s).

5.3 STATEMENT OF PROBLEM

Consider a three-dimensional non-uniform wall-frame structure with a rigid foundation. Changes in structural properties are assumed to occur at a number of discrete levels along the height of the structure. Each level of change, including the top and the base of the structure, is defined as a station. The part of the structure between two stations is defined as a segment, within which no structural change is permitted. Permissible structural changes at stations include changes in floor height, material properties and wall thickness, and in the sectional properties of the connecting beams and the columns and girders of the frames. Changes in wall thickness are such that the shear centre and centroid of each wall pier lie on the same vertical axis in all segments and that the same relative change occurs for all wall piers from one segment to another. Changes in the sectional properties of the columns in those frames that are coupled to walls must be such that the same relative change in cross-sectional area occurs for all the columns from one segment to another as for the walls. The layout of connecting beams must be constant in all segments.

A schematic picture of the wall-frame structure with stepwise structural changes is given in Figure 5-1. An orthogonal global co-ordinate system with horizontal axes X and

Y, vertical axis Z, and origin O is defined for the structure. Stations and segments are numbered in ascending order starting from the base. Assuming there are N segments in the structure, the base is taken to be station zero, the next higher station to be station 1, and so forth. Thus, the top of the structure is denoted as station N. Segment i, where i = 1, 2, ... N, is then the part of the structure between stations (i-1) and i. The state in terms of deformation and force quantities at any particular location along the height of the structure is defined by a state vector. Referring to Figure 5-2, the state vectors immediately above and below station i are denoted by $\{\Phi\}_{iA}$ and $\{\Phi\}_{iB}$ respectively. Thus, the state vectors at the top and the bottom of segment i are denoted by $\{\Phi\}_{iB}$ and $\{\Phi\}_{(i-1)A}$ respectively. External lateral and torsional loads are represented by concentrated loads applied at the stations. Thus, at station i, P_{xi} and P_{yi} are the concentrated loads acting in the X- and Y-directions, respectively, and P_{ti} is the applied torque. At the top of segment i, the internal shear forces acting in the X- and Y-directions and the internal torque are denoted by V_{xiB}, V_{yiB}, and Q_{tiB}, respectively, while the internal moments about the X- and Y-directions are denoted by M_{xiB} and M_{yiB}, respectively. The internal shear forces, torque, and moments acting at the bottom of station i are of the same magnitude as their counterparts acting at the top of segment i but in the oppo-

site directions. At the top of station i, the corresponding internal shear forces, torque, and moments are denoted by V_{xiA}, V_{yiA}, Q_{tiA}, M_{xiA}, and M_{yiA}. Lastly, the X- and Y-direction and the rotational generalised displacements at the bottom of station i or at the top of segment i are denoted by ξ_{iB}, η_{iB} and θ_{iB}, respectively. The corresponding generalised displacements at the top of station i are denoted by ξ_{iA}, η_{iA} and θ_{iA}.

5.4 ANALYSIS OF TYPICAL SEGMENT — SEGMENT i

The analysis of a typical segment of the non-uniform wall-frame structure is essentially similar to that of the uniform counterpart subjected to concentrated loads at the top. Thus the analysis proposed in Chapter IV can be utilised here.

5.4.1 EQUILIBRIUM CONDITIONS

Referring to Eqn(4-56), the horizontal translational and the rotational equilibriums of segment i are given by:

$$[K_o]_i\{\Delta\}_i''' - [K_s]_i\{\Delta\}_i' - [R_s]^T\{\tilde{q}\}_i - [\bar{R}]^T\{\bar{q}\}_i = -\{V\}_{iB} \qquad (5\text{-}1)$$

where $[K_o]_i$, $[K_s]_i$, $\{\Delta\}_i$, $\{\tilde{q}\}_i$, and $\{\bar{q}\}_i$ are as defined by Eqns(4-56a), (4-56b), (4-56e), (4-56f), and (4-56g), respectively, for segment i; $[R_s]$ and $[\bar{R}]$ are given by Eqns(4-56c) and (4-56d) and are constant for all segments; and $\{V\}_{iB}$ is the load vector at the top of segment i and is given by

$$\{V\}_{iB} = \text{col.}\{\ V_{xiB}\ \ V_{yiB}\ \ Q_{tiB}\ \} \qquad (5\text{-}1a)$$

5.4.2 COMPATIBILITY CONDITIONS

The compatibility equations for all three types of

connecting laminae in segment i can be obtained following the development presented in Section 4.6.

For the k^{th} band of type 1 laminae that connects walls m and n, where k = 1, 2,...K, the axial deformations of the walls accumulated over all segments below segment i give rise to an initial relative vertical displacement at the midspan of the laminae at the base of the segment. Denoting this initial relative displacement by δ_{ki}, the compatibility equation for the k^{th} type 1 laminae band is given by

$$r_{xk}\xi_i' + r_{yk}\eta_i' + r_{\theta k}\theta_i' - \int_o^z \left(\frac{T_m}{EA_m}\right)_i d\bar{z} + \int_o^z \left(\frac{T_n}{EA_n}\right)_i d\bar{z} - \left(\frac{q_k}{E\gamma_k}\right)_i + \delta_{ki} = 0 \quad (k=1,2,\ldots K) \qquad (5\text{-}2)$$

where r_{xk}, r_{yk}, and $r_{\theta k}$ are given by Eqns(4-21a), (4-21b), and (4-34f), respectively; γ_{ki} is as defined by Eqn(4-43e) for segment i; and δ_{ki} is given by

$$\delta_{ki} = -\sum_{j=1}^{i-1} \int_o^{H_j} \left(\frac{T_m}{EA_m}\right)_j d\bar{z} - \sum_{j=1}^{i-1} \int_o^{H_j} \left(\frac{T_n}{EA_n}\right)_j d\bar{z} \qquad (5\text{-}3)$$

with H_j = length of segment j.

For the n^{th} band of type 2 laminae, where n = 1, 2, ... I, the compatibility equation is given by

$$\bar{r}_{\theta n}\theta'_i - \left(\frac{\bar{q}_n}{E\bar{\gamma}_n}\right)_i = 0 \qquad (n=1,2,\ldots I) \qquad (5\text{-}4)$$

where $\bar{r}_{\theta n}$ is given by Eqn(4-36a), and $\bar{\gamma}_{ni}$ is as defined by Eqn(4-46a) for segment i.

For the j^{th} band of type 3 laminae that connects wall m and frame ℓ, where j = 1, 2, ... J, the axial deformations of the wall and column $C_{j\ell}$ of the frame accumulated over all segments below segment i give rise to an initial relative vertical displacement $\hat{\delta}_{ji}$ at the midspan of the laminae at the base of the segment. Thus, referring to Eqn(4-51b), the compatibility equation for the j^{th} type 3 laminae band is given by

$$(\hat{r}^*_{xj}\xi')_i + (\hat{r}^*_{yj}n')_i + (\hat{r}^*_{\theta j}\theta')_i - \left(\frac{\hat{q}_j}{E\hat{\gamma}_j}\right)_i - \int_o^z \left(\frac{T_m}{EA_m}\right)_i d\bar{z}$$

$$- f_{j\ell} \int_o^z \left(\frac{T_m}{EA_{cj\ell}}\right)_i d\bar{z} + \frac{D_{cj\ell}}{d_{cj\ell}} \int_o^z \left(\frac{T_{cj\ell}}{EA_{cj\ell}}\right)_i d\bar{z} + \hat{\delta}_{ji} = 0$$

$$(j = 1, 2, \ldots J) \qquad (5\text{-}5)$$

where $\hat{r}^*_{xji}$, $\hat{r}^*_{yji}$ and $\hat{r}^*_{\theta ji}$, and $\hat{\gamma}_{ji}$ are as defined by Eqns(4-51c) and (4-47e), respectively, for segment i; $f_{j\ell}$ is assumed to be constant for all segments and takes on a value ranging between 1.1 and 1.4; $D_{cj\ell}$ is given by Eqn(4-50a); $(T_{cj\ell})_i$ is as defined by Eqn(4-48a) or Eqn(4-48b) for segment i; and

$$\hat{\delta}_{ji} = -\sum_{k=1}^{i-1} \int_{o}^{H_k} \left(\frac{T_m}{EA_m}\right)_k d\bar{z} - f_{j\ell} \sum_{k=1}^{i-1} \int_{o}^{H_k} \left(\frac{T_m}{EA_{cj1}}\right)_k d\bar{z}$$

$$+ \frac{D_{cj1}}{d_{cj1}} \sum_{k=1}^{i-1} \int_{o}^{H_k} \left(\frac{T_{cj1}}{EA_{cj1}}\right)_k d\bar{z} \qquad (5\text{-}6)$$

The I compatibility equations for type 2 laminae can be represented by the following matrix equation:

$$[\bar{R}]\{\Delta\}_i' - [\bar{\Gamma}]_i\{\bar{q}\}_i = \{0\} \qquad (5\text{-}7)$$

where $[\bar{\Gamma}]_i$ is as defined by Eqn(4-57a) for segment i.

Referring to Sections 4.6.1 and 4.6.3, it can be shown that the compatibility equations for type 1 and type 3 laminae can be combined together to form the following matrix equation:

$$[R_c]_i\{\Delta\}_i''' - [\Psi]_i\{\Delta\}_i' + [\tilde{A}]_i\{\bar{q}\}_i - [\tilde{\Gamma}]\{\bar{q}\}_i'' = \{0\} \qquad (5\text{-}8)$$

where $[R_c]_i$, $[\Psi]_i$, and $[\tilde{\Gamma}]_i$ are as defined by Eqns(4-58a), (4-58b), and (4-58e), respectively, for segment i, and $[\tilde{A}]_i$ is as explained in Appendix G.

5.4.3 FINAL DIFFERENTIAL EQUATION

The $\{\bar{q}\}_i$ term can be eliminated from Eqn(5-1) by the

use of Eqn(5-7) to form the following equation:

$$[K_o]_i\{\Delta\}_i''' - [\bar{K}_s]_i\{\Delta\}_i' - [R_s]^T\{\tilde{q}\}_i = -\{V\}_{iB} \qquad (5\text{-}9)$$

where $$[\bar{K}_s]_i = [K_s]_i + [\bar{R}]^T[\bar{\Gamma}]_i^{-1}[\bar{R}] \qquad (5\text{-}9a)$$

Differentiating Eqn(5-9) once, there is obtained

$$[K_o]_i\{\Delta\}_i^{iv} - [\bar{K}_s]_i\{\Delta\}_i'' - [R_s]^T\{\tilde{q}\}_i' = \{0\} \qquad (5\text{-}10)$$

Defining a 3x1 vector $\{e\}_i$ as follows:

$$\{\tilde{q}\}_i = [\tilde{\Gamma}]_i^{-1}[R_c]_i\{e\}_i \qquad (5\text{-}11)$$

there is obtained from Eqn(5-9)

$$\{e\}_i = [R_s^T\tilde{\Gamma}_i^{-1}R_{ci}]^{-1}[K_o]_i\{\Delta\}_i''' - [R_s^T\Gamma_i^{-1}R_{ci}]^{-1}[\bar{K}_s]_i\{\Delta\}_i'$$

$$+ [R_s^T\tilde{\Gamma}_i^{-1}R_{ci}]^{-1}\{V\}_{iB} \qquad (5\text{-}12)$$

Substituting Eqn(5-11) into Eqn(5-8), there is obtained

$$[R_c]_i\{e\}_i'' = [\tilde{A}\tilde{\Gamma}^{-1}R_c]_i\{e\}_i + [R_c]_i\{\Delta\}_i''' - [\Psi]_i\{\Delta\}_i' \qquad (5\text{-}13)$$

Substituting Eqn(5-12) into Eqn(5-13), there is obtained the

final differential equation for segment i:

$$[K_o]_i\{\Delta\}_i^{v} - [K_1]_i\{\Delta\}_i''' + [K_2]_i\{\Delta\}_i' = [B]_i\{V\}_{iB} \quad (5\text{-}14)$$

where
$$\left.\begin{aligned} [B]_i &= [R_s]^T[\tilde{\Gamma}]_i^{-1}[\tilde{A}\tilde{\Gamma}^{-1}R_c]_i[R_s^T\tilde{\Gamma}_i^{-1}R_{ci}]^{-1} \\ [K_1]_i &= [B]_i[K_o]_i + [R_s^T\tilde{\Gamma}_i^{-1}R_{ci}] + [\bar{K}_s]_i \\ [K_2]_i &= [B]_i[\bar{K}_s]_i + [R_s]^T[\tilde{\Gamma}]_i^{-1}[\Psi]_i \end{aligned}\right\} \quad (5\text{-}14a)$$

Eqn(5-14) can be reduced to a fourth order differential equation as shown below:

$$[K_o]_i\{\Delta\}_i^{iv} - [K_1]_i\{\Delta\}_i'' + [K_2]_i\{\Delta\}_i = \int [B]_i\{V\}_{iB}\,d\bar{z} + \{C_k\}_i \quad (5\text{-}15)$$

where $\{C_k\}_i$ is a 3x1 vector of constants.

Referring to Section 4.8, the complete solution to Eqn(5-15) can be shown to be given by

$$\{\Delta\}_i = \sum_{j=1}^{6} [C_j\cosh(\lambda_j Z)\{\phi\}_j + S_j\sinh(\lambda_j Z)\{\phi\}_j]_i + [\bar{B}]_i\{V\}_{iB}z + \{k\}_i \quad (5\text{-}16)$$

where
$$[\bar{B}]_i = [K_2]_i^{-1}[B]_i \quad (5\text{-}16a)$$

$$\{k\}_i = 3x1 \text{ constant vector}$$

$$= \text{col.}\{ k_1 \; k_2 \; k_3 \}_i \qquad (5\text{-}16b)$$

λ_j^2, where j = 1, 2, ... 6, is the j^{th} eigen-value of the characteristic equation of Eqn(5-15) given by

$$| \lambda^4[K_o]_i - \lambda^2[K_1]_i + [K_2]_i | = 0 \qquad (5\text{-}17)$$

and $\{\phi\}_j$ is the eigen-vector associated with $|\lambda_j|$. C_{ji} and S_{ji}, where j = 1, 2, ... 6, and k_{mi}, where m = 1, 2, 3, constitute fifteen constants to be determined from the boundary conditions of segment i of the structure.

5.5 SOLUTION BY TRANSFER MATRIX TECHNIQUE

The state vector at any height z within segment i is defined by

$$\{\Phi(z)\}_i = \text{col.}\{\xi(z) \quad \eta(z) \quad \theta(z) \quad \xi'(z) \quad \eta'(z) \quad \theta'(z)$$
$$\xi''(z) \quad \eta''(z) \quad \theta''(z) \quad \xi'''(z) \quad \eta'''(z) \quad \theta'''(z)$$
$$\xi^{iv}(z) \quad \eta^{iv}(z) \quad \theta^{iv}(z) \quad M_y(z) \quad M_x(z)$$
$$V_x(z) \quad V_y(z) \quad Q_t(z)\}_i \qquad (5\text{-}18)$$

From the complete solution to Eqn(5-15), namely, Eqn(5-16), the state vector $\{\Phi\}_i$ can be shown to be given by

$$\{\Phi(z)\}_i = [\,X(z)\,]_i \{R\}_i \qquad (5\text{-}19)$$

where $[X(z)]_i$ is a 20 x 20 matrix and is shown in details in Appendix H, and $\{R\}_i$ is a vector of constants given by

$$\{R\}_i = \text{col.}\{C_{1i} \; S_{1i} \; C_{2i} \; S_{2i} \; \ldots\ldots \; C_{6i} \; S_{6i} \; k_{1i} \; k_{2i} \; k_{3i}$$
$$M_{yiB} \; M_{xiB} \; V_{xiB} \; V_{yiB} \; Q_{tiB}\} \qquad (5\text{-}19a)$$

The state vectors at the top and the bottom of segment

i, namely, $\{\Phi\}_{iB}$ and $\{\Phi\}_{(i-1)A}$, respectively, are therefore given by

$$\{\Phi\}_{iA} = [X(H_i)]_i \{R\}_i \tag{5-20}$$

$$\{\Phi\}_{(i-1)A} = [X(0)]_i \{R\}_i \tag{5-21}$$

and can be related to each other by a segment transfer matrix $[F]_i$ such that

$$\{\Phi\}_{iB} = [F]_i \{\Phi\}_{(i-1)A} \tag{5-22}$$

where $$[F]_i = [X(H_i)]_i [X(0)]_i^{-1} \tag{5-22a}$$

From considerations of continuity requirements between segments and equilibrium conditions at stations, the state vector at the top of segment i, $\{\Phi\}_{iB}$, can further be related to that at the bottom of segment (i+1), $\{\Phi\}_{iA}$, by a station transfer matrix $[S]_i$ and a load transfer vector $\{L\}_i$ Such that

$$\{\Phi\}_{iA} = [S]_i\{\Phi\}_{iB} + \{L\}_i \tag{5-23}$$

The elements of $[S]_i$ and $\{L\}_i$ are determined from the following continuity and equilibrium requirements:

(1) The lateral displacements and rotations at the top and the bottom of station i are equal. Thus

$$\{\Delta\}_{iA} = \{\Delta\}_{iB} \tag{5-24}$$

(2) The slopes of the generalised displacement curves at the top and the bottom of station i are equal. Thus

$$\{\Delta\}'_{iA} = \{\Delta\}'_{iB} \tag{5-25}$$

(3) Taking note that (a) the axial force in any wall pier or column at the top of station i is equal to that at the bottom of the same station, (b) the moments and bimoment in any wall pier at the top of station i are equal to the corresponding moments and bimoment at the bottom of the same station, and (c) the same relative change in thickness occurs in all wall piers from one segment to another, it can be shown that

$$\{\Delta\}''_{iA} = [C_1]_i \{\Delta\}''_{iB} \tag{5-26}$$

where

$$[C_1]_i = \begin{bmatrix} (Et)_i/(Et)_{i+1} & 0 & 0 \\ 0 & (Et)_i/(Et)_{i+1} & 0 \\ 0 & 0 & (Et)_i/(Et)_{i+1} \end{bmatrix} \tag{5-26a}$$

with t_i being the relative thickness of the shear walls in segment i.

Moreover, the total internal moments just above and below station i are equal. Thus,

$$\begin{Bmatrix} M_y \\ M_x \end{Bmatrix}_{iA} = \begin{Bmatrix} M_y \\ M_x \end{Bmatrix}_{iB} \tag{5-27}$$

(4) It can be shown that by applying the compatibility equations for the three types of connecting laminae at the top of segment i and at the base of segment (i+1), the following continuity equations for the distributed beam shears in the three types of laminae are obtained:

(a) For the k^{th} band of type 1 laminae, where k=1,2,...K,

$$q_{kiA} = \frac{(E\gamma_k)_{i+1}}{(E\gamma_k)_i} q_{kiB} \tag{5-28a}$$

(b) For the n^{th} band of type 2 laminae, where n = 1,2,...I,

$$\bar{q}_{niA} = \frac{(E\bar{\gamma}_n)_{i+1}}{(E\bar{\gamma}_n)_i} \bar{q}_{niB} \tag{5-28b}$$

(c) For the j^{th} band of type 3 laminae, where j = 1,2,

...J,

$$\hat{q}_{jiA} = \frac{(E\hat{\gamma}_j)_{i+1}}{(E\hat{\gamma}_j)_i}\,\hat{q}_{jiB} + (E\hat{\gamma}_j)_{i+1}$$

$$\cdot\{[(\hat{r}^*_{xj})_{i+1} - (\hat{r}^*_{xj})_i]\cdot\xi'_{iB}$$

$$+ [(\hat{r}^*_{yj})_{i+1} - (\hat{r}^*_{yj})_i]\cdot\eta'_{iB}$$

$$+ [(\hat{r}^*_{\theta j})_{i+1} - (\hat{r}^*_{\theta j})_i]\cdot\theta'_{iB}\ \} \qquad (5\text{-}28c)$$

Eqns(5-28a) and (5-28c) can be combined together in the following matrix form:

$$\{\tilde{q}\}_{iA} = [\tilde{\Gamma}]^{-1}_{i+1}[\tilde{\Gamma}]_i\{\tilde{q}\}_{iB} + [\tilde{\Gamma}]^{-1}_{i+1}[D]_i\{\Delta\}'_{iB} \qquad (5\text{-}28d)$$

where $$[D]_i = [R_c]_{i+1} - [R_c]_i \qquad (5\text{-}28e)$$

Considering the equilibrium of shear forces and torques at station i, there is obtained

$$\{V\}_{iA} = \{V\}_{iB} - \{P\}_i \qquad (5\text{-}28f)$$

where $\{P\}_i$ is the vector of the lateral loads and torque applied at station i and is given by

$$\{P\}_i = \text{col.}\{\ P_{xi}\ \ P_{yi}\ \ P_{ti}\ \} \qquad (5\text{-}28g)$$

Applying Eqn(5-9) at the top and bottom of station i, eliminating $\{\tilde{q}\}_{iA}$ and $\{\tilde{q}\}_{iB}$ using Eqn(5-28d), and taking note of Eqn(5-28f), the following continuity equation is obtained for the third derivative of the generalised displacement vector $\{\Delta\}_i$:

$$\{\Delta\}'''_{iA} = [C_2]_i\{\Delta\}'''_{iB} + [C_3]_i\{\Delta\}'_{iB} - [C_4]_i\{V\}_{iB} + \{C_7\}_i \tag{5-29}$$

where

$$\left.\begin{aligned}
[C_2]_i &= [K_o]^{-1}_{i+1}[R_s]^T[\tilde{\Gamma}]^{-1}_{i+1}[R_c]_i[R_s^T\tilde{\Gamma}_i^{-1}R_{ci}]^{-1}[K_o]_i \\
[C_3]_i &= [K_o]^{-1}_{i+1}[\bar{K}_s]_{i+1} + [K_o]^{-1}_{i+1}[R_s]^T[\tilde{\Gamma}]^{-1}_{i+1}[D]_i \\
&\quad - [K_o]^{-1}_{i+1}[R_s]^T[\tilde{\Gamma}]^{-1}_{i+1}[R_c]_i[R_s^T\tilde{\Gamma}_i^{-1}R_{ci}]^{-1}[\bar{K}_s]_i \\
[C_4]_i &= [K_o]^{-1}_{i+1} - [K_o]^{-1}_{i+1}[R_s]^T[\tilde{\Gamma}]^{-1}_{i+1}[R_c]_i[R_s^T\tilde{\Gamma}_i^{-1}R_{ci}]^{-1} \\
\{C_7\}_i &= [K_o]^{-1}_{i+1}\{P\}_i
\end{aligned}\right\} \tag{5-29a}$$

(5) Differentiating once the compatibility equations for type 1 and type 3 laminae, namely, Eqn(5-2) and Eqn(5-5), respectively, and applying the resulting equations at the top and bottom of station i, the following continuity equation for $\{\tilde{q}\}'$ can be obtained:

$$\{\tilde{q}\}'_{iA} = \frac{(Et)_i}{(Et)_{i+1}} [\tilde{f}]^{-1}_{i+1}[D]_i\{\Delta\}''_{iB} + \frac{(Et)_i}{(Et)_{i+1}} [\tilde{f}]^{-1}_{i+1}[\tilde{f}]_i\{\tilde{q}\}'_{iB} \quad (5\text{-}30)$$

Applying Eqn(5-10) at the top and bottom of station i, and making use of Eqns(5-12), (5-26), and (5-30) to eliminate $\{\Delta\}''_{iA}$, $\{\tilde{q}\}'_{iA}$, and $\{\tilde{q}\}'_{iB}$, the following continuity equation for $\{\Delta\}^{iv}$ can be obtained:

$$\{\Delta\}^{iv}_{iA} = [C_5]_i\{\Delta\}^{iv}_{iB} + [C_6]_i\{\Delta\}''_{iB} \quad (5\text{-}31)$$

where

$$\left.\begin{aligned} [C_5]_i &= \frac{(Et)_i}{(Et)_{i+1}} [K_o]^{-1}_{i+1}[R_s]^T[\tilde{f}]^{-1}_{i+1}[R_c]_i[R_s^T\tilde{f}_i^{-1}R_{ci}]^{-1}[K_o]_i \\ [C_6]_i &= \frac{(Et)_i}{(Et)_{i+1}} [K_o]^{-1}_{i+1}\{[\bar{K}_s]_{i+1} + [R_s]^T[\tilde{f}]^{-1}_{i+1}[D]_i \\ &\quad - [R_s]^T[\tilde{f}]^{-1}_{i+1}[R_c]_i[R_s^T\tilde{f}_i^{-1}R_{ci}]^{-1}[\bar{K}_s]_i\} \end{aligned}\right\} \quad (5\text{-}31a)$$

The station transfer matrix $[S]_i$ and the load transfer vector $\{L\}_i$ for station i can then be constructed from Eqns(5-24), (5-25), (5-26), (5-27), (5-28f), (5-29), and (5-31). $[S]_i$ and $\{L\}_i$ are shown in details in Appendix I.

Following a development similar to that presented in Section 3.5.3, the relationship between the states at the top and bottom of the structure can be established as

$$\{\Phi\}_{NB} = [\bar{F}]\{\Phi\}_{oA} + \{\bar{L}\} \tag{5-32}$$

where $[\bar{F}]$ = structure transfer matrix

$$= \prod_{i=1}^{N} [S]_i[F]_i \tag{5-32a}$$

$\{\bar{L}\}$ = structure load vector

$$= \sum_{i=1}^{N-1} \left(\prod_{r=i+1}^{N} [S]_r[F]_r \right)\{L\}_i \tag{5-32b}$$

with the "Π" operation representing pre-multiplication.

The state vectors at the top and base of the structure, namely, $\{\Phi\}_{NB}$ and $\{\Phi\}_{oA}$, can be determined from the following boundary conditions:

(1) At the base, displacement and slope are zero. Thus,

$$\{\Delta\}_{oA} = \{o\} \tag{5-33a}$$

$$\{\Delta\}'_{oA} = \{o\} \tag{5-33b}$$

(2) Moments and bimoments vanish at the top. Thus,

$$\{\Delta\}''_{NB} = \{o\} \tag{5-33c}$$

$$\begin{Bmatrix} M_y \\ M_x \end{Bmatrix}_{NB} = \{o\} \tag{5-33d}$$

(3) The distributed beam shears in the connecting laminae vanish at the base. Thus there can be obtained from Eqns(5-9) and (5-33b) the following condition:

$$\{\Delta\}'''_{oA} = - [K_o]_i^{-1} \{V\}_{oA} \tag{5-33e}$$

(4) Axial forces vanish at the top. Thus, taking note of Eqn(5-33c), it can be shown by differentiating the compatibility equations once that the first derivatives of the distributed beam shears in all three types of laminae are zero at the top. Accordingly, there can be obtained from Eqn(5-10)

$$\{\Delta\}^{iv}_{NB} = \{o\} \tag{5-33f}$$

(5) Equilibrium of station N leads to

$$\{V\}_{NB} = \{P\}_N \tag{5-33g}$$

Equilibrium of the overall structure leads to

$$\begin{Bmatrix} M_y \\ M_x \end{Bmatrix}_{oA} = \sum_{i=1}^{N} \left[\left(\sum_{j=1}^{i} H_j \right) \begin{Bmatrix} P_x \\ P_y \end{Bmatrix}_i \right] \qquad (5\text{-}33h)$$

$$\{V\}_{oA} = \sum_{i=1}^{N} \{P\}_i \qquad (5\text{-}33i)$$

By substituting Eqns(5-33a) through (5-33i) into Eqn (5-32), a system of six simultaneous equations will be obtained. The state vectors $\{\Phi\}_{oA}$ and $\{\Phi\}_{NB}$ can then be determined completely by solving these simultaneous equations. The state vector at any intermediate station can be found by a process of successive substitution making use of Eqns(5-22) and (5-23) [ref. Section 3.5.3]. Distributed beam shears in the connecting laminae can be determined from Eqn(5-7) for type 2 laminae, and from Eqns(5-11) and (5-12) for type 1 and type 3 laminae. The axial force at height z within segment i of a wall m which is coupled to a frame via the j^{th} band of type 3 laminae is given by

$$T_{mi}(z) = T_{miB} + \int_{z}^{H_i} \hat{q}_{ji}(\bar{z})\, d\bar{z} \qquad (5\text{-}34)$$

where T_{miB} is the axial force in the wall at the top of seg-

ment i. In Eqn(5-34), it is assumed that the distributed beam shear $\hat{q}_{ji}$ acts upwards on the wall. For a wall m which is connected by more than one band of type 1 laminae, the axial force in the wall is given by

$$T_{mi}(z) = T_{miB} + \sum_{k,m}^{Bl} s_k \int_z^{H_i} q_{ki}(z)\, d\bar{z} \qquad (5\text{-}35)$$

where $\sum_{k,m}^{Bl}$ indicates summation over all type 1 laminae bands that are connected to wall m, and s_k is +1 or -1 if the distributed beam shear in the k^{th} band of the type 1 laminae acts upwards or downwards, respectively, on wall m.

5.6 EXAMPLE

A non-uniform example structure has been analysed using the proposed method. This structure is basically similar to the example discussed in Chapter IV except that the storey height in the bottom four storeys is changed to 5.50 m (18 ft.). An external lateral load of 10 kN/m (0.685 klf) along the height of the structure, acting at wall pier 4 in the direction of the Y-axis, is approximated by a series of point loads applied at the floor levels (Figure 5-3).

Results for structure rotation and the X- and Y-translational displacements at the centroid of wall pier 4 are shown in Figures 5-4 through 5-6. Results for the wall moment of wall pier 3, the interstorey shear of frame 2, and the beam shear of connecting beam 4 are presented in Figures 5-7, 5-8, and 5-9 respectively. Corresponding results by SAP-IV [62] for the same structure are also shown for comparison. Close agreement between the two sets of results can be generally observed.

For this non-uniform example structure, the computer time required by the proposed method was about 8.5 decimal seconds on the CDC CYBER 170/730 computer (excluding time required for solving for the member forces in the frames by plane frame analysis) while that required by SAP-IV was about 126 decimal seconds. It can therefore be seen that, apart

from other advantages such as less tedious data preparation processes and direct computation of wall stresses, enormous savings in computer time can be achieved with the proposed method.

5.7 CONCLUSION

A method of analysis for three-dimensional non-uniform wall-frame building structures subjected to lateral and torsional loads has been presented. The method is essentially based upon the continuum approach, and utilises the transfer matrix technique to take into account structural non-uniformity in the form of stepwise changes along the height of the structure. Permissible structural changes include changes in storey height, material properties, wall thickness, and the sectional properties of connecting beams, columns and girders. An example structure has been analysed using the proposed method and the results checked against those given by SAP-IV [62]. Good agreement has been observed generally.

The proposed method exhibits the following advantages:

(1) Use of the continuum approach by the proposed method renders its basic computer storage requirements independent of the number of storeys in the structure. Despite the requirement by the transfer matrix technique of a number of 20 x 20 matrices, which increases with the number of segments in the structure, the computer storage requirements for the proposed method are in general significantly lower than

for matrix methods in analysing a structure of the same complexity. The proposed method also requires considerably less computer time, and fewer efforts in data preparation than matrix methods.

(2) With the proposed method, any arbitrary lateral and torsional loading can be approximated as a number of concentrated loads and torques acting at the floor levels. Thus the flexibility matrix for the structure can be determined by successively applying a number of unit loads, one at a time, at various floor levels and finding the resulting structure displacements. The flexibility matrix so obtained can be used in the dynamic analysis of the structure based on the lumped-mass approach.

Finally, it is believed that the proposed method of analysis, which combines the convenience of the continuum approach and the flexibility of the transfer matrix technique in accounting for structural non-uniformity, does provide a viable means for the study of three-dimensional non-uniform wall-frame building structures subjected to lateral and torsional loads.

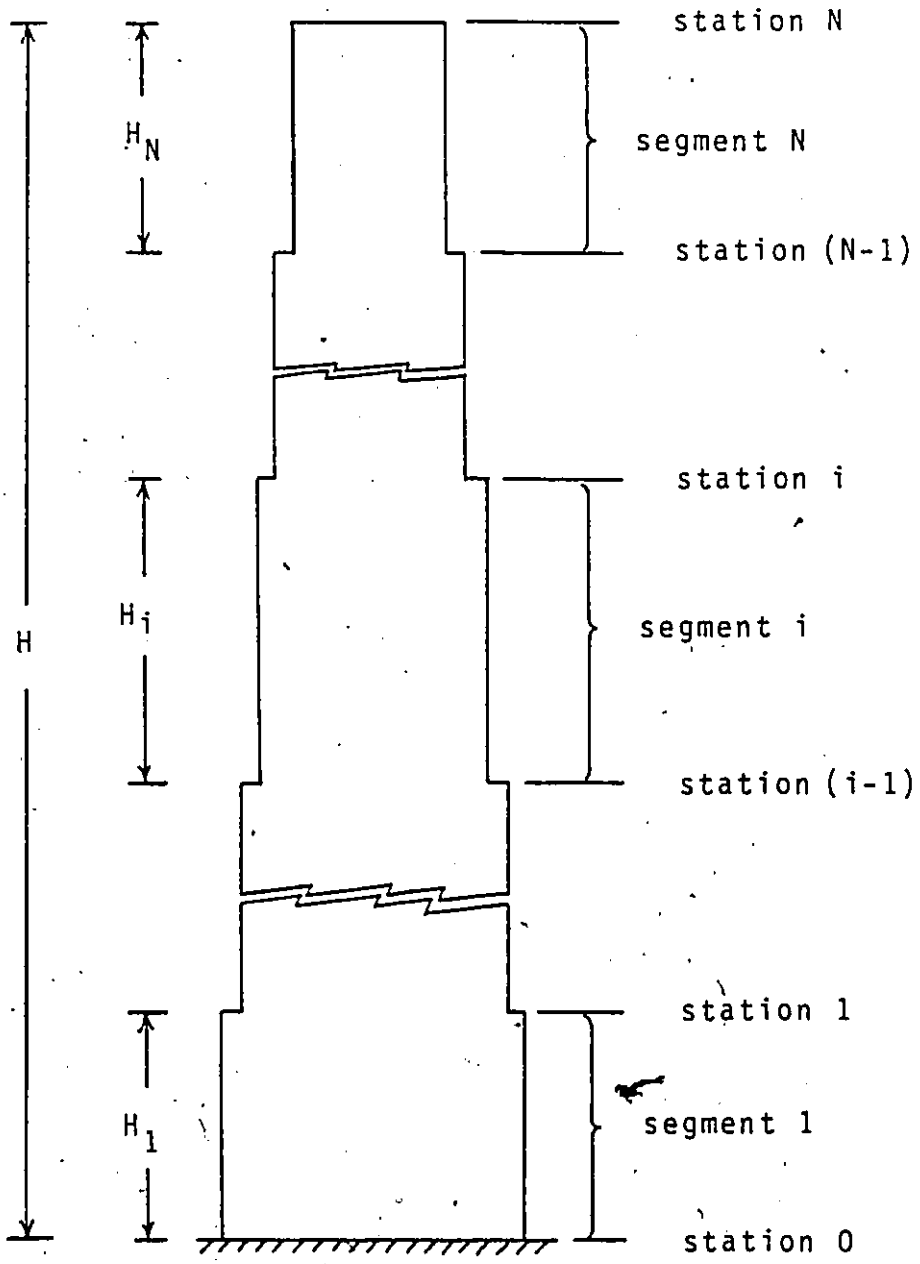

FIG. 5-1: SCHEMATIC REPRESENTATION OF NON-UNIFORM STRUCTURE

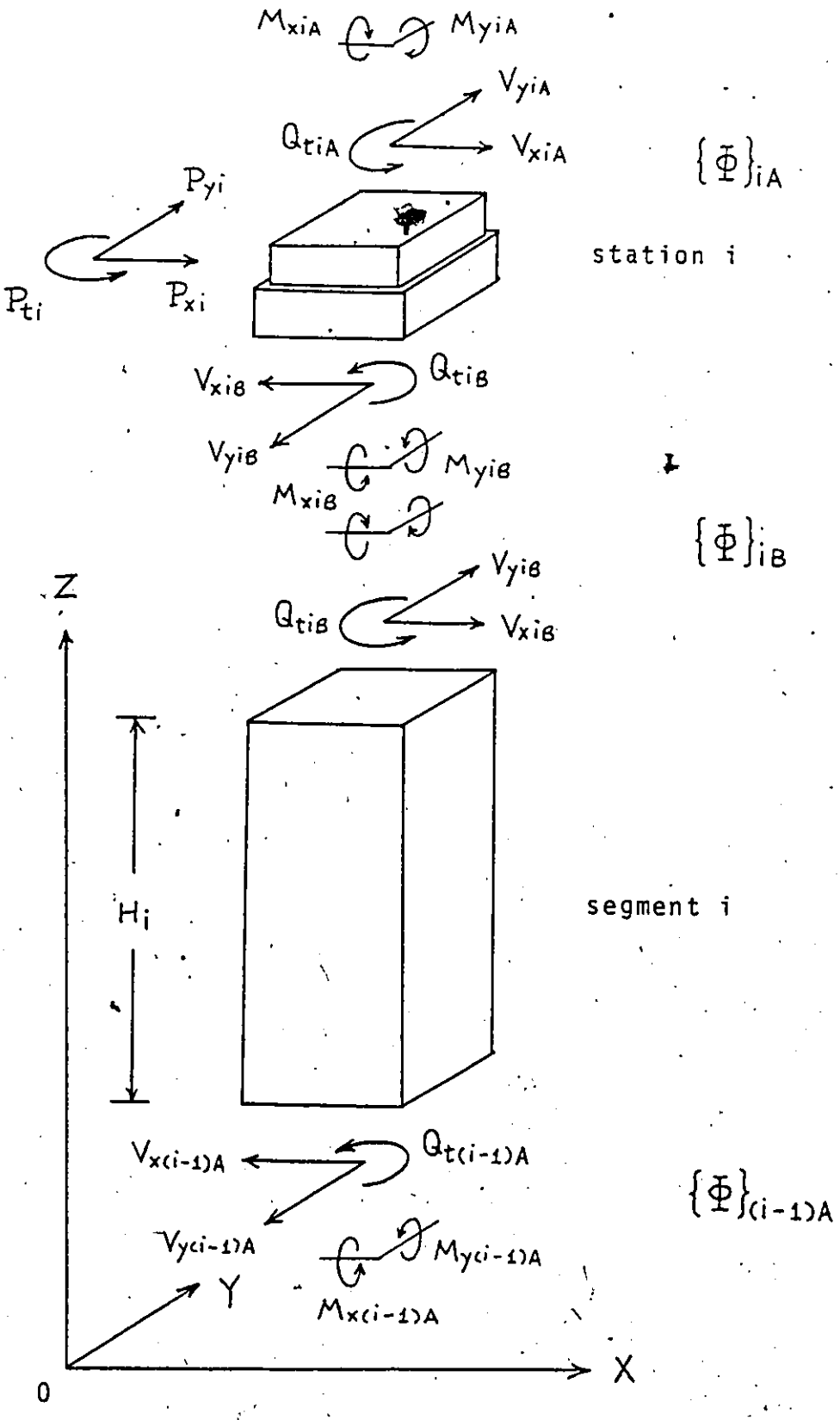

FIG. 5-2: FREE-BODY DIAGRAM OF STATION i AND SEGMENT i

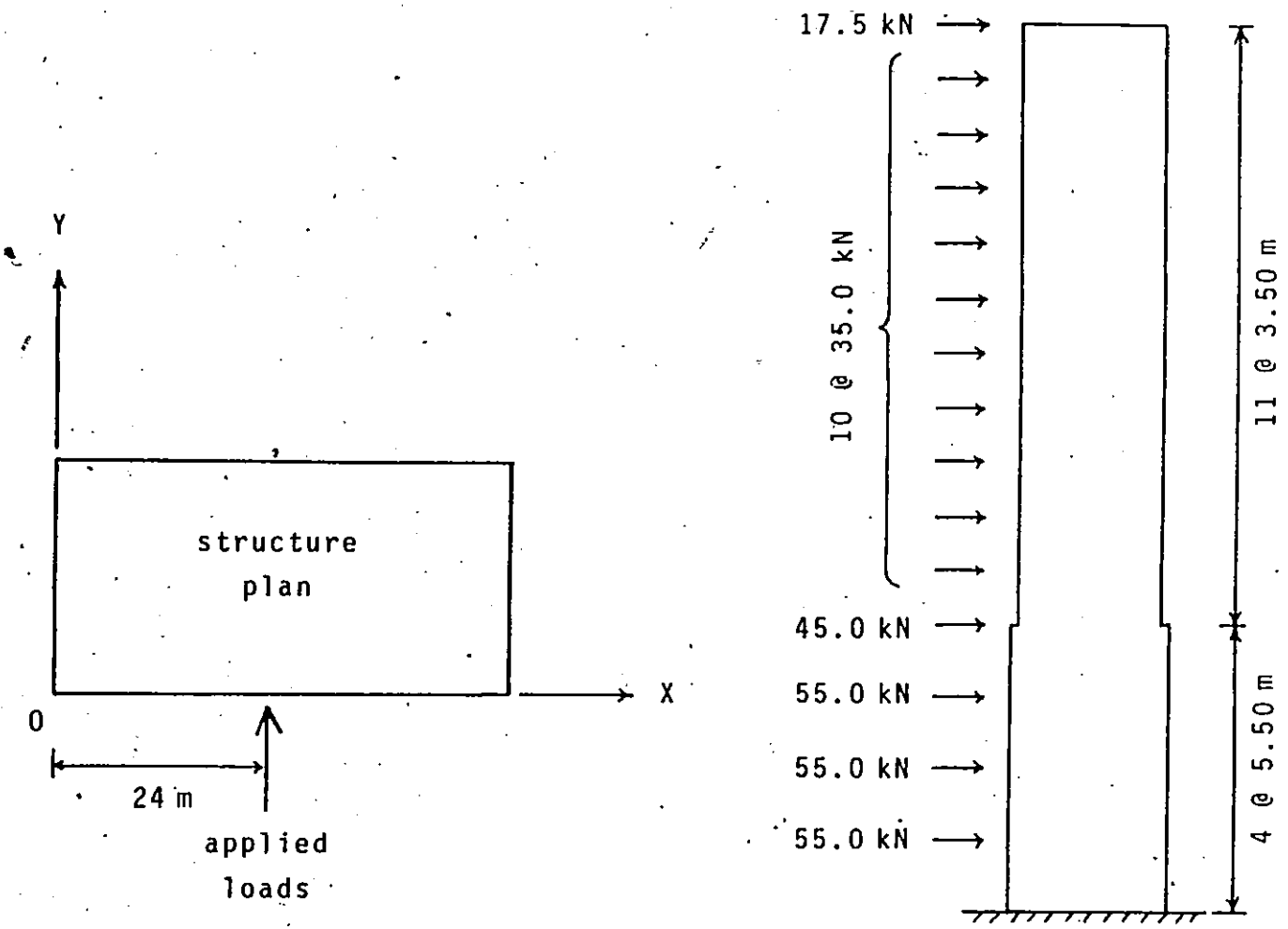

FIG. 5-3: LOADING CONDITIONS FOR NON-UNIFORM EXAMPLE STRUCTURE

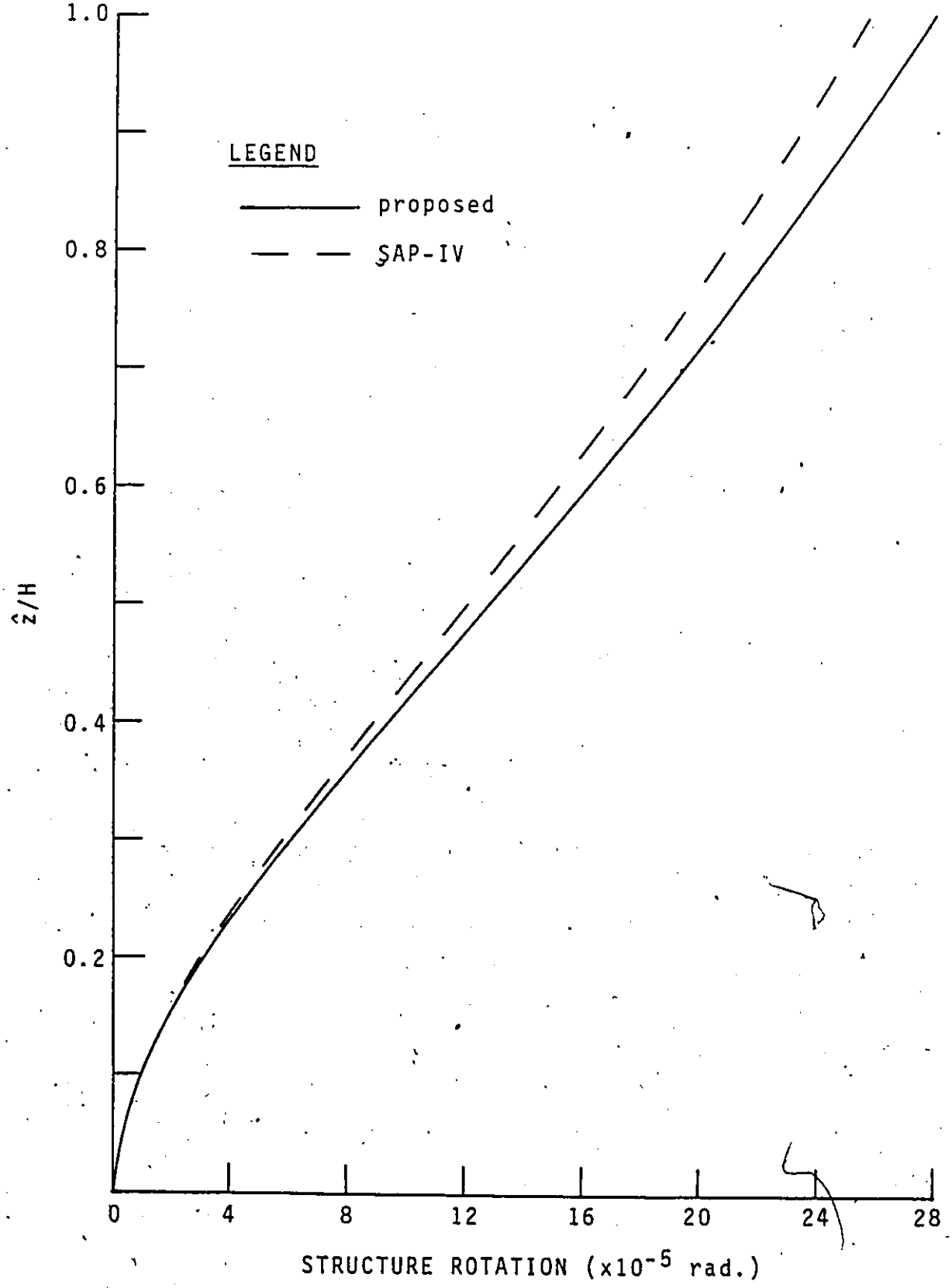

FIG. 5-4: ROTATION OF NON-UNIFORM EXAMPLE STRUCTURE

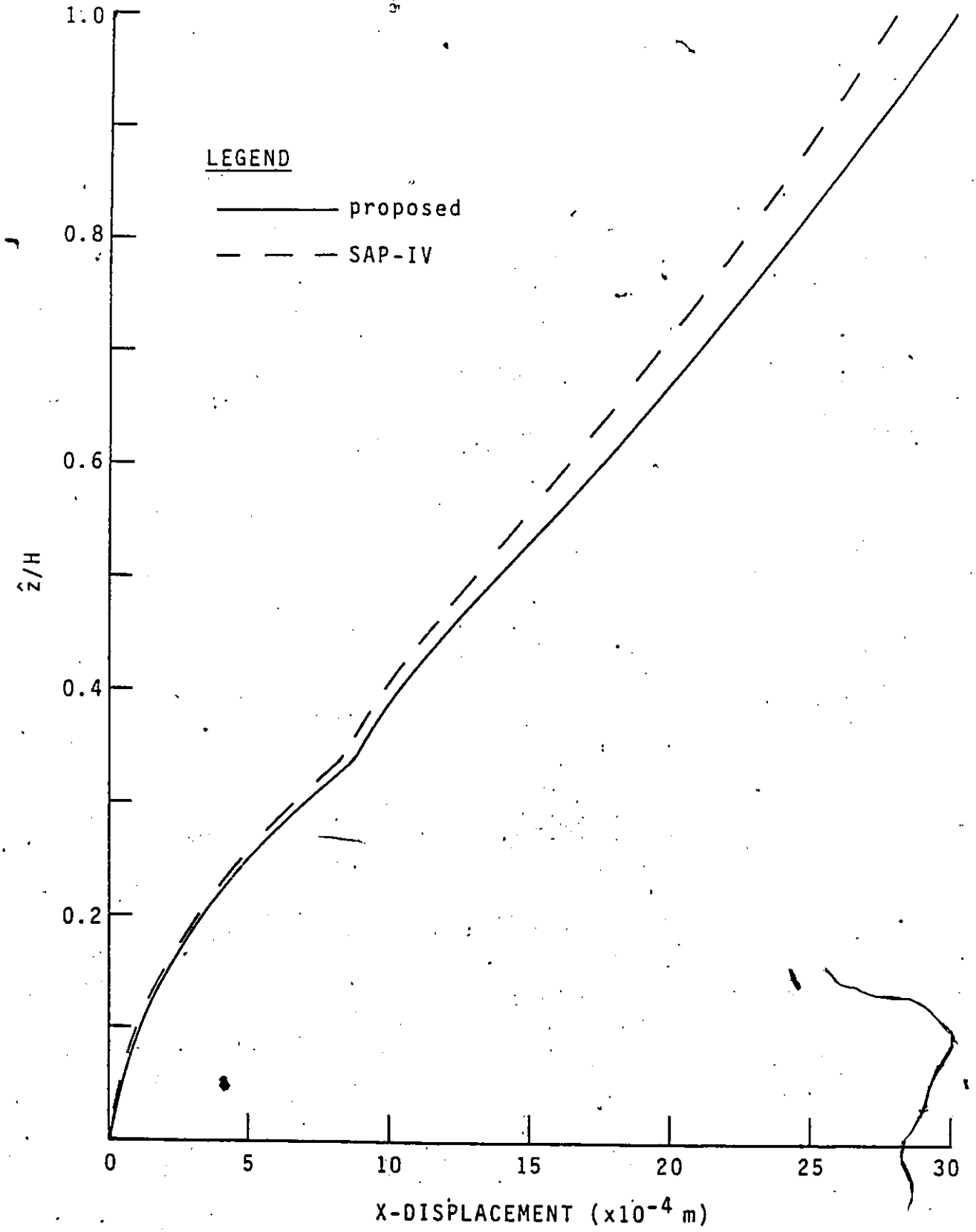

FIG. 5-5: X-DISPLACEMENT AT CENTROID OF WALL PIER 4

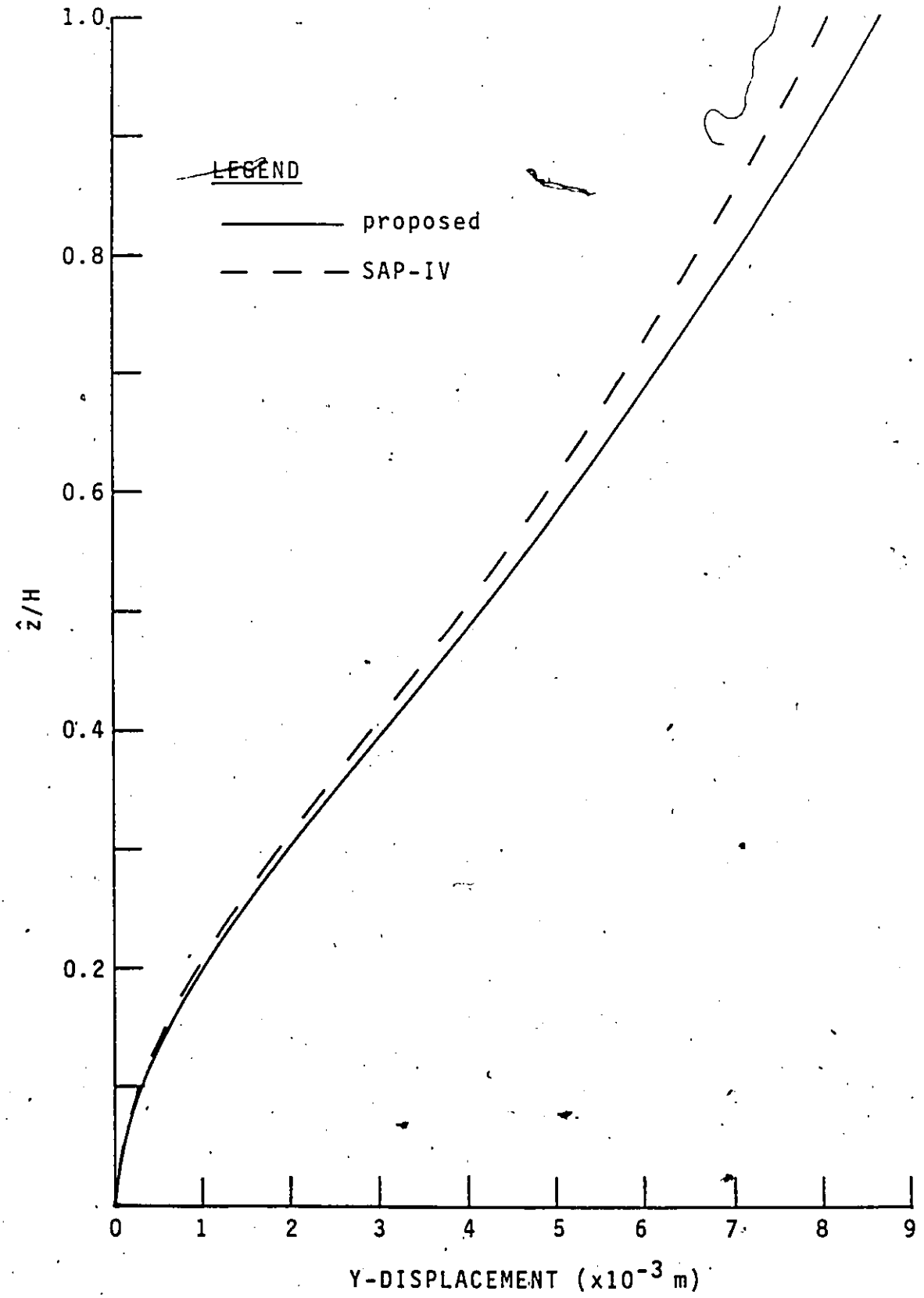

FIG. 5-6: Y-DISPLACEMENT AT CENTROID OF WALL PIER 4

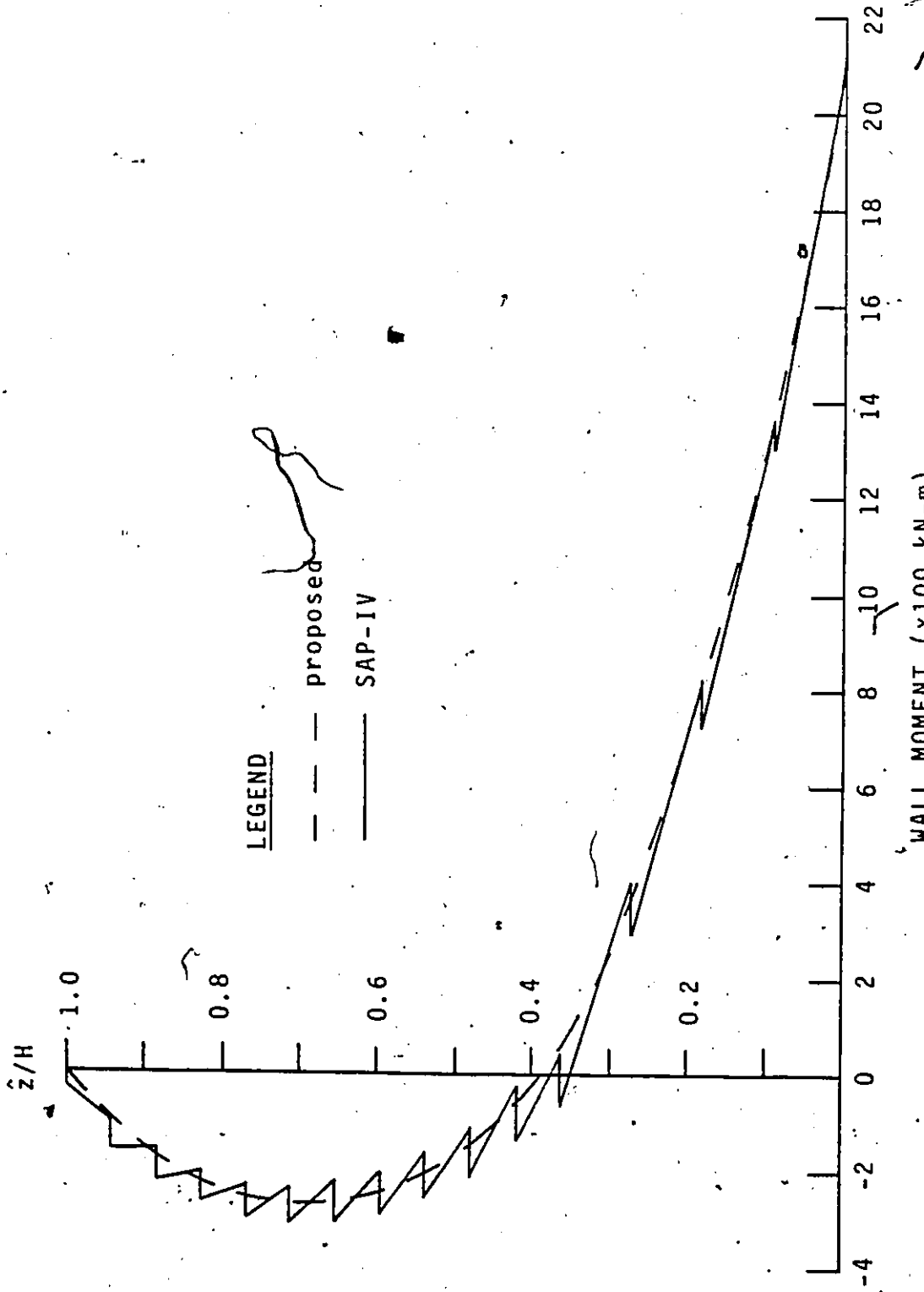

FIG. 5-7: INTERNAL MOMENT OF WALL PIER 3

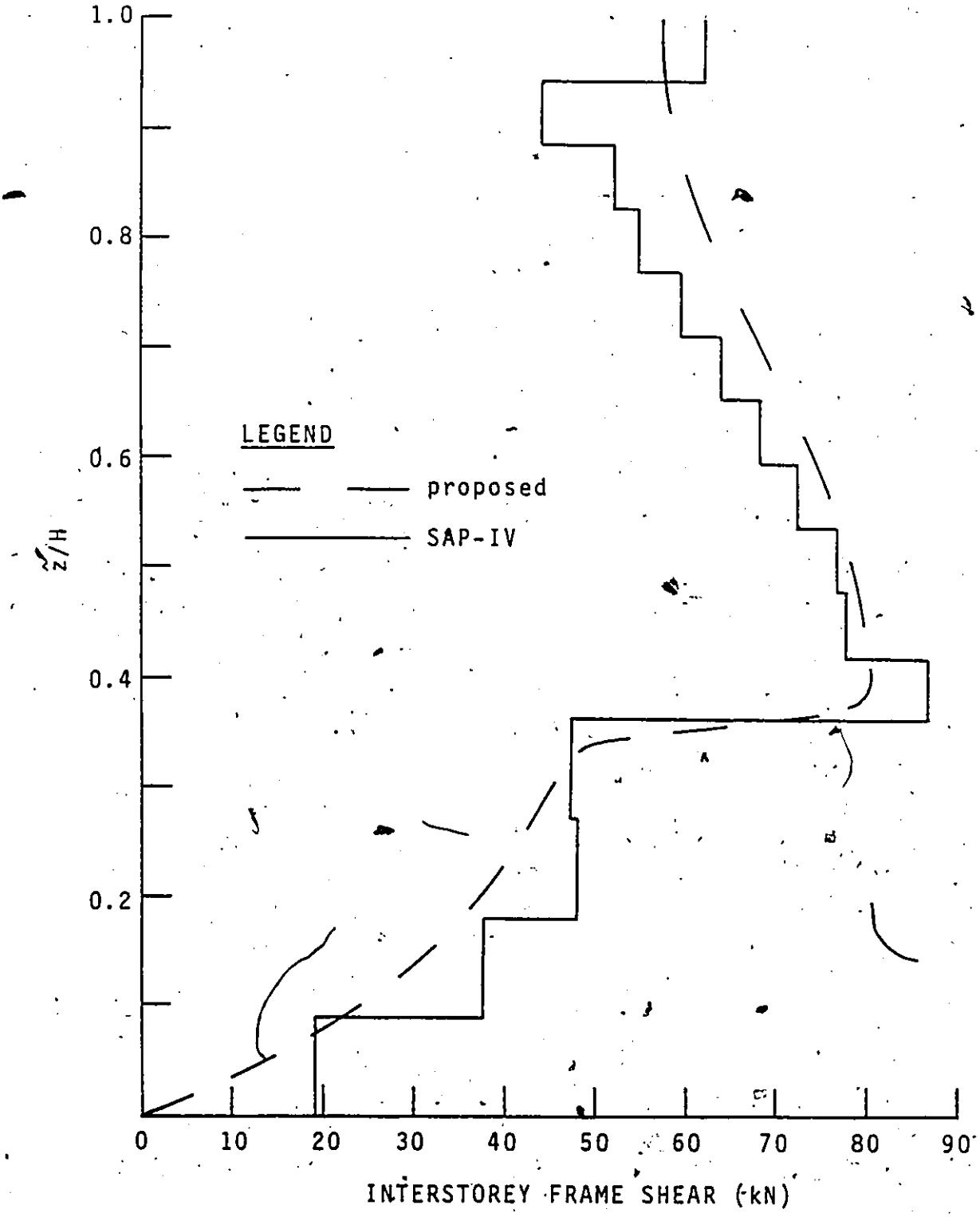

FIG. 5-8: INTERSTOREY SHEAR IN FRAME 2

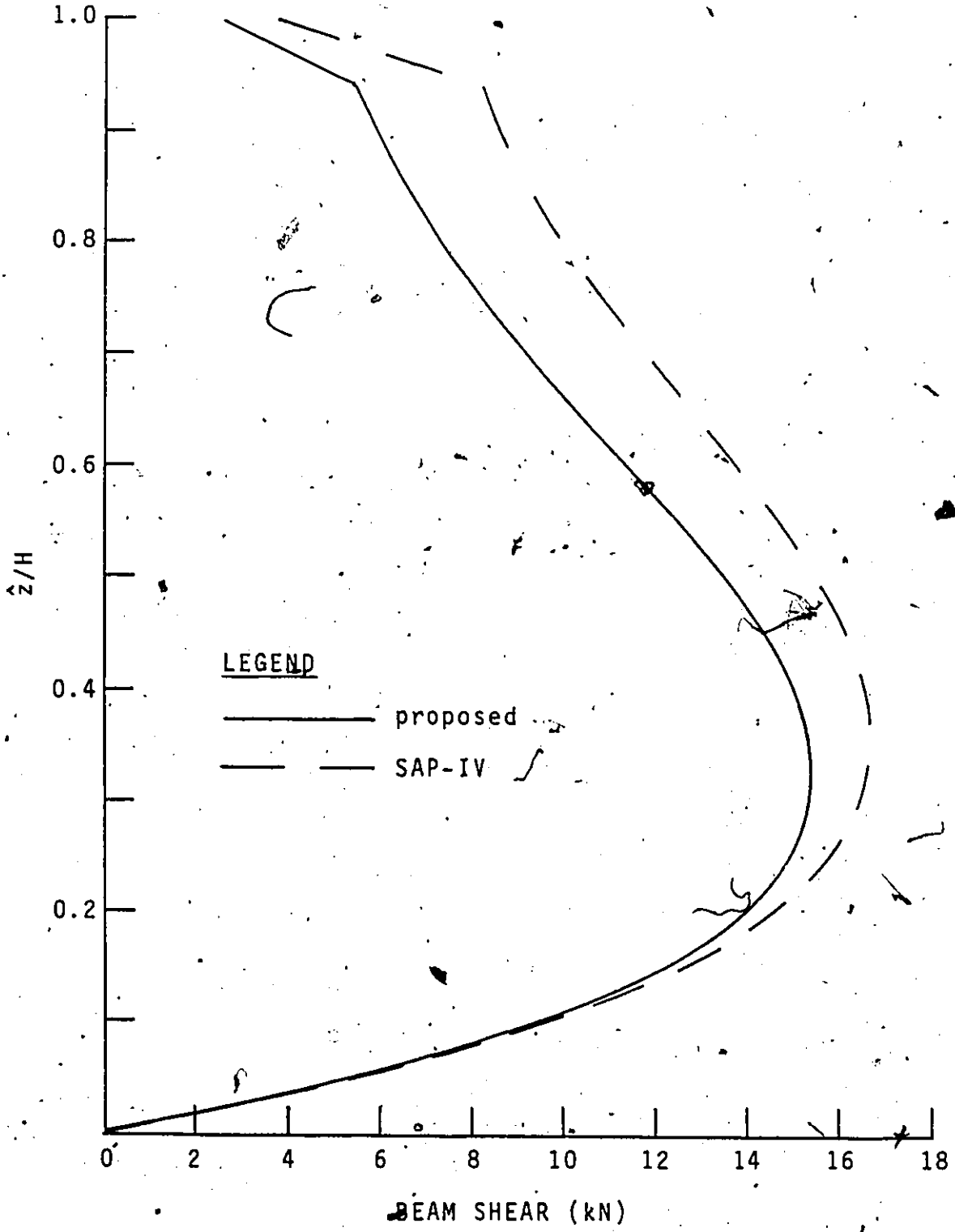

FIG. 5-9: SHEARS IN CONNECTING BEAM 4

CHAPTER VI

THREE-DIMENSIONAL ANALYSIS OF GENERAL BUILDING STRUCTURES

6.1 INTRODUCTION

The lateral load analysis of a multi-storey building structure can be undertaken from a two-dimensional perspective when the structure has a symmetrical layout with respect to the direction of the external load and the latter does not produce torsion in it. Otherwise, a three-dimensional analysis must be considered.

Numerous analytical methods have been proposed for the three-dimensional analysis of various types of building structures. These methods in general fall into two basic categories, namely, discrete methods and continuum methods. Discrete methods include the standard matrix metnods [50], and the finite element method [85]. The feasibility of applying the finite element method to three-dimensional building analysis is severely restricted due to reasons of economy, efficiency, and practicality. The matrix methods also suffer drawbacks due to the complexity of the process of data input and the heavy demand of computer resources.

Several modified stiffness matrix methods [9,81,82] have been developed with a view to economise on computer resource requirements. All these matrix methods, standard or modified, in general suffer the more important drawback of analytical inefficacy in the three-dimensional analysis of building structures which comprise non-planar shear walls. In contrast, continuum methods in general require relatively little computer storage and have been found to be convenient, economical, and efficient in dealing with shear wall structures in particular. The continuum approach has also been applied to the analysis of wall-frame building structures in previous chapters of this thesis and by other researchers [6, 29, 57, 60,70]. However, the application of a continuum method is usually restricted by its basic assumption of constant structure height.

Considering from the analytical perspective the broad spectrum of analytical methods which have been developed over the past couple of decades and which have been reviewed in Chapter I, the four principal lateral load-resisting systems, namely, the frame system, the shear wall system, the shear wall-frame system, and the tube system, can in general be broken down into the following basic analytical systems (Figures 6-1a through 6-1i):

(a) plane frame system

(b) plane shear wall system

(c) non-planar shear wall wystem

(d) planar two-pier coupled shear wall system with one row of connecting beams [78]

(e) non-planar two-pier coupled shear wall system with one row of connecting beams [76]

(f) general three-dimensional coupled shear wall system with more than two rows of connecting beams [4]

(g) planar shear wall-frame system with one row of wall-frame connecting beams (Chapter III)

(h) general three-dimensional shear wall-frame system with more than two rows of wall-wall or wall-frame connecting beams (Chapter V)

(i) framed-tube system [12,19]

Each of the above nine basic analytical systems by itself pertains to a distinct analytical formulation for the determination of its response to lateral and/or torsional loads. In cases where the analytical method is based on the continuum approach, the transfer matrix technique can be used in conjunction with that method in order to allow structural non-uniformity and arbitrary loading conditions along the height of the associated structure.

A general building structure may comprise one or more

of the above-mentioned basic analytical systems as its substructures such that analysis of the overall structure is not amenable to any single characteristic method. Practical examples of this nature include a set-back asymmetric shear wall building, a low-rise frame type construction attached to a high rise shear wall tower, or the tube-in-tube structure. Thus, it is obvious that there exists a need for a versatile method of analysis for general multi-storey building structures.

Methods proposed by Coull and Irwin [16], and by Coull and Subedi [20] point in this direction. A number of methods of a similar nature have also been proposed. All these methods are based on an analogy of the stiffness matrix method. Some of them allow for an arbitrary structure layout [8, 71] while others assume the structural elements to be arranged in parallel planes [16, 41]. Typically, the building structure is divided into individual resisting components, which can be frames, shear walls, or planar assemblies of these. Flexibility matrices with respect to lateral and/or rotational deformations are determined by appropriate techniques for these components. The corresponding stiffness matrices can then be found by inverting these flexibility matrices. Subsequent solution procedures are analogous to those of the stiffness matrix method by way of energy considerations [8] or direct equilibrium considerations [16, 41,

71]. In all of these methods, the resisting components are in general assumed to be two-dimensional elements having in-plane stiffness only. For non-planar elements such as open-section shear walls, they are treated as an assemblage of uncoupled plannar components. Thus, the scope of these methods is in general limited.

In this chapter, a method of three-dimensional analysis for general multi-storey buildings which comprise a combination of substructures of distinct analytical character will be presented. In the analysis, each substructure is defined as a macro-element for which an analytical method is available. The proposed method, referred to as the macro-element method of analysis, is essentially based on the stiffness matrix approach. An example will be worked out to illustrate application of the proposed analysis. The advantages and limitations of the analysis as a design tool will then be discussed.

6.2 NOTATIONS

The following notations will be used in this chapter:

$[K_T]$ = stiffness matrix of total structure with respect to global co-ordinate system (3N x 3N).

$[\bar{k}]_m$ = stiffness matrix of planar macro-element m with respect to lateral deflection along $\bar{Y}_m$ (N_m x N_m).

$[\hat{k}]_m$ = stiffness matrix of non-planar macro-element m with respect to lateral deflections along $\bar{X}_m$ and $\bar{Y}_m$, and rotation about $\bar{Z}_m$ ($3N_m$ x $3N_m$).

$[\bar{K}]_m$ = stiffness matrix of planar macro-element m with respect to global co-ordinate system ($3N_m$ x $3N_m$).

$[\hat{K}]_m$ = stiffness matrix of non-planar macro-element m with respect to global co-ordinate system ($3N_m$ x $3N_m$).

$\{L\}$ = global external load vector of overall structure.

M = number of macro-elements in total structure.

N_m = number of floor levels present in macro-element m.

N = maximum number of floor levels in structure.

$\{P_x\}_m$ $\{P_y\}_m$ $\{P_t\}_m$ = vectors of loads acting along X, Y, and about Z, respectively, that are taken up by macro-element m.

$\{P\}_m$ = $[\ \{P_x\}_m^T\ \{P_y\}_m^T\ \{P_t\}_m^T\ ]^T$.

$\{\bar{P}_x\}_m$ $\{\bar{P}_y\}_m$ $\{\bar{P}_t\}_m$ = vectors of loads acting on macro-element m along $\bar{X}_m$, $\bar{Y}_m$, and about $\bar{Z}_m$, respectively.

$\{\bar{P}\}_m$ = $[\ \{\bar{P}_X\}_m^T\ \{\bar{P}_y\}_m^T\ \{\bar{P}_t\}_m^T\ ]^T$.

$[R_D]_m$ = displacement transformation matrix for macro-element m.

$[R_L]_m$ = load transformation matrix for non-planar macro-element m.

X Y Z O = horizontal axes, vertical axis, and origin, respectively, of global co-ordinate system.

$\bar{X}_m$ $\bar{Y}_m$ $\bar{Z}_m$ O_m = horizontal axes, vertical axis, and origin, respectively, of local co-ordinate system for macro-element m.

$\{\xi\}_m$ $\{\eta\}_m$ $\{\theta\}_m$ = displacement vectors of macro-element m with respect to X, Y, and Z, respectively.

$\{\bar{\xi}\}_m$ $\{\bar{\eta}\}_m$ $\{\bar{\theta}\}_m$ = displacement vectors of macro-element m with respect to $\bar{X}_m$, $\bar{Y}_m$, and $\bar{Z}_m$,

respectively.

$\{\Delta\}_m$ = $[\ \{\xi\}_m^T\ \ \{\eta\}_m^T\ \ \{\theta\}_m^T\ ]^T$.

$\{\bar{\Delta}\}_m$ = $[\ \{\bar{\xi}\}_m^T\ \ \{\bar{\eta}\}_m^T\ \ \{\bar{\theta}\}_m^T\ ]^T$.

$\{\Delta\}$ = displacement vector of overall structure with respect to global coordinate system.

col. = column.

Eqn(s) = Equation(s).

6.3 STATEMENT OF PROBLEM

Consider a general three-dimensional building structure comprised of M mocro-elements linked together through the floor system. A macro-element is said to be planar or non-planar when its resultant lateral resistance to external loads acts in only one or more than one principal direction, respectively. For the overall structure, a right-handed orthogonal global co-ordinate system with origin O, horizontal axes X and Y, and vertical axis Z, is defined as shown in Figure 6-2. For macro-element m, where m = 1, 2, ... M, a local co-ordinate system with origin O_m located at (x_m, y_m) measured along X and Y with respect to O, horizontal axes $\overline{X}_m$ and $\overline{Y}_m$ oriented at an angle ϕ_m with respect to the global counterparts, and vertical axis $\overline{Z}_m$, is also defined (Figure 6-3). In the case of a planar macro-element, the $\overline{Y}_m$ - axis is assumed to lie in the principal plane of the element (Figure 6-3(b)). With N_m denoting the number of floors present in macro-element m, the displacements of the element at floor level ℓ, where ℓ = 1, 2, 3, ... N_m, will be defined by the horizontal displacements, $\overline{\xi}_\ell$ and $\overline{\eta}_\ell$, of O_m along $\overline{X}_m$ and $\overline{Y}_m$, respectively, and rotation $\overline{\theta}_\ell$ about $\overline{Z}_m$. External loads for the overall structure are approximated as concentrated loads applied at floor levels along the X - and Y - axes for lateral loads and about the Z - axis for torques.

Other assumptions made in this analysis are:

(1) Rigid diaphragm action of the floor system is assumed so that only three degrees of freedom are involved at any floor ℓ of the total structure, these being lateral deflections ξ_ℓ and η_ℓ along X and Y, respectively, and rotation θ_ℓ about Z.

(2) Macro-elements are assumed to be linked together by hinge-ended connections so that no interaction between macro-elements exists in the vertical direction.

(3) The structure which forms a macro-element is assumed to be amenable to analysis so that its behaviour under applied lateral and/or torsional loads is known.

6.4 FORMULTATION OF ANALYSIS

6.4.1 CONCEPT

For the m^{th} macro-element, the pertinent analytical method will be used to generate a flexibility matrix. In the case of a planar element, the flexibility matrix pertains to lateral deflection along $\overline{Y}_m$. In the case of a non-planar element, the flexibility matrix pertains to lateral deflections along $\overline{X}_m$ and $\overline{Y}_m$, and rotation about $\overline{Z}_m$. From this flexibility matrix, the corresponding stiffness matrix is obtained by matrix inversion. The total stiffness matrix for the overall structure is then obtained by superimposing the stiffness matrices of all macro-elements referred to the global co-ordinate system. The displacements of the overall structure can thus be determined. The applied external loads are then distributed among all macro-elements. With these distributed loads, each macro-element can be analysed accordingly for internal stresses by the respective analytical method which has been used to establish the flexibility matrix of the marco-element.

6.4.2 CO-ORDINATE TRANSFORMATION

The displacements of macro-element m, planar or non-

planar, relative to the respective local co-ordinate system can be transformed into displacements relative to the global co-ordinate system by the following relationship:

$$\{\bar{\Delta}\}_m = [R_D]_m \{\Delta\}_m \tag{6-1}$$

where $\{\bar{\Delta}\}_m$ and $\{\Delta\}_m$ are the vectors of lateral and rotational displacements at all floors of macro-element m relative to the respective local and global co-ordinate systems, respectively, and are defined by

$$\{\bar{\Delta}\}_m = \text{col.}\{\bar{\xi}_1\ \bar{\xi}_2 \cdots \bar{\xi}_{N_m}\ \bar{\eta}_1\ \bar{\eta}_2 \cdots \bar{\eta}_{N_m}\ \bar{\theta}_1\ \bar{\theta}_2 \cdots \bar{\theta}_{N_m}\} \tag{6-1a}$$

$$\{\Delta\}_m = \text{col.}\{\xi_1\ \xi_2 \cdots \xi_{N_m}\ \eta_1\ \eta_2 \cdots \eta_{N_m}\ \theta_1\ \theta_2 \cdots \theta_{N_m}\} \tag{6-1b}$$

The displacement transformation matrix of macro-element m, $[R_D]_m$, is defined by

$$[R_D]_m = \begin{bmatrix} \cos\phi_m[I]_m & \sin\phi_m[I]_m & -\bar{y}_m[I]_m \\ -\sin\phi_m[I]_m & \cos\phi_m[I]_m & \bar{x}_m[I]_m \\ [0]_m & [0]_m & [I]_m \end{bmatrix} \tag{6-1c}$$

in which $\bar{x}_m$ and $\bar{y}_m$ are the co-ordinates of O_m with respect to O but measured along the directions of $\bar{X}_m$ and $\bar{Y}_m$, respectively, while

$$[I]_m = \text{identity matrix of size } N_m \times N_m \qquad (6\text{-}1d)$$

$$[O]_m = \text{null matrix of size } N_m \times N_m \qquad (6\text{-}1e)$$

6.4.3 STIFFNESS CONTRIBUTION OF PLANAR MACRO-ELEMENTS TO TOTAL STRUCTURE

The lateral loads acting on planar macro-element m at all floor levels along the $\bar{Y}_m$-axis are given by the vector $\{\bar{P}_y\}_m$ such that

$$\{\bar{P}_y\}_m = [\bar{k}]_m \{\bar{n}\}_m \qquad (6\text{-}2)$$

where $[\bar{k}]_m$ is the $N_m \times N_m$ stiffness matrix of planar macro-element m with respect to lateral deflection along $\bar{Y}_m$, and $\{\bar{n}\}_m$ is the vector of displacements at all floor levels of the macro-element along $\bar{Y}_m$ and is given by

$$\{\bar{n}\}_m = \text{col.}\{\bar{n}_1 \;\; \bar{n}_2 \;\; \bar{n}_3 \;\; \ldots\ldots \;\; \bar{n}_{N_m}\}_m \qquad (6\text{-}2a)$$

Referring to Figure 6-3(b), it can be shown that by

Resolving $\{\bar{P}_y\}_m$ into components acting at the global origin O with respect to the directions of the global axes, there is obtained

$$\{P_x\}_m = -\{\bar{P}_y\}_m \sin\phi_m \qquad (6\text{-}3)$$

$$\{P_y\}_m = \{\bar{P}_y\}_m \cos\phi_m \qquad (6\text{-}4)$$

$$\{P_t\}_m = \{\bar{P}_y\}_m \bar{x}_m \qquad (6\text{-}5)$$

where $\{P_x\}_m$, $\{P_y\}_m$, and $\{P_t\}_m$ are the vectors of load components acting at all floors of macro-element m with respect to the X-, Y-, and Z-axes, respectively, such that

$$\{P_x\}_m = \text{col.}\{\, P_1^x \;\; P_2^x \;\; P_3^x \;\; \ldots\; P_{N_m}^x \,\}_m \qquad (6\text{-}3a)$$

$$\{P_y\}_m = \text{col.}\{\, P_1^y \;\; P_2^y \;\; P_3^y \;\; \ldots\; P_{N_m}^y \,\}_m \qquad (6\text{-}4a)$$

$$\{P_t\}_m = \text{col.}\{\, P_1^t \;\; P_2^t \;\; P_3^t \;\; \ldots\; P_{N_m}^t \,\}_m \qquad (6\text{-}5a)$$

where P_ℓ^x, P_ℓ^y, and P_ℓ^t with $\ell = 1,2,\ldots,N_m$ represent the corresponding load components at floor level ℓ.

Substituting Eqn(6-2) into each of Eqns(6-3), (6-4), (6-5) separately, and making use of the transformation relationship of Eqn(6-1), the following equations are obtained:

$$\{P_x\}_m = [\bar{K}_m^{xx}]\{\xi\}_m + [\bar{K}_m^{xy}]\{\eta\}_m + [\bar{K}_m^{x\theta}]\{\theta\}_m \qquad (6\text{-}6)$$

$$\{P_y\}_m = [\bar{K}_m^{yx}]\{\xi\}_m + [\bar{K}_m^{yy}]\{\eta\}_m + [\bar{K}_m^{y\theta}]\{\theta\}_m \qquad (6\text{-}7)$$

$$\{P_t\}_m = [\bar{K}_m^{\theta x}]\{\xi\}_m + [\bar{K}_m^{\theta y}]\{\xi\}_m + [\bar{K}_m^{\theta\theta}]\{\theta\}_m \qquad (6\text{-}8)$$

where $\{\xi\}_m$, $\{\eta\}_m$, and $\{\theta\}_m$ are the vectors of displacements at all floors of macro-element m with respect to the X-, Y-, and Z-axes, respectively, such that

$$\begin{aligned} \{\xi\}_m &= \text{col.}\{\ \xi_1 \quad \xi_2 \quad \cdots \quad \xi_{N_m}\ \}_m \\ \{\eta\}_m &= \text{col.}\{\ \eta_1 \quad \eta_2 \quad \cdots \quad \eta_{N_m}\ \}_m \\ \{\theta\}_m &= \text{col.}\{\ \theta_1 \quad \theta_2 \quad \cdots \quad \theta_{N_m}\ \}_m \end{aligned} \qquad (6\text{-}9a)$$

$$\left.\begin{aligned} [\bar{K}_m^{xx}] &= [\bar{k}]_m \sin^2\phi_m \\ [\bar{K}_m^{xy}] &= -[\bar{k}]_m \sin\phi_m \cos\phi_m \\ [\bar{K}_m^{x\theta}] &= [\bar{K}_m^{xy}]\cdot x_m - [\bar{K}_m^{xx}]\cdot y_m \\ [\bar{K}_m^{yx}] &= [\bar{K}_m^{xy}] \\ [\bar{K}_m^{yy}] &= [\bar{k}]_m \cos^2\phi_m \\ [\bar{K}_m^{y\theta}] &= [\bar{K}_m^{yy}]\cdot x_m - [\bar{K}_m^{xy}]\cdot y_m \\ [\bar{K}_m^{\theta x}] &= [\bar{K}_m^{x\theta}] \\ [\bar{K}_m^{\theta y}] &= [\bar{K}_m^{y\theta}] \ ; \quad [\bar{K}_m^{\theta\theta}] = [\bar{k}]_m \cdot \bar{x}_m^2 \end{aligned}\right\} \qquad (6\text{-}9b)$$

Combining Eqns(6-6), (6-7), and (6-8) into one single matrix equation, there is obtained

$$\{P\}_m = [\bar{K}]_m \{\Delta\}_m \tag{6-10}$$

where $\{\Delta\}_m$ is as defined by Eqn(6-1b), $[\bar{K}]_m$ is the stiffness matrix of planar macro-element m with respect to the global co-ordinate system and is given by

$$[\bar{K}]_m = \begin{bmatrix} [\bar{K}_m^{xx}] & [\bar{K}_m^{xy}] & [\bar{K}_m^{x\theta}] \\ [\bar{K}_m^{yx}] & [\bar{K}_m^{yy}] & [\bar{K}_m^{y\theta}] \\ [\bar{K}_m^{\theta x}] & [\bar{K}_m^{\theta y}] & [\bar{K}_m^{\theta\theta}] \end{bmatrix} \tag{6-10a}$$

$$\{P\}_m^T = [\ \{P_x\}_m^T \ \ \{P_y\}_m^T \ \ \{P_t\}_m^T\ ] \tag{6-10b}$$

Thus Eqn(6-10) defines the contribution of planar macro-element m to the stiffness of the total structure with respect to the global co-ordinate system.

6.4.4 STIFFNESS CONTRIBUTION OF NON-PLANAR MACRO-ELEMENTS TO TOTAL STRUCTURE

The lateral and torsional loads acting on non-planar macro-element m relative to the respective local co-

ordinate system are given by $\{\bar{P}\}_m$ such that

$$\{\bar{P}\}_m = [\hat{k}]_m \{\bar{\Delta}\}_m \qquad (6\text{-}11)$$

where $\{\bar{\Delta}\}_m$ is as defined by Eqn(6-1a), $[\hat{k}]_m$ is the stiffness matrix of non-planar macro-element m with respect to lateral and rotational displacements relative to the respective local co-ordinate system, and

$$\{\bar{P}\}_m^T \equiv [\ \{\bar{P}_x\}_m^T \ \ \{\bar{P}_y\}_m^T \ \ \{\bar{P}_t\}_m^T\ ] \qquad (6\text{-}11a)$$

where $\{\bar{P}_x\}_m$, $\{\bar{P}_y\}_m$, and $\{\bar{P}_t\}_m$ are the vectors of loads acting at all floors of macro-element m relative to the $\bar{X}_m$-, $\bar{Y}_m$-, and $\bar{Z}_m$-axes respectively..

Transforming $\{\bar{P}\}_m$ from the local to the global co-ordinate system, there is obtained

$$\{P\}_m = [R_L]_m \{\bar{P}\}_m \qquad (6\text{-}12)$$

where $\{P\}_m$ is as defined by Eqn(6-10a), and $[R_L]_m$ is the load transformation matrix of size $N_m \times N_m$ for non-planar macro-element m and is given by

$$[R_L]_m = \begin{bmatrix} \cos\phi_m[I]_m & -\sin\phi_m[I]_m & [0]_m \\ \sin\phi_m[I]_m & \cos\phi_m[I]_m & [0]_m \\ -\bar{y}_m\cdot[I]_m & \bar{x}_m\cdot[I]_m & [I]_m \end{bmatrix} \qquad (6\text{-}12a)$$

Substituting Eqn(6-1) into Eqn(6-11), there is obtained

$$\{\bar{P}\}_m = [\hat{k}]_m [R_D]_m \{\Delta\}_m \qquad (6\text{-}13)$$

Substituting Eqn(6-13) into Eqn(6-12), there is obtained

$$\{P\}_m = [\hat{K}]_m \{\Delta\}_m \qquad (6\text{-}14)$$

where $[\hat{K}]_m$ is the stiffness matrix of non-planar macro-element m with respect to lateral and rotational displacements relative to the global co-ordinate system, and is given by

$$[\hat{K}]_m = [R_L]_m [\hat{k}]_m [R_D]_m \qquad (6\text{-}14a)$$

Thus Eqn(6-14) defines the contribution of non-planar macro-element m to the stiffness of the total structure with respect to the global co-ordinate system.

6.4.5 STIFFNESS OF TOTAL STRUCTURE

Considering the equilibrium of the overall structure, there is obtained.

$$\sum_{m=1}^{M} \{P\}_m = \{L\} \qquad (6\text{-}15)$$

where $\{L\}$ is the vector of external lateral and torsional loads applied at the global origin with respect to the directions of the global axes.

Substituting Eqn(6-10) for planar macro-elements or Eqn(6-14) for non-planar macro-elements into Eqn(6-15) there is obtained

$$\sum_{m=1}^{M} [K]_m \{\Delta\}_m = \{L\}_m \tag{6-16}$$

where $$[K]_m \equiv \begin{cases} [\bar{K}]_m \text{ for planar macro-elements.} \\ [\hat{K}]_m \text{ for non-planar macro-elements.} \end{cases} \tag{6-16a}$$

By the assumption of rigid diaphragm action, for all macro-elements

$$\{\Delta\}_m = \{\Delta\} \tag{6-17}$$

where $\{\Delta\}$ is the tri-directional displacement vector of the overall structure with respect to the global co-ordinate system such that

$$\{\Delta\} = \text{col.}\{\ \xi_1\ \xi_2 \cdots \xi_N\ \eta_1\ \eta_2 \cdots \eta_N\ \theta_1\ \theta_2 \cdots \theta_N\ \} \tag{6-17a}$$

where N is the maximum number of floor levels among all

planar and non-planar macro-elements.

Therefore, substituting Eqn(6-17) into Eqn(6-15), there is obtained

$$[K_T]\ \{\Delta\} = \{L\} \qquad (6\text{-}18)$$

where $[K_T]$ is the stiffness matrix of the total structure with respect to the global co-ordinate system and is given by

$$[K_T] = \sum_{m=1}^{M} [K]_m \qquad (6\text{-}18a)$$

6.4.6 DISTRIBUTION OF EXTERNAL LOADS

The displacements of the total structure with respect to the global co-ordinate system are determined by solving Eqn(6-18) and are given by

$$\{\Delta\} = [K_T]^{-1}\ \{L\} \qquad (6\text{-}19)$$

The displacements of each macro-element relative to the respective local co-ordinate system can be found by transformation using Eqn(6-1). The loads taken by each macro-element, with respect to the respective local co-

ordinate system, can then be obtained from Eqn(6-10) in the case of a planar macro-element, or from Eqn(6-14) in the case of a non-planar macro-element. With the respective loads computed, each macro-element is then analysed by the associated analytical method for internal stresses.

6.5 IMPLEMENTATION OF PROPOSED METHOD

6.5.1 COMPUTER PROGRAM

A Fortran computer program has been developed based on the proposed method of analysis. It contains a base program which carries out such routines as assembling the stiffness matrices of individual macro-elements to form the global stiffness matrix for the total structure, computing the generalised displacements of the structure, and distributing loads to various macro-elements for the evaluation of member forces and/or deformations within each of them. Linked to this base program are a number of subroutines each of which serves to evaluate the flexibility matrix for a particular type of substructure and to compute the member forces and/or deformations within that substructure after loads are distributed to it by the base program. The following types of substructure, or macro-element, have been included in the program:

(1) plane frame
(2) plane cantilever wall
(3) non-planar cantilever wall
(4) planar two-pier coupled shear wall [78]
(5) planar wall-frame (see Chapter III)

(6) three-dimensional coupled shear wall [4]

(7) three-dimensional wall-frame (see Chapter V)

Except for the plane frame macro-element, to which the stiffness matrix method is applied, all the other macro-elements listed above are analysed by continuum methods.

6.5.2 EXAMPLE

The example structure of Chapter IV has been analysed using the computer program described in the previous section. The structure is divided up into seven macro-elements as shown in Figure 6-4. Two separate cases, namely, Case A and Case B, have been considered. In Case A, the planar coupled shear wall and planar wall-frame macro-elements(macro-elements 2, 3, 4, 5, and 6) are analysed by the appropriate continuum methods while in Case B, these are analysed as plane frame structures. In both cases, the I-section shear wall (macro-element 1) is analysed as a non-planar cantilever wall macro-element while the single-bay frame (macro-element 7) is analysed as a plane frame. A lateral load of 10 kN/m (0.685 klf) along the height of the structure is applied at wall pier 4 in the direction of the Y-axis, and is approximated as five point loads acting at floor levels 3, 6, 9, 12, and 15 (Figure 6-5).

Results for structure rotation, the X- and Y-translational displacements at the centroid of wall pier 4, the wall moment of wall pier 3, the interstorey shear in frame 2, and the beam shear in connecting beam 4 are presented in Figures 6-6 through 6-11. Corresponding results by SAP-IV [62] are also shown for comparison. It can be observed that the results for both Case A and Case B compare favourably with those by SAP-IV. It can also be found that Case B shows closer agreement than Case A. This is understandable since Case B is essentially a matrix method analysis similar to SAP-IV.

Finally, it is worth mentioning that the computer execution times required for Case A and Case B on the CDC CYBER 170/730 computer are 10.66 and 16.28 decimal seconds, respectively, while that for SAP-IV is 126 decimal seconds.

6.6 DISCUSSION

The proposed method is simple in concept. It also exhibits the following advantages:

(1) Effects of various sub-structures, each forming a macro-element, on the behaviour of the total structure in terms of external load allocation, control of overall deformation, etc., can be individually visualised. This will be helpful in achieving an optimum structure that is capable of satisfying prescribed structural requirements.

(2) During the early stages of a design process, structural modifications are not infrequent. The building in question can be broken up into several areas of interest, each of which constitutes one macro-element. Thus design changes made in a particular macro-element do not affect the process of data preparation in other macro-elements. Meanwhile, the effects of these changes on the overall behaviour of the total structure can be recognised readily.

(3) In loose terms, the computer storage requirement of any structure to be analysed does not depend on its overall complexity but rather on that of its constituent macro-elements and on the specific analytical

techniques associated with these macro-elements. Thus, when analysing a large structure, computer storage requirements can be optimised by breaking up the structure into macro-elements. For example, a large three-dimensional orthogonal frame structure could be analysed essentially by a plane frame program [9,82]. It is to be noted that, in general, more computing time will be called for when a structure is divided up into more macro-elements than is anaytically required.

(4) Flexibility in structural non-uniformity along the height is enhanced where the macro-elements involve continuum analysis, because independent structural changes can be imposed as intended for within individual macro-elements.

(5) A computer program written on the basis of the method will be essentially open-ended so that new or improved analytical techniques can be easily accomodated in the form of subprograms when the need so arises.

(6) For structures which are deemed to be more amenable to experimental analysis than otherwise for reasons of economy, efficiency, or practicality, or because of the lack of an appropriate analytical method, experimental findings in the form of flexibility or stiffness coefficients can be incorporated as direct input data.

Thus, in view of the simplicity of the proposed method and the advantages discussed above, it is believed that the method does provide a viable and versatile tool for the lateral load analysis of general building structures.

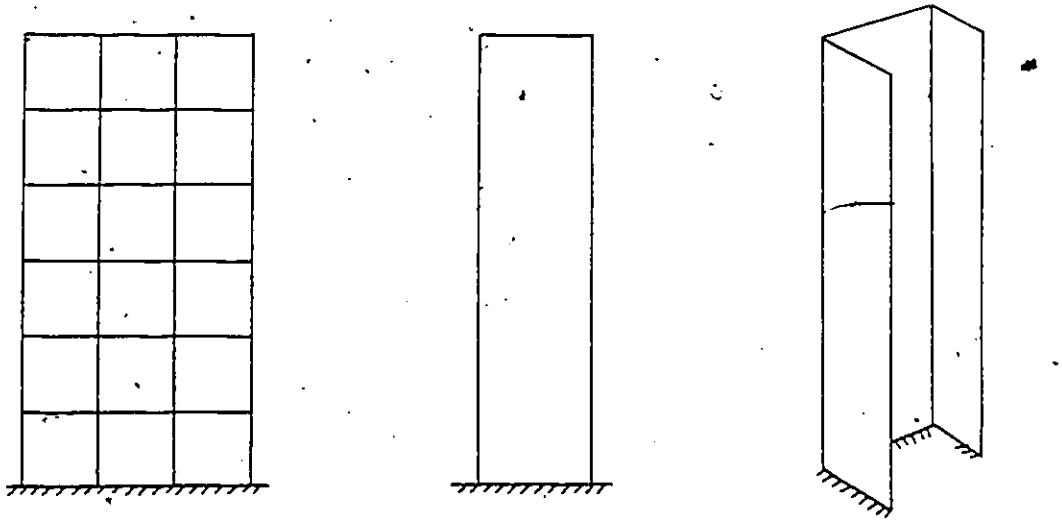

(a) plane frame (b) plane shear wall (c) non-planar shear wall

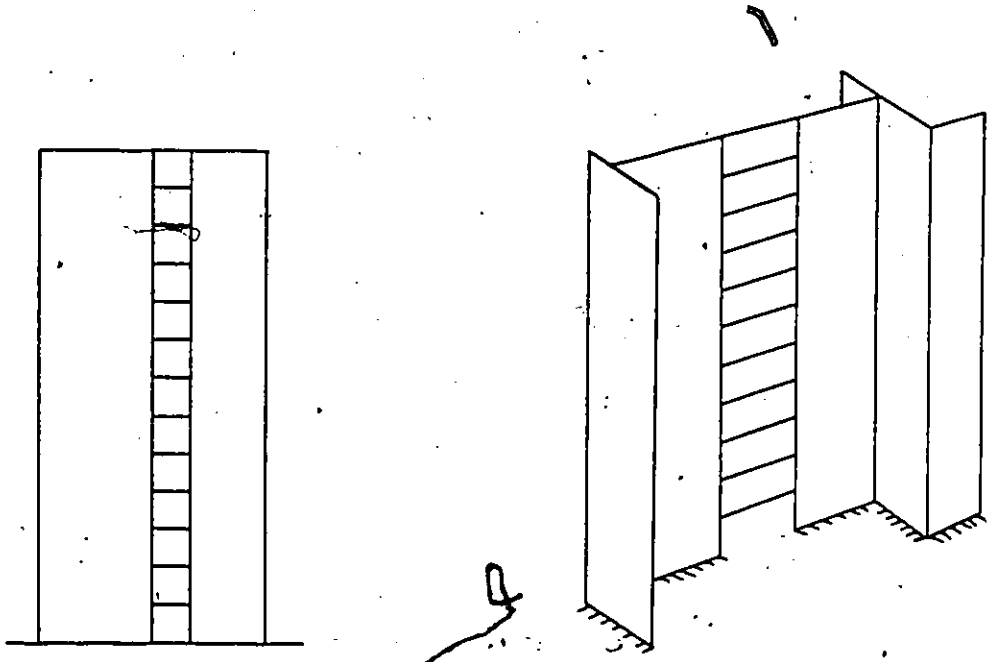

(d) planar 2-pier coupled shear wall (e) non-planar 2-pier coupled shear wall

FIG. 6-1: TYPES OF ANALYTICAL SYSTEMS

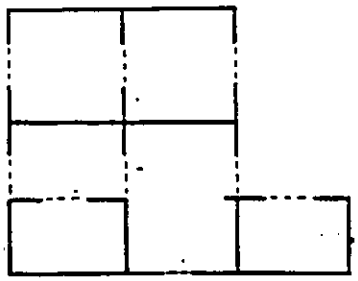

—— wall elements
---- conn. beams

(f) three-dimensional coupled shear wall

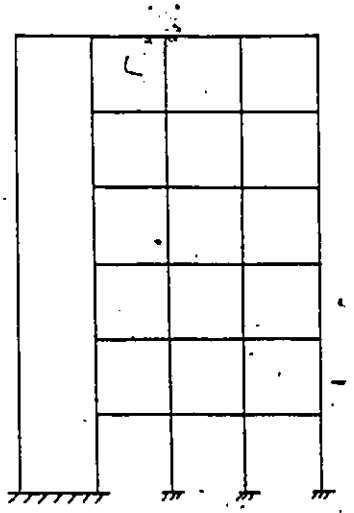

(g) planar wall-frame

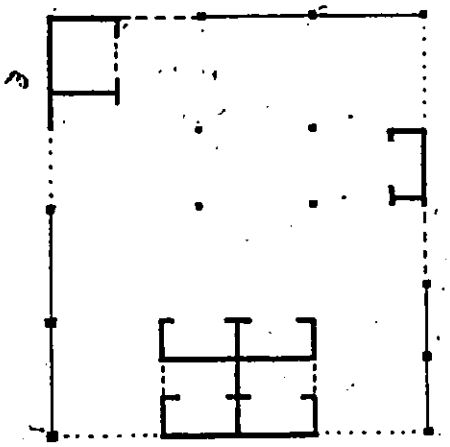

····· plan boundaries
—— walls ▪ ▪ columns
--- conn. beams —▪— frames

(h) three-dimensional wall-frame

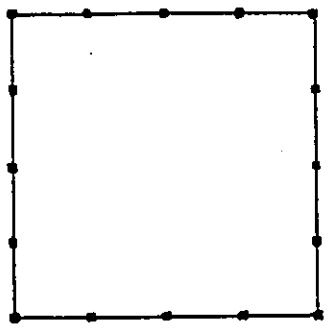

(i) framed-tube

(FIG. 6-1 CONTINUED)

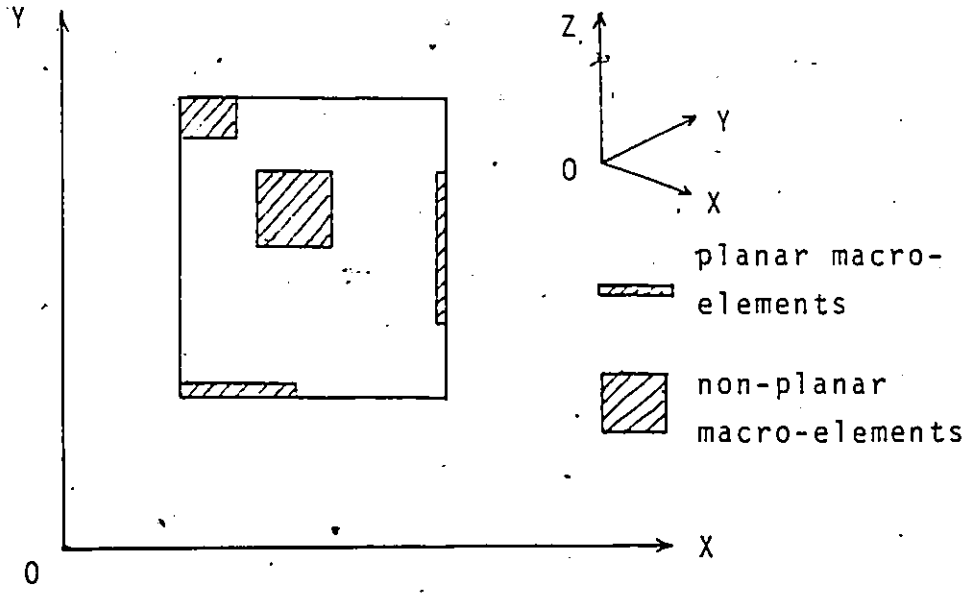

FIG. 6-2: SCHEMATIC PLAN OF STRUCTURE AND GLOBAL CO-ORDINATE SYSTEM

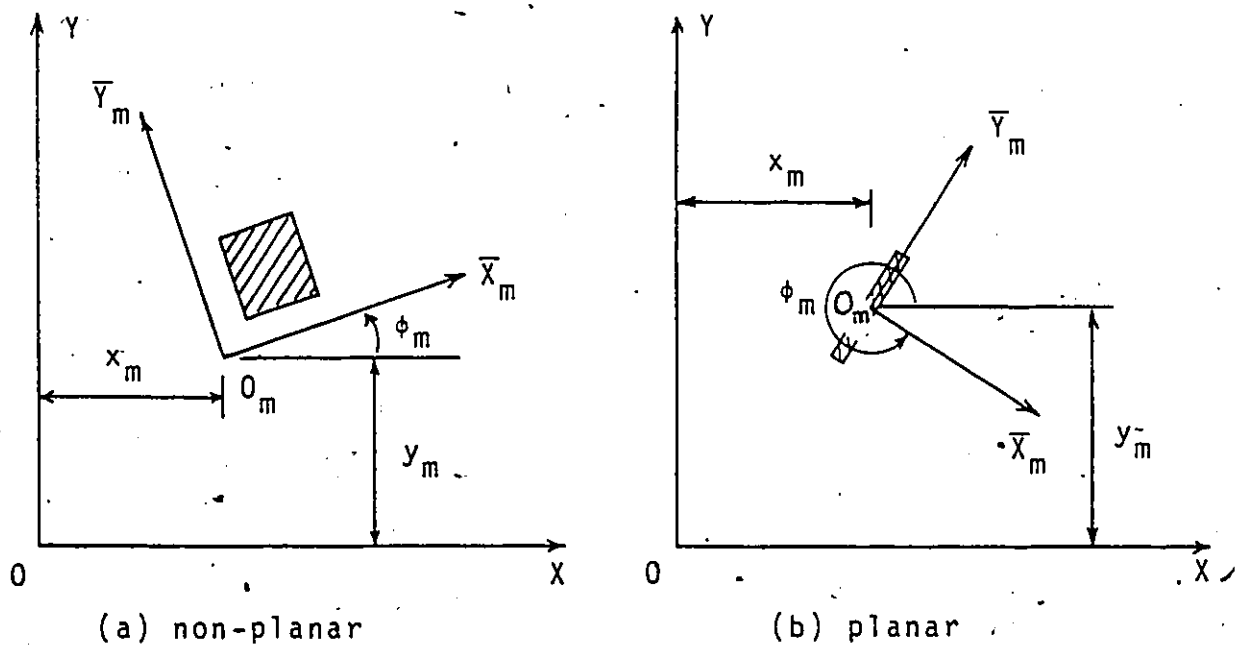

FIG. 6-3: LOCAL CO-ORDINATE SYSTEM OF MACRO-ELEMENT m

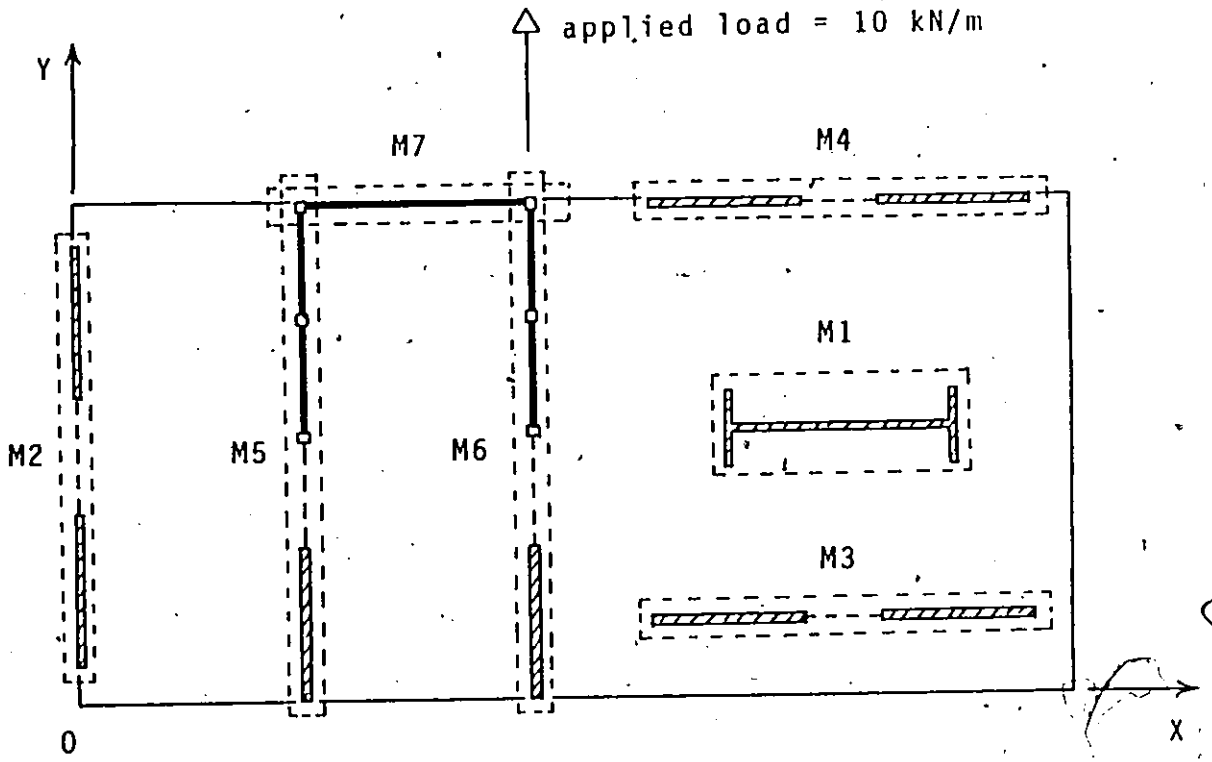

NOTATIONS: M1 = macro-element 1
M2 = macro-element 2
⋮ ⋮
M7 = macro-element 7

(for structural details, refer to FIG. 4-13)

FIG. 6-4: DIVISION OF EXAMPLE STRUCTURE INTO MACRO-ELEMENTS

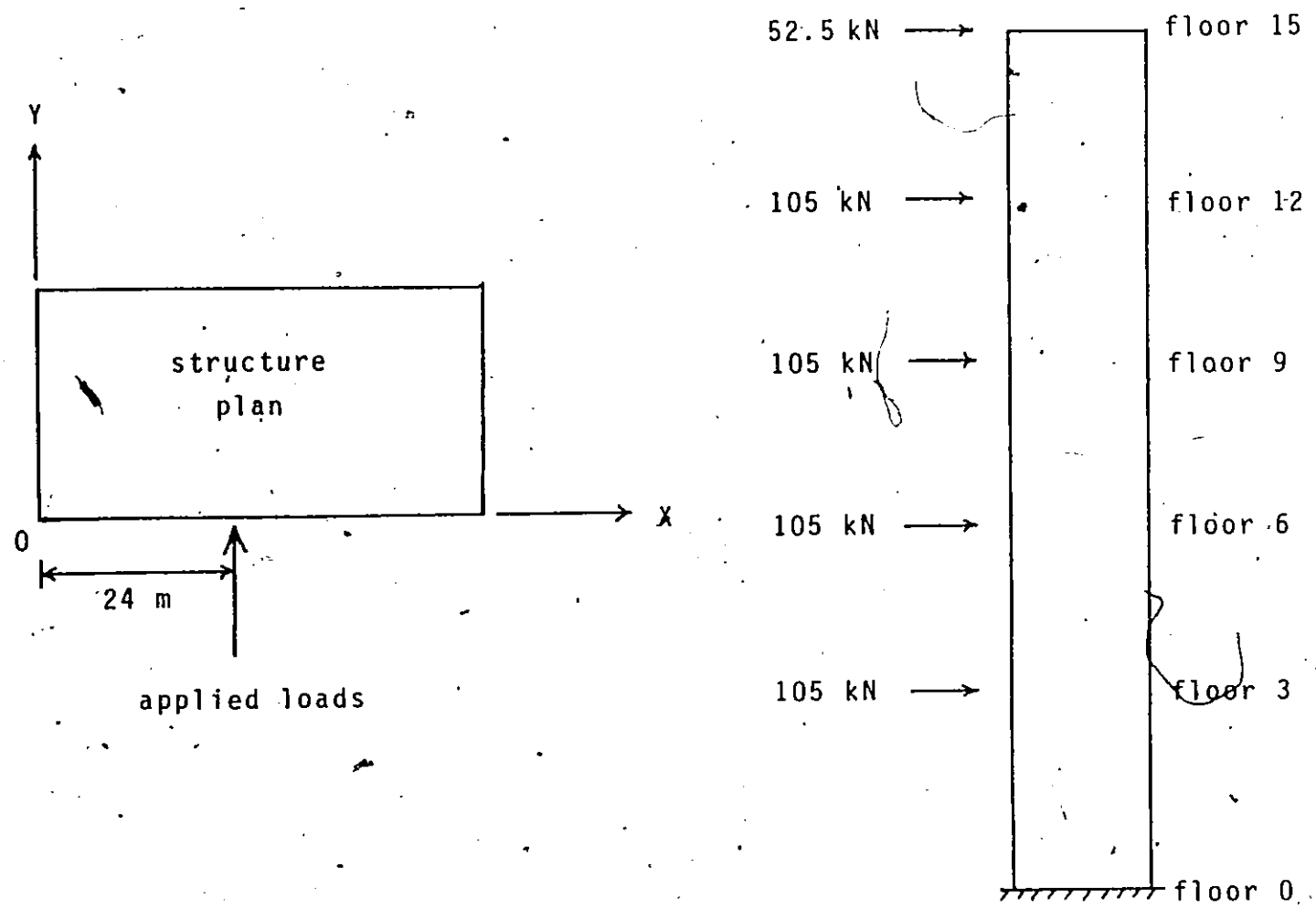

FIG. 6-5: LOADING CONDITIONS OF EXAMPLE STRUCTURE

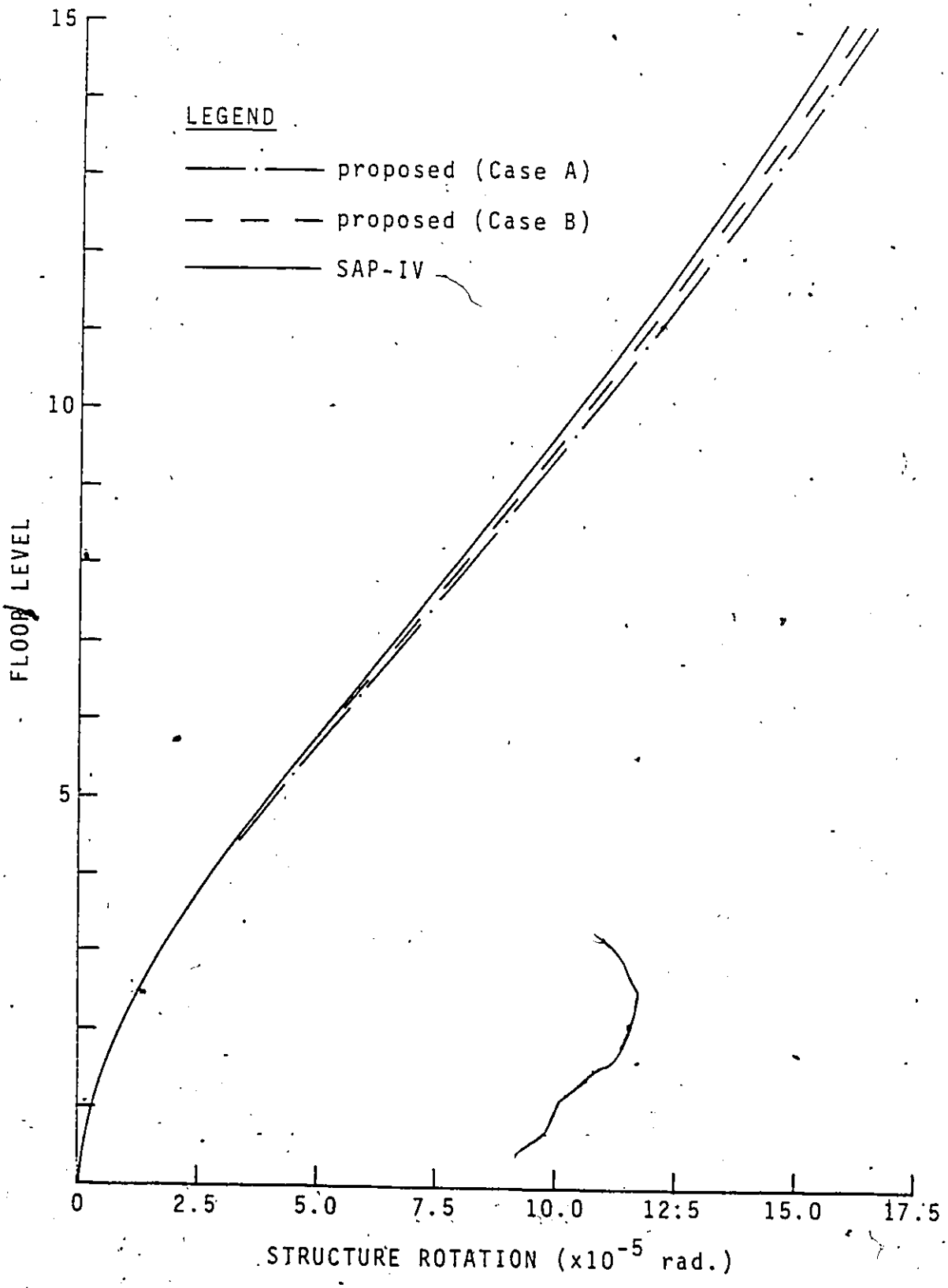

FIG. 6-6: ROTATION OF EXAMPLE STRUCTURE

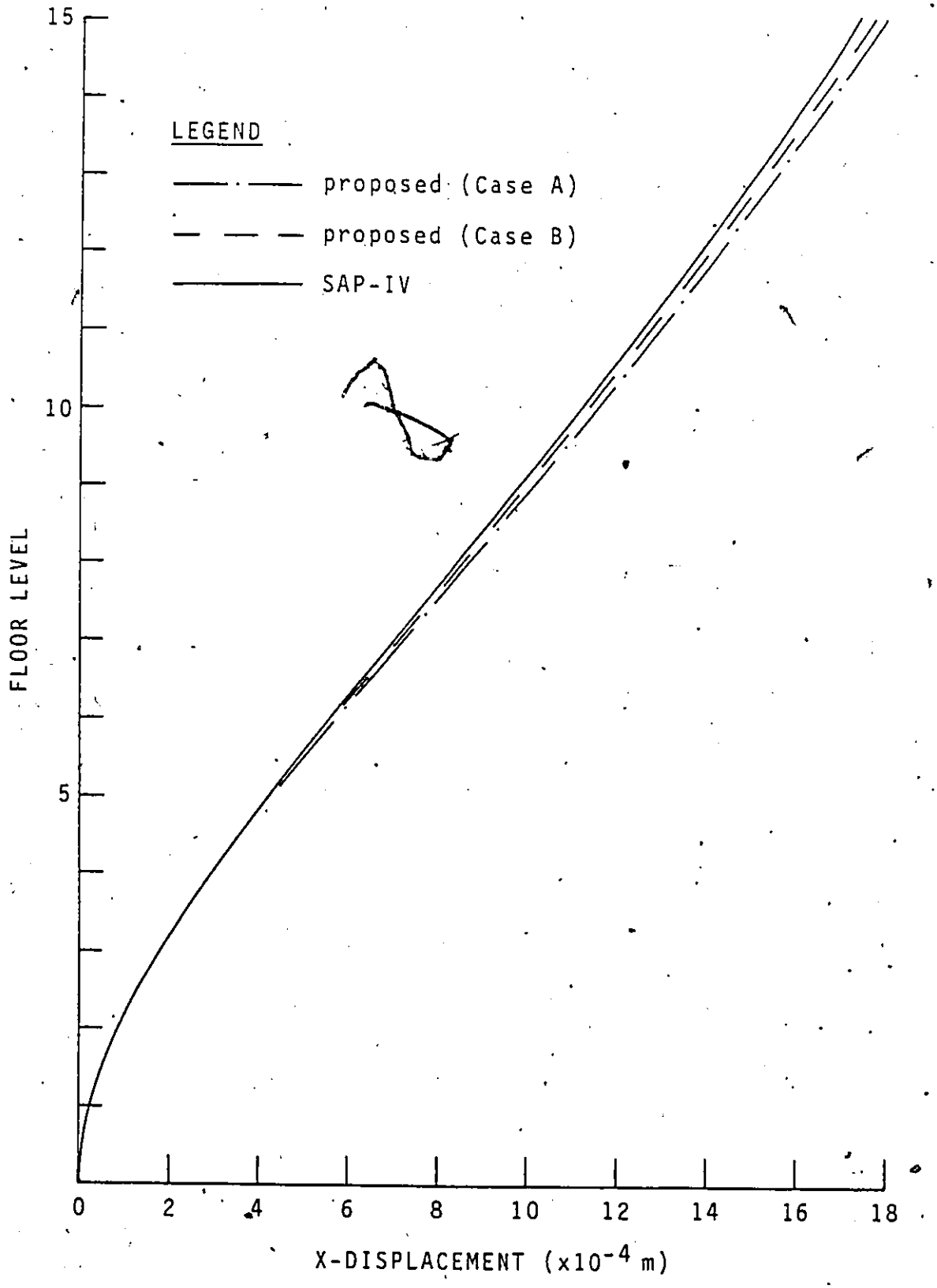

FIG. 6-7: X-DISPLACEMENT AT CENTROID OF WALL PIER 4

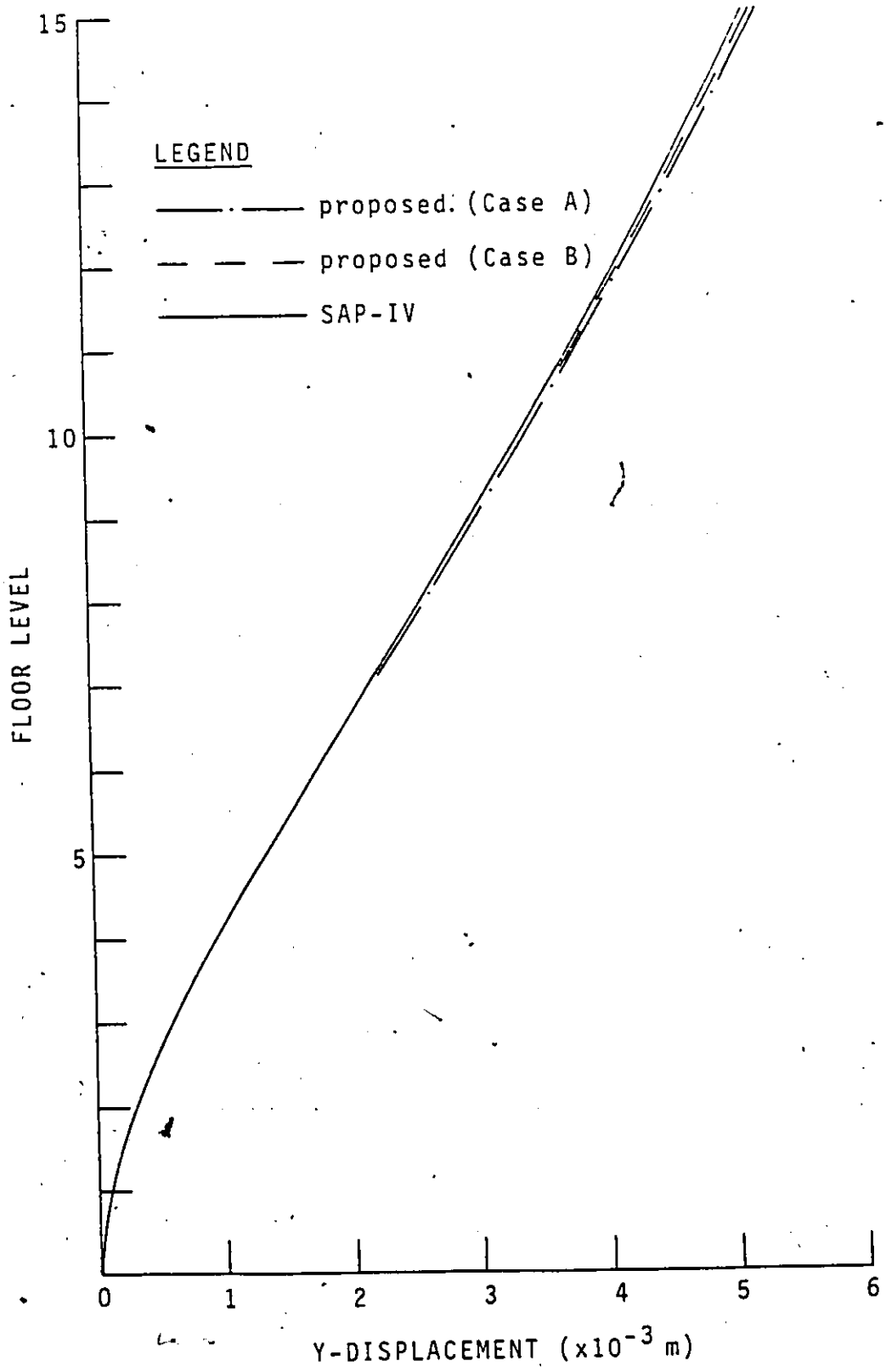

FIG. 6-8: Y-DISPLACEMENT AT CENTROID OF WALL PIER 4

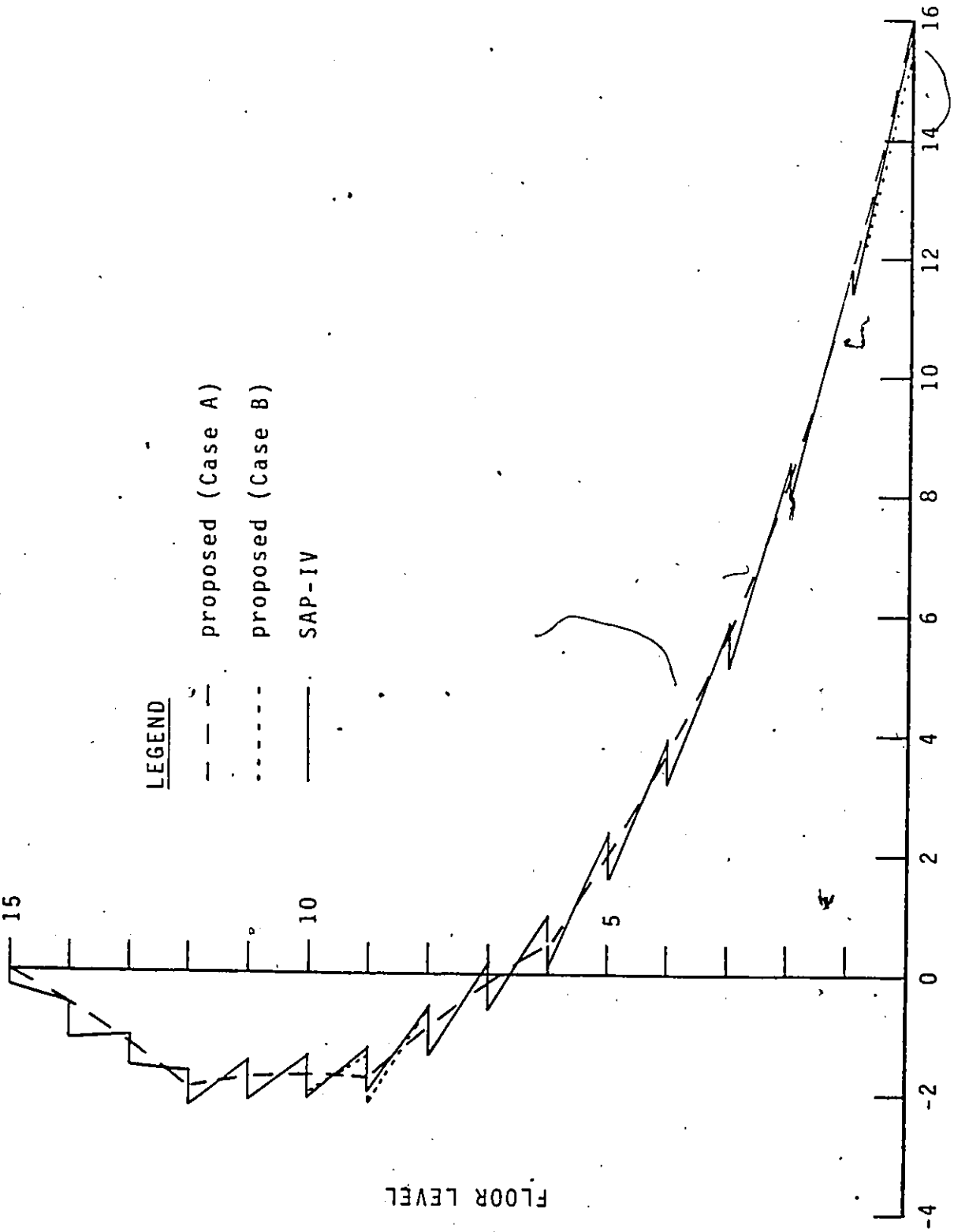

FIG. 6-9: INTERNAL MOMENT OF WALL PIER 3

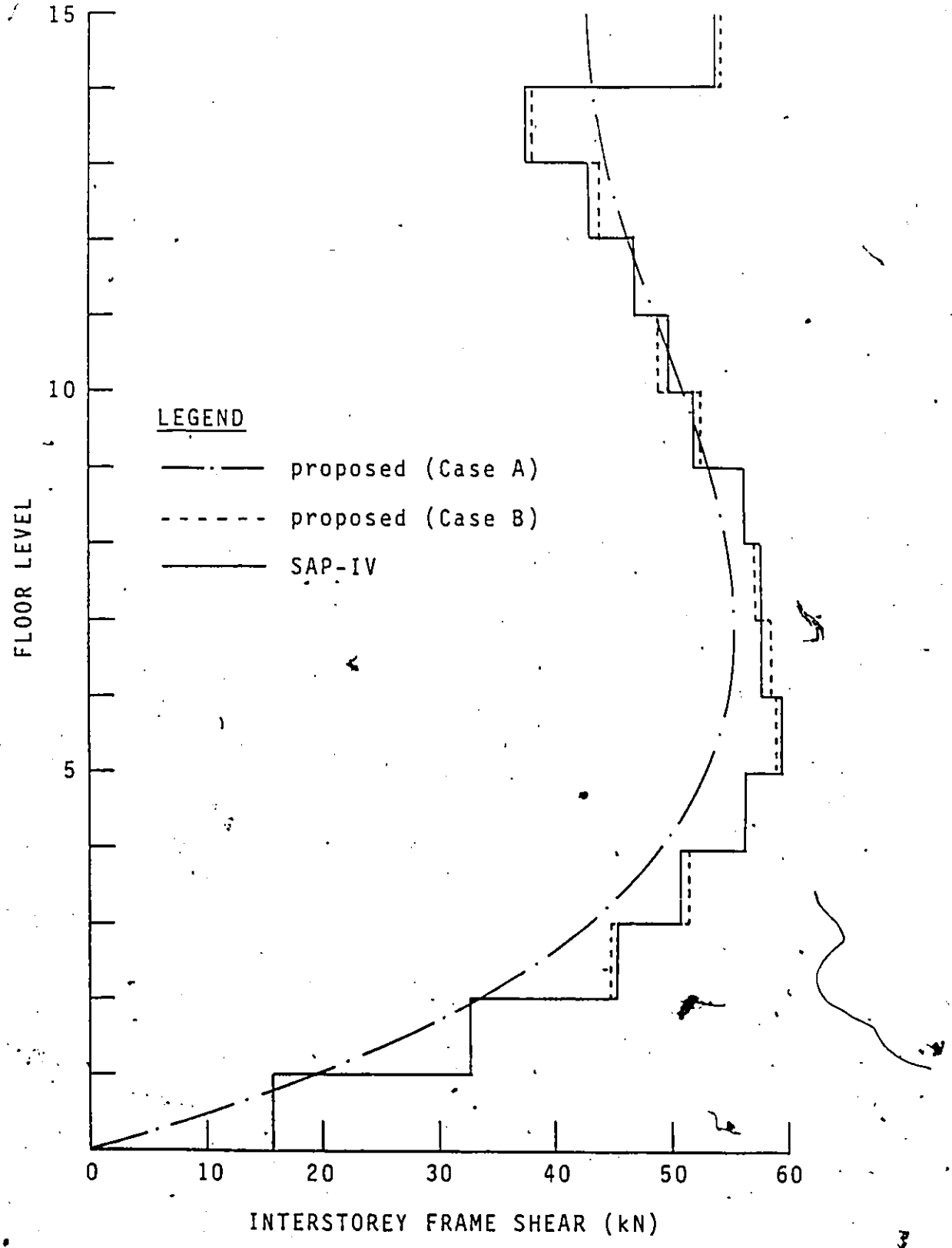

FIG. 6-10: INTERSTOREY SHEAR IN FRAME 2

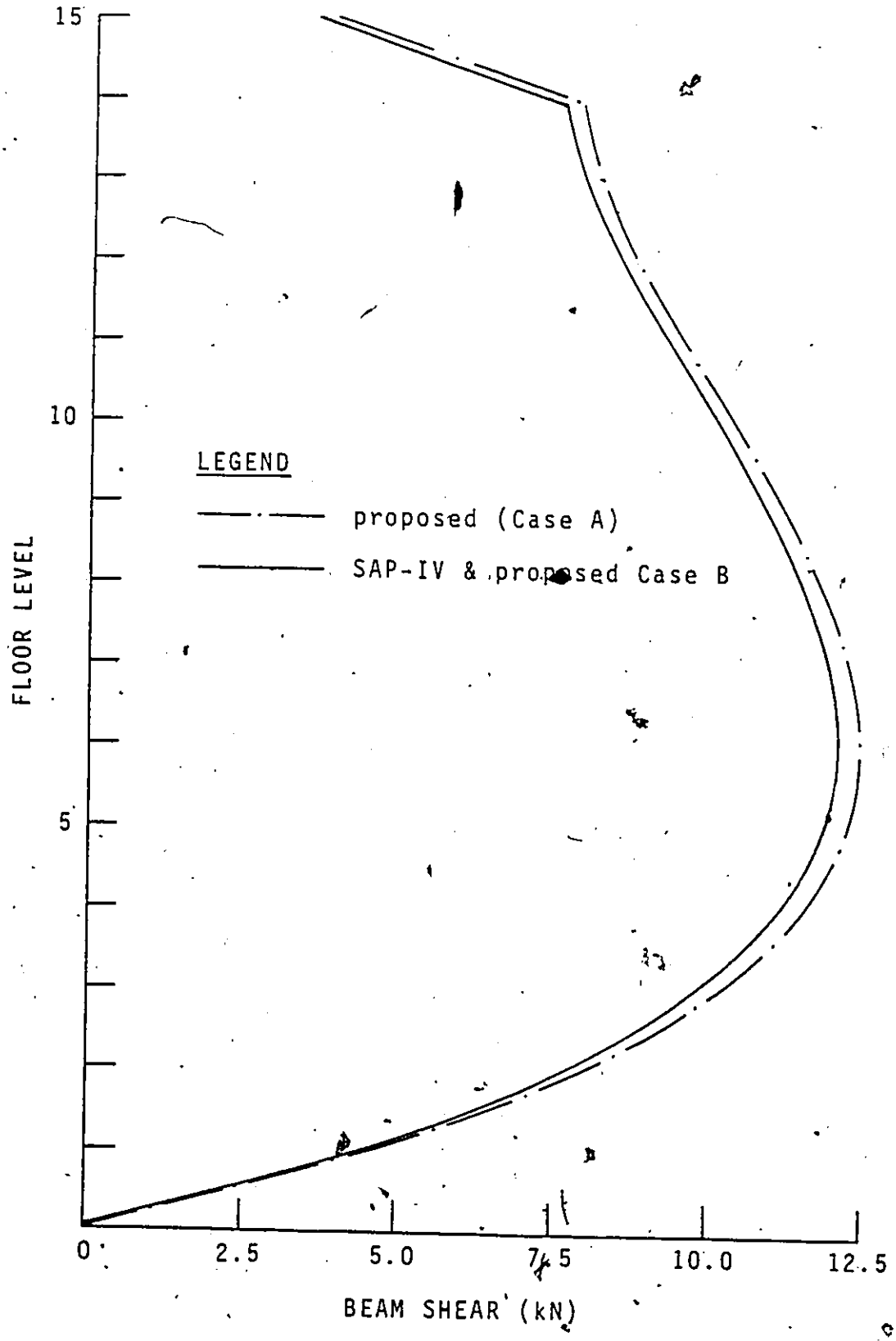

FIG. 6-11: SHEARS IN CONNECTING BEAM 4

CHAPTER VII

DYNAMIC MODELLING OF BUILDING STRUCTURES

7.1 INTRODUCTION

The dynamic response of multi-storey building structures to earthquake excitation is of increasing concern to the structural engineer. The dynamic behaviour of a three-dimensional building structure in general consists of three types of vibration modes, namely, two horizontal translational modes perpendicular to each other and a torsional mode about the vertical.

Equivalent static methods of estimating the dynamic response of building structures are usually provided in building codes, including the National Building Code of Canada(NBCC), 1977[45]. However, in view of the complexity of the three-dimensional dynamic behaviour of a multi-storey building structure, which so often possesses eccentric centres of mass and rigidity and hence invites modal coupling, such static methods may turn out to be grossly inadequate. Thus, a dynamic analysis becomes necessary.

A dynamic analysis can be undertaken according to

standard procedures[3], either by way of a continuous model wherein the mass of the building is assumed to be continuously distributed over the entire building height, or by way of a discrete model wherein the total building mass is divided up into a number of masses located at specified levels along the building height. By the latter so-called lumped-mass approach, the building is in effect idealised as a multi-degree-of-freedom system, the solution to which can be found with relative ease. Most of the published research work on the dynamic behaviour of building structures has been based on the lumped-mass idealisation [34, 42, 52, 59, 61, 66, 82].

In this chapter, the undamped free vibration response of a general three-dimensional building structure with a rigid foundation will be investigated using the lumped-mass approach. An attempt will then be made to obtain the natural frequencies of an actual building - the Banco de America - both before and after damage was sustained by the structure during the Managua, Nicaragua earthquake of December 23, 1972. In this study, the stiffness matrix for the structure is determined by the static analysis presented in Chapter VI. Results will be compared with those obtained analytically and experimentally by other researchers [53, 67].

7.2 NOTATIONS

The following notations will be used in this chapter:

C_m = centre of mass at level m (m = 1, 2, ... N).

I_m = mass moment of inertia of mass m about its own centre of mass.

$[K]$ = stiffness matrix of structure, with respect to horizontal displacements of reference point O along X and Y, and rotation about the vertical (size 3Nx3N).

$[M]$ = Mass matrix of structure (size 3Nx3N).

M_m = mass at level m.

N = number of lumped masses.

u_m, v_m = horizontal displacements of C_m in the X- and Y-directions, respectively.

x_m, y_m = co-ordinates of C_m in X-Y plane.

$\{\Delta\}$ = displacement vector (size 3N).

$\{\ddot{\Delta}\}$ = acceleration vector (size 3N).

ξ_m, η_m, θ_m = horizontal displacements of reference point O, along X and Y and rotation about the vertical at level m.

ω_m, $\{\phi\}_m$ = natural frequency and associated mode shape vector for m^{th} mode.

7.3 STATEMENT OF PROBLEM

A general three-dimensional multi-storey wall-frame building structure is considered. An arbitrary orthogonal co-ordinate system with origin O, horizontal axes X and Y, and vertical axis Z, is defined. The total mass of the structure is divided up into N lumped masses each of which is located at a discrete level (Figure 7-1). The centre of mass at level m, where m = 1, 2, ... N, is denoted by C_m and is located at (x_m, y_m) in the X-Y plane (Figure 7-2a). The motion of mass m is defined by the horizontal translational displacements of the reference point O in the X- and Y-directions — denoted by ξ_m and η_m respectively — and rotation θ_m about the vertical (Figure 7-2b). Thus, there are altogether 3N degrees of freedom for the total structure. The horizontal displacements of the centre of mass at level m, C_m, in the X- and Y-directions are denoted by u_m and v_m respectively. These are related to the displacements of O by the following relationships:

$$u_m = \xi_m - y_m\theta_m \qquad (7\text{-}1a)$$

$$v_m = \eta_m + x_m\theta_m \qquad (7\text{-}1b)$$

Using the static analysis proposed in Chapter V or VI, the flexibility matrix for the structure is determined

by successively applying unit lateral loads and torques, one at a time, at each of the N levels and finding the displacements and rotations at all levels. The corresponding stiffness matrix [K] can then be obtained by inverting the flexibility matrix.

In the following analysis, the structure is assumed to undergo free vibration without damping. Linearly elastic behaviour of the structure is also assumed.

7.4 EQUATION OF FREE VIBRATION AND SOLUTION

When the structure undergoes free vibration, mass m is subjected to horizontal inertial forces and an inertial torque as shown in Figure 7-3. These inertial effects are given by

$$F_{mx} = M_m \ddot{u}_m \tag{7-2a}$$

$$F_{my} = M_m \ddot{v}_m \tag{7-2b}$$

$$F_{m\theta} = I_m \ddot{\theta}_m \tag{7-2c}$$

where M_m is the mass at level m, I_m is the mass moment of inertia of M_m about C_m, F_{mx} and F_{my} are the inertial forces acting at C_m in the X- and Y-directions respectively, and $F_{m\theta}$ is the inertial torque about C_m.

These inertial effects are resisted by the internal forces and torques of the structure at the corresponding levels as shown in Figure 7-3. Letting P_{mx} and P_{my} be the internal forces acting at level m along the X- and Y-axes, respectively, and $P_{m\theta}$ be the internal torque about Z, these internal effects are given by

$$P_{mx} = \sum_{n=1}^{N} (K_{xx}^{mn} \xi_n + K_{xy}^{mn} \eta_n + K_{x\theta}^{mn} \theta_n) \tag{7-3a}$$

$$P_{my} = \sum_{n=1}^{N} (K_{yx}^{mn}\xi_n + K_{yy}^{mn}\eta_n + K_{y\theta}^{mn}\theta_n) \qquad (7\text{-}3b)$$

$$P_{m\theta} = \sum_{n=1}^{N} (K_{\theta x}^{mn}\xi_n + K_{\theta y}^{mn}\eta_n + K_{\theta\theta}^{mn}\theta_n) \qquad (7\text{-}3c)$$

where K_{xx}^{mn}, K_{xy}^{mn}, ... $K_{\theta\theta}^{mn}$ are the elements of the stiffness matrix [K] such that K_{xy}^{mn} is the force acting along X at level m due to a unit displacement along Y at level n, $K_{y\theta}^{mn}$ is the force along Y at level m due to a unit rotation at level n, and so forth. The stiffness matrix [K] is shown in details in Appendix J.

Considering the equilibrium of forces in the X- and Y-directions and torques about the Z-axis, and making use of Eqns(7-1a) and (7-1b), there can be obtained at the m^{th} level, where m = 1,2,...N,

$$M_m\ddot{\xi}_m - \bar{y}_m M_m\ddot{\theta}_m + \sum_{n=1}^{N} (K_{xx}^{mn}\xi_n + K_{xy}^{mn}\eta_n + K_{x\theta}^{mn}\theta_n) = 0 \qquad (7\text{-}4)$$

$$M_m\ddot{\eta}_m + \bar{x}_m M_m\ddot{\theta}_m + \sum_{n=1}^{N} (K_{yx}^{mn}\xi_n + K_{yy}^{mn}\eta_n + K_{y\theta}^{mn}\theta_n) = 0 \qquad (7\text{-}5)$$

$$-\bar{y}_m M_m\ddot{\xi}_m + \bar{x}_m M_m\ddot{\eta}_m + I_m^*\ddot{\theta}_m + \sum_{n=1}^{N} (K_{\theta x}^{mn}\xi_n + K_{\theta y}^{mn}\eta_n + K_{\theta\theta}^{mn}\theta_n) = 0 \qquad (7\text{-}6)$$

where $I_m^* = I_m + M_m (x_m^2 + y_m^2)$ (7-6a)

The above three equations of equilibrium can be written in matrix form as follows:

$$[M]\{\ddot{\Delta}\} + [K]\{\Delta\} = \{0\} \tag{7-7}$$

where [M] and [K] are the mass matrix and the stiffness matrix, respectively, of the structure, $\{\ddot{\Delta}\}$ and $\{\Delta\}$ are the acceleration and displacement vectors, respectively, such that

$$\{\Delta\} = \text{col.}\{ \xi_1 \ \eta_1 \ \theta_1 \ \xi_2 \ \eta_2 \ \theta_2 \ \cdots \ \xi_N \ \eta_N \ \theta_N \} \tag{7-7a}$$

$$\{\ddot{\Delta}\} = \text{col.}\{ \ddot{\xi}_1 \ \ddot{\eta}_1 \ \ddot{\theta}_1 \ \ddot{\xi}_2 \ \ddot{\eta}_2 \ \ddot{\theta}_2 \ \cdots \ \ddot{\xi}_N \ \ddot{\eta}_N \ \ddot{\theta}_N \} \tag{7-7b}$$

and $\{0\}$ is a null vector of order 3N. The mass matrix [M] is shown in details in Appendix K.

Eqn(7-7) is the equation of undamped free vibration for the structure. The undamped natural frequencies of vibration and the associated mode shapes can be determined from the solution to the equation. To this end, the solution to Eqn(7-7) is assumed to be of the following form:

$$\{\Delta\} = \{\phi\} \cdot \sin(\omega t) \tag{7-8a}$$

Therefore,

$$\{\ddot{\Delta}\} = -\omega^2 \{\phi\} \cdot \sin(\omega t) \qquad (7\text{-}8b)$$

Substituting Eqns(7-8a) and (7-8b) into Eqn(7-7), the following eigen-value problem is obtained:

$$\left(-\omega^2 [I] + [M]^{-1}[K] \right) \{\phi\} = \{0\} \qquad (7\text{-}9)$$

where [I] is a 3N x 3N identity matrix.

Solving the eigen-value problem will give rise to 3N natural frequencies ($\omega_1, \omega_2, \ldots \omega_{3N}$) and the associated mode shapes ($\{\phi\}_1, \{\phi\}_2, \ldots \{\phi\}_{3N}$).

7.5 DYNAMIC MODELLING OF THE BANCO DE AMERICA BUILDING

Structural damage was sustained by the Banco de America Building during the Managua, Nicaragua earthquake of December 23, 1972. A model study for the evaluation of the dynamic characteristics of the structure both before and after damage was incurred will be presented in the following.

7.5.1 DESCRIPTION OF BUILDING

The Banco de America Building is an 18-storey reinforced concrete wall-frame structure of height 68.65 m (225 ft) above ground and comprised of a central core of four wall piers and narrowly spaced peripheral columns (Figure 7-4). The wall piers are connected by pairs of lintel beams while the columns are connected via the floor slabs only. A complete description of the structural details of the building has been given by Sozen and Shibata [67]. Damage suffered by the building was light in general [64]. While some diagonal cracking was observed in the wall piers, most of the damage was sustained by the lintel beams. A simplified description of the lintel beam damage is shown in Table 7-1.

7.5.2 MODELLING OF BUILDING

A rigid foundation is assumed at the ground level,

thereby neglecting the effect of the basement floors. Steel reinforcement is neglected. The configuration of the wall piers in the top floor is taken to be the same as that in the typical floor. In order to allow for structural non-uniformity along the height of the building, the total structure is divided into six segments (Figure 7-5). The various structural properties pertaining to the building model as used in the present study are given in Table 7-2. It should be noted that in order to account for, approximately, the effect of finite joint size for the equivalent "edge" beams of the peripheral columns, the moment of inertias as obtained by Sozen and Shibata [67] for these beams have been modified by a factor of 6.54, which is the ratio of the centre to centre length to the clear span length for the "edge" beams raised to the third power.

Assuming a unit weight of 23.6 kN/m^3 (150 pcf) for concrete, the mass and polar mass of inertia per typical storey of the building are estimated to be 5.48×10^5 $N\text{-}sec^2/m$ and 2.36×10^8 $Nm\ sec^2$ respectively. The total mass and polar mass of inertia of the building are equally lumped at floor levels 2, 5, 8, 11, 14, and 17 (Figure 7-5). The mass centres for all six lumped masses are taken to be located at the centre of the building plan.

In simulating the damaged condition of the building, the stiffness of the lintel beams is the most critical factor.

Based on the observations noted in Table 7-1, two damage zones are identified for the lintel beams, with damage zone I extending from floor levels 1 through 8 and damage zone II from floor levels 9 through 18. Within each zone, a constant rate of damage is assumed for all beams. Six models will first be considered: Model 1 pertains to the undamaged condition of the building while Models 2, 3, 4, 5, and 6 assume varying degrees of damage in the lintel beams. The relative stiffness of the lintel beams for these various models are given in Table 7-3. For each model, the static method of analysis proposed in Chapter VI is used to form the stiffness matrix [K] for the total structure. The peripheral columns with the equivalent edge beams formed from the floor slabs are treated as four plane frame macro-elements for all models. Vertical compatibility is therefore ignored at the corner columns. The central wall core is treated as one three-dimensional coupled shear wall macro-element for Models 2, 3, 4, and 5, and as four non-planar cantilever wall macro-elements for Model 6.

7.5.3 RESULTS AND DISCUSSION

Owing to the fact that the structure being studied is symmetric about the north-south direction and exhibits very little asymmetry about the other, the frequencies for each of the three modes of vibration, namely, the north-south and east-

west translational modes and the torsional mode, can be identified readily for all models. In fact, results do show light modal coupling between the east-west translational and the torsional modes only. As an illustration, the mode shapes for the first six modes are shown in Figure 7-6. The computed frequencies and the corresponding frequency ratios for the various models are shown in Tables 7-4 through 7-6. The typical frequency ratios for uniform wall structures and uniform frame structures are shown in Table 7-7 for reference.

Results for the north-south translational mode for Model 1 are compared with those obtained via a two-dimensional model study by Sozen and Shibata [67] in Table 7-8. Close agreement can be observed in the frequency ratios despite the relatively large apparent discrepancies in the frequency values. This should lend sufficient credibility to the validity of the basic structural model used in the present model study.

Models 2 through 6 are intended to provide an approximate simulation of the damaged condition of the Banco de America Building. Field data obtained by Rojahn [53] after the earthquake are presented as shown in Table 7-9 for comparison. Considering Tables 7-4 through 7-9, the following observations can be drawn:

(1) The field results indicate the predominance of frame

action in the dynamic response of the damaged structure where as results of the model study indicate the predominance of cantilever wall action.

(2) The field results reveal a much less stiff structure after damage than is indicated by any of the simulated models.

(3) The torsional frequencies are found to be higher than the translational frequencies for the field results whereas the opposite is true for the computed results.

(4) It appears that from considerations of both frequency values and frequency ratios, Models 1 and 4 give the best simulated damage with respect to the torsional vibration mode and the translational vibration modes, respectively.

Generally, it can be noted that the computed results for the dynamic models, which allow for varying degrees of lintel beam damage, deviate significantly from the field results. However, the very possibility of inevitable discrepancies between the structural and mass characteristics assumed for the basic mathematical model being used in this study and those of the actual building must be recognised. The extreme difficulty of quantifying the actual structural damage suffered by the building must also be reckoned with. Nevertheless, observa-

tions (1) and (2) tend to show that other significant damage exists in the building — especially in the wall piers — in addition to the lintel beam damage allowed for by the simulated models. In fact, some damage in the walls and the floor slabs between the peripheral columns has been reported [64]. However, it is felt that information regarding such damage is too scarce to permit a reasonably realistic and useful assumption of the extent of the damage. Finally, observations (3) and (4) tend to show that the actual lintel beam damages are such that their softening effect on the torsional vibration of the structure is less than that on its translational vibration.

7.6 CONCLUSION

The undamped free vibration response of a general three-dimensional multi-storey building structure has been investigated. Based on the analysis, a model study has been conducted on the Banco de America Building. In this study, the stiffness matrix for the total structure is determined by the static method of analysis proposed in Chapter VI. The wall core is analysed by the continuum approach while the peripheral frames are analysed by the stiffness matrix method of analysis. The results of the model study have been compared with those obtained analytically and experimentally by other researchers [53, 67]. Discrepancies between the results of the model study and the field results have also been discussed. The primary purpose of this model study is to show the use and limitations of analytical techniques in studying the dynamic behaviour of real structures.

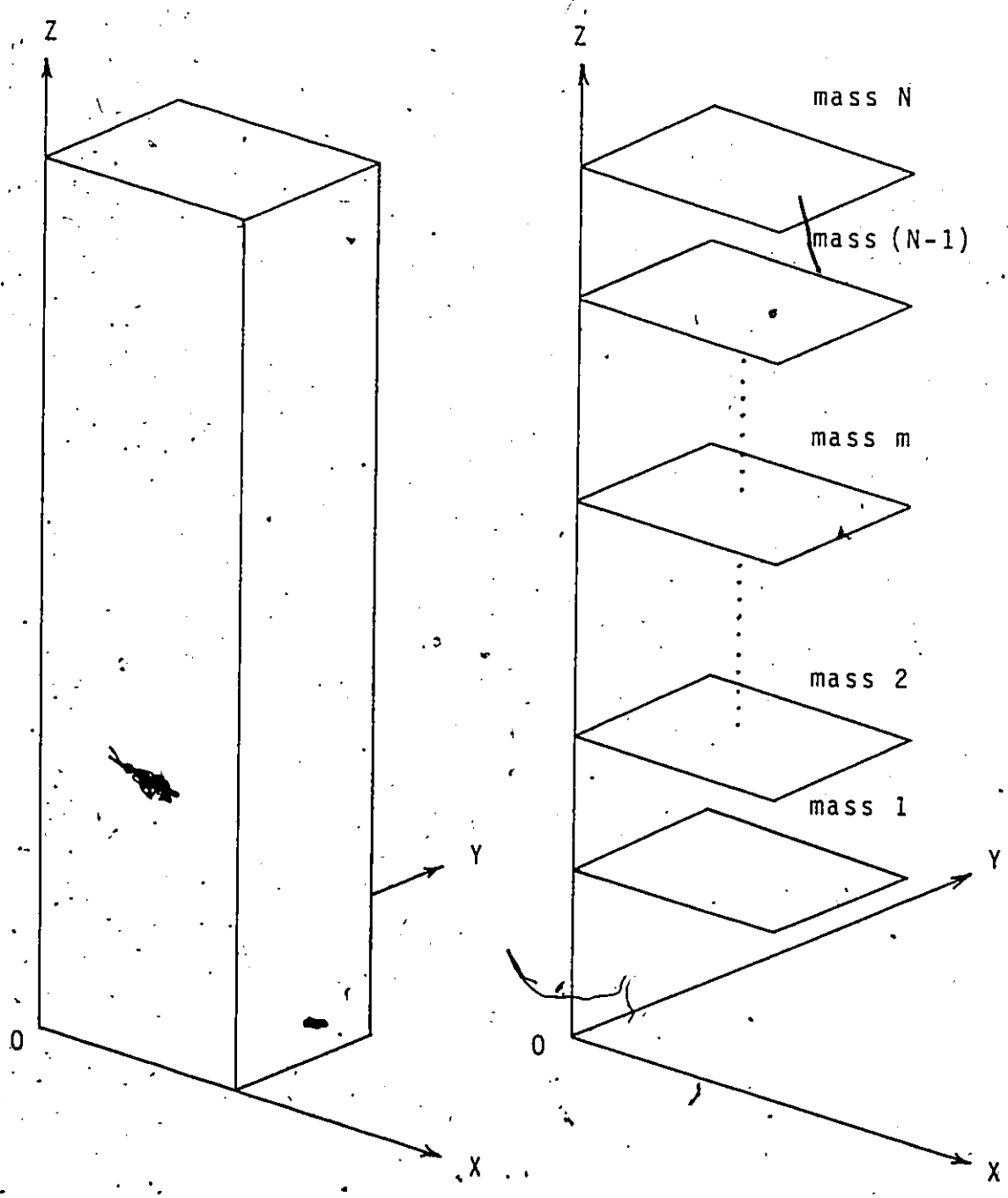

(a) actual structure (b) idealised model

FIG. 7-1: LUMPED MASS IDEALISATION OF STRUCTURE

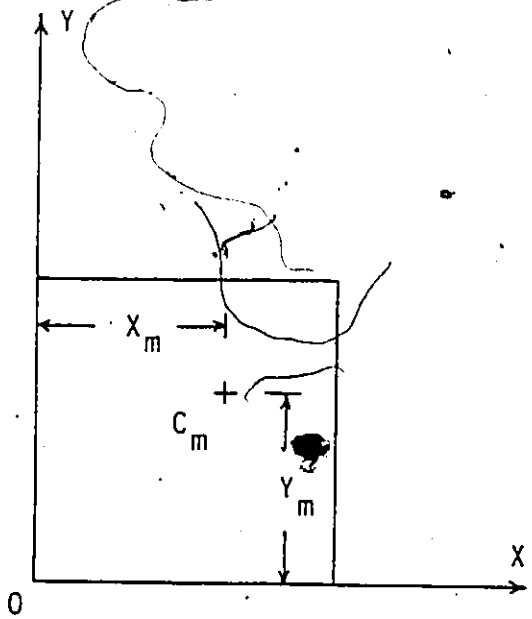

FIG. 7-2a: MASS CENTRE

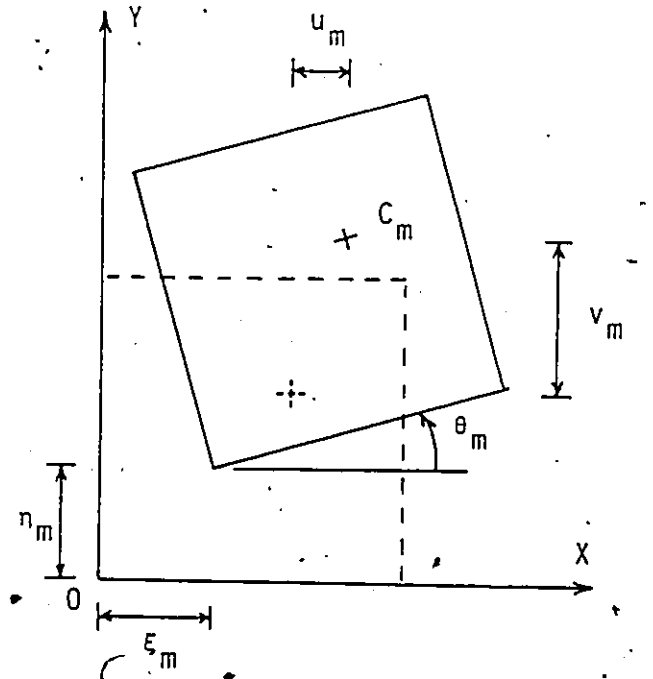

FIG. 7-2b: DEGREES OF FREEDOM FOR MASS m

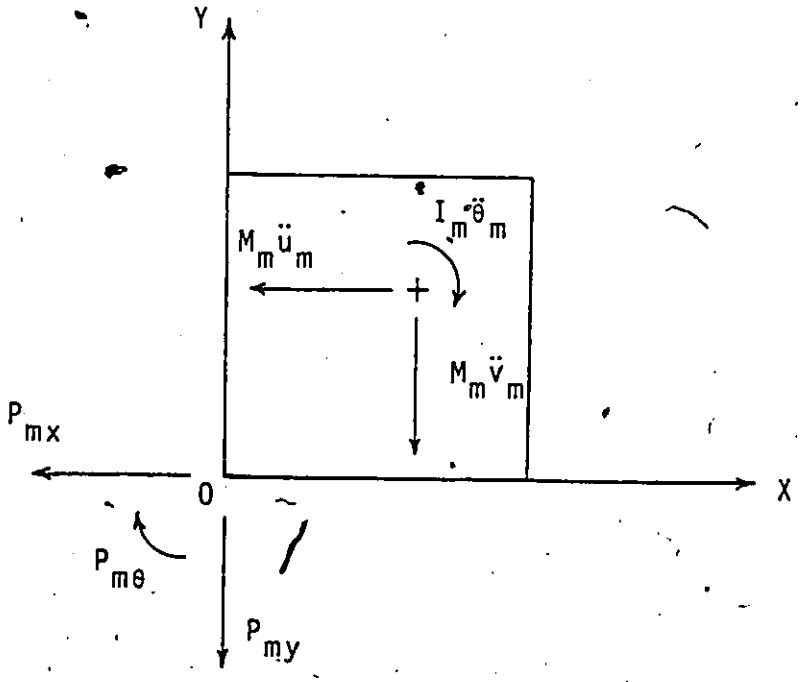

FIG. 7-3: FORCES AND TORQUES ACTING ON MASS m

(NOTE: all units in metres)

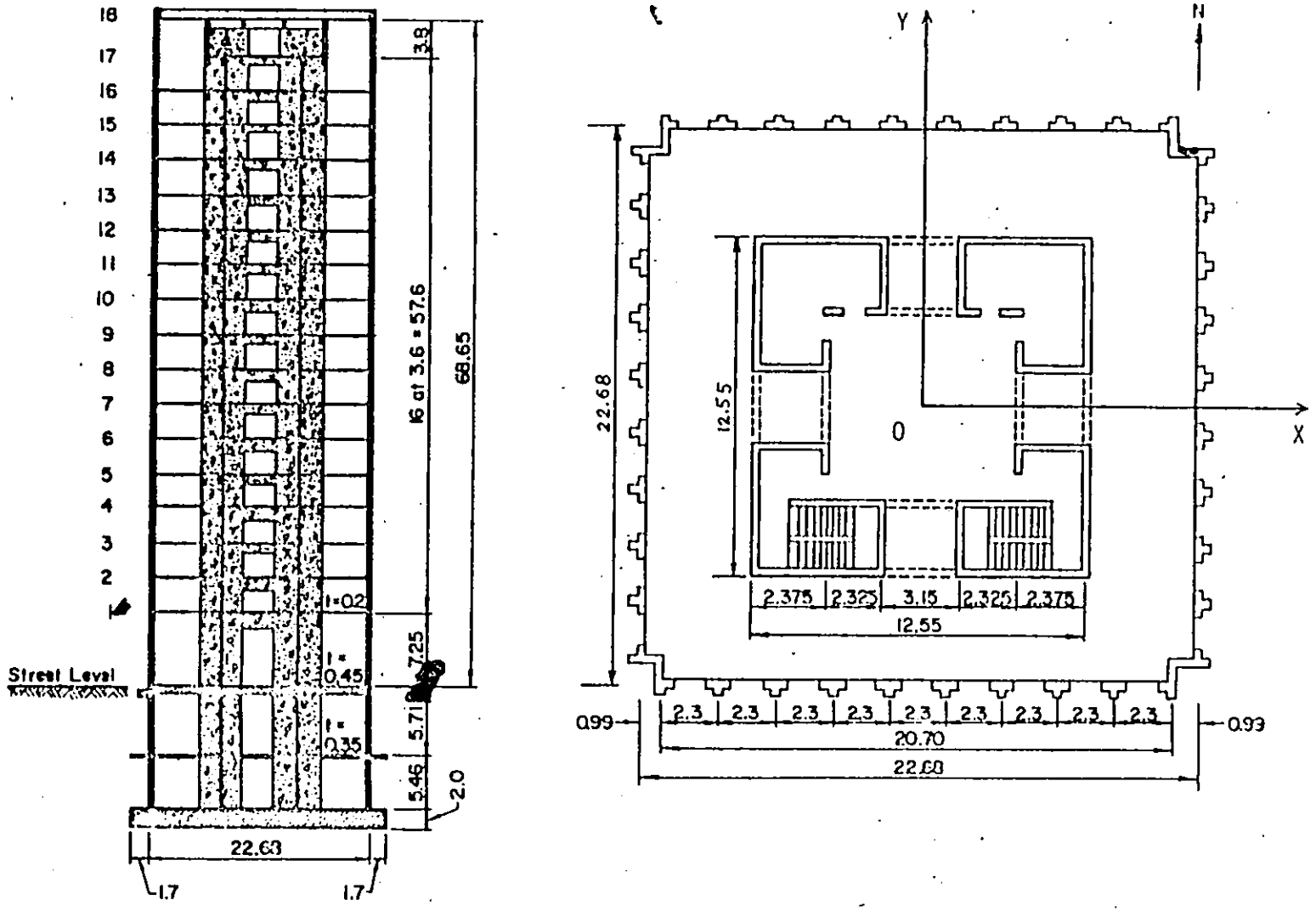

(a) ELEVATION

(b) PLAN

FIG. 7-4: BANCO DE AMERICA BUILDING [67]

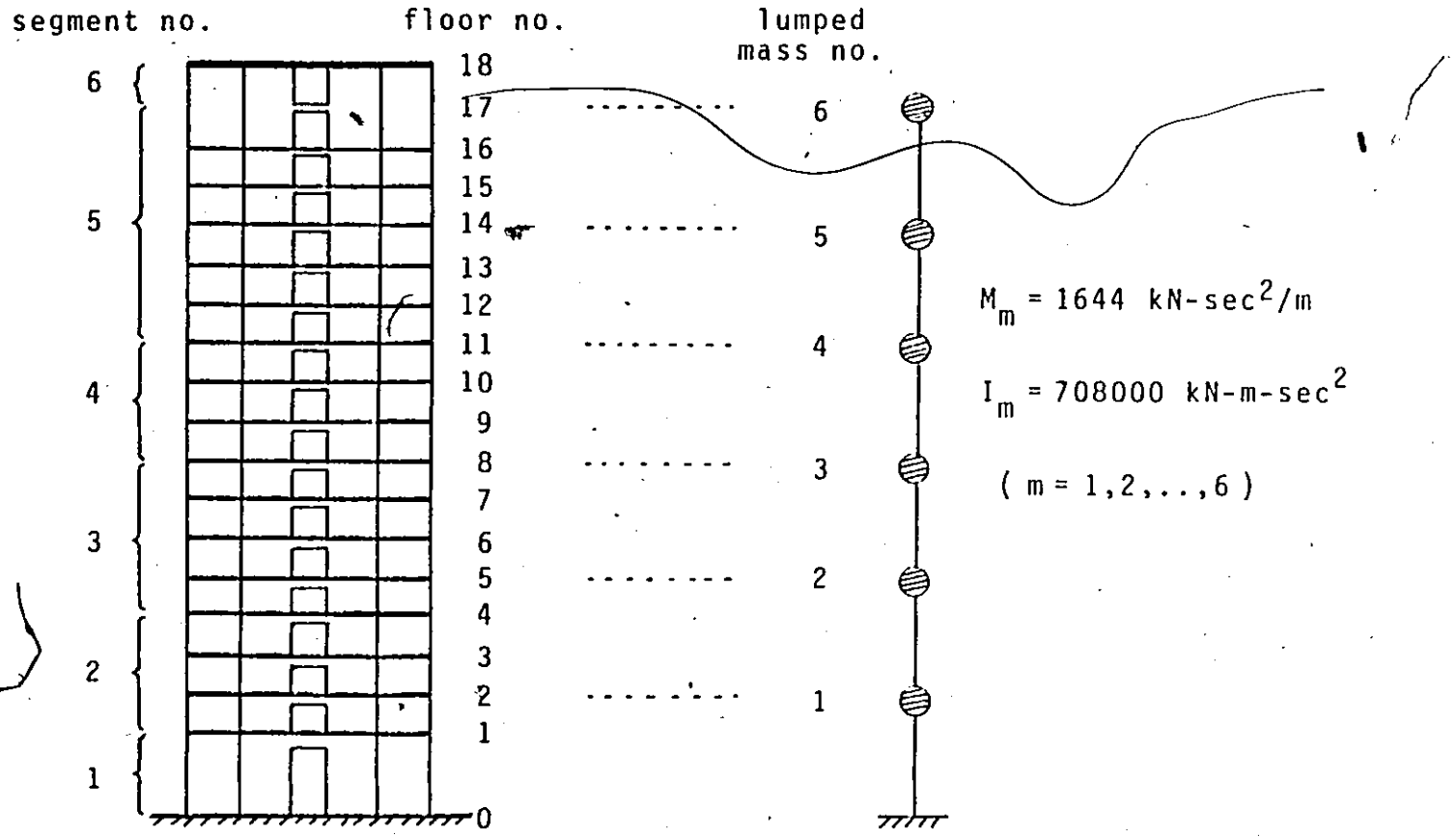

FIG. 7-5: DYNAMIC MODEL OF BANCO DE AMERICA

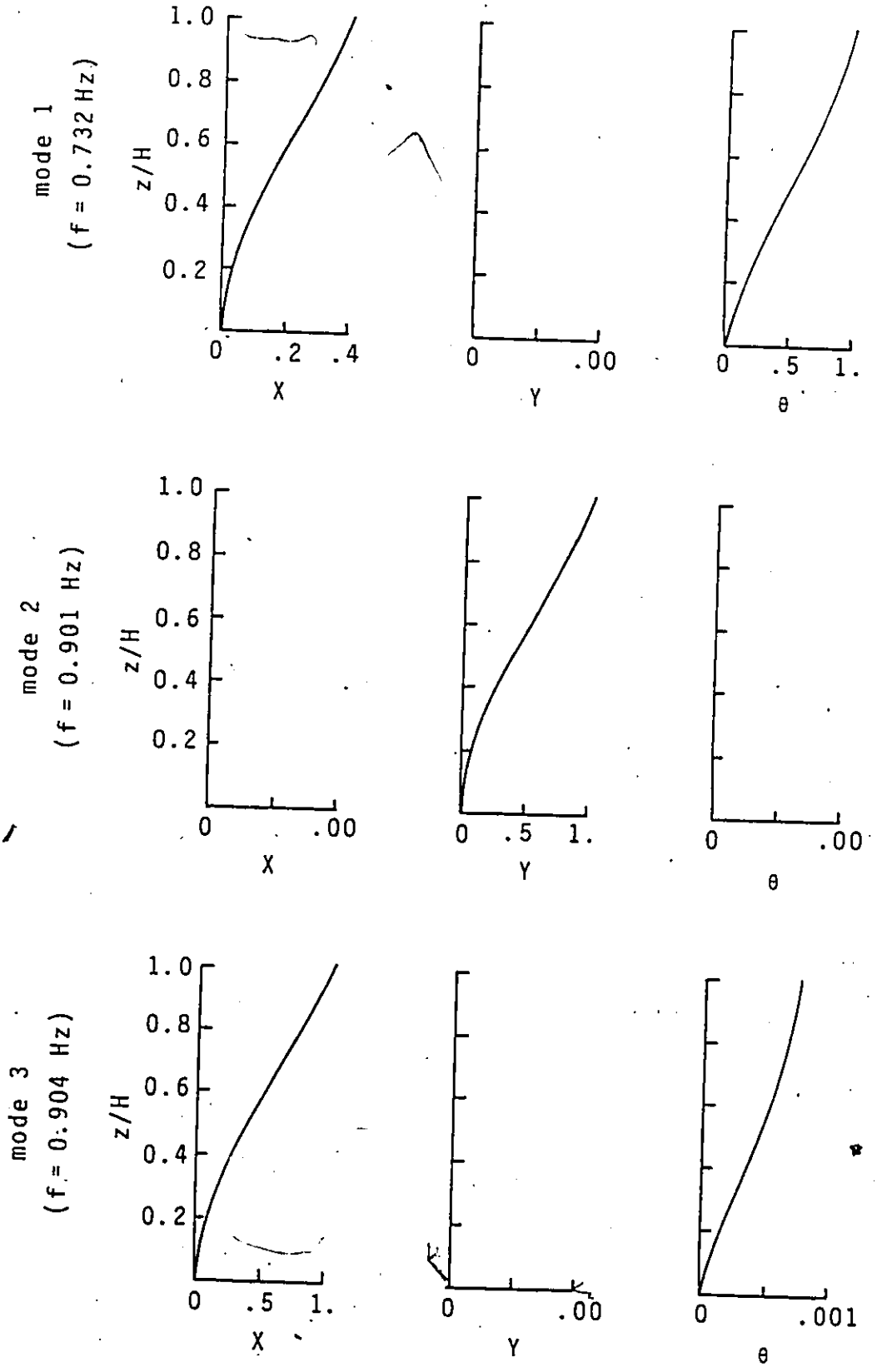

FIG. 7-6: NORMALISED MODE SHAPES FOR FIRST SIX MODES

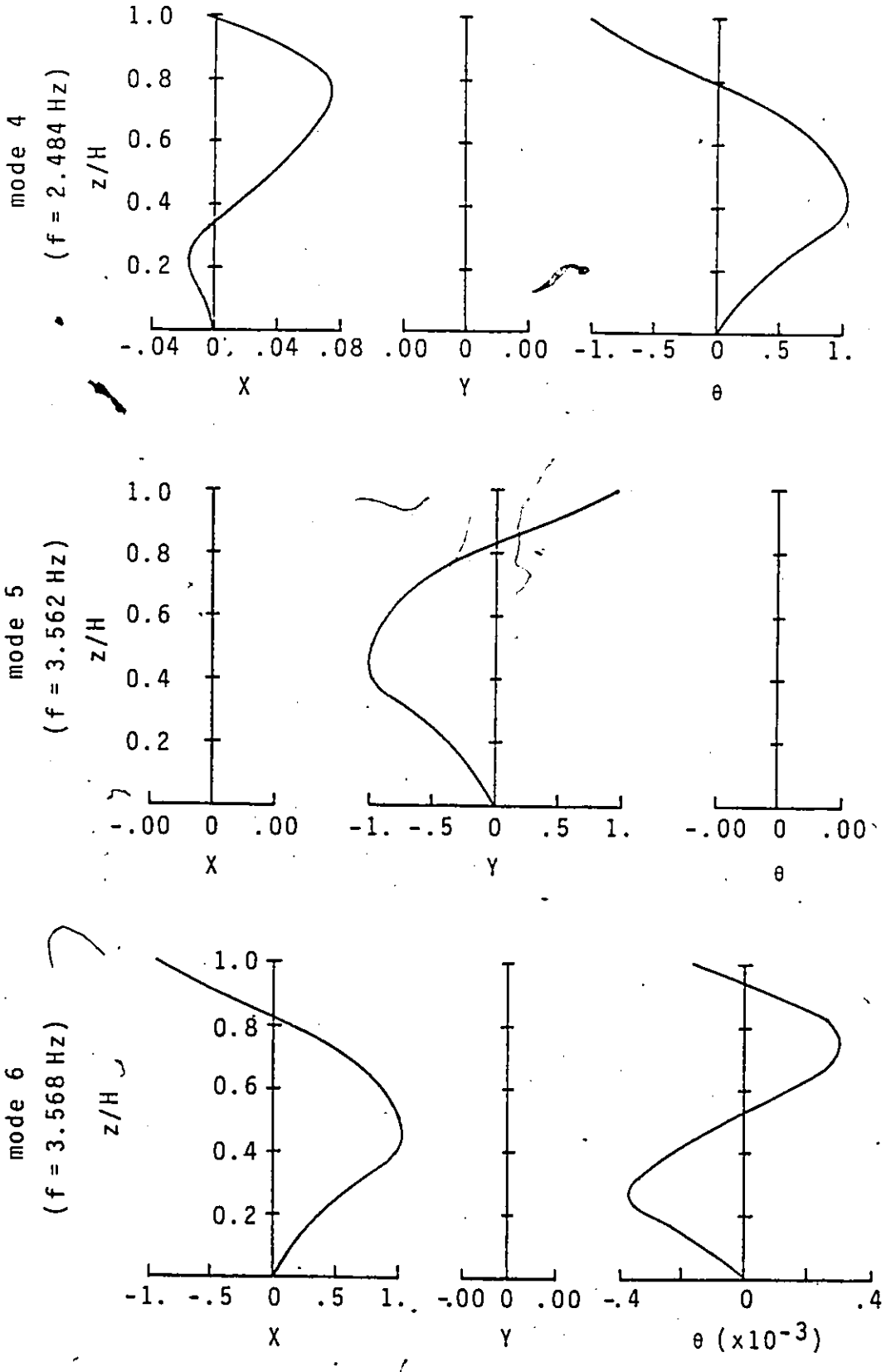

(FIG. 7-6 CONTINUED)

FLOOR	N.		E.		S.		W.	
	I	O	I	O	I	O	I	O
ROOF	NC	LXC TFB	NC	NC TFB	NC	LXC TFB	NC	LXC TFB
P	HXC	HXC TFA	NC	NC TFA	HXC	HXC TFA	HXC	XC TFA
17	CO	CO	NC	NC	CO	CO	LC	LC
16	HXC	CO	LC	LC BF	CO	CO	XC	XC
15	CO	CO	LC	XC	CO	CO	XC	XC
14	CO	CO	LC	LC	CO	CO	SCH	SCH
13	CO	CO	NC	SCH	CO	CO	XC	HXC
12	CO	CO	N/O	HXC	CO	CO	XC	XC
11	CO	CO	XC	XC	CO	CO	XC	HXC
10	CO	CO	HXC	HXC	CO	CO	XC	CO
9	CO	CO	N/O	CO	CO	CO	XC	CO
8	CO	CO	XC	CO	CO	CO	SCH	SCH
7	CO	CO	XC	XC	CO	CO	XC	XC
6	CO	CO	NC	NC	CO	CO	NC	N/O
5	CO	CO	NC TF	LC TF	CO	CO	NDT NC	NDT NC
4	CO	CO	NC	NC	CO	CO	NDT NC	NDT NC
3	NDT XC	NDT XC	NDT NC	NDT NC	NDT XC	NDT XC	NDT NC	NDT NC
2	N/O	N/O	N/O	N/O	N/O	N/O	N/O	N/O

Legend:

1. N/O - not observable
2. NDT - no duct
3. XC - X cracking below hole
4. NC - no cracking
5. CO - concrete out below hole
6. LC - light cracking below hole
7. LXC - light X cracking
8. TF - tile filler wall present below
9. SCH - shear crack below hole
10. HXC - heavy X crack below hole
11. BF - brick filler wall
12. TFB - tile filler below
13. TFA - tile filler above

TABLE 7-1: DESCRIPTION OF LINTEL BEAM DAMAGE [64]

TABLE 7-2: STRUCTURAL PROPERTIES OF BUILDING MODEL

segment number		1	2	3	4	5	6
storey numbers		1	2-4	5-8	9-11	12-17	18
storey height		7.25m	3.60m	3.60m	3.60m	3.60m	3.80m
wall thickness*		30cm	30cm	25cm	25cm	20cm	20cm
I of lintels ($\times 10^{-2} m^4$)	out.	8.44	1.82	1.52	1.52	1.52	6.66
	in.	7.03	1.52	1.52	1.52	1.22	4.44
edge columns	I**	$0.0258\ m^4$					
	A**	$0.33\ m^2$					
corner columns	I	$0.1720\ m^4$					
	A	$0.8875\ m^2$					
I@ of "edge" beams		$0.005 m^4$ for st.1-16, zero for st.17					$1.12 m^4$
Young's modulus		$24{,}900{,}000\ N/m^2$					

* assumed constant for all wall elements in a given storey

** assumed constant for all storeys

@ modified by a factor of 6.54 to account for effects of finite joint size

TABLE 7-3: RELATIVE STIFFNESSES OF LINTEL BEAMS

MODEL	DAMAGE ZONE I	DAMAGE ZONE II
1	1.00	1.00
2	0.50	0.50
3	0.10	0.10
4	0.50	0.01
5	0.10	0.01
6	0	0

TABLE 7-4: NATURAL FREQUENCIES (HZ) AND FREQUENCY RATIOS OF DYNAMIC MODELS – NORTH-SOUTH TRANSLATION

		mode 1	mode 2	mode 3	mode 4	mode 5
model 1	f[@]	0.901	3.562	7.969	13.948	20.993
	r[#]	1.000	3.953	8.845	15.481	23.300
model 2	f	0.842	3.288	7.428	13.323	20.372
	r	1.000	3.905	8.822	15.823	24.195
model 3	f	0.710	2.841	6.692	12.557	19.687
	r	1.000	4.001	9.425	17.686	27.728
model 4	f	0.735	2.793	6.677	12.666	19.783
	r	1.000	3.800	9.084	17.233	26.916
model 5	f	0.658	2.666	6.482	12.389	19.544
	r	1.000	4.052	9.851	18.828	29.702
model 6	f	0.615	2.593	6.392	12.277	19.449
	r	1.000	4.216	10.393	19.963	31.624

[@] natural frequencies in Hz

[#] frequency ratios

TABLE 7-5: NATURAL FREQUENCIES (HZ) AND FREQUENCY RATIOS OF DYNAMIC MODELS — EAST-WEST TRANSLATION

		mode 1	mode 2	mode 3	mode 4	mode 5
model 1	f[@]	0.904	3.568	7.969	13.929	20.945
	r[#]	1.000	3.947	8.815	15.408	23.169
model 2	f	0.844	3.290	7.421	13.294	20.324
	r	1.000	3.898	8.793	15.751	24.081
model 3	f	0.711	2.838	6.677	12.518	19.608
	r	1.000	3.992	9.391	17.606	27.578
model 4	f	0.736	2.790	6.659	12.627	19.719
	r	1.000	3.791	9.048	17.156	26.792
model 5	f	0.657	2.659	6.462	12.344	19.465
	r	1.000	4.047	9.836	18.788	29.627
model 6	f	0.614	2.585	6.369	12.233	19.369
	r	1.000	4.210	10.373	19.923	31.546

[@] natural frequencies in Hz

[#] frequency ratios

TABLE 7-6: NATURAL FREQUENCIES (HZ) AND FREQUENCY RATIOS OF DYNAMIC MODELS – TORSION

		mode 1	mode 2	mode 3	mode 4	mode 5
model 1	f@	0.732	2.484	4.991	8.446	12.497
	r#	1.000	3.393	6.818	11.538	17.072
model 2	f	0.625	2.200	4.593	8.023	12.112
	r	1.000	3.520	7.349	12.837	19.379
model 3	f	0.487	1.826	4.097	7.522	11.680
	r	1.000	3.749	8.413	15.446	23.984
model 4	f	0.511	1.795	4.080	7.589	11.738
	r	1.000	3.513	7.984	14.851	22.971
model 5	f	0.456	1.716	3.969	7.418	11.596
	r	1.000	3.763	8.704	16.268	25.430
model 6	f	0.433	1.675	3.918	7.355	11.544
	r	1.000	3.868	9.048	16.986	26.661

@ natural frequencies in Hz

frequency ratios

TABLE 7-7: TYPICAL FREQUENCY RATIOS

	mode 1	mode 2	mode 3	mode 4
uniform wall structure	1.00	6.25	16.67	33.33
uniform frame structure	1.00	3.03	5.00	7.14

TABLE 7-8: NORTH-SOUTH TRANSLATIONAL FREQUENCIES OF MODEL 1 VERSUS SOZEN'S RESULTS ("MODEL A")

		mode 1	mode 2	mode 3	mode 4	mode 5
SOZEN[67]	f@	0.806	3.268	7.042	11.628	16.949
	r#	1.000	4.055	8.737	14.427	21.029
MODEL 1	f	0.901	3.562	7.969	13.948	20.993
	r	1.000	3.953	8.845	15.481	23.300
difference* in freq. ratios (%)		0	-2.5	1.2	7.3	10.8

@ frequencies in Hz

frequency ratios

* relative to Sozen's results

TABLE 7-9: FIELD DATA BY ROJAHN [53]

		mode 1	mode 2	mode 3	mode 4
N-S	f[@]	0.54	1.96	3.88	6.20
	r[#]	1.00	3.63	7.19	11.50
E-W	f	0.47	1.76	3.76	6.39
	r	1.00	3.74	8.00	13.60
TORSION	f	0.68	2.29	4.32	7.00
	r	1.00	3.37	6.35	10.30

[@] frequencies in Hz

[#] frequency ratios

CHAPTER VIII

CONCLUSIONS

8.1 BEHAVIOUR OF WALL-FRAME STRUCTURES

A method of analysis for planar wall-frame building structures has been presented. Based on the analysis, parametric studies are conducted on a nominal structure to investigate the effects of wall-frame connections and structure height on the general behaviour of wall-frame structures. These studies give rise to the following observations:

(1) In the top storeys of a wall-frame system, the frame often resists more load than is actually applied to the system.

(2) In a "dual structural system" such as the wall-frame system, design of the frame is in general governed by the requirement of resisting the load that is apportioned the frame in interacting with the wall except in the bottom few storeys, where the requirement of resisting not less than 25% of the total lateral load prevails.

(3) The critical interstorey frame shears in a wall-frame system in general occur in the vicinity of the lowest third-point of the structure height.

(4) Frames are more efficient in contributing to lateral stiffness with taller structures. However, the increase in efficiency tends to become marginal in structures towering beyond about 40 storeys in height.

(5) Wall-frame coupling contributes considerably to reducing structure sway, interstorey frame shear, and wall moment. Moreover, the critical shears in wall-frame connections occur in the vicinity of the lowest third-point of the structure height.

In the light of the above observations, the following recommendations regarding the design of wall-frame structures against lateral loads are made:

(a) Design practices which disregard the interaction between the wall and the frame should not be encouraged.

(b) The significant contribution of wall-frame coupling to improving the general performance of a wall-frame system renders such coupling a worthwhile design consideration.

(c) In the perspective of seismic design, the wall-frame system provides a promising structural system by combining both stiffness, which is mainly due to the wall and is required to reduce interstorey drift and hence non-structural damage, and ductility, which can be built into the system via the wall-frame and/or shear wall connections, or the frame members at selected locations. Thus, a three-stage seismic strategy is possible: the wall-frame and/or shear wall connections can act as the first line of defence by dissipating seismic energy, the walls as the second and main line of defence for major lateral resistance, and the frames as the final line of defence to provide back-up lateral resistance and gravity support.

8.2 COMPARISON OF PROPOSED THREE-DIMENSIONAL ANALYTICAL METHODS

Two methods of analysis for three-dimensional wall-frame building structures have been presented. The first method (Chapters IV and V), called Method A herein for ease of reference, is based upon the continuum approach and is limited to wall-frame structures. The second method (Chapter VI), or Method B, is basically analogous to the stiffness matrix method of analysis, and assumes the availability of a number of other analytical methods to deal with various structural assemblages that normally make up a building structure.

The following comparisons regarding the applicabilities and limitations of these two methods can be made:

(1) The shear beam model employed in Method A in approximation of the lateral stiffness of the frame does not take into account chord drift effects. Thus in dealing with very tall wall-frame structures, significant inaccuracies may arise. However, it is believed that when the number of storeys does not exceed 20, the method will provide reasonably accurate results. On the contrary, Method B can account for

chord drift in frames via plane frame analysis for most wall-frame structural configurations, and is therefore capable of giving better results than Method A in cases where both methods are equally applicable.

(2) Method A is limited to structures where the structure height is constant, and hence cannot deal with, say, set-back buildings. Method B is more flexible and can deal with more structural configurations. It also provides more flexibility in regard to the variation of structural properties along the height of the structure.

(3) In cases where both methods are equally applicable, Method A is in general more efficient in terms of computing time than Method B.

Finally, it can be stated that both methods are general enough to deal with a wide variety of actual structural configurations, are convenient to apply and efficient in terms of computing time and computer storage requirements, and hence are plausible alternatives to existing matrix methods of analysis in dealing with three-dimensional building structures.

APPENDIX A

DERIVATION OF SHEAR STIFFNESS (GA) OF FRAME

The shear stiffness GA of a frame is derived on the basis of the following assumptions:

(1) Chord drift effects are negligible.

(2) Contraflexural points in the columns and girders are located at the midspan.

A typical 1-storey segment of a deflected multi-storey multi-bay frame is isolated as shown in Figure A-1. Each column in the segment, along with the attached girder or girders, constitutes a basic shearing element. One such element is isolated as shown in Figure A-2. The interstorey drift Δ is due to the rotation of the column-girder joint θ and the flexural and shear deformation of the column. Neglecting shear deformation in the column and the girders, it can be shown that

$$\theta = \frac{P_i h}{6E(I_{g1}/g_1 + I_{g2}/g_2)} \qquad \text{(A-1)}$$

$$\Delta = 2\left[\theta\frac{h}{2} + \frac{P_i (h/2)^3}{3EI_{gi}}\right] \qquad \text{(A-2)}$$

Substituting Eqn(A-1) into Eqn(A-2) and isolating P_i, it can be shown that

$$P_i = \frac{12EI_{ci}}{h^2}\left[\, 1 + \frac{2I_{ci}}{h(I_{g1}/g_1 + I_{g2}/g_2)} \,\right]^{-1}\left(\frac{\Delta}{h}\right) \qquad \text{(A-3)}$$

where h = storey height; I_{ci} = moment of inertia of column i; I_{g1}, I_{g2} = moments of inertia of adjacent girders; g_1, g_2 = lengths of adjacent girders; and P_i = shear force in column i.

It is noted that in Eqn (A-3), the term (Δ/h) gives the approximate average slope of the deflected shape of the frame segment. Therefore, by definition, the shear stiffness of column i is given by GA_i such that

$$GA_i = \frac{12EI_{ci}}{h^2}\left[\, 1 + \frac{2I_{ci}}{h(I_{g1}/g_1 + I_{g2}/g_2)} \,\right]^{-1} \qquad \text{(A-4)}$$

For columns having girders on one side only, one of the two moments of inertia for the girders vanishes. For columns at the base of the frame, it can be shown that the corresponding shear stiffness is given by

$$(GA_i)_B = \frac{12EI_{ci}}{h^2}\left[\, 1 + \frac{I_{ci}}{h(I_{g1}/g_1 + I_{g2}/g_2)} \,\right]^{-1} \qquad \text{(A-4a)}$$

while for columns in the top storey of the frame, the shear stiffness becomes

$$(GA_i)_T = \frac{12EI_{ci}}{h^2}\left[\, 1 + \frac{3I_{ci}}{2h(I_{g1}/g_1 + I_{g2}/g_2)} \,\right]^{-1} \qquad \text{(A-4b)}$$

For frames having more than ten storeys, the discrepancy introduced by adopting GA_i, given by Eqn(A-2), as the typical shear stiffness of the respective column on all floors can be neglected. Therefore, the shear stiffness of an n-column frame is given by

$$GA = \sum_{i=1}^{n} GA_i \qquad \text{(A-5)}$$

where GA_i is as defined by Eqn(A-4)

Meanwhile, the joint rotation θ can be found by substituting Eqn(A-3) into Eqn(A-1) so that

$$\theta = \frac{2I_{ci}}{[\, 2I_{ci} + h(I_{gi}/g_i + I_{g2}/g_2) \,]} \left(\frac{\Delta}{h}\right) \qquad \text{(A-6)}$$

Replacing (Δ/h) by y', where y is the average overall lateral deflection of the frame, and rearranging terms, there is obtained

$$\theta = 2\left[\, 2 + \left(\frac{I_{gi}h}{I_{ci}g_i}\right) + \left(\frac{I_{g2}h}{I_{ci}g_2}\right) \,\right]^{-1} y' \qquad \text{(A-6a)}$$

Eqn(A-6a) is the same equation as Eqn(2-8) except that in the latter case, ℓ_{g1} replaces g_1, ℓ_b replaces g_2, I_b replaces I_{g2}, and i is 1.

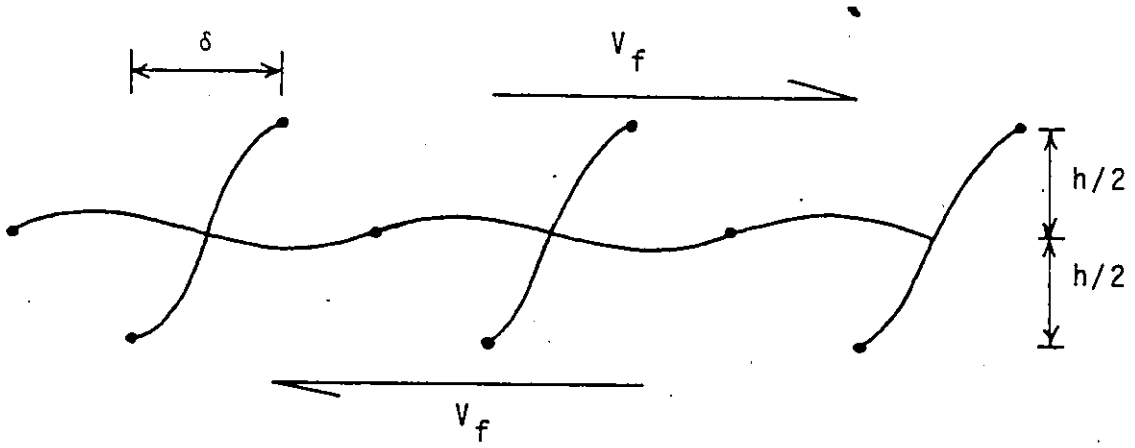

FIG. A-1: TYPICAL SINGLE-STOREY SEGMENT OF FRAME

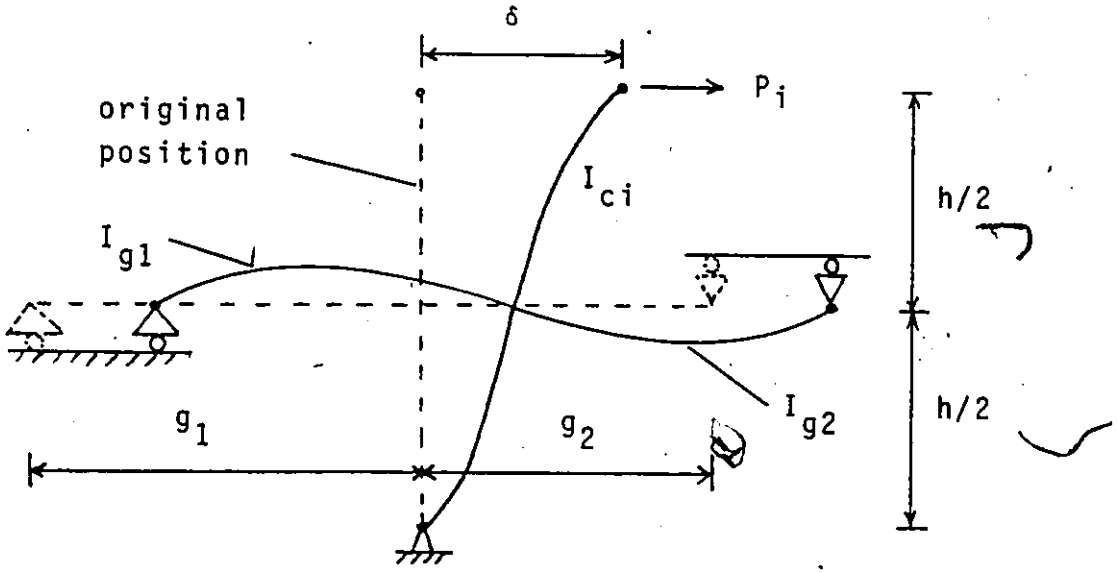

FIG. A-2: BASIC SHEAR ELEMENT i

APPENDIX B

USE OF f_c VALUES

The range of values recommended for f_c, namely,

$$1.1 \leq f_c \leq 1.4 \tag{B-1}$$

when the frame contains not less than one row of girders has been found empirically based upon the following general proportions of the columns, girders, and connecting beams:

$$\begin{aligned} \ell_{g1}/h &\geq 1 \\ I_{g1} &\leq 10 I_{c1} \\ \ell_b/\ell_{g1} &\leq 1 \end{aligned} \tag{B-2}$$

It seems that the value of f_c is mostly controlled by the (ℓ_{g1}/h) ratio. Thus, with I_{g1} and I_{c1} being of the same order of magnitude, the following will suffice as a guide:

(ℓ_{g1}/h)	1.0	1.5	2.0
f_c	1.4	1.2	1.1

(B-3)

It can be shown that an increase in the f_c value tends to decrease q, increase y, and increase the base moment of the wall. However, it is found that these changes are relatively small compared to changes in f_c.

Finally, it is noted that the effect of q in causing axial forces in columns other than column 1 and column 2 in an n-column frame with $n \geq 2$ is neglected based upon the conditions laid down in Eqn(B-2).

APPENDIX C

DERIVATION OF DISTRIBUTED MOMENT AT MIDSPAN OF CONNECTING BEAMS

If the assumption of midspan contraflexural points in the connecting beams or laminae is dispensed with, then when a midspan cut is made, there will be exposed a distribution of moments m(z) in addition to the distribution of shears q(z) (Figure C-1). With these distributed moments present, the shear stiffness of the column 1, GA_1, will be slightly reduced since the rotation of the connecting beam-column joint will be larger than when only the column shear is acting (Figure C-2). Moreover, with the GA_1 reduced, Eqn(2-2) will become

$$-EI_w y''' + GA^* y' + \ell_w q + m = V \qquad (C)$$

where the GA^* contains the reduced GA_1. It should be noted that the resultant effect of m(z) on the horizontal shear resistance of the total structure is zero, so that if its reducing effect on GA_1 is neglected, the m(z) term must also be eliminated from Eqn(C).

The moment distribution can be obtained by considering the continuity at the midspan of the connecting beams or laminae. Thus, if a cut is made at the midspan, the beams

or laminae on one side will undergo rotation relative to those on the other. Referring to Figure C-3, and letting, on the frame side of the cut:

$(\theta_1)_f$ = change in slope at cut due to q(z),

$(\theta_2)_f$ = change in slope at cut due to m(z),

$(\theta_3)_f$ = change in slope at cut due to rotation of connecting beam-column joint,

and on the wall side of the cut:

$(\theta_1)_w$ = change in slope at cut due to q(z),

$(\theta_2)_w$ = change in slope at cut due to m(z),

$(\theta_3)_w$ = change in slope at cut due to rotation of wall,

there is obtained, assuming clockwise rotation to be negative,

$$(\theta_1)_f = \frac{h\ell_b^2}{8EI_b}\, q(z) \qquad \text{(C-1)}$$

$$(\theta_2)_f = -\frac{h\ell_b}{2EI_b}\, m(z) \qquad \text{(C-2)}$$

From Eqn(A-6a) and neglecting the effect of m(z),

$$(\theta_3)_f = 2\left[\, 2 + \frac{I_{g1}h}{I_{c1}\ell_{g1}} + \frac{I_b h}{I_{c1}\ell_b}\,\right]^{-1} y' \qquad \text{(C-3)}$$

Also, $(\theta_1)_w = (\theta_1)_f$ (C-4)

$(\theta_2)_w = -(\theta_2)_f$ (C-5)

$$(\theta_3)_w = - y' \qquad (C\text{-}6)$$

By continuity at the midspan,

$$(\theta_1)_f+(\theta_2)_f+(\theta_3)_f+(\theta_1)_w+(\theta_2)_w+(\theta_3)_w = 0 \qquad (C\text{-}7)$$

Therefore, by substituting Eqns(C-1) through (C-6) into Eqn(C-7), there is finally obtained

$$m(z) = \left(\frac{1 - r}{\varepsilon} \right) y' \qquad (C\text{-}8)$$

where $$r = 2\left[2 + \frac{I_{g1} h}{I_{c1} \ell_{g1}} + \frac{I_b h}{I_{c1} \ell_b} \right]^{-1} \qquad (C\text{-}8a)$$

$$\varepsilon = \frac{h \ell_b}{E I_b} + \frac{h}{12E}(I_{g1}/\ell_{g1} + I_b/\ell_b)^{-1} \qquad (C\text{-}8b)$$

It should be noted that the effect of frame rocking due to chord drift is neglected in deriving Eqn(C-8).

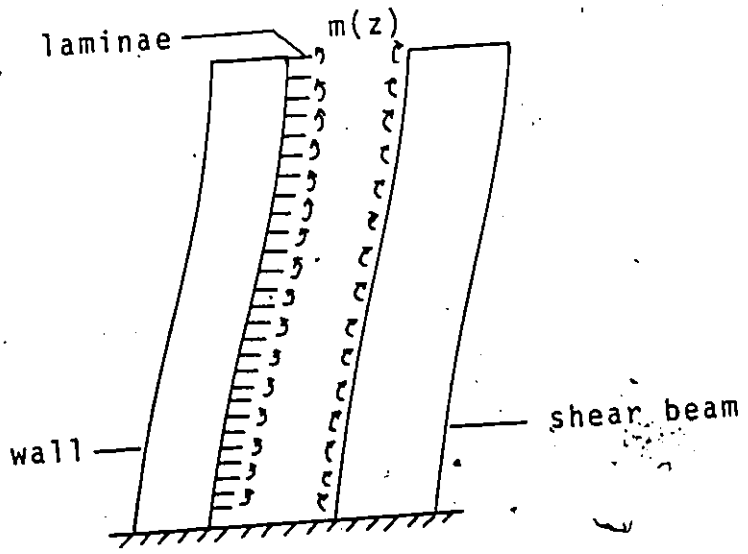

FIG. C-1: DISTRIBUTED MOMENT AT MIDSPAN OF LAMINAE

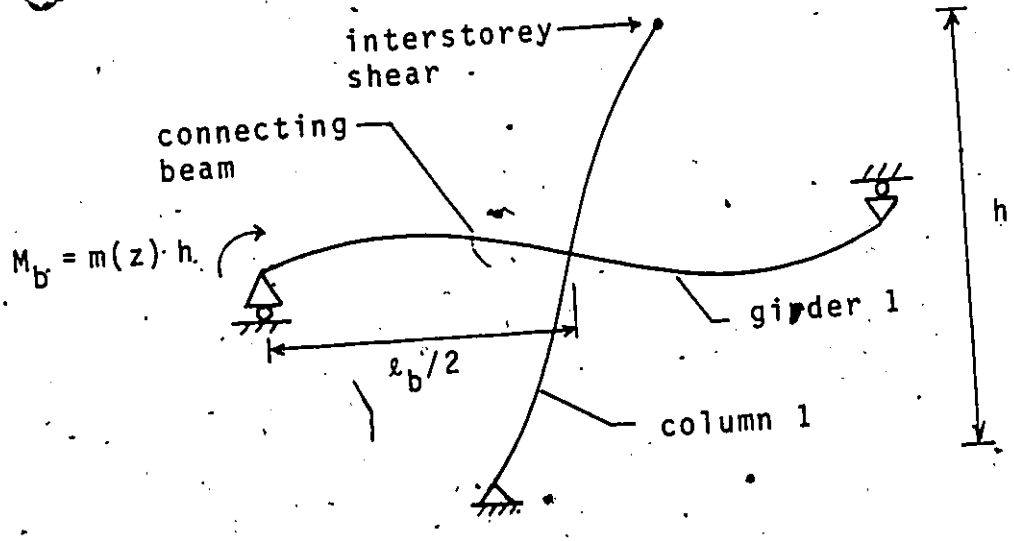

FIG. C-2: DISCRETE CONNECTING BEAM MOMENT

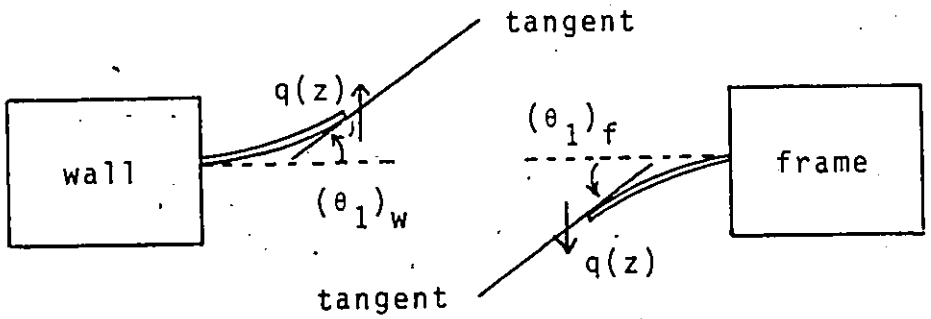

(a) effect of distributed beam shear q(z)

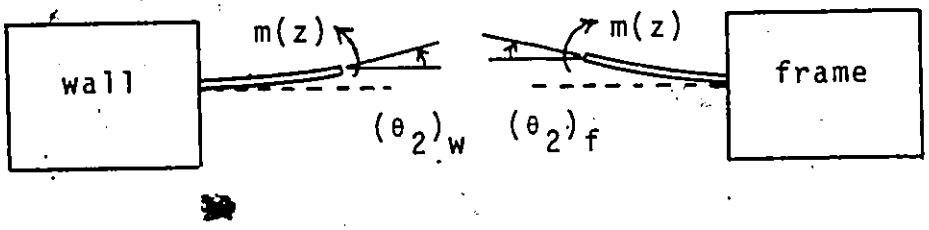

(b) effect of distributed beam moment m(z)

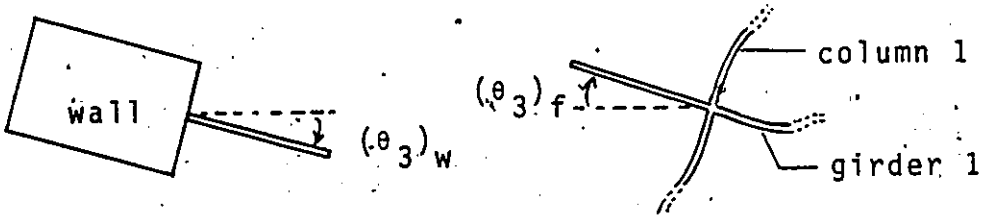

(c) effect of rotation of wall and beam-column joint

FIG. C-3: CONTINUITY AT MIDSPAN OF CONNECTING BEAM

APPENDIX D

MATRIX $[\lambda(z)]_i$

The matrix $[\lambda(z)]_i$ is given by

$$[\lambda(z)]_i = \begin{bmatrix} \lambda_{11} & \lambda_{12} & \lambda_{13} & \lambda_{14} & \lambda_{15} & \lambda_{16} & \lambda_{17} & \lambda_{18} \\ \lambda_{21} & & & & & & & \cdot \\ \lambda_{31} & & & & & & & \cdot \\ \lambda_{41} & & & & & & & \cdot \\ \lambda_{51} & & & & & & & \cdot \\ \lambda_{61} & & & & & & & \cdot \\ \lambda_{71} & & & & & & & \cdot \\ \lambda_{81} & \cdot & \cdot & \cdot & \cdot & \cdot & \cdot & \lambda_{88} \end{bmatrix}$$

where

$\lambda_{11} = \cosh(m_i z)$; $\lambda_{12} = \sinh(m_i z)$; $\lambda_{13} = \cosh(n_i z)$;
$\lambda_{14} = \sinh(n_i z)$; $\lambda_{17} = (\zeta/\phi)_i$;

$\lambda_{21} = m_i \sinh(m_i z)$; $\lambda_{22} = m_i \cosh(m_i z)$;
$\lambda_{23} = n_i \sinh(n_i z)$; $\lambda_{24} = n_i \cosh(n_i z)$;

$\lambda_{31} = m_i^3 \sinh(m_i z)$; $\lambda_{32} = m_i^3 \cosh(m_i z)$;
$\lambda_{33} = n_i^3 \sinh(n_i z)$; $\lambda_{34} = n_i^3 \cosh(n_i z)$;

$$\lambda_{41} = [\sinh(m_i H_i) - \sinh(m_i z)]/m_i;$$

$$\lambda_{42} = [\cosh(m_i H_i) - \cosh(m_i z)]/m_i;$$

$$\lambda_{43} = [\sinh(n_i H_i) - \sinh(n_i z)]/n_i;$$

$$\lambda_{44} = [\cosh(n_i H_i) - \cosh(n_i z)]/n_i;$$

$$\lambda_{45} = 1; \quad \lambda_{47} = (\zeta/\phi)_i (H_i - z)$$

$$\lambda_{51} = (\kappa_i - m_i^2 \chi_i)\lambda_{41}; \quad \lambda_{52} = (\kappa_i - m_i^2 \chi_i)\lambda_{42};$$

$$\lambda_{53} = (\kappa_i - n_i^2 \chi_i)\lambda_{43}; \quad \lambda_{54} = (\kappa_i - n_i^2 \chi_i)\lambda_{44}; \quad \lambda_{56} = 1;$$

$$\lambda_{57} = \{\kappa_i (\zeta/\phi)_i - [(\rho E I_w/\mu)_i + 1]/GA_i\}(H_i - z)$$

$$\lambda_{61} = -(\kappa_i - m_i^2 \chi_i)\cosh(m_i z); \quad \lambda_{62} = -(\kappa_i - m_i^2 \chi_i)\sinh(m_i z);$$

$$\lambda_{63} = -(\kappa_i - n_i^2 \chi_i)\cosh(n_i z); \quad \lambda_{64} = -(\kappa_i - n_i^2 \chi_i)\sinh(n_i z);$$

$$\lambda_{67} = -\{\kappa_i (\zeta/\phi)_i - [(\rho E I_w/\mu)_i + 1]/GA_i\};$$

$$\lambda_{77} = 1;$$

$$\lambda_{87} = H_i - z; \quad \lambda_{88} = 1$$

with $\kappa_i = [(sEI_w/\mu + \ell_w)/GA]_i$

$\chi_i = [I/(GA\mu\gamma)]_i$

All other elements in the matrix are zero.

APPENDIX E

STATION TRANSFER MATRIX $[S]_i$ AND LOAD TRANSFER VECTOR $\{L\}_i$

(FOR TWO-DIMENSIONAL CASE)

The station transfer matrix $[S]_i$ is given by

$$[S]_i = \begin{bmatrix} S_{11} & S_{12} & S_{13} & S_{14} & S_{15} & S_{16} & S_{17} & S_{18} \\ S_{21} & & & & & & & \cdot \\ S_{31} & & & & & & & \cdot \\ S_{41} & & & & & & & \cdot \\ S_{51} & & & & & & & \cdot \\ S_{61} & & & & & & & \cdot \\ S_{71} & & & & & & & \cdot \\ S_{81} & \cdot & \cdot & \cdot & \cdot & \cdot & \cdot & S_{88} \end{bmatrix}$$

where

$$S_{11} = (E\gamma)_{i+1}/(E\gamma)_i;$$

$$S_{16} = (E\gamma)_{i+1}[(\mu + \rho EI_w)_{i+1} - (\mu + \rho EI_w)_i];$$

$$S_{22} = \alpha_i/\alpha_{i+1};\ S_{24} = [(sEI_w/\mu)_i - (sEI_w/\mu)_{i+1}]/\alpha_{i+1};$$

$$S_{28} = [(\rho EI_w/\mu)_{i+1} - (\rho EI_w/\mu)_i]/\alpha_{i+1};$$

$$S_{33} = (\beta_{i+1}S_{24} + \phi_{i+1})/\phi_i;\ S_{32} = \beta_{i+1}\alpha_i/\alpha_{i+1} - \beta_i S_{33};$$

$$S_{38} = \zeta_i S_{33} + \beta_{i+1}S_{28} - \zeta_{i+1};$$

$$S_{44} = S_{55} = S_{66} = S_{77} = S_{88} = 1$$

All other elements in $[S]_i$ are zero.

The load transfer vector $\{L\}_i$ is given by

$$\{L\}_i = \text{col.}\{\ 0\quad 0\quad 0\quad 0\quad 0\quad 0\quad -P_i\quad 0\ \}:$$

APPENDIX F

SIGN CONVENTION FOR CHAPTER IV

Consider an arbitrary thin-walled beam section as shown in Figure F-1. The centroid and principal axes of the section form the local co-ordinate system. The relations between the generalised displacement variables of the section and the forces acting on it are given by

$$T(z) = EA\zeta'(z) \tag{F-1}$$

$$M_x(z) = EI_x\eta''(z) \tag{F-2}$$

$$M_y(z) = EI_y\xi''(z) \tag{F-3}$$

$$B(z) = -EI_\omega\theta''(z) \tag{F-4}$$

$$Q_t(z) = -EI_\omega\theta'''(z) + GJ\theta'(Z) \tag{F-5}$$

$$V_x(z) = -EI_y\xi'''(z) \tag{F-6}$$

$$V_y(z) = -EI_x\eta'''(z) \tag{F-7}$$

where ξ, η, and θ are the generalised displacements, T is the axial force acting at the centroid along the Z-axis, M_x and M_y are the internal moments about the X- and Y-directions,

respectively, B is the bimoment, Q_t is the internal torque, and V_x and V_y are the X- and Y-direction internal shears acting at the shear centre. These generalised displacements and internal forces and moments are shown in their respective positive directions in Figure F-1.

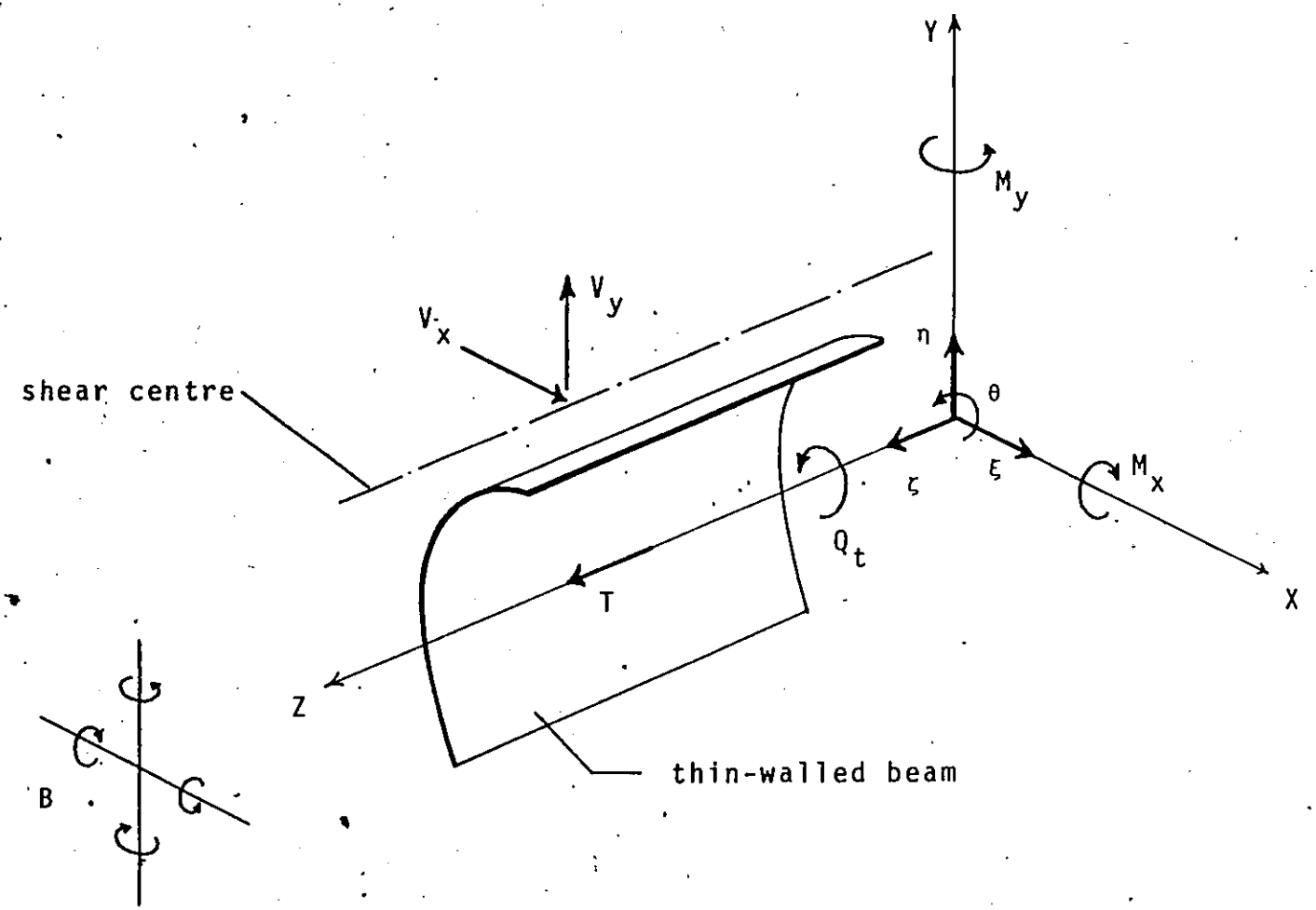

FIG. F-1: SIGN CONVENTION FOR GENERALISED FORCES AND DISPLACEMENTS

APPENDIX G

MATRIX [$\tilde{A}$]

Eqn(4-45) has been derived for a coupled shear wall unit with only one single band of type 1 laminae. When either or both of the walls are connected by more than one band of type 1 laminae — and taking note of Eqn(4-42a) — Eqn (4-45) will take the following form:

$$r_{xk}\xi''' + r_{yk}\eta''' + r_{\theta k}\theta''' + \frac{1}{EA_m}\sum_{j,m}^{Bl} s_j q_j - \frac{1}{EA_n}\sum_{j,n}^{Bl} s_j q_j - \frac{q_k}{E\gamma_k} = 0 \qquad (G\text{-}1)$$

where $\sum_{j,m}^{Bl}$ and $\sum_{j,n}^{Bl}$ represent summation over all type 1 laminae bands that are connected to wall m and wall n, respectively.

Based on Eqns(G-1), and (4-54) or (4-55), an element in the u^{th} row and v^{th} column of [$\tilde{A}$], denoted by a_{uv}, can be defined as follows:

(1) For $u \leq K$ and $v \leq K$, a_{uv} represents the contribution to relative displacement at the midspan cut of the u^{th} band of type 1 laminae, which connects walls m and n,

due to the distributed beam shear in the v^{th} band of type 1 laminae. a_{uv} is given by

$$a_{uv} = \frac{s_{vm}}{EA_m} + \frac{s_{vn}}{EA_n} \qquad (G\text{-}2)$$

where for $m < n$:

(a) $s_{vm}, s_{vn} = 0$ if the laminae band in which q_v acts does not connect wall m or wall n, respectively;

(b) $s_{vm} = +1, -1$ if q_v acts upwards of downwards, respectively, on wall m;

(c) $s_{vn} = +1, -1$ if q_v acts downwards or upwards, respectively, on wall n.

(2) For $u = v = j + k$, where $j = 1, 2, \ldots J$, a_{uv} represents the contribution to relative displacement at the midspan cut of the j^{th} band of type 3 laminae, which connects wall m and frame ℓ, due to the axial effect of $\hat{q}_j$ on the wall and the adjoining column from the frame. In the light of Eqn(4-54),

$$a_{uv} = S_{xj} \qquad (G\text{-}3a)$$

or in the light of Eqn(4-55),

$$a_{uv} = S_{yj} \qquad (G\text{-}3b)$$

where S_{xj} and S_{yj} are given by Eqns(4-54a) and (4-55a), respectively.

(3) For $u \leq K$ and $v > K$, $a_{uv} = 0$.

(4) For $u > K$ and $v \neq u$, $a_{uv} = 0$.

Referring to the wall-frame configuration shown in Figure G-1, $[\tilde{A}]$ is given by

$$[\tilde{A}] = \begin{bmatrix} \frac{1}{EA_1} + \frac{1}{EA_2} & \frac{1}{EA_1} + \frac{1}{EA_2} & -\frac{1}{EA_2} & \frac{1}{EA_1} & 0 & 0 \\ \frac{1}{EA_1} + \frac{1}{EA_2} & \frac{1}{EA_1} + \frac{1}{EA_2} & -\frac{1}{EA_2} & \frac{1}{EA_1} & 0 & 0 \\ -\frac{1}{EA_2} & -\frac{1}{EA_2} & \frac{1}{EA_2} + \frac{1}{EA_3} & 0 & 0 & 0 \\ \frac{1}{EA_1} & \frac{1}{EA_1} & 0 & \frac{1}{EA_1} + \frac{1}{EA_5} & 0 & 0 \\ 0 & 0 & 0 & 0 & S_{x1} & 0 \\ 0 & 0 & 0 & 0 & 0 & S_{y2} \end{bmatrix}$$

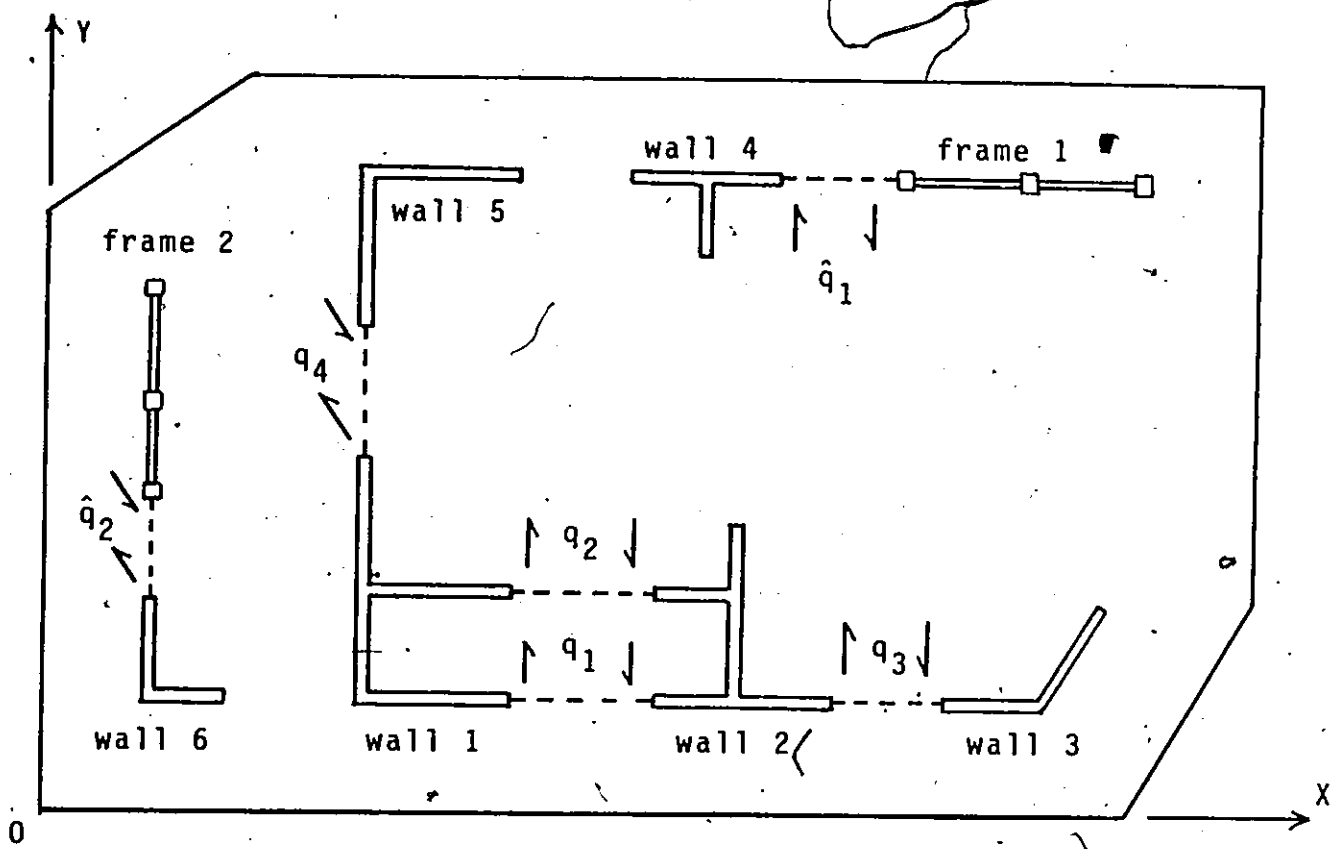

FIG. G-1: EXAMPLE WALL-FRAME COUPLING CONFIGURATION

APPENDIX H

ELEMENTS OF MATRIX $[X(z)]_i$

$$
\begin{bmatrix}
\phi_{11}^{ch_1} & \phi_{11}^{sh_1} & \phi_{12}^{ch_2} & \phi_{12}^{sh_2} & \phi_{13}^{ch_3} & \phi_{13}^{sh_3} \\
\phi_{21}^{ch_1} & \phi_{21}^{sh_1} & \phi_{22}^{ch_2} & \phi_{22}^{sh_2} & \phi_{23}^{ch_3} & \phi_{23}^{sh_3} \\
\phi_{31}^{ch_1} & \phi_{31}^{sh_1} & \phi_{32}^{ch_2} & \phi_{32}^{sh_2} & \phi_{33}^{ch_3} & \phi_{33}^{sh_3} \\
\phi_{11}^{ch_1\lambda_1} & \phi_{11}^{sh_1\lambda_1} & \phi_{12}^{ch_2\lambda_2} & \phi_{12}^{sh_2\lambda_2} & \phi_{13}^{ch_3\lambda_3} & \phi_{13}^{sh_3\lambda_3} \\
\phi_{21}^{ch_1\lambda_1} & \phi_{21}^{sh_1\lambda_1} & \phi_{22}^{ch_2\lambda_2} & \phi_{22}^{sh_2\lambda_2} & \phi_{23}^{ch_3\lambda_3} & \phi_{23}^{sh_3\lambda_3} \\
\phi_{31}^{ch_1\lambda_1} & \phi_{31}^{sh_1\lambda_1} & \phi_{32}^{ch_2\lambda_2} & \phi_{32}^{sh_2\lambda_2} & \phi_{33}^{ch_3\lambda_3} & \phi_{33}^{sh_3\lambda_3} \\
\phi_{11}^{ch_1\lambda_1^2} & \phi_{11}^{sh_1\lambda_1^2} & \phi_{12}^{ch_2\lambda_2^2} & \phi_{12}^{sh_2\lambda_2^2} & \phi_{13}^{ch_3\lambda_3^2} & \phi_{13}^{sh_3\lambda_3^2} \\
\phi_{21}^{ch_1\lambda_1^2} & \phi_{21}^{sh_1\lambda_1^2} & \phi_{22}^{ch_2\lambda_2^2} & \phi_{22}^{sh_2\lambda_2^2} & \phi_{23}^{ch_3\lambda_3^2} & \phi_{23}^{sh_3\lambda_3^2} \\
\phi_{31}^{ch_1\lambda_1^2} & \phi_{31}^{sh_1\lambda_1^2} & \phi_{32}^{ch_2\lambda_2^2} & \phi_{32}^{sh_2\lambda_2^2} & \phi_{33}^{ch_3\lambda_3^2} & \phi_{33}^{sh_3\lambda_3^2} \\
\phi_{11}^{ch_1\lambda_1^3} & \phi_{11}^{sh_1\lambda_1^3} & \phi_{12}^{ch_2\lambda_2^3} & \phi_{12}^{sh_2\lambda_2^3} & \phi_{13}^{ch_3\lambda_3^3} & \phi_{13}^{sh_3\lambda_3^3} \\
\phi_{21}^{ch_1\lambda_1^3} & \phi_{21}^{sh_1\lambda_1^3} & \phi_{22}^{ch_2\lambda_2^3} & \phi_{22}^{sh_2\lambda_2^3} & \phi_{23}^{ch_3\lambda_3^3} & \phi_{23}^{sh_3\lambda_3^3} \\
\phi_{31}^{ch_1\lambda_1^3} & \phi_{31}^{sh_1\lambda_1^3} & \phi_{32}^{ch_2\lambda_2^3} & \phi_{32}^{sh_2\lambda_2^3} & \phi_{33}^{ch_3\lambda_3^3} & \phi_{33}^{sh_3\lambda_3^3} \\
\phi_{11}^{ch_1\lambda_1^4} & \phi_{11}^{sh_1\lambda_1^4} & \phi_{12}^{ch_2\lambda_2^4} & \phi_{12}^{sh_2\lambda_2^4} & \phi_{13}^{ch_3\lambda_3^4} & \phi_{13}^{sh_3\lambda_3^4} \\
\phi_{21}^{ch_1\lambda_1^4} & \phi_{21}^{sh_1\lambda_1^4} & \phi_{22}^{ch_2\lambda_2^4} & \phi_{22}^{sh_2\lambda_2^4} & \phi_{23}^{ch_3\lambda_3^4} & \phi_{23}^{sh_3\lambda_3^4} \\
\phi_{31}^{ch_1\lambda_1^4} & \phi_{31}^{sh_1\lambda_1^4} & \phi_{32}^{ch_2\lambda_2^4} & \phi_{32}^{sh_2\lambda_2^4} & \phi_{33}^{ch_3\lambda_3^4} & \phi_{33}^{sh_3\lambda_3^4} \\
0 & 0 & 0 & 0 & 0 & 0 \\
0 & 0 & 0 & 0 & 0 & 0 \\
0 & 0 & 0 & 0 & 0 & 0 \\
0 & 0 & 0 & 0 & 0 & 0 \\
0 & 0 & 0 & 0 & 0 & 0
\end{bmatrix}
$$

(continued next page)

(matrix $[x(z)]_i$ continued)

$\phi_{14}^{ch_4}$	$\phi_{14}^{sh_4}$	$\phi_{15}^{ch_5}$	$\phi_{15}^{sh_5}$	$\phi_{16}^{ch_6}$	$\phi_{16}^{sh_6}$
$\phi_{24}^{ch_4}$	$\phi_{24}^{sh_4}$	$\phi_{25}^{ch_5}$	$\phi_{25}^{sh_5}$	$\phi_{26}^{ch_6}$	$\phi_{26}^{sh_6}$
$\phi_{34}^{ch_4}$	$\phi_{34}^{sh_4}$	$\phi_{35}^{ch_5}$	$\phi_{35}^{sh_5}$	$\phi_{36}^{ch_6}$	$\phi_{36}^{sh_6}$
$\phi_{14}^{ch_4\lambda_4}$	$\phi_{14}^{sh_4\lambda_4}$	$\phi_{15}^{ch_5\lambda_5}$	$\phi_{15}^{sh_5\lambda_5}$	$\phi_{16}^{ch_6\lambda_6}$	$\phi_{16}^{sh_6\lambda_6}$
$\phi_{24}^{ch_4\lambda_4}$	$\phi_{24}^{sh_4\lambda_4}$	$\phi_{25}^{ch_5\lambda_5}$	$\phi_{25}^{sh_5\lambda_5}$	$\phi_{26}^{ch_6\lambda_6}$	$\phi_{26}^{sh_6\lambda_6}$
$\phi_{34}^{ch_4\lambda_4}$	$\phi_{34}^{sh_4\lambda_4}$	$\phi_{35}^{ch_5\lambda_5}$	$\phi_{35}^{sh_5\lambda_5}$	$\phi_{36}^{ch_6\lambda_6}$	$\phi_{36}^{sh_6\lambda_6}$
$\phi_{14}^{ch_4\lambda_4^2}$	$\phi_{14}^{sh_4\lambda_4^2}$	$\phi_{15}^{ch_5\lambda_5^2}$	$\phi_{15}^{sh_5\lambda_5^2}$	$\phi_{16}^{ch_6\lambda_6^2}$	$\phi_{16}^{sh_6\lambda_6^2}$
$\phi_{24}^{ch_4\lambda_4^2}$	$\phi_{24}^{sh_4\lambda_4^2}$	$\phi_{25}^{ch_5\lambda_5^2}$	$\phi_{25}^{sh_5\lambda_5^2}$	$\phi_{26}^{ch_6\lambda_6^2}$	$\phi_{26}^{sh_6\lambda_6^2}$
$\phi_{34}^{ch_4\lambda_4^2}$	$\phi_{34}^{sh_4\lambda_4^2}$	$\phi_{35}^{ch_5\lambda_5^2}$	$\phi_{35}^{sh_5\lambda_5^2}$	$\phi_{36}^{ch_6\lambda_6^2}$	$\phi_{36}^{sh_6\lambda_6^2}$
$\phi_{14}^{ch_4\lambda_4^3}$	$\phi_{14}^{sh_4\lambda_4^3}$	$\phi_{15}^{ch_5\lambda_5^3}$	$\phi_{15}^{sh_5\lambda_5^3}$	$\phi_{16}^{ch_6\lambda_6^3}$	$\phi_{16}^{sh_6\lambda_6^3}$
$\phi_{24}^{ch_4\lambda_4^3}$	$\phi_{24}^{sh_4\lambda_4^3}$	$\phi_{25}^{ch_5\lambda_5^3}$	$\phi_{25}^{sh_5\lambda_5^3}$	$\phi_{26}^{ch_6\lambda_6^3}$	$\phi_{26}^{sh_6\lambda_6^3}$
$\phi_{34}^{ch_4\lambda_4^3}$	$\phi_{34}^{sh_4\lambda_4^3}$	$\phi_{35}^{ch_5\lambda_5^3}$	$\phi_{35}^{sh_5\lambda_5^3}$	$\phi_{36}^{ch_6\lambda_6^3}$	$\phi_{36}^{sh_6\lambda_6^3}$
$\phi_{14}^{ch_4\lambda_4^4}$	$\phi_{14}^{sh_4\lambda_4^4}$	$\phi_{15}^{ch_5\lambda_5^4}$	$\phi_{15}^{sh_5\lambda_5^4}$	$\phi_{16}^{ch_6\lambda_6^4}$	$\phi_{16}^{sh_6\lambda_6^4}$
$\phi_{24}^{ch_4\lambda_4^4}$	$\phi_{24}^{sh_4\lambda_4^4}$	$\phi_{25}^{ch_5\lambda_5^4}$	$\phi_{25}^{sh_5\lambda_5^4}$	$\phi_{26}^{ch_6\lambda_6^4}$	$\phi_{26}^{sh_6\lambda_6^4}$
$\phi_{34}^{ch_4\lambda_4^4}$	$\phi_{34}^{sh_4\lambda_4^4}$	$\phi_{35}^{ch_5\lambda_5^4}$	$\phi_{35}^{sh_5\lambda_5^4}$	$\phi_{36}^{ch_6\lambda_6^4}$	$\phi_{36}^{sh_6\lambda_6^4}$
0	0	0	0	0	0
0	0	0	0	0	0
0	0	0	0	0	0
0	0	0	0	0	0
0	0	0	0	0	0

(continued next page)

(matrix $[\chi(z)]_i$ continued)

$$
\begin{bmatrix}
1 & 0 & 0 & 0 & 0 & b_{11}z & b_{12}z & b_{13}z \\
0 & 1 & 0 & 0 & 0 & b_{21}z & b_{22}z & b_{23}z \\
0 & 0 & 1 & 0 & 0 & b_{31}z & b_{32}z & b_{33}z \\
0 & 0 & 0 & 0 & 0 & b_{11} & b_{12} & b_{13} \\
0 & 0 & 0 & 0 & 0 & b_{21} & b_{22} & b_{23} \\
0 & 0 & 0 & 0 & 0 & b_{31} & b_{32} & b_{33} \\
0 & 0 & 0 & 0 & 0 & 0 & 0 & 0 \\
0 & 0 & 0 & 0 & 0 & 0 & 0 & 0 \\
0 & 0 & 0 & 0 & 0 & 0 & 0 & 0 \\
0 & 0 & 0 & 0 & 0 & 0 & 0 & 0 \\
0 & 0 & 0 & 0 & 0 & 0 & 0 & 0 \\
0 & 0 & 0 & 0 & 0 & 0 & 0 & 0 \\
0 & 0 & 0 & 0 & 0 & 0 & 0 & 0 \\
0 & 0 & 0 & 0 & 0 & 0 & 0 & 0 \\
0 & 0 & 0 & 0 & 0 & 0 & 0 & 0 \\
0 & 0 & 0 & 1 & 0 & (H_i-z) & 0 & 0 \\
0 & 0 & 0 & 0 & 1 & 0 & (H_i-z) & 0 \\
0 & 0 & 0 & 0 & 0 & 1 & 0 & 0 \\
0 & 0 & 0 & 0 & 0 & 0 & 1 & 0 \\
0 & 0 & 0 & 0 & 0 & 0 & 0 & 1
\end{bmatrix}
$$

NOTE: $ch_j = \cosh(\lambda_j z)$; $sh_j = \sinh(\lambda_j z)$; $\phi_{ij} = i^{th}$ element of eigen-vector $\{\phi\}_j$ ($i = 1,2,3$; $j = 1,2,\ldots 6$).

b_{mn} = element in m^{th} row and n^{th} column of $[\bar{B}]_i$.

APPENDIX I

STATION TRANSFER MATRIX $[S]_i$ AND LOAD TRANSFER VECTOR $\{L\}_i$

(FOR THREE-DIMENSIONAL CASE)

$$[S]_i = \begin{bmatrix}
1 & 0 & 0 & 0 & 0 & 0 & 0 & 0 & 0 & 0 & 0 & 0 & 0 & 0 & 0 & 0 & 0 & 0 & 0 & 0 \\
0 & 1 & & & & & & & & & & & & & & & & & & \\
 & & 1 & & & & & & & & & & & & & & & & & \\
 & & & 1 & & & & & & & & & & & & & & & & \\
 & & & & 1 & & & & & & & & & & & & & & & \\
 & & & & & 1 & & & & & & & & & & & & & & \\
 & & & & & & [C_1]_i & & & & & & & & & & & & & \\
 & & [C_3]_i & & & & & [C_2]_i & & & & & & & & & [C_4]_i & & \\
 & & & & & & [C_6]_i & & & & [C_5]_i & & & & & & & & & \\
 & & & & & & & & & & & 1 & & & & & & & & \\
 & & & & & & & & & & & & 1 & & & & & & & \\
 & & & & & & & & & & & & & 1 & & & & & & \\
 & & & & & & & & & & & & & & 1 & 0 & & & & \\
0 & . & . & . & . & . & . & . & . & . & . & . & . & . & . & 0 & 1 & & & &
\end{bmatrix}$$

$$\{L\}_i = \text{col.}\{\ 0,\ 0,\ 0,\ 0,\ 0,\ 0,\ 0,\ 0,\ 0,\ \{C_7\}_i,$$

$$0,\ 0,\ 0,\ 0,\ 0,\ -P_{xi},\ -P_{yi},\ -P_{ti}\ \}$$

NOTE: The submatrices $[C_1]_i$, $[C_2]_i$, $[C_3]_i$, $[C_4]_i$, $[C_5]_i$, and $[C_6]_i$ in $[S]_i$ and the subvector $\{C_7\}_i$ in $\{L\}_i$ are as given by Eqns (5-26a), (5-29a), and (5-31a). Elements not entered in $[S]_i$ are zero.

APPENDIX J

STIFFNESS MATRIX [K]

$$[K] = \begin{bmatrix}
K_{xx}^{11} & K_{xy}^{11} & K_{x\theta}^{11} & K_{xx}^{12} & K_{xy}^{12} & K_{x\theta}^{12} & \cdots & K_{xx}^{1N} & K_{xy}^{1N} & K_{x\theta}^{1N} \\
K_{yx}^{11} & K_{yy}^{11} & K_{y\theta}^{11} & K_{yx}^{12} & K_{yy}^{12} & K_{y\theta}^{12} & & K_{yx}^{1N} & K_{yy}^{1N} & K_{y\theta}^{1N} \\
K_{\theta x}^{11} & K_{\theta y}^{11} & K_{\theta\theta}^{11} & K_{\theta x}^{12} & K_{\theta y}^{12} & K_{\theta\theta}^{12} & & K_{\theta x}^{1N} & K_{\theta y}^{1N} & K_{\theta\theta}^{1N} \\
K_{xx}^{21} & K_{xy}^{21} & K_{x\theta}^{21} & K_{xx}^{22} & K_{xy}^{22} & K_{x\theta}^{22} & & K_{xx}^{2N} & K_{xy}^{2N} & K_{x\theta}^{2N} \\
K_{yx}^{21} & K_{yy}^{21} & K_{y\theta}^{21} & K_{yx}^{22} & K_{yy}^{22} & K_{y\theta}^{22} & & K_{yx}^{2N} & K_{yy}^{2N} & K_{y\theta}^{2N} \\
K_{\theta x}^{21} & K_{\theta y}^{21} & K_{\theta\theta}^{21} & K_{\theta x}^{22} & K_{\theta y}^{22} & K_{\theta\theta}^{22} & & K_{\theta x}^{2N} & K_{\theta y}^{2N} & K_{\theta\theta}^{2N} \\
\vdots & & & & & & & & & \\
K_{xx}^{N1} & K_{xy}^{N1} & K_{x\theta}^{N1} & K_{xx}^{N2} & K_{xy}^{N2} & K_{x\theta}^{N2} & & K_{xx}^{NN} & K_{xy}^{NN} & K_{x\theta}^{NN} \\
K_{yx}^{N1} & K_{yy}^{N1} & K_{y\theta}^{N1} & K_{yx}^{N2} & K_{yy}^{N2} & K_{y\theta}^{N2} & & K_{yx}^{NN} & K_{yy}^{NN} & K_{y\theta}^{NN} \\
K_{\theta x}^{N1} & K_{\theta y}^{N1} & K_{\theta\theta}^{N1} & K_{\theta x}^{N2} & K_{\theta y}^{N2} & K_{\theta\theta}^{N2} & \cdots & K_{\theta x}^{NN} & K_{\theta y}^{NN} & K_{\theta\theta}^{NN}
\end{bmatrix}$$

APPENDIX K

MASS MATRIX [M]

The mass matrix [M] is given by

$$[M] = \begin{bmatrix} [\bar{M}_1] & & & & \\ & [\bar{M}_2] & & & \\ & & \ddots & & \\ & & & [\bar{M}_m] & \\ & & & & \ddots \\ & & & & & [\bar{M}_N] \end{bmatrix}$$

where

$$[\bar{M}_m] = \begin{bmatrix} M_m & 0 & -y_m M_m \\ 0 & M_m & x_m M_m \\ -y_m M_m & x_m M_m & I_m + M_m(x_m^2 + y_m^2) \end{bmatrix}$$

for m = 1, 2,....N. Elements not entered in [M] are zero.

BIBLIOGRAPHY

1. Barnard, P. R. and Schwaighofer, J., "The Interaction of Shear Walls Connected Solely through Slabs", Tall Buildings, Pergamon Press, 1967, pp. 157-173.
2. Beck, H., "Contribution to the Analysis of Coupled Shear Walls", Journal of the Am. Conc. Inst., Aug. 1962, pp. 1055-1070.
3. Biggs, J. M., Introduction to Structural Dynamics, McGraw Hill, New York.
4. Biswas, J. K., "Three-Dimensional Analysis of Shear Wall Multi-Storey Buildings", Ph.D. Thesis, McMaster University, Hamilton, Ontario, Canada, Sept. 1974.
5. Butlin, G. A. and McMillan, C. M., "An Improved Finite Element for Analysis of Plane Coupled Shear Walls", Civil Engg. and Public Works Review, Dec. 1971, pp. 1299-1303.
6. Cardan, B., "Concrete Shear Walls Combined with Rigid Frames in Multi-Storey Buildings Subjected to Lateral Loads", Journal of the Am. Conc. Inst., Sept. 1961, pp. 299-316.
7. Chan, P. C. K., "Static and Dynamic Analysis of Framed-Tube Structures", Ph.D. Thesis, McMaster University, Hamilton, Ontario, Canada, Oct.1973.
8. Chriss, S., "Analysis of Shear Wall-Frame Systems", Jour-

nal of Boston Soc. of Civil Engineers, 1970, pp. 94-144.

9. Clough, R. W., King, I. P., and Wilson, E. L., "Structural Analysis of Multi-storey Buildings", Journal of Struct. Div., ASCE, Vol. 90, ST3, June 1964, pp. 19-34.

10. Coull, A., "Interaction of Coupled Shear Walls with Elastic Foundations", Journal of the Am. Conc. Inst., June 1971, pp. 456-461.

11. Coull, A., "Coupled Shear Walls Subjected to Differential Settlement", Build. Sci., Vol. 6, 1971, pp. 209-212.

12. Coull, A. and Bose B., "Simplified Analysis of Frame-Tube Structures", Journal of the Struct. Div., ASCE, Vol. 101, No. ST11, Nov. 1975, pp. 2223-2240.

13. Coull, A. and Choudhurry, J. R., "Stresses and Deflections in Coupled Shear Walls", Journal of the Am. Conc. Inst., Feb. 1967, pp. 65-72.

14. Coull, A. and Choudhurry, J. R., "Analysis of Coupled Shear Walls", Journal of the Am. Conc. Inst., Sept. 1967, pp. 587-593.

15. Coull, A. and choudhurry, J. R., "Analysis of Coupled Shear Walls of Variable Thickness", Build. Sci., Vol. 2, 1967, pp. 181-188.

16. Coull, A. and Irwin, A. W., "Analysis of Load Distribution in Multi-storey Shear Wall Structures", Structural Engineer, Aug. 1970, pp. 301-306.

17. Coull, A. and Puri, R. D., "Analysis of Pierced Shear Walls", Journal of Struct. Div., ASCE, Vol. 94, ST1, Jan. 1968, pp. 71-82.

18. Coull, A. and Puri, R. D., "Analysis of Coupled Shear Walls of Variable Cross-section", Build. Sci., Vol. 2, 1968, pp. 313-320.

19. Coull, A. and Subedi, N. K., "Framed-Tube Structures for High-rise Buildings", Journal of Struct. Div., ASCE, Vol. 97, ST8, Aug. 1971, pp. 2097-2105.

20. Coull, A. and Subedi, N. K., "Hull-Core Structures Subjected to Bending and Torsion", Preliminary Report, International ASSOC. of Bridge and Struct. Engg., Amsterdam, May 1972, pp. 613-622.

21. Elkholy, I. A. S., "Static Analysis of Plane Coupled Shear Walls", M. Eng. Thesis, McMaster University, Hamilton, Ontario, Canada, Dec. 1971.

22. Frischmann, W. W., Prabhu, S. S., and Toppler, J. F., "Multi-storey Frames and Interconnected Shear Walls Subjected to Lateral Loads", Concrete and Construction Engg., June 1963, pp. 227-233.

23. Gluck, J. and Gellert, M., "Three Dimensional Lateral Load Analysis of Multi-storey Structures", International ASSOC. of Bridge and Struct. Engg., 1972, pp. 77-90.

24. Gluck, J., Gellert, M., and Danay, A., "Dynamics of Asymmetric Multi-storey Structures", International ASSOC.

of Bridge and Struct. Engg., Vol. 33-III, 1973, pp. 91-106.

25. Goldberg, J. E., "Analysis of Multi-storey Buildings Considering Shear Wall and Floor Deformations", Tall Buildings, Pergamon Press, 1967, pp. 349-373.

26. Gould, P. L., "Interaction of Shear Wall-Frame Systems in Multi-stoery Buildings", Journal of the Am. Conc. Inst., Jan. 1965, pp. 45-70.

27. Goyal, B. K. and Sharma, S. P., "Matrix Analysis of Frames with Shear Walls", Build. Sci., Vol. 3, 1968. pp. 93-98.

28. Grundy, P. and Wathen, G. R., "Frame-Shear Wall Interaction", Civ. Engg. Trans. I. E. Aust., Vol. CE14, NO. 1, April 1972, pp. 102-109.

29. Heidebrecht, A. C. and Stafford Smith, B., "Approximate Analysis of Tall Wall-Frame Structures", Journal of Struct. Div., ASCE, Vol. 99, ST2, Feb. 1973, pp. 199-221.

30. Heidebrecht, A. C. and Stafford Smith, B., "Approximate Analysis of Open-section Shear Walls Subject to Torsional Loading", Dept. Research Report No. 72-8, Dept. of Civil Eng. & Eng. Mech., McMaster University, Hamilton, Ontario, Canada, Sept. 1972.

31. Heidebrecht, A. C. and Swift, R. D., "Analysis of Asymmetrical Coupled Shear Walls", Journal of Struct. Div.,

ASCE, Vol. 97, ST5, May 1971, pp. 1407-1422.

32. Hussein, W. A., "Analysis of Multi-Bay Shear Wall Structures by the Shear Connection Method", Build. Sci., Vol. 7, 1972, pp. 69-73.

33. Jenkins, W. M. and Harrison, T., "Analysis of Tall Buildings with Shear Walls under Bending and Torsion", Tall Buildings, Pergamon Press, 1967, pp. 413-439.

34. Kan, C. L. and Chopra, A. K., "Elastic Earthquake Analysis of Torsionally Coupled Multi-storey Buildings", Earthquake Engg. and Struct. Dynamics, Vol. 5, pp. 395-412, 1977.

35. Khan, F. R. and Navinchandra, R. A., "Analysis and Design of Framed-Tube Structures for Tall Concrete Buildings", Structural Engineer, March 1973, pp. 85-92.

36. Khan, F. R. and Sbarounis, J. A., "Interaction of Shear Walls and Frames", Journal of Struct. Div., ASCE, Vol. 93, ST3, 1964, pp. 285-332.

37. Macleod, I. A., "New Rectangular Finite Element for Shear Wall Analysis", Journal of the Struct. Div., ASCE, Vol. 95, ST3, March 1969, pp. 399-409.

38. Macleod, I. A., "Connected Shear WAlls of Unequal Width", Journal of the Am. Conc. Inst., May 1970, pp. 408-412.

39. Macleod, I. A., "Simplified Equations for Deflection of Multi-storey Frames", Build. Sci., Vol. 6, 1971, pp. 25-31.

40. Macleod, I. A., "Simplified Analysis for Shear Wall-Frame Interaction", Build. Sci., Vol. 7, 1972, pp. 121-125.

41. Majib, k. I. and Croxton, P. C. L., "Wind Analysis of Complete Building Structures by Influence Co-efficients", Proc. of the Inst. of Civil Engineers, Oct. 1970, pp. 169-184.

42. Medearis, K., "Coupled Bending and Torsional Oscillations of a Modern Skyscraper", Bull. of Seism. Soc. of Am., Vol. 56, No. 4, Aug. 1966, pp. 937-946.

43. Michael, D., "The Effect of Local Wall Deformations on the Elastic Interaction of Cross Walls Coupled by Beams", Tall Buildings, Pergamon Press, 1967, pp. 253-270.

44. Michael, D., "Torsional Coupling of Core Walls in Tall Buildings", Structural Engineer, Feb. 1969, pp. 67-71.

45. National Building Code of Canada, 1977, National Research Council of Canada, Canada.

46. Oakberg, R. G. and Weaver, W., "Analysis of Frames with Shear Walls by Finite Elements", Proc., Sym. on Application of Finite Element Methods in Civil Engg., Vanderbilt University, Nashville, Tennessee, Nov. 1969, pp. 567-607.

47. Parme, A. L., "Design of Combined Frames and Shear Walls", Tall Buildings, Pergamon Press, 1967, pp. 291-317.

48. Pauley, T., "An Elastic-plastic Analysis of Coupled Shear Walls", Journal of the Am. Conc. Inst., Nov.1970, pp. 915-922.

49. Pisanty, A. and Traum, E. E., "Simplified Analysis of Coupled Shear Walls of Variable Cross-section", Build. Sci., Vol. 5, 1970, pp. 11-20.

50. Przemieniecki, J. S., Theory of Matrix Structural Analysis, McGraw Hill, New York, 1968.

51. Qadeer, A. and Stafford Smith, B., "The Bending Stiffness of Slabs Connecting Shear Walls", Journal of the Am. Conc. Inst., June 1969, pp. 464-473.

52. Reinhorn,A., Rutenberg, A., and Gluck, J., "Dynamic Torsional Coupling in Asymmetric Building Structures", Building and Environment, Vol. 12, pp. 251-261, 1977.

53. Rojahn, C., "Analysis of Banco de America and Banco Central Postearthquake Ambient Vibration Observations", Managua, Nicaragua Earthquake of December 23, 1972, Earthquake Engineering Research Institute Conference Proceedings, Volume II, pp. 674-692.

54. Rosenblueth, E. and Holtz, I., "Elastic Analysis of Shear Walls in Tall Buildings", Journal of the Am. Conc. June 1960, pp. 1209-1222.

55. Rosman, R., "An Approximate Method of Analysis of Walls of Multi-storey Buildings", Civil Engg. and Public Works

Review, London, Vol. 59, Jan. 1964, pp. 67-69.

56. Rosman, R., "Approximate Analysis of Shear Walls Subjected to Lateral Loads", Journal of the Am. Conc. Inst., June 1964, pp. 717-732.

57. Rosman, R., "Laterally Loaded Systems Consisting of Walls and Frames", Tall Buildings, Pergamon Press, 1967, pp. 273-289.

58. Rosman, R., "Torsion of Perforated Concrete Shafts", Journal of the Struct. Div., ASCE, Vol. 95, ST5, May 1969, pp. 991-1010.

59. Rutenberg, A., "A Consideration of the Torsional Response of Building Frames", Bull. New Zealand Nat. Soc. Earthq. Engg., Vol. 12, No. 1, March 1979.

60. Rutenberg, A. and Heidebrecht, A. C., "Approximate Analysis of Asymmetric Wall-Frame Structures", Build. Sci., Vol. 10, 1975, pp. 27-35.

61. Rutenberg, A., Tso, W. K., and Heidebrecht, A. C., "Dynamic Properties of Asymmetric Wall-Frame Structures", Earthquake Engg. and Struct. Dynamics, Vol. 5, pp. 41-51 , 1977.

62. SAP-IV: A Structural Analysis Program for Static and Dynamic Response of Linear Systems, University of California, Berkeley, June 1973.

63. Schwaighofer, J. and Microys, H. F., "Analysis of Shear

Walls Using Standard Computer Programs", Journal of the Am. Conc. Inst., Dec. 1969, pp. 1005-1007.

64. Selna, L. G. and Cho, M. D., "Banco de America, Managua: A High-rise Shear Wall Building Withstands a Strong Earthquake", Managua, Nicaragua Earthquake of December 23, 1972, Earthquake Engineering Research Institute Conference Proceedings, Volume II, pp. 551-570.

65. Shah, H. C., Nicoletti, J., and Kulka, F., "Post Earthquake Dynamic Measurements of Four Structures in Managua", Managua, Nicaragua Earthquake of December 23, 1972, Earthquake Engineering Research Institute Conference Proceedings, Volume II, pp. 693-708.

66. Sheppard, R. and Donald, R. A., "Seismic Response of Torsionally Unbalanced Buildings", Journal of Sound and Vibration, Vol. 6, No. 1, 1967, pp. 20-37.

67. Sozen, M. A. and Shibata, A., "An Evaluation of the Performance of the Banco de America Building, Managua, Nicaragua", Managua, Nicaragua Earthquake of December 23, 1972, Earthquake Engineering Research Institute Conference Proceedings, Volume II, pp. 529-550.

68. Stafford Smith, B., "Modified Beam Method for Analysing Symmetrical Interconnected Shear Walls", Journal of the Am. Conc. Inst., Dec. 1970, pp. 977-980.

69. Stafford Smith, B. and Tananath, B.C., "The Analysis of

Tall Core-Supported Structures Subjected to Torsion", Proc. of the Inst. of Civil Engineers, Vol. 53, Sept. 1972, pp. 173-187.

70. Stomato, M. C. and Mancini, E., "Three-Dimensional Interaction of Walls and Frames", Journal of the Struct. Div., ASCE, Vol. 99, No. ST12, Dec. 1973.

71. Stomato, M. C. and Stafford Smith, "Approximate Method for the Three-Dimensional Analysis of Tall Buildings", Proc. of the Inst. of Civil Engineers, July 1969, pp. 361-379.

72. Traum, E. E., "Multi-storey Pierced Shear Walls of Variable Cross-section", Tall Buildings, Pergamon Press, 1967,, pp. 181-206.

73. Tso, W. K., "Stresses in Coupled Shear Walls Induced by Foundation Deformation", Build. Sci., Vol. 7, 1972, pp. 197-203.

74. Tso, W. K. and Biswas, J. K., "Analysis of Core Wall Structures Subjected to Applied Torque", Building Science, Vol. 8, pp. 251-257, Pergamon Press 1973.

75. Tso, W. K. and Biswas, J. K., "Torsional Analysis of Core Wall Structures", preprints of the Fifth World Conference on Earthquake Engineering, Vol. I, paper no. 17, Rome, Italy, June 1973.

76. Tso, W. K. and Biswas, J. K., " General Analysis of Non-planar Coupled Shear Walls", Journal of Struct. Div., ASCE, Vol. 99, ST3, March 1973, pp. 365-380.

77. Tso, W. k. and Chan, P. C. K., "Flexible Foundation Effect on Coupled Shear Walls", Journal of the Am. Conc. Inst., Nov. 1972, pp. 678-683.

78. Tso, W. k. and Chan, P. C. K., "Static Analysis of Stepped Coupled Shear Walls by Transfer Matrix Method", Build. Sci., Vol. 8, 1973, pp. 167-177.

79. Tso, W. K. and Mahmond, A. A., "Effective Width of Coupling Slabs in Shear Wall Buildings", Journal of the Struct. Div., Vol. 103, No. ST3, March 1977.

80. Vlasov, V. S., "Thin Walled Elastic Beams", English Translation, National Science Foundation, Washington, D. C., 1961.

81. Weaver, W. and Nelson, M. F., "Three-Dimensional Analysis of Tier Buildings", Journal of the Struct. Div., ASCE, Vol. 92, ST6, Dec. 1966, pp. 385-404.

82. Webster, J. A., "The Static and Dynamic Analysis of Orthogonal Structures Composed of Shear Walls and Frames", Tall Buildings, Pergamon Press, 1967, pp. 377-395.

83. Winokur, A. and Gluck, J., "Lateral Loads in Asymmetric Multi-storey Structures", Journal of the Struct. Div., ASCE, Vol. 94, ST3, March 1968, pp. 645-656.

84. Winokur, A. and Gluck, J., "Ultimate Strength Analysis

of Coupled Shear Walls", Journal of the Am. Conc. Inst., Dec. 1968, pp. 1029-1036.

85. Zienkiewicz, O. C., The Finite Element Method in Structural and Continuum Mechanics, McGraw Hill, 1967.